



**THÈSE DE DOCTORAT DE  
L'UNIVERSITÉ PIERRE ET MARIE CURIE**

Spécialité

**Physique Théorique**

École doctorale de la région parisienne – ED 107

# **Phase transitions and diffusion in dissipative classical and quantum systems**

Réalisée au

**Laboratoire de Physique Théorique et Hautes Energies**

Présentée par

**Julius BONART**

Pour obtenir le grade de

**DOCTEUR de l'UNIVERSITÉ PIERRE ET MARIE CURIE**

soutenue le 04 octobre 2013

devant le jury composé de :

Mme Leticia F. CUGLIANDOLO	Directrice de thèse
M. Thierry GIAMARCHI	Rapporteur
M. Rosario FAZIO	Rapporteur
M. Pierre LE DOUSSAL	Examineur
M. Pascal SIMON	Membre invité
M. Alberto ROSSO	Membre invité



à *Laetitia*



# Transitions de phase et diffusion dans des systèmes classiques et quantiques dissipatifs

## Résumé

Cette thèse est structurée autour de trois chapitres principaux. Dans le premier chapitre, je présente de nouveaux résultats obtenus pour la théorie  $\phi^4$  hors équilibre, dont la dynamique est décrite par une équation de Langevin en présence d'un bruit coloré. Les corrélations temporelles du bruit décroissent avec une loi de puissance déterminée par un certain exposant que j'appellerai  $\alpha$ . Il s'avère qu'il y a un  $\alpha_c$  de transition qui dépend de la dimension  $D$  du système et qui sépare le plan  $(\alpha, D)$  en une région où la couleur du bruit modifie le comportement critique et une autre où cette couleur est non pertinente. Je discute également le comportement d'échelle des fonctions de corrélation hors équilibre. Dans le deuxième chapitre de ma thèse j'introduis un formalisme d'intégrale de chemin pour décrire le mouvement Brownien hors équilibre. Je présente de nouveaux résultats qui ont été obtenus pendant mon doctorat sur les fonctions de corrélation hors équilibre après une trempe quantique. La troisième partie de ma thèse est consacrée à la diffusion d'impuretés dans des liquides quantiques en une dimension, communément appelés des liquides de Luttinger. Après une introduction aux problèmes divers liés à un tel système composé d'une impureté et d'un liquide de Luttinger, je présente une nouvelle description de la dynamique de l'impureté en présence d'un piège harmonique. La densité du liquide de Luttinger non-homogène influence fortement la dynamique de l'impureté et mène à des comportements inédits. De tels systèmes physiques sont actuellement étudiés dans des expériences d'atomes froids.

## Abstract

This thesis is structured around three main chapters. In the first chapter I present new results which have been obtained for the out-of-equilibrium critical  $\phi^4$ -theory. Its dynamics are described by a Langevin equation driven by a colored noise. The temporal correlation of this noise features a power-law decrease which is governed by a certain exponent  $\alpha$ . It turns out that there exists a crossover  $\alpha_c$  which depends on the dimension  $D$  of the system and separates the  $(\alpha, D)$ -plane into a region where the color of the noise alters the critical behaviour and a region where the color is non relevant. I also discuss the scaling behaviour of the non equilibrium correlation functions. In the second chapter I introduce a path integral formalism to describe non equilibrium quantum Brownian motion. I present the results which have been obtained during my PhD on the evolution of the non equilibrium correlation functions after a quantum quench. The third part of my thesis focuses on the impurity diffusion in one-dimensional quantum liquids which are commonly called Luttinger liquids. After an introductory part which covers the main issues related to such a system, I present a novel description of the impurity dynamics in the case where an external trapping potential is present. The non-homogeneous density profile of the Luttinger liquid then strongly influences on the impurity dynamics in a fascinating way. Such systems are currently being studied in cold atoms experiments.



## Remerciements

*Tout d'abord j'aimerais exprimer ma gratitude envers Leticia Cugliandolo qui a accepté d'être ma directrice de thèse il y a maintenant trois ans. Elle m'a fait profiter de son vaste savoir et de sa mémoire bibliographique. Pendant ces trois ans je suis devenu, du moins j'ose l'espérer, un jeune chercheur indépendant et rigoureux.*

*Ensuite, je remercie tous les membres du LPTHE de m'avoir accueilli et permis de m'épanouir ; je remercie également l'enseignement supérieur de France qui m'a instruit et soutenu.*

*Pendant les trois ans de ma thèse j'ai passé de très bons moments notamment grâce à Demian Levis et Adam Raçon, et plus généralement à tous les autres "jeunes" du LPTHE ainsi qu'à mes autres amis physiciens, en particulier Fred Jendrzejewski et Thomas Plisson.*

*Je tiens également à exprimer ma gratitude envers toute ma famille. Ich danke meinen Eltern und Großeltern, die sich stets bemüht haben mir die Welt zu erklären und mich des Weiteren immer dazu ermuntert haben selbst verstehen zu wollen. Ich danke ebenso meinen Brüdern für interessante und endlose Diskussionen.*

*Je ne peux conclure sans remercier Laetitia. Dir, meinem Stern, möchte ich diese Dissertation widmen.*



<b>1</b>	<b>Introduction</b>	<b>1</b>
<b>2</b>	<b>Classical phase transitions and colored noise</b>	<b>7</b>
2.1	Introduction and preliminary remarks . . . . .	7
2.1.1	Subcritical ordering dynamics . . . . .	8
2.1.2	Colored noise . . . . .	10
2.1.3	Fractional noises in nature . . . . .	12
2.2	Critical dynamics: Introduction . . . . .	14
2.2.1	Scaling . . . . .	18
2.2.2	Large- $N$ limit for Ohmic dissipation . . . . .	19
2.3	Critical dynamics and colored noise . . . . .	20
2.3.1	Equilibrium dynamics . . . . .	20
2.3.2	Gaussian theory . . . . .	21
2.3.3	The interaction part . . . . .	24
2.3.4	Perturbative expansion . . . . .	25
	Renormalization of the noise vertex. . . . .	26
	The Wilsonian renormalization scheme. . . . .	28
	The flow equation of $z$ and the crossover $\alpha_c$ . . . . .	28
	Renormalization of the self-energy and FDT. . . . .	31
	Renormalization of the self-energy: the anomalous exponent $\eta$ . . . . .	32
2.3.5	Non-equilibrium dynamics . . . . .	33
	Preliminary remarks . . . . .	33
	General non-equilibrium renormalization group analysis . . . . .	35
	The initial-slip exponent $\theta$ . . . . .	37
	Fluctuation-dissipation ratio and effective temperature. . . . .	40
2.4	Appendix A . . . . .	42
2.4.1	Fourier and Laplace conventions . . . . .	42
2.4.2	The equilibrium propagators . . . . .	43
	Scaling in real time . . . . .	43
	Generalized Mittag-Leffler functions . . . . .	44
2.4.3	Calculation of $\mathcal{E}_w^{0,2}$ and $\mathcal{E}^{1,1}$ . . . . .	45

2.4.4	Non-equilibrium propagators . . . . .	47
<b>3</b>	<b>Out of equilibrium quantum Brownian motion</b>	<b>49</b>
3.1	What is Quantum Brownian motion? . . . . .	50
3.1.1	Some equilibrium results for Ohmic dissipation . . . . .	55
3.1.2	Other important dissipative quantum systems . . . . .	57
3.2	The Hamiltonian of a quantum Brownian particle . . . . .	58
3.3	The non-equilibrium generating functional . . . . .	60
3.3.1	The density matrix . . . . .	62
3.3.2	Reduced density matrix for a system initially coupled to an equilibrium bath . . . . .	63
3.3.3	Generic Gaussian initial conditions . . . . .	64
3.3.4	The sources . . . . .	65
3.3.5	The harmonic case . . . . .	66
3.3.6	Integration over the initial condition . . . . .	66
3.3.7	Real time minimal action paths with external sources . . . . .	67
3.3.8	Integration over the end-points . . . . .	69
3.3.9	The correlation function . . . . .	70
3.4	Non equilibrium dynamics after quantum quenches. . . . .	71
3.4.1	A particle in a harmonic potential with an initial position measurement . . . . .	71
3.4.2	Quantum quench in the confining potential. . . . .	73
3.5	Appendix B . . . . .	74
3.5.1	Coherent state path integral formulation . . . . .	74
	Integration over the bath variables . . . . .	77
3.5.2	Classical Brownian particle in a harmonic potential: Initial position measurement and quenches in the trapping potential . . . . .	81
3.5.3	The equilibrium initial condition . . . . .	82
	The fluctuation-dissipation theorem . . . . .	82
3.5.4	Asymptotic behavior of $\mathcal{G}_+(t)$ and $\mathcal{C}^{1eq}(t)$ for Ohmic dissipation . . . . .	84
<b>4</b>	<b>Dissipative impurity dynamics in a 1D quantum liquid</b>	<b>87</b>
4.1	Introduction to Luttinger liquid theory . . . . .	87
4.1.1	Phenomenological bosonization . . . . .	89
4.1.2	The Tomonaga-Luttinger Hamiltonian . . . . .	92
4.1.3	The interaction between an impurity and a Luttinger liquid . . . . .	94
4.1.4	The Lieb-Liniger gas as a Luttinger liquid . . . . .	94
4.2	Drag force and critical velocities in a 1D quantum liquid . . . . .	96
4.2.1	First order dissipation rate: Fermi's golden rule approach . . . . .	96
4.2.2	Forward scattering Bremsstrahlung of accelerated impurities . . . . .	98
4.2.3	Backscattering: Renormalization group approach . . . . .	100
4.2.4	Drag force and quantum stirring in a Luttinger liquid . . . . .	102
4.3	Trapped Luttinger liquids . . . . .	103
4.3.1	Ground state of a trapped Lieb-Liniger gas: Thomas-Fermi approximation and Tonks-Girardeau regime . . . . .	104
4.3.2	Hydrodynamic excitations in a trapped Luttinger liquid . . . . .	106
4.4	A Luttinger liquid as a quantum bath . . . . .	110
4.4.1	The impurity model . . . . .	110

4.4.2	Steep potential: The Luttinger bath and the initial condition . . . . .	113
4.4.3	Signature of a Luttinger liquid bath . . . . .	114
4.5	Some notions about polaron theory . . . . .	118
4.6	An impurity in a trapped 1D gas: Dynamical linear response theory . . . . .	121
4.6.1	The experimental evidence . . . . .	123
4.6.2	The dynamical mass shift . . . . .	123
4.6.3	The potential renormalization . . . . .	125
4.6.4	Long time dynamics . . . . .	127
4.6.5	The impurity influence functional . . . . .	127
4.6.6	Discussion of the results . . . . .	128
<b>5</b>	<b>Conclusion and Outlook</b>	<b>131</b>
5.1	Critical dynamics driven by colored noise . . . . .	131
5.2	Out-of-equilibrium quantum Brownian motion . . . . .	133
5.3	Impurity dynamics in 1D Bose liquids . . . . .	134
5.4	Outlook . . . . .	138
<b>6</b>	<b>Bibliography and index of most important symbols</b>	<b>141</b>



# CHAPTER 1

---

## Introduction

---

*“Dieu n’avait fait que l’eau, l’homme a fait le vin!”*  
Victor Hugo

In Mai 1905 Albert Einstein challenged in the last paragraph<sup>1</sup> of his celebrated article [1] experimental physicists all over the world: With a simple microscope – he stated – could one observe the stochastic motion of (dust) particles suspended in a liquid such as simple water. This appeal triggered widespread interest in his work; moreover, Robert Brown had already observed this phenomenon as early as in 1827, but in this ancient world the details of his discovery had attained Einstein 70 years later in such a fragmented form that he was not able to decide whether his theory actually explained or rather predicted something. Einstein’s theory, based on an analysis of the osmotic forces induced by the stochastic motion of the water molecules, was indeed confirmed only three years later by J. Perrin. This discovery led immediately to the final victory of Dalton’s atomistic hypothesis<sup>2</sup>.

Today, we mostly remember his famous formula (the Stokes-Einstein equation) which established that the diffusion coefficient  $D$  is proportional to the temperature<sup>3</sup>  $\beta^{-1}$ : a sphere with a radius  $r$  suspended in a liquid with friction coefficient  $\gamma$  undergoes stochastic motion with  $D = \beta^{-1}/(6\pi\gamma r)$ . The underlying assumption is that classical statistical physics holds. The number of degrees of freedom of the dust particle-liquid system is enormous such that every approach based on the calculation of the trajectory of each liquid molecule has to inevitably fail<sup>4</sup>. Statistical physics reduces the complexity of the problem by introducing several average quantities, such as temperature, pressure or volume, which can then be used to characterize the system. The price to pay is the loss of knowledge of the dynamics of each degree of freedom.

---

<sup>1</sup>Möge es bald einem Forscher gelingen, die hier aufgeworfene, für die Theorie der Wärme wichtige Frage zu entscheiden! – I hope that a scientist will soon be able to answer the question I have raised in this work and which is important for the theory of heat!

<sup>2</sup>For the sake of a fluid presentation of the historical context I did not mention the contributions of M. Smoluchowski and L. Bachelier to the theory of Brownian motion, contributions which are likely as important as Einstein’s.

<sup>3</sup>Throughout this manuscript I avoid the notation  $T$  for the temperature and I rather work with  $\beta = 1/k_B T$ .

<sup>4</sup>Note that L. Boltzmann always believed in atoms and molecules.

Hence, equilibrium thermodynamics (rather thermostatics) is based on the theory of thermodynamic potentials such as the internal energy and the entropy which are linked with the mean quantities such as temperature by static equations of state. While its success is undeniable it cannot be generalized to dynamical out-of-equilibrium phenomena.

Diffusion is a genuine non-equilibrium phenomenon. If we follow the same line of arguments which lead to classical statistical physics we can argue that the impact of each degree of freedom of the environment on the main particle is so small and the subsequent impacts so frequent, that the main particle only feels some *stochastic noise* with some well-defined properties. In conjunction with the central limit theorem one is then guided towards Gaussian noise. This Gaussian noise exerts a random force on the particle. From now on, two different descriptions of the particle dynamics are possible. Either one directly writes a Newtonian equation of motion where the noise plays the role of the force and one tries to solve this so called *Langevin equation* [2, 3]. In this case the resulting particle trajectory depends in general on the noise history. By averaging over the possible noise configurations one then arrives at mean values which sufficiently describe the particle dynamics. However, one has also the choice to do the opposite as long as the noise is uncorrelated in time: One writes down first a *Fokker-Planck equation* [2, 3] of the probability density for the particle position and searches for a solution of this generalized diffusion equation. Since all higher-order cumulants are identically zero for a Gaussian noise, one can easily convert a Langevin equation into a Fokker-Planck equation and vice-versa.

The Langevin equation contains only useful information if the noise can be specified. There are however many cases where no such noise exists. One often encounters situations where a system changes stochastically its state with some known transition rates. Imagine for example a particle on a one-dimensional lattice which jumps one step with some probability  $p$  to the left or to the right. Such a process can be conveniently described with a *master equation* [2, 3, 4]. Fortunately, in many cases this master equation can again be mapped to a Fokker-Planck equation *via* the *Kramers-Moyal expansion* [2]. For instance, in the hopping example cited above the result is a simple Brownian diffusion equation.

Soon after the discovery of diffusion driven by stochastic forces and conveniently described by *classical* Langevin or Fokker-Planck equations, quantum mechanics paced its path through physics. The very first work which pointed towards quantum mechanics was Max Planck's analysis of the black body radiation. He showed that a simple trick could cure all undesired divergences in the formula for the black body radiation density of states which resulted from the classical statistical analysis of a photon gas. By assuming discrete energy values (in contrast to a continuous energy spectrum) for the quantum harmonic oscillator he derived the correct black body radiation formula. This raises the important question of the validity of Einstein's result at low temperatures, i.e. in the quantum regime. Quantum baths differ greatly from classical baths. Due to Heisenberg's uncertainty relation a quantum bath can exchange energy even at absolute zero. If we forget about any quantum effects for the particle, i.e. if we only measure its mean displacement  $Q(t)$ , where  $t$  is the time lag, one can ask whether quantum mechanics modifies the classical diffusion law. The answer is yes. Einstein's relation  $Q(t) \sim Dt$  has to be replaced by  $Q(t) \sim \log(\gamma t)$ <sup>5</sup>. Such *quantum Brownian motion* can be conveniently dealt with by using a path integral approach. Grabert et al. [5, 6, 7, 8] were the first to find the stationary

---

<sup>5</sup>These two relations hold for a so-called *Ohmic* bath. In classical physics such an Ohmic bath leads to uncorrelated noise which drives the stochastic process called "Brownian motion". Quantum stochastic processes driven by a non-Ohmic environment are, however, also called "quantum Brownian motion" in contrast to their classical equivalents where the term "fractional Brownian motion" or "generalized Brownian motion" is preferred.

quantum Brownian motion correlation functions within such a path integral formalism, without relying on simplifying assumptions such as an initial decoupling between the particle and the environment [9]. The second chapter of my thesis will be dedicated to a generalization of their formalism which works also for non-stationary cases.

One can easily imagine more complicated quantum environments for which the term “bath” may even seem inappropriate; however I will use it also for the “exotic” quantum baths I shall describe in what follows. One of the main features of a quantum harmonic oscillator bath is that it is not entangled on its own: Only the coupling to the particle leads to quantum entanglement of different oscillators, which are independent from each other without the central coupling to a particle. A highly entangled bath, on the other hand, is formed by a one-dimensional liquid of interacting bosons or fermions which, as is well established, forms a so-called Luttinger liquid [10] which features non Fermi-liquid [11] behaviour, such as collective excitation and a power-law decrease of correlation functions. In particular, the Landau quasiparticles [12, 11] do not exist anymore and the physics has to be described in terms of density and charge fluctuations [10]. Moreover, such one-dimensional systems can be realized nowadays with cold-atom techniques. An impurity immersed in this *Luttinger liquid* can then be considered as a particle coupled to an exotic quantum bath under certain circumstances, i.e. rather weak intra-quantum liquid interactions (see the discussion in chapter 5 for more details on this delicate issue). The non equilibrium dynamics of these impurities is extremely complex. In the third chapter I will focus on a small aspect of these very rich physics and I will present results on the impurity diffusion in ultracold Bose liquids, which can be obtained without making use of heavy methods such as Bethe ansatz techniques and sophisticated numerical simulations. The point of view I will adopt there will place the impurity in the center of our attention. I will not too much care about its effects on the Luttinger liquid, as I will be mostly interested in the impurity dynamics.

It is as interesting to adopt the opposite point of view and to ask about the effects the impurity has on the Luttinger liquid. If the impurity is not mobile, i.e. if it represents a fixed obstacle, quantum tunneling still allows in principle the Luttinger liquid to cross the barrier. One is immediately guided towards the question: Is this always the case? The answer is negative and it depends on the physical properties of the underlying Luttinger liquid. The analysis of this problem has been performed by, e.g., Kane and Fisher [13] for an isolated impurity and by Giamarchi and Schulz [14] for an infinite number of impurities, i.e. for disorder, by using a *renormalization group approach*. This key word now leads us to another important topic which will be relevant for the first part of my thesis.

Collective phenomena have always fascinated physicists. A system of many molecules, electrons, photons or, why not, pedestrians, shows often an intriguing behaviour although the underlying physical laws which govern the dynamics of each “unit” are very often very simple (This may be subject to debate for the pedestrians in the – say – subway stations). However, the fact that many of these units interact with each other renders the physics of the whole system very complex. When an external parameter is varied one often observes a *phase transition* where the system abruptly changes its state (for the pedestrians this parameter may be the density and the phase transition may be the onset of a collective panic or a jam). At the *critical point* the system becomes scale-free; the typical correlation length dominates all the other microscopic length scales of the system and even diverges at criticality. The system becomes self-similar and it is thus often possible to integrate over fast fluctuations to recover an effective description of the system at large spatial or temporal scales. This is the heart of the renormalization group approach. It implies in particular that many properties of the critical or

near-critical system are *universal* in the sense that they only depend on macroscopic quantities such as dimensionality, topological constraints and the internal symmetries of the system. By using such techniques the authors cited above showed that the impurity is a relevant barrier for the Luttinger liquid if  $K < 1$  where  $K$  [13] is one of the two parameters which fully characterize such a Luttinger liquid. In the case of a Gaussian disorder the critical value is  $K = 3/2$  [14].

We now come back to the starting point of this introduction. In general, the critical point always separates two equilibrium phases. However, if the system is quenched (e.g. the system is cooled down from some high temperature to the critical one) it needs time to equilibrate. During this equilibration time both phases are present and, if the system is infinite and in the case of a critical quench, neither of them disappears: In this case the equilibration time is infinite and the system shows *critical slow dynamics* [15, 16] during which the equilibration dynamics has universal properties. In order to model such critical dynamics a force is needed, which drives the phase transition. For *subcritical dynamics* (i.e. a quench below the critical temperature) the dynamics are often governed by internal a-thermal forces such as the surface tension between regions of different low-temperature phases (here I mean the two low-temperature phases which are two distinct realization, related by a symmetry, of the low-temperature equilibrium phase). Usually, the two different phases are clearly separated: in, for instance, boiling water moving vapour bubbles can be distinguished from the surrounding liquid water or in binary alloys the regions consisting of the substance  $A$  are separated from the regions consisting of  $B$  during the demixing process through a clear boundary. This phase boundary minimizes its surface tension and therefore drives the phase transition [17].

At criticality the picture is different. The boundary now has a fractal structure and even infinitesimal fluctuations in the medium heavily influence on its shape [18, 19, 20]. These fluctuations can have a thermal or quantum origin and they can enhance or slow down the critical ordering process. Hence, due to the fractal nature of the boundaries the kinetic arguments used for subcritical ordering dynamics are flawed and a renormalization group approach is needed. Since the precise nature of the thermal (quantum) fluctuations is now important for the ordering dynamics, one needs to specify its statistical properties to be able to fully describe the system. From the central limit theorem we expect that the noise is Gaussian. But its internal spatial and temporal correlations can be very important. Do such internal correlations, in particular if they are long-range, influence on the critical properties of the system? It may come as a surprise that this problem has not been intensely studied in the literature. Thus, in the first part of my thesis I will show that strongly temporally correlated noises change the critical exponents of the phase transition of ferromagnetic systems, which are conveniently described by the  $\phi^4$ -theory. The critical dynamics of this  $\phi^4$  phase transition are then driven by the internal potential and by the stochastic noise.

Let me close this introductory chapter by presenting the structure of my thesis in more details. The first part of my thesis is devoted – as already pointed out above – to the study of the dynamics of the critical  $\phi^4$ -theory in presence of heavily temporally correlated thermal noise. This analysis will go beyond the standard Ornstein-Uhlenbeck case of exponentially correlated noise by focusing on power-law correlated noise which is extensively studied in the field of fractional Brownian motion, but which has to date not been applied to the critical  $\phi^4$ -theory. I will present a renormalization group analysis up to second order in the coupling constants which yields a quite complete picture of the equilibrium and non-equilibrium dynamics of the system.

The second part of this work focuses on quantum Brownian motion. After an introductory

chapter I will present new results on out-of-equilibrium quantum Brownian motion. The analysis involves path integral techniques previously used in [8] in this context. In contrast to previous studies I will not rely on a density matrix formalism, which only yields one-time quantities, but rather on an approach based on a generating functional from which all non-equilibrium correlation functions can be obtained.

The third part is about impurity dynamics in ultracold quantum liquids. Quantum Brownian motion can be directly applied to this problem if one assumes that Luttinger theory is valid in the parameter regime in question; however, the outcome is only partially satisfactory. Note that the Luttinger liquid behaves essentially as a bath of harmonic oscillators since it is a Gaussian theory and every momentum mode can be identified with one oscillator. However, the coupling between the Luttinger liquid and the impurity conserves the total momentum. In this case the coupling is non-linear in the impurity position in strong contrast to standard quantum Brownian motion. The density-density coupling of the impurity-quantum liquid system leads to novel effects, such as an effective mass of the impurity and an enhancement of the external potential. These phenomena have been recently observed in cold-atom experiments and they can be explained within an approach based on the equations of motion of the system.

Finally, the last part of my thesis concludes the work presented here and compares the results to very recent studies.

## How to read this thesis

The present thesis has three main research parts (chapters 2 to 4 of this manuscript). Chapter 2 is completely independent from chapters 3 and 4. Thus, a reader only interested in quantum Brownian motion or in impurity dynamics in Luttinger liquids can directly go to chapter 3 and 4, respectively. Each part is meant to be self-consistent. Note however, that chapter 4 makes use of results and methods presented in chapter 3, in particular concerning the influence functional of quantum Brownian motion which is subsequently used as a starting point for the description of impurity dynamics. The Sec. 3.3 can be considered as a junction between chapters 3 and 4.

The introductory parts of each chapter are supposed to provide the reader with the necessary background information in order to be able to understand the following parts where I present new results and to be able to put these new results in their respective context. It is however impossible for these background information to be exhaustive within the scope of the present thesis. Some techniques such as path integral methods and the renormalization group are not explained in this thesis.

Note that the results presented in the main body of the thesis (ch. 2 to ch. 4) are almost never directly followed by a conclusion or any general comments. It is in chapter 5 that I have decided to comment on the results presented in this thesis. This is also where I compare the results to slightly different but related approaches in the existing literature.

## Published articles

The present thesis is based on three articles which I wrote in collaboration with L. F. Cugliandolo and A. Gambassi [21, 22, 23]. During my writing of the present manuscript I worked on yet another project on the dissipative phase transition of the spin-boson model. This work is not included in the present text but can be found in its published form in [24]. An article which I wrote in collaboration with A. Rançon can be found in [25].



---

## Classical phase transitions and colored noise

---

*“Le hasard est le pseudonyme de Dieu lorsqu’il ne voulait pas signer.”*  
Anatole France

### 2.1 Introduction and preliminary remarks

In the first part of the present thesis I focus on the dynamical aspects of classical uniaxial ferromagnetic systems close to the Curie point. In this case thermal fluctuations are responsible for the critical ordering dynamics and I will neglect all quantal effects in this chapter. While classical problems are usually easier to solve than their quantum counterparts, classical statistical mechanics does not provide us with a natural dynamics in contrast to quantum mechanics which determines the fluctuations of the time-dependent order parameter. One way to solve the problem posed by the absence of a natural dynamics in the classical case is to impose some suitably chosen dynamics to the system by hand. For instance, in the classical Ising model the only dynamic event is a “spin flip” and every dynamic theory is solely governed by its spin flip probability. Thus, “Glauber dynamics” [26] amounts to setting the spin flip rate of the  $j$ -th spin equal to  $w_{s_j} = 1/2 - \tanh(2\beta J)s_j[s_{j-1} + s_{j+1}]/4$  with  $J$  the ferromagnetic coupling strength and  $\beta$  the inverse temperature. These dynamics satisfy detailed balance such that the system remains in equilibrium once it has reached it. One way of testing if a system is in equilibrium is to compare the time derivative of its correlation function  $\partial_s C(t, s)$  to its linear response (to an infinitesimal external field)  $R(t, s)$ . If

$$R(t, s) = \beta \partial_s C(t, s) \tag{2.1}$$

the system satisfies the fluctuation-dissipation theorem which is a necessary condition for equilibrium. However, an infinite system which is at initial time in a generic (non equilibrium) spin configuration does not necessarily reach equilibrium within a finite time interval. During the spin ordering process these *ordering dynamics* show universal features which are in general

different from the equilibrium dynamics. If the system is critical, these ordering dynamics are commonly called *critical dynamics*.

Before concentrating on critical systems, the reader might appreciate to obtain an overview of what is known of general ordering dynamics. Dynamical ferromagnetic systems are conveniently described in terms of a coarse-grained order parameter field  $\vec{\phi}(\vec{x}, t)$  by using the fact that the correlation length is much larger than the lattice constant of the original spin system. We use the short-hand notation  $\vec{\phi}$  for the ensemble of  $N$  fields  $\phi_j$  which depend on time and  $D$ -dimensional space. The static behaviour of the system is then controlled by a Hamiltonian of the Ginzburg-Landau type

$$\mathcal{H}[\vec{\phi}] = \int d^D x \left[ \frac{1}{2} (\vec{\nabla} \vec{\phi})^2 + \frac{1}{2} r \vec{\phi}^2 + \frac{g}{4!} \vec{\phi}^4 \right]. \quad (2.2)$$

$g$  is the strength of the non-linearity that drives the phase transition,  $r$  is the control parameter for it, and the coefficient in front of the elastic term  $\propto (\vec{\nabla} \vec{\phi})^2$  has been absorbed in the definition of the field.

Dynamics are now incorporated in a twofold way. First, we expect that (unless one considers very short times) the friction force  $\gamma \partial_t \vec{\phi}$  exactly balances the potential force  $\vec{F}[\mathcal{H}]$  which is some functional of the energy  $\mathcal{H}$ . The diffusive dynamics are thus governed by an equation of the form

$$\gamma \frac{\partial}{\partial t} \vec{\phi}(\vec{x}, t) = \vec{F}[\mathcal{H}] \quad (2.3)$$

as long as thermal fluctuations are absent. However, if the effect of thermal fluctuations is important Eq. (2.3), has to be complemented by an additional stochastic force term  $\vec{\zeta}(\vec{x}, t)$  so that

$$\gamma \frac{\partial}{\partial t} \vec{\phi}(\vec{x}, t) = \vec{F}[\mathcal{H}] + \vec{\zeta}(\vec{x}, t). \quad (2.4)$$

When do we have to take explicitly into account the stochastic fluctuations, i.e. when is Eq. (2.3) sufficient to correctly describe the ordering dynamics? Taking into account the thermal noise is crucial in the case of critical ordering dynamics where the fractal structure of the phase boundaries is unstable against the weakest fluctuations in the medium. Hence, it turns out that the noise statistics are irrelevant for most off-critical systems but crucial for critical dynamics. Let me first briefly discuss off-critical dynamics (or sub-critical coarsening) from a simple kinetic point of view where the phase transition is essentially driven by the surface tension of the phase boundary.

### 2.1.1 Subcritical ordering dynamics

If the order parameter field  $\vec{\phi}$  is not conserved the potential force is simply given by

$$\vec{F}(\vec{x}, t) = - \frac{\delta \mathcal{H}}{\delta \vec{\phi}(\vec{x}, t)}. \quad (2.5)$$

According to the widely used classification of Halperin [27, 28] dynamics based on Eq. (2.5) are known as “model A” dynamics and one can show that they generalize the Glauber dynamics valid for lattice spin systems to the continuum case.

In conjunction with Eq. (2.3) one can then show [17] that the driving force for the domain growth during the ordering dynamics is the wall curvature. It then follows that the typical domain has the shape of a circle in  $D = 2$  dimensions and the form of a hyper-sphere in general

$D$  dimensions. It is instructive to seek for a spherical solution to Eq. (2.3) for a 1-component non conserved spherically symmetric field  $\phi(r, t)$  with  $r = |\vec{x}|$ . By using Eq. (2.5) one immediately obtains

$$\gamma \frac{\partial \phi}{\partial t} = \frac{\partial^2 \phi}{\partial r^2} + \frac{d-1}{r} \frac{\partial \phi}{\partial r} - \frac{1}{3!} \phi^3. \quad (2.6)$$

By assuming that the typical droplet radius  $\rho$  is much larger than the interface width one can make the *ansatz*  $\phi(r, t) = f(r - \gamma^{-1} \rho(t))$ .  $f'$  is assumed to be sharply peaked around  $r = \rho$  and to vanish for  $r \rightarrow \pm\infty$ . Inserting this *ansatz* into Eq. (2.6) yields

$$f'' + \left[ \frac{d-1}{r} + \dot{\rho} \right] f' - \frac{1}{3!} f^3 = 0. \quad (2.7)$$

Multiply Eq. (2.7) by  $f'$  and integrate  $r$  from  $\rho - \delta$  to  $\rho + \delta$  where  $\delta$  is chosen small but large enough such that  $f'(\pm\delta) \rightarrow 0$ . By using the continuity of the function  $f$  the final results reads  $\dot{\rho}(t) = (d-1)/\rho(t)$  and it can be recast in the form

$$\rho^2(t) = \rho^2(0) - 2(d-1)t. \quad (2.8)$$

Hence, the isolated bubble vanishes during the ordering dynamics with a collapse time which scales as  $t \sim \rho^2(0)$ . This holds true for general curved regions as well [29] which shows that time and space scale according to

$$t \sim x^z \quad (2.9)$$

with the *dynamic exponent*  $z = 2$ .

In many cases external constraints impose a different growth mechanism than model A. The Halperin classification ranges from model A to model E but I will only briefly discuss the so-called model B dynamics which describes a general demixing process of binary alloys or below the liquid-gas critical point (where the quantity of liquid is approximately conserved). In all cases one expects the continuity equation has to be satisfied so that the order parameter is subject to the constraint

$$\frac{\partial \phi}{\partial t} + \nabla \cdot \vec{J}[\mathcal{H}] = 0, \quad (2.10)$$

where I focus on the single order parameter case ( $N = 1$ ) and where  $\vec{J}$  is some  $D$ -dimensional vector functional of  $\mathcal{H}$ . The simplest equation one can write is

$$\vec{J}(\vec{x}, t) = -\sigma \nabla \left[ \frac{\delta \mathcal{H}}{\delta \phi(\vec{x}, t)} \right], \quad (2.11)$$

with  $\sigma$  a kinetic coefficient related to the mobility. In  $D = 3$  dimensions it can be shown with similar methods (albeit the analysis is technically more demanding for a conserved order parameter and after a long controversy the issue had only been settled by D. A. Huse in 1986 [30]) as in the previous section that

$$\rho^3(t) = \rho^3(0) - \frac{3\sigma t}{2}. \quad (2.12)$$

The collapse time for the model B dynamics hence scales according to  $t \sim \rho(0)^3$  in contrast to the result for a non-conserved order parameter Eq. (2.8) for which  $z = 2$ . Accordingly, the dynamic exponent for a conserved order parameter is  $z = 3$ .

After these two warm-up sections I now turn to critical dynamics for which the thermal noise statistics cannot be neglected anymore. I will first discuss uncorrelated noise and then ultimately present the new results which were found during my PhD on correlated noise.

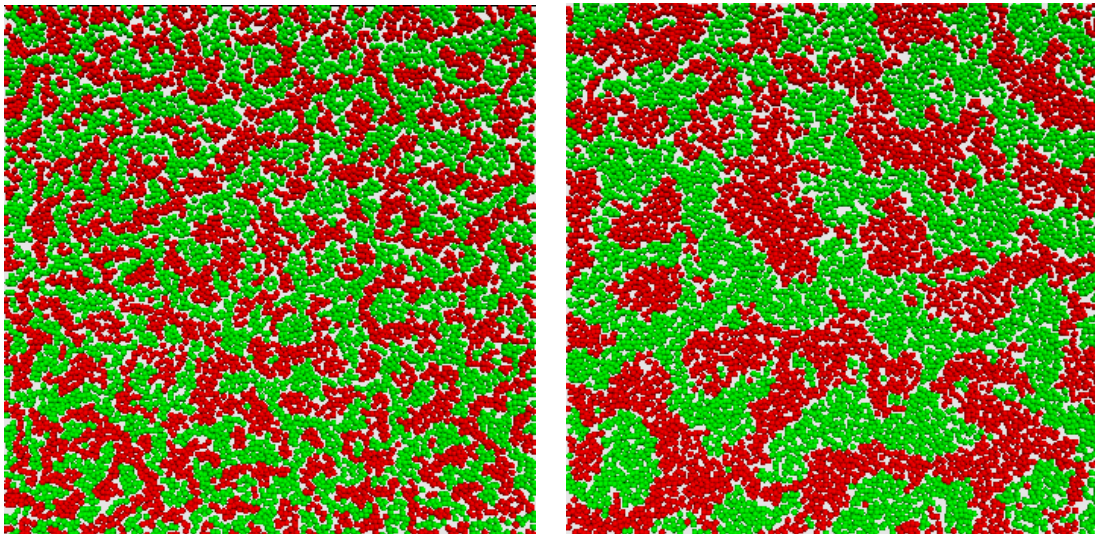


Figure 2.1: Simulation of a two-dimensional gas of a binary mixture of  $2 \times 5000$  hard spheres with a non-additive radius ( $r_{12} = 1.5r_{11} = 1.5r_{22}$ ): Intra-species scattering events are simulated by the hard-sphere constraint with  $r_{11}$  (or  $r_{22}$ , respectively), whereas inter-species collisions are simulated by the hard-sphere constraint with  $r_{12}$ . Left image: Snapshot after a short relaxation time. Right picture: Snapshot after a large relaxation time. The simulation corresponds to subcritical ordering dynamics with a conserved order parameter (here the number of spheres of each species).

### 2.1.2 Colored noise

In the last I have presented an analysis of subcritical dynamics. Since the main subject of the present chapter are critical dynamics driven by colored noise let me introduce colored, i.e. time-correlated, noise in this subsection.

By definition, white noise processes have a vanishing correlation time, which can be directly seen from the correlation function (I do not consider here a spatial dependence to simplify the presentation)

$$\langle \xi(t)\xi(t') \rangle = 2\beta^{-1}\gamma_w\delta(t-t') = D\delta(t-t') . \quad (2.13)$$

Since the correlator only depends on the time difference  $t-t'$  such a process is stationary. The constant  $\gamma_w$  measures the amplitude of the noise and it is related to the noise strength coefficient  $\gamma_w$  of the previous section by  $D = 2\beta^{-1}\gamma_w$  with  $\beta$  the (inverse) temperature of the noise<sup>1</sup>. Let this white noise drive a particle *via* the Langevin equation

$$\dot{x}(t) = \xi(t) , \quad (2.14)$$

then  $\langle x(t)x(t') \rangle = x(0)^2 + D \min(t, t')$  thus leading to

$$\langle (x(t) - x(t')) \rangle = D|t - t'| , \quad (2.15)$$

which is independent of the initial condition  $x(0)$ . Our particle hence undergoes *Browian motion* with the diffusion coefficient  $D$ . At this point it becomes important to distinguish two kinds

<sup>1</sup>I will use the convention  $\int_0^t ds \delta(t-s)f(s) = f(t)/2$  in the following, hence the factor 2 in the definition of  $D$ .

of noises, stationary and non-stationary ones. Obviously, the white noise is stationary while the Brownian motion is *not*; indeed, the mean displacement function of the Brownian motion rather than its correlation function is stationary. The term *colored noise* refers throughout the whole manuscript exclusively to *stationary* colored noise  $\zeta(t)$  with a correlation function

$$\langle \zeta(t)\zeta(t') \rangle = \beta^{-1}\Gamma(t-t'), \quad (2.16)$$

with  $\Gamma(t-t')$  some function other than the Dirac  $\delta$ -function. We denote the Euler  $\Gamma$ -function by  $\Gamma_E$  in the following to avoid confusion with the noise kernel. Such a noise will be considered in Secs. 2.2 and 2.3 where I will focus on *power-law* correlated noise with

$$\Gamma(t) \sim t^{-\alpha} \quad (2.17)$$

for large  $t$ . Examples of such noises occurring in nature will be listed in Sec. 2.1.3.

Let us relate the white noise  $\xi$  to the colored noise  $\zeta$  with a power-law correlator (2.16). If  $\alpha > 1$  the noise kernel is not integrable and a small-time cutoff  $t_0$  has to be introduced. By defining the kernel  $A(t) = 1/(t_0 + |t|)^\gamma$ , with  $\gamma > 1/2$ , we have

$$\zeta(t) \propto \int_{-\infty}^t dt' A(t-t')\xi(t'). \quad (2.18)$$

Indeed, if we define  $\zeta$  in this way we find the correlation

$$\langle \zeta(t)\zeta(t') \rangle = \int_0^{\min(t,s)} ds A(t-s)A(t'-s) \propto (t_0 + |t-t'|)^{1-2\gamma}. \quad (2.19)$$

Accordingly, after the identification  $\gamma = 1/2 + \alpha/2$  one recovers the form (2.16). This colored noise can now be used to model a driven stochastic system whose relevant Langevin equation reads [16, 21] in equilibrium

$$\int_{-\infty}^t ds \Gamma(t-s)\dot{x}(s) = \zeta(t). \quad (2.20)$$

Let me introduce the formal inverse function  $\Gamma^{-1}$  of  $\Gamma$ , then obviously  $\Gamma^{-1}(t) \sim t^{\alpha-2}$  for large times. We thus find formally by standard power counting

$$x(t) \sim \int_{-\infty}^t ds (t-s)^{H-1/2}\xi(s), \quad (2.21)$$

where I introduced the so-called *Hurst exponent* [31, 32]

$$H = \frac{\alpha}{2}. \quad (2.22)$$

The relation (2.21), although in this manuscript established on a somewhat shallow arguments, can be put on firmer grounds and it is essentially correct and it leads to the time power counting which establishes Eq. (2.22). The physical meaningful analogue of Eq. (2.21) has been extensively studied since the 1950s [31, 32, 33, 34] and is called *fractional Brownian motion*. It is a generalization of the standard Wiener process  $x(t) = \int_{-\infty}^t ds \xi(s)$  (i.e. the standard Brownian motion) and B. B. Mandelbrot defines it as [33]

$$b(t) = b_0 + \frac{1}{\Gamma_E(H+1/2)} \left\{ \int_{-\infty}^0 ds \xi(s) \left[ (t-s)^{H-1/2} - (-s)^{H-1/2} \right] + \int_0^t ds \xi(s)(t-s)^{H-1/2} \right\}. \quad (2.23)$$

The introduction of  $\Gamma_E(H + 1/2)$  in the denominator has the following motivation: it ensures that, when  $H - 1/2$  is an integer, a fractional integral becomes an ordinary integral. Also, the definition of the fractional Brownian motion  $x(t)$  can be made more symmetric by writing it as the following convergent difference of divergent integrals:

$$b(t) - b(t') = \frac{1}{\Gamma_E(H + 1/2)} \left\{ \int_{-\infty}^t ds \xi(s)(t - s)^{H-1/2} - \int_{-\infty}^{t'} ds \xi(s)(t' - s)^{H-1/2} \right\}. \quad (2.24)$$

Very similar to standard Brownian motion, which corresponds to  $H = 1/2$  or  $\alpha = 1$ , fractional Brownian motion is, strictly speaking, not a stationary process while, however, the displacement  $x(t) - x(t')$  is. From Eq. (2.24) we directly find that fractional Brownian motion has the correlation function

$$\langle b(t)b(t') \rangle = \frac{1}{2} [ |t|^{2H} + |s|^{2H} - |t - s|^{2H} ]. \quad (2.25)$$

Again, we see that for  $H = 1/2$  the process is diffusion-like. In this case the process is *Markovian* such that the probability distribution of the actual increment does not depend on any past information. However, for  $H > 1/2$  the process is positively correlated and hence super-diffusive with a variance that grows stronger than linearly in time,

$$\langle b(t)^2 \rangle \sim t^{2H}, \quad (2.26)$$

while for  $H < 1/2$  the process is negatively correlated which leads to subdiffusion.

It is well known that Brownian motion has a fractal nature in the sense that it is self-affine [34]. Its generalization, the fractional Brownian motion, satisfies also self-affinity relations as can be readily seen from Eq. (2.24). Indeed, we have

$$b(at) \sim |a|^H b(t), \quad (2.27)$$

where the equivalence relation  $\sim$  is established with respect to the equivalence of the respective probability distributions. Since  $b(t)$  is a Gaussian process this can be proven by the two relations

$$\langle b(at) - b(at') \rangle = 0 = \langle b(t) - b(t') \rangle, \quad (2.28)$$

$$\langle (b(at) - b(at'))^2 \rangle \sim |a|^{2H} |t - t'|^{2H} \sim |a|^{2H} \langle (b(t) - b(t'))^2 \rangle. \quad (2.29)$$

I remind the reader again of the fact that fractional Brownian motion is only a Markov process<sup>2</sup> if  $H = 1/2$ .

### 2.1.3 Fractional noises in nature

Fractional Brownian motion is closely related to stochastic processes in biology [35] and physics [4] where it can be used to model anomalous diffusion. These findings complement the original discovery by Hurst on long-range correlations of river flood records [31]. In the interdisciplinary overlap between physics, chemistry and biology fractional Brownian motion occurs on numerous occasions. The following list will not be – in any case – exhaustive; it is rather meant

<sup>2</sup>A stochastic process  $b_i$  defined on a discrete time  $t_i = i\Delta t$  is called Markovian, if the conditional probability distribution of future states of  $b$  depends only upon the present state, i.e. if for  $j' < j < i$  arbitrary,  $\mathcal{P}(b_i = B_i | b_j = B_j, \{b_{j'} = B_{j'}\}) = \mathcal{P}(b_i = B_i | b_j = B_j)$ , where  $\mathcal{P}(\cdot)$  is the conditional probability of  $b$ . In the limit  $\Delta t \rightarrow 0$  one thus defines a Markov process on the continuum.

as a teaser to arouse some interest in this multidisciplinary research field. I will also cite examples where fractional Brownian motion can be useful in combination with field theoretical approaches; this will build a bridge to the forthcoming sections which will deal with critical dynamics driven by such colored noise.

To begin with rather remote fields of research, fractional Brownian motion has been used to determine statistical properties of interstellar gas [36], to describe certain arbitrage opportunities in finance [37] and to improve image processing [38]. In solid state physics fractional Gaussian processes occur for instance when dealing with director fluctuations of nematic ordering [39] and when considering structural and flow properties of binary media generated by fractional Brownian motion models [40]. The authors of [41] have recently studied a fractional Brownian motion approach to polymer translocation and in [42] elastic membranes and polymers were considered whose stochastic motion yields fractional Brownian noise. Moreover, in [43] it has been shown that the membrane potential fluctuations of some type of cells have fractal properties that can be modeled by using fractional Brownian motion and the authors of [44] have introduced a new approach to cell mechanisms concerning DNA sequences based also on fractional Brownian motion. More generally, colored noise occurs in many aspects of biophysics such as cell membrane fluctuations [45] and DNA dynamics [46] already mentioned above.

The physical circumstances in which generally temporally correlated noise arises are also manifold including polymer translocation through a nanopore [47] or the effective description of a tracer in a glassy medium [48]. A review of the effects of colored noise in dynamical systems is given in [49]. Last but not least, the environment fluctuations in quantum dissipative systems give rise rather naturally to temporally correlated noises [50]. Indeed, it is well known that the generalization of the classical influence functional of Brownian motion to quantum dynamics yields a power-law correlated noise even in the case of an Ohmic bath [see part 3 of the thesis].

Let me now cite one example where field theory approaches play a role. It is well known that polymerized membranes undergo a melting transition between a crystalline phase, a hexatic phase and a fluid phase which can be dealt with by using field theory and renormalization group techniques [51]. Although the relevant free energy functionals do not contain the same terms as the ones I shall consider in the following, a variant of the methods that will be presented in this manuscript can be generalized to such melting transitions of membranes. Since these cell membranes are immersed in hydrodynamic media, the stochastic properties of such hydrodynamic environments should greatly influence the critical membrane dynamics. Indeed, recently it has been shown in [52] by demonstrating that these hydrodynamic correlations lead to a resonant peak in the power spectral density, that hydrodynamic “memory” translates into thermal forces which have a non-white noise spectrum. In many situations of practical interest a full treatment of such a *colored* noise is therefore necessary. For example, the escape rate of particles confined within a potential well crucially depends on the statistics of the thermal bath [53, 54, 55] as observed in the desorption of molecules from a substrate undergoing a second-order phase transition which effectively provides a colored noise for the stochastic dynamics of the molecules (this phenomenon is called Hedvall effect and it was studied theoretically in, e.g., [56]). Another important instance is the stochastic Burgers modeling of turbulence where the noise is correlated in both time and space [57]. This equation is, in addition, closely related to the Kardar-Parisi-Zhang description of surface growth that was analyzed with spatially correlated noise in, e.g., [58, 59] and references therein.

In the last paragraph of this subsection the so-called “pink noises” should not remain unmentioned. Such pink noise has a spectral density which decreases as  $1/f^\beta$  (where  $f$  is the

frequency) with  $\beta \approx 1$  and it is believed to be stationary. In particular, the  $1/f$  noise has been found on numerous occasions in physical systems: It is omnipresent in solid states [60, 61, 62] and in general in condensed matter systems [63] where it is often associated to fluctuation of the electrical resistance [64]. Moreover,  $1/f$ -noise has been observed when studying the dynamics of granular media [65] and it has been used to characterize the statistical properties of avalanches and cascades [66] occurring in various contexts, such as sandpile dynamics [67], self-organizing traffic flows [68] and the statistical features of cascades in heartbeats [69]. Furthermore,  $1/f$ -noise has been experimentally found for the dynamics of some proteins [70] and in connexion with the evolution of fractal correlations in DNA base sequences [71].

I hope that the reader is now – if he hadn’t been already before – convinced that colored noise occurs in various contexts in all fields of physics. As pointed out, the physics of  $1/f$ -noise are rich and complex but they go beyond the scope of this thesis; in the next chapter I will focus more on noise with heavy time correlations. Such a noise has a spectral density which *grows* in general with the frequency in contrast to the pink noise briefly discusses above. I will show that such colored noise qualitatively changes the critical behaviour of the ferromagnetic transition in spin models, conveniently described by a  $\phi^4$ -theory. This might be expected from a bolt analogy: Long-range spatial correlations are known to change the critical behaviour of – for instance – the classical Ising chain [72]. Such spatial correlations are typically static. Temporal correlations, on the other hand, are usually associated to some statistical environment which induces noise on the system. The analogy is therefore not totally given. However, we will show that long-range correlated noises do change the critical ferromagnetic transition dramatically – as long as they are “sufficiently” correlated.

## 2.2 Critical dynamics: Introduction

For more than 30 years critical dynamics have been explored with field theoretical methods [73, 74, 75, 76, 77, 78, 79, 80, 81]. A variety of dynamic models were introduced to describe the collective evolution of systems close to critical points. Among these, the most common ones are the dynamics of non-conserved or conserved order parameters which successfully describe the evolution of uniaxial magnetic systems close to the Curie point or the dynamics of binary alloys close to the demixing transition, respectively. The subcritical dynamics of these systems have been discussed in Sec. 2.1.1. I insist here, that these problems as well as many of their generalizations discussed in [76, 77, 79, 81] are *classical* in the sense that their stochastic nature can be essentially ascribed to thermal fluctuations. Therefore, as in the simpler diffusion processes, the evolution of the interacting degrees of freedom – described via a field  $\phi$  – is modeled by a functional Langevin equation in which the coupling to the environment is responsible for both thermal fluctuations, encoded in a stochastic external noise, and the friction [see Sec. 2.1]. If the environment, which acts as a thermal bath for  $\phi$ , is in equilibrium at a certain temperature  $\beta^{-1}$ , the space and time dependence of the friction coefficient and of the correlations of the thermal fluctuations are related via the fluctuation-dissipation theorem, see Eq. 2.1. The selected model bath determines then the remaining functional form of the noise-noise correlation and the usual choice is to take it to be delta-correlated in time which corresponds to white noise.

In cases in which the initial conditions of the system are drawn from an equilibrium Gibbs-Boltzmann distribution, or the system is allowed to evolve for a sufficiently long time such that this distribution function is reached, the space-time behavior of dynamic quantities is characterized by scaling laws in which the usual static exponents ( $\nu$ ,  $\eta$  etc.) appear but a new critical

exponent  $z$  is needed to relate the space and time dependencies. In the case of subcritical dynamics we have seen that  $z = 2$  ( $z = 3$ ) for an unconserved order parameter (conserved order parameter, respectively). Besides the analysis of equilibrium dynamics, field-theoretical methods allow one to study the *non-equilibrium* dynamics after a sudden quench from a suitably chosen initial condition to the critical point [82]. A Gaussian distribution of the initial field configuration with zero average and short-range correlations mimics a quench from the disordered phase [82]. A distribution with non-zero average but still short-range correlations describes (in the case of a scalar field  $\phi$ ) a quench from the ordered state [83, 84]. In these non-equilibrium cases a new critical exponent — usually denoted by  $\theta$  and called the “initial slip exponent” — characterizes the short-time behavior of the average order parameter as well as of the correlation and response functions [82] (see, e.g., [85, 86, 87] for summaries).

In all the studies mentioned above, the noise is assumed to have a Gaussian distribution with no temporal correlations, i.e., to be Gaussian and *white*. The first assumptions can be justified in many cases by the central limit theorem: If one considers a coarse-grained thermal noise, that is the sum  $\zeta(t) = n^{-1/2} \sum_{i=1}^n \xi_{t+i}$ , with  $\xi_i$  the microscopic random force at instant  $i$ , the probability distribution of  $\zeta(t)$  *locally* converges to a Gaussian as long as the mean and the variance of the  $\xi_i$  are finite. Note however that the absence of uniform convergence implies that only the events  $\zeta(t)$  of order  $\leq \mathcal{O}(\sqrt{n})$  are distributed according to a Gaussian; extreme events are thus excluded from the central limit theorem. The Gaussian distribution does not emerge uniformly but it rather gradually “eats up” the extreme events situated far away from the bulk. If these extreme events are rare (for example if  $\zeta(t)$  is bounded) the bulk distribution dominates and the central limit theorem is valid for the *whole* event space. However, there are well-known cases where extreme events are frequent enough that they need a special analysis (one important example are financial markets) although the Gaussian central limit theorem applies [see also Bouchaud and Potters [88]].

The second hypothesis is yet less justified. Indeed, the very coupling to thermal reservoirs yields, in general, non-Markovian Langevin equations in which the noise is correlated in time and the friction coefficient has some memory [89, 90, 50]. Although one can argue in some cases that the typical correlation time of the thermal bath is much smaller than the typical time scales in the system, it is known that some environments exhibit *power-law* correlated thermal fluctuations which are scalefree: In such cases assuming Markovian statistics is *never* justified a priori. I refer the reader to Sec. 2.1.3 where I present some examples of such scalefree environments which occur in nature.

In the present manuscript I will essentially focus on critical dynamics of an unconserved order parameter, i.e. described by [see Eqs. (2.4 and (2.5)]

$$\int_{-T}^t dt' \Gamma(t-t') \partial_{t'} \vec{\phi}(\vec{x}, t') + \frac{\delta \mathcal{H}}{\delta \vec{\phi}(\vec{x}, t)} = \vec{\zeta}(\vec{x}, t), \quad (2.30)$$

where  $-T$  is the initial time of the process and  $\vec{\zeta}$  is a zero-mean Gaussian colored noise with

$$\langle \zeta_i(\vec{x}, t) \zeta_j(\vec{x}', t') \rangle = \beta^{-1} \Gamma(t-t') \delta(\vec{x} - \vec{x}') \delta_{ij}. \quad (2.31)$$

Note that the function  $\Gamma$  determines both the noise-noise correlation [see Eq. (2.31)] and the time-dependent retarded friction coefficient [see Eq. (2.30)] since we have assumed the thermal bath (which is weakly coupled to the system) to be in equilibrium at temperature  $\beta^{-1}$ . The Markovian examples of this dynamics are characterized by a  $\delta$ -correlated (‘white’) noise, i.e.,

$$\Gamma(t) = 2\gamma_w \delta(t), \quad (2.32)$$

where  $\gamma_w$  is the friction coefficient. In this case Eq. (2.30) has been extensively studied both in and out of equilibrium, see, e.g., [75, 82, 86, 91]. Such *Ohmic* dissipation is the simplest form of *short-range correlated* noise. It can be formally obtained as the limit  $t_0 \rightarrow 0$  of the exponentially correlated Ornstein-Uhlenbeck (OU) process

$$\Gamma_{\text{OU}}(t) = \frac{\gamma_{\text{OU}}}{t_0} e^{-|t|/t_0}, \quad (2.33)$$

where the finite characteristic relaxation time  $t_0$  plays the role of an internal scale. Under renormalization one expects the exponentially correlated noise to become equivalent to a white (delta-correlated) one, Eq. (2.32), and the critical behavior of the OU process be identical to the Markovian one. In the *absence of an internal scale*, instead, there is no reason to expect a white noise limit and the critical behavior might be affected. The simplest example with no explicit time scale is

$$\Gamma(t) = \frac{\gamma}{\Gamma_E(1-\alpha)} |t|^{-\alpha} \quad \text{with } \alpha > 0. \quad (2.34)$$

( $\Gamma_E$  the Euler  $\Gamma$ -function). For  $\alpha > 1$ , i.e., *super Ohmic dissipation*, expression (2.34) is not integrable, unless a short-time cut-off and thus an internal scale is introduced. One can show that under naive scaling (introduced in Sec. 3) the Fourier or Laplace transform of  $\Gamma(t)$  generate a white noise vertex that dominates over the colored noise part. Hence, the appearance of a cut-off scale suggests the non relevance of the colored noise for *super-Ohmic* dissipation, i.e.,  $\alpha > 1$ . This statement will be made precise in the following. Instead, for *sub-Ohmic dissipation*, i.e.,  $\alpha < 1$ , the noise is truly long-range correlated and its influence on the dynamics will turn out to be non-trivial. The naive cross-over value between these two cases is  $\alpha = \alpha_c = 1$ , that is white noise or *Ohmic dissipation*. In the presence of interactions we shall show that this scenario is slightly modified, with the cross-over value  $\alpha_c(D, N)$  depending upon  $D$  and  $N$ .

A functional-integral representation of the stochastic process, Markovian or not, is better suited for an analytic treatment of critical dynamics than the Langevin equation (2.30). In particular, it allows one to express the average  $\langle \dots \rangle_\zeta$  over the possible realizations of the noise  $\vec{\zeta}$  in Eq. (2.30) as a functional integral (which will be denoted by  $\langle \dots \rangle$  in what follows)

$$\langle \dots \rangle_\zeta = \int [d\phi d\bar{\phi}] \dots e^{-S[\phi, \bar{\phi}]} \quad (2.35)$$

over  $\phi$  and an auxiliary field  $\bar{\phi}$  with  $\mathcal{S} = \mathcal{S}_0 + \mathcal{S}_{\text{int}} - \ln \mathcal{P}_{IC}$  [73, 74, 75, 92]<sup>3</sup>,

$$\begin{aligned} \mathcal{S}_0 = & \int d^D x \int_{-T}^{\infty} dt \bar{\phi}_i(\vec{x}, t) \left[ \int_{-T}^t dt' \Gamma(t-t') \partial_{t'} \phi_i(\vec{x}, t') + (r - \nabla^2) \phi_i(\vec{x}, t) \right] \\ & - \beta^{-1} \int d^D x \int_{-T}^{\infty} dt \int_{-T}^t dt' \bar{\phi}_i(\vec{x}, t) \Gamma(t-t') \bar{\phi}_i(\vec{x}, t') \end{aligned} \quad (2.36)$$

and

$$\mathcal{S}_{\text{int}} = \int d^D x \int_{-T}^{\infty} dt \frac{g}{3!} \bar{\phi}_i(\vec{x}, t) \phi_i(\vec{x}, t) \phi_j(\vec{x}, t) \phi_j(\vec{x}, t). \quad (2.37)$$

We used Einstein's convention of summation over repeated indices. The zero-source functional integral is identical to 1 due to the normalization of the noise probability distribution.

<sup>3</sup>In the presence of colored noise no discretization problems arise, see, e.g., [92].

$\mathcal{P}_{IC}[\vec{\phi}(\vec{x}, -T)]$  is the statistical weight of the initial condition. The auxiliary field  $\vec{\phi}$ <sup>4</sup> is conjugated to an external perturbation  $\vec{h}$ , in such a way that if  $\mathcal{H}[\vec{\phi}, \vec{h}] = \mathcal{H}[\vec{\phi}] - \vec{\phi} \cdot \vec{h}$ , the linear response of the order parameter to the field  $\vec{h}$  is given by

$$R(\vec{x} - \vec{x}'; t, t')\delta_{ij} = \left. \frac{\delta \langle \phi_i(\vec{x}, t) \rangle_{\vec{h}}}{\delta h_j(\vec{x}', t')} \right|_{\vec{h}=\vec{0}} = \langle \phi_i(\vec{x}, t) \bar{\phi}_j(\vec{x}', t') \rangle, \quad (2.38)$$

where  $\langle \dots \rangle_{\vec{h}}$  is the average over the stochastic process in the presence of the external perturbation, i.e., Eq. (2.30) with  $\mathcal{H} \mapsto \mathcal{H}[\vec{\phi}, \vec{h}]$ . The response function is causal irrespectively of the noise statistics and the Jacobian of the transformation of variables from  $\vec{\zeta}$  to  $\vec{\phi}$  which allows us to write the average over the stochastic process as in Eq. (2.35) is also a factor with no consequences [92]. In addition to the (linear) response function, we shall consider below the correlation function of the order parameter, defined by

$$C(\vec{x} - \vec{x}', t, t')\delta_{ij} = \langle \phi_i(\vec{x}, t) \phi_j(\vec{x}', t') \rangle \quad (2.39)$$

where we assumed translational invariance in space. The action  $\mathcal{S}_0 + \mathcal{S}_{int}$  is the sum of two contributions each one made of several terms. The part with density  $\bar{\phi}_i \delta \mathcal{H} / \delta \phi_i$  represents the deterministic dynamics whereas the remaining part is due to the coupling to the bath. The latter consists of the friction term and the noise-noise correlation and both involve the kernel  $\Gamma$ . In this formulation the problem is recast in the form of a field theory in  $D + 1$  dimensions with two vector fields, the analysis of which can be done via standard field-theoretical tools, such as the renormalization group (RG) approach that we shall use below.

Since, in general, there is no tractable Fokker-Planck equation for the non-Markov stochastic processes we are presently interested in, the usual and relatively simple proof of equilibration explained in, e.g., [19, 20] for the white-noise problem does not apply. However, we recall here that Eq. (2.30) is an effective description of the dynamics of a classical system with Hamiltonian  $\mathcal{H}'$  which is weakly and linearly coupled to a (large) equilibrium bath of harmonic oscillators at temperature  $\beta^{-1}$ , acting as a source of the stochastic noise  $\vec{\zeta}$  effectively induced by such a coupling. Indeed, the temperature that characterizes the correlations of the noise in Eq. (2.31) is  $\beta^{-1}$ , whereas the distribution of the frequencies of the harmonic oscillators within the bath determines the functional form of  $\Gamma$ . In addition,  $\Gamma$  appears in Eq. (2.30) and Eq. (2.31) in such a way to ensure the fluctuation-dissipation theorem for the bath variables. As a result, even with this effective non-Markov dynamics the system should still lose memory of its initial condition and equilibrate with the equilibrium bath of oscillators, resulting in a canonical distribution  $e^{-\beta \mathcal{H}[\vec{\phi}]} / \mathcal{Z}(\beta)$  of one-time quantities at sufficiently long times (possibly divergent with the system size) where  $\mathcal{Z}(\beta)$  is the partition function and  $\mathcal{H}$  differs from  $\mathcal{H}'$  by a term which is quadratic in the relevant degrees of freedom (see, e.g., [50, 15] for details). The asymptotic critical *equilibrium dynamics* is expected to be described by the limit  $T \rightarrow \infty$  of the action in which one neglects the specific distribution  $\mathcal{P}_{IC}$  of the initial conditions that in any case should be forgotten dynamically. Since we shall be interested in the critical dynamics, we set  $\beta = \beta_c$  and we absorb this constant into a redefinition of the fields and of the coupling constant  $g$ . In equilibrium the response and the correlation functions are invariant under time translations, i.e.,  $R(\vec{x}, t, t') = R(\vec{x}, t - t')$  [see Eq. (2.38)] and  $C(\vec{x}, t, t') = C(\vec{x}, t - t')$  [see Eq. (2.39)], and they are related to each other by the fluctuation-dissipation theorem (FDT) that reads  $R(\vec{x}, t) = -\beta \partial_t C(\vec{x}, t) \Theta(t)$ , where  $t$  represents the time delay,  $\Theta(t \leq 0) = 0$  and

<sup>4</sup> $\vec{\phi}$  is purely imaginary and it is sometimes written as  $i\vec{\phi}$  in the literature.

$\Theta(t > 0) = 1$ <sup>5</sup>, and which is completely independent of the specific characteristics of the system and the bath apart from its temperature. (A proof of this relation for generic colored noise Langevin dynamics can be found in [92].) Once the latter has been absorbed in the redefinition of  $\phi_i$  and  $g$  the FDT becomes

$$R(\vec{x}, t) = -\partial_t C(\vec{x}, t)\Theta(t), \quad (2.40)$$

and this is the form that we shall use in our calculations. Moreover, the time-dependent correlation is invariant under time-reversal, i.e.,  $C(\vec{x}, t) = C(\vec{x}, -t)$ .

*Non-equilibrium dynamics*, instead, can be studied by leaving  $T$  finite and by making the initial distribution  $\mathcal{P}_{IC}$  explicit [82, 86]. A typical choice is a Gaussian weight in which case  $\beta_c$  can still be absorbed into a redefinition of the fields and  $g$ . Stationarity is lost out of equilibrium and correlation and linear response functions depend on all times involved in their definitions ( $t$  and  $t'$  in Eq. (2.38) and Eq. (2.39)). Moreover, the FDT is no longer valid [86, 93, 94].

In addition to  $R$  defined in Eq. (2.38) and  $C$  defined in Eq. (2.39), one can construct the quadratic correlator  $\langle \bar{\phi}_i(\vec{x}, t)\bar{\phi}_j(\vec{x}', t') \rangle$  which, independently of the color of the noise, vanishes identically due to causality.

### 2.2.1 Scaling

In the case of stochastic dynamics with white noise, a systematic RG analysis confirms the phenomenological scaling behavior of the linear response and correlation functions both for  $T \rightarrow \infty$  and  $T$  finite corresponding, respectively, to equilibrium and non-equilibrium relaxational dynamics. In terms of the equilibrium correlation length  $\xi_{\text{eq}} \simeq |r - r_c|^{-\nu}$ , where  $r_c$  is the critical value of the parameter  $r$  in Eq. (2.2), and of a dynamic growing length  $\xi(t) \simeq t^{1/z}$ , one expects [82, 86]

$$R(\vec{p}, t, t') = p^{-2+\eta+z} [\xi(t)/\xi(t')]^{z\theta} f_R(p\xi_{\text{eq}}, \xi(t)/\xi_{\text{eq}}, \xi(t')/\xi(t)) \quad (2.41)$$

and

$$C(\vec{p}, t, t') = p^{-2+\eta} [\xi(t)/\xi(t')]^{z(\theta-\hat{\alpha})} f_C(p\xi_{\text{eq}}, \xi(t)/\xi_{\text{eq}}, \xi(t')/\xi(t)), \quad (2.42)$$

for the Fourier transform in space of  $R(\vec{x}, t, t')$  and  $C(\vec{x}, t, t')$ , respectively, with the white noise value  $\hat{\alpha} = 1$  [82]. In the previous expressions,  $\nu$  is the standard static critical exponent associated with the correlation length,  $z$  is the dynamic critical exponent which characterizes the different scaling behavior of space and time, whereas  $\eta$  is the static anomalous dimension of the field  $\phi$  and it controls the power-law spatial decay of the static correlation function.  $\theta$  is the so-called initial-slip exponent [82, 85, 86] that accounts for the effects of the initial condition in the case of finite  $T$ . It is a novel universal quantity if the relaxation occurs from a disordered initial state, whereas it is related to known equilibrium exponents if the initial state has a non-vanishing average value of the order parameter [83, 84]. In (2.41) and (2.42)  $f_{R,C}$  are scaling functions which become universal after the introduction of proper normalization. Equilibrium dynamical scaling is recovered in the limiting case  $\xi(t') \simeq \xi(t) \gg \xi_{\text{eq}}$  (i.e., in the limit of long times  $t, t'$  with finite  $t - t'$ ), whereas aging phenomena are expected to emerge for  $\xi(t), \xi(t') \ll \xi_{\text{eq}}$  and, in particular, right at the critical point  $r = r_c$ . In the presence of specific instances of correlated noise we expect the scaling behavior in (2.41) and (2.42) to be modified

<sup>5</sup>Note that the Itô prescription of the Langevin equation Eq. (2.30) implies  $\Theta(0) = 0$  in the stochastic path integral description [19, 75].

both as far as the exponents and the scaling functions are concerned. The changes appear at the level of the Gaussian theory and non-trivial effects survive in the presence of interactions for certain noise correlations, as we shall explain in the following.

### 2.2.2 Large- $N$ limit for Ohmic dissipation

The limit where the number of components  $N$  of  $\vec{\phi}$  is infinite can be solved exactly for the full out of equilibrium dynamics driven by white noise Eq. (2.32). First, one replaces the coupling  $g$  by  $g \mapsto g/N$  in order to obtain a homogeneous scaling in  $N$ . Second, one notices that the stochastic variable  $\sum_{j=1}^N \phi_j^2(\vec{x}, t)/N$  tends to a Gaussian with mean  $\sum_{j=1}^N \langle \phi_j^2(\vec{x}, t) \rangle / N = \langle \phi_i^2(\vec{x}, t) \rangle$  (for all  $i \in \{1, \dots, N\}$ ) and variance of  $\mathcal{O}(N^{-1/2})$ . Hence, for large  $N$ , a sensible approximation is to replace the expression  $\vec{\phi}^2$  in the interaction part (2.30) by its mean  $C(\vec{x} = \vec{0}, t = 0)$ . This is the usual large- $N$  approximation which becomes exact for  $N \rightarrow \infty$ . The equation of motion (2.30) for Ohmic dissipation then reads

$$\gamma_w \dot{\phi}(\vec{x}, t) = -[\nabla^2 + I(t)]\phi(\vec{x}, t) + \zeta(\vec{x}, t), \quad (2.43)$$

where  $\phi$  stands for each (now independent) component  $\phi_i$  which are all equivalent for large  $N$ . We introduced the time-dependent function

$$I(t) = r + g C(\vec{0}, 0), \quad (2.44)$$

which has to be determined self-consistently. The scalar Gaussian noise  $\zeta(\vec{x}, t)$  has the correlation

$$\langle \zeta(\vec{x}, t) \zeta(\vec{x}', t') \rangle = \beta^{-1} \gamma_w \delta(\vec{x} - \vec{x}') \delta(t - t'). \quad (2.45)$$

The model (2.43) has to be complemented by information on the initial condition. We choose a completely disordered high-temperature initial condition to mimic a quench to the critical point:

$$\langle \vec{\phi}(\vec{x}, 0) \rangle = 0, \quad (2.46)$$

$$\langle \phi_i(\vec{x}, 0) \phi_j(\vec{x}', 0) \rangle = \frac{1}{\tau_0}. \quad (2.47)$$

This initial condition will be reused in Sec. 2.3.5.

The noise amplitude  $\gamma_w$  can be scaled away by setting  $t \mapsto \gamma_w t$ . Then, the formal solution of Eq. (2.43) can be written in the Fourier domain as

$$\phi(\vec{k}, t) = R(\vec{k}, t, 0) \phi(\vec{k}, 0) + \int_0^t ds R(\vec{k}, t, s) \zeta(\vec{k}, s), \quad (2.48)$$

where

$$R(\vec{k}, t, s) = \frac{Y(s)}{Y(t)} e^{-k^2(t-s)} \quad (2.49)$$

is the non-equilibrium response functions (which depends on two times  $t$  and  $s$ ) with  $Y(s) = \exp[\int_0^s dt' I(t')]$ . Consequently, solving the Langevin equation (2.43) amounts to determine  $Y(s)$  self-consistently.

From the very definition of  $Y(t)$  follows that

$$\frac{\partial Y^2(t)}{\partial t} = 2 \left[ r + g C(\vec{x} = \vec{0}, 0) \right] Y^2(t). \quad (2.50)$$

Now, introduce an ultraviolet cutoff function  $\chi(\vec{k})$  to write

$$C(\vec{x} = \vec{0}, 0) = \int \frac{d^D k}{(2\pi)^D} C(\vec{k}, t) \chi(\vec{k}) . \quad (2.51)$$

We are only interested in the long-time dynamics which are expected to be universal and hence independent of the precise form of  $\chi(\vec{k})$ . Therefore, we can choose a specific  $\chi(\vec{k})$  which is suitable for the calculation:  $\chi(\vec{k}) = \exp[-k^2/\Lambda^2]$  with  $\Lambda$  some ultraviolet cutoff. By using Eq. (2.48) we can write

$$C(\vec{k}, t) = R^2(\vec{k}, t, 0)\tau^{-1} + 2\beta^{-1} \int_0^t ds R^2(\vec{k}, t, s) , \quad (2.52)$$

which leads in conjunction with Eq. (2.51) to an integro-differential equation for  $Y(t)$ :

$$\frac{\partial Y^2(t)}{\partial t} = 2rY^2(t) + 2g\tau^{-1} h(t + 1/2\Lambda^2) + 4g\beta^{-1} \int_0^t ds h(t - s + 1/2\Lambda^2)Y^2(s) , \quad (2.53)$$

where we defined  $h(z) = \int \frac{dk^D}{(2\pi)^D} e^{-2k^2 z} = (8\pi z)^{-D/2}$ . By applying a Laplace transform it is straightforward to find the asymptotic behaviour

$$Y(t) \sim \begin{cases} t^{-(4-D)/4} & \text{for } D < 4 , \\ \text{const.} & \text{for } D \geq 4 \end{cases} \quad (2.54)$$

at the well known critical large- $N$  point defined by  $r^* + gT^*B = 0$ .  $B$  is the standard critical one-loop bubble of the (regularized)  $\phi^4$ -theory:  $B(0) = \int \frac{d^D k}{(2\pi)^D} \chi(\vec{k})/k^2$ . From the general scaling relation (2.41) one immediately finds for the Ohmic large- $N$  model in the non-mean-field case  $D < 4$

$$z = 2 , \quad (2.55)$$

$$\theta = (4 - D)/4 . \quad (2.56)$$

The large- $N$  approximation thus gives a qualitative behaviour that confirms (2.41) and (2.42). In the next section I present a renormalization group analysis for the more difficult case: The out of equilibrium dynamics of model A driven by power-law correlated noise. A generalization to the full colored noise case is not straightforward and has to my knowledge not been performed, yet.

## 2.3 Critical dynamics and colored noise

### 2.3.1 Equilibrium dynamics

According to the interpretation of the Langevin dynamics in Eq. (2.30) as resulting from the coupling to an equilibrium thermal bath, after a sufficiently long time the system is expected to relax towards an equilibrium state characterized by the effective Hamiltonian  $\mathcal{H}$ , i.e., by the static  $\phi^4$ -theory. This relaxation occurs generically and for arbitrary initial conditions as long as the asymptotic values of the control parameters of the system ( $r$  in the case we are concerned with) imply for  $\mathcal{H}$  neither a spontaneous symmetry breaking nor criticality, which would indeed provide instances of *aging* (see, e.g., [15]). However, the existence of a wide region of parameter

space ( $r > 0$ ) for which equilibration occurs, allows us to conclude that all static properties of a theory with effective Hamiltonian  $\mathcal{H}$  carry over to the dynamic field-theoretical action  $\mathcal{S}$  [see Eqs. (2.36) and (2.37)] which generates the dynamic correlation functions and therefore the static ones as a special case. The upper critical dimensionality  $D_c$  above which the Gaussian theory becomes exact is therefore the same as in the  $\phi^4$  theory, i.e.,  $D_c = 4$  (see, e.g., [19]). Analogously, the same applies to the static exponents  $\nu$  and  $\eta$ . In this section we show how this arises within perturbation theory. In particular, we determine the conditions under which the critical dynamics is modified by the colored part of the noise with special focus on the emergence of a cross-over line  $\alpha_c(D, N)$  which bounds the region within which the dynamic exponent  $z$  is affected by the color of the noise. We calculate this exponent in the white and colored noise cases.

### 2.3.2 Gaussian theory

In the  $T \rightarrow \infty$  limit the Gaussian part of the action  $\mathcal{S}_0$  can be diagonalized via a Fourier transform of the fields defined in Eq. (2.151). One obtains

$$\mathcal{S}_0 = \frac{1}{2} \int \frac{d\omega}{2\pi} \frac{d\omega'}{2\pi} \int \frac{d^D p}{(2\pi)^D} \frac{d^D p'}{(2\pi)^D} \vec{\varphi}^T(\vec{p}, \omega) \mathcal{C}(\vec{p}, \omega; \vec{p}', \omega') \vec{\varphi}(\vec{p}', \omega'), \quad (2.57)$$

where we used a vector notation  $\vec{\varphi} = (\vec{\phi}(\vec{p}, \omega), \vec{\bar{\phi}}(\vec{p}, \omega))^T$  for the  $2N$ -component field  $\vec{\varphi}$  and we introduced the correlation matrix

$$\mathcal{C} = \delta_{ij} \delta(\vec{p} + \vec{p}') \delta(\omega + \omega') \begin{pmatrix} 0 & i\omega \Gamma_{i\omega} + (p^2 + r) \\ -i\omega \Gamma_{i\omega}^* + (p^2 + r) & -(\Gamma_{i\omega} + \Gamma_{i\omega}^*) \end{pmatrix}. \quad (2.58)$$

Here and in what follows we denote a function and its Fourier transform with the same symbol, the difference being made clear by their arguments. In Eq. (2.58)  $\Gamma_{i\omega}$  stands for the Fourier transform of  $\Theta(t)\Gamma(t)$  [the  $\Theta(t)$  factor is a consequence of the causal structure of Eq. (2.30)]. As usual,  $*$  denotes the complex conjugate. For the colored noise in Eq. (2.34) one finds

$$\Gamma_{i\omega} = \gamma |\omega|^{\alpha-1} [\sin(\pi\alpha/2) - i \operatorname{sign}(\omega) \cos(\pi\alpha/2)] + \gamma_w. \quad (2.59)$$

[Note that for  $\alpha > 1$  a short-time cut-off has to be introduced in order to transform Eq. (2.34). However, the dynamic properties we are presently interested in are determined by the leading behavior at small  $\omega$ , which is not affected by the introduction of such a cut-off and is correctly captured by Eq. (2.59). Accordingly, we shall use this form irrespectively of the value of  $\alpha$ .] In this expression we have added a supplementary *white-noise vertex*  $\gamma_w$  for reasons that will become clear in the following [note that the cut-off that has to be introduced in order to make Eq. (2.34) integrable for  $\alpha > 1$  effectively leads to this supplementary white-noise vertex]. The propagators<sup>6</sup> are deduced by inverting  $\mathcal{C}$ :

$$R_0(\vec{p}, \omega) \delta_{ij} = \langle \phi_i(\vec{p}, \omega) \bar{\phi}_j(-\vec{p}, -\omega) \rangle = \frac{1}{i\omega \Gamma_{i\omega} + p^2 + r} \delta_{ij} \quad (2.60)$$

and

$$\begin{aligned} C_0(\vec{p}, \omega) \delta_{ij} &= \langle \phi_i(\vec{p}, \omega) \phi_j(-\vec{p}, -\omega) \rangle \\ &= \frac{\Gamma_{i\omega} + \Gamma_{i\omega}^*}{\omega^2 \Gamma_{i\omega} \Gamma_{i\omega}^* + i\omega(p^2 + r)(\Gamma_{i\omega} - \Gamma_{i\omega}^*) + (p^2 + r)^2} \delta_{ij}. \end{aligned} \quad (2.61)$$

<sup>6</sup>In what follows we denote the response and correlation function by  $R$  and  $C$ , respectively. The various propagators and quantities within the Gaussian approximation are denoted by the subscript  $0$ .

By construction they satisfy the FDT [see Eq. (2.40)] that in the frequency domain reads:

$$2i \operatorname{Im} R_0(\vec{p}, \omega) = -i\omega C_0(\vec{p}, \omega). \quad (2.62)$$

We recall that we absorbed the temperature  $\beta^{-1}$  in a redefinition of the fields and the coupling constant  $g$ , and that  $C_0(\vec{p}, \omega)$  is a real function.

The static correlation function  $C_0(\vec{p}, t = 0)$  can be obtained by integrating Eq. (2.61) over the frequency  $\omega$  and, as expected, the result agrees with the static Gaussian correlation that one would infer from the Hamiltonian  $\mathcal{H}$  [see, c.f., the calculation leading to Eq. (2.155)]. Consequently, the static critical exponents  $\nu$  and  $\eta$  are not modified at this order by the dynamics and they take the Gaussian values  $\nu_0 = 1/2$  and  $\eta_0 = 0$ , respectively.

We anticipate here that in Sec. 2.3.5, while discussing the non-equilibrium dynamics of the present model, we consider the Laplace transform [see Eq. (2.152)] of Eq. (2.30) with  $g = 0$  and the colored noise given in Eq. (2.34) (i.e., with  $\gamma_w = 0$ ). This allows us to determine the Laplace transform of the response function  $R_0$ , formally obtained by replacing  $i\omega$  with  $\lambda$  in Eq. (2.60); compare Eq. (2.151) and Eq. (2.152). This transform can be inverted to a form given in terms of the so-called generalized Mittag-Leffler functions  $E_{\alpha,\beta}$  defined in (2.169) and provides a closed expression for  $R_0(\vec{p}, t)$ :

$$R_0(\vec{p}, t) = \Theta(t) \frac{t^{\alpha-1}}{\gamma} E_{\alpha,\alpha}(-At^\alpha/\gamma), \quad (2.63)$$

where  $A \equiv p^2 + r$ . The equilibrium correlation function  $C_0$  is readily determined from this expression via the fluctuation-dissipation theorem (2.40) (see, c.f., App. 2.4.2 for details):

$$C_0(\vec{p}, t) = \frac{1}{A} E_{\alpha}(-A|t|^\alpha/\gamma) \quad (2.64)$$

where  $E_{\alpha}(z) \equiv E_{\alpha,1}(z)$ . In Fig. 2.2(a) we plot  $AC_0$  as a function of the (dimensionless) scaling variable  $u \equiv |t|(A/\gamma)^{1/\alpha}$  associated with time  $t$ . For  $\alpha \rightarrow 1$  one recovers the purely exponential dependence  $e^{-u}$  (indicated by the decreasing dashed curve in Fig. 2.2) which characterizes the case of white noise. As  $\alpha$  decreases, instead, the correlation function displays a faster initial drop followed by a slower decay at large values of  $u$ . Indeed, taking into account the known asymptotic behavior of the Mittag-Leffler functions [c.f., Eq. (2.170)], these curves decay algebraically as  $\sim 1/[\Gamma_E(1-\alpha)u^\alpha]$  for  $u \rightarrow \infty$ . In panel (b) of Fig. 2.2 we use a log-log-scale to compare the curves shown in panel (a) with their corresponding leading asymptotic algebraic decays, indicated by the straight dashed curves for  $u \gtrsim 5$ . As  $\alpha \rightarrow 0$  the approximation provided by the leading term of the asymptotic expansion becomes less accurate in this time span and one needs to go to longer times to reach the asymptotic regime. The curves in Fig. 2.2 clearly illustrate the crossover between an exponential and an algebraic asymptotic behavior of the correlation function as  $\alpha$  decreases below the value  $\alpha = 1$ .

For the generic case of the noise in Eq. (2.59) with  $\gamma, \gamma_w \neq 0$ , the propagators  $R_0$  and  $C_0$  do not have a simple analytic form in the time domain, in contrast to the familiar exponential relaxation which characterizes the case with white noise ( $\gamma = 0, \gamma_w \neq 0$ ) briefly recalled in Eqs. (2.153) and (2.153) and to the purely colored case discussed in the previous paragraph ( $\gamma \neq 0$  and  $\gamma_w = 0$ ). In spite of this difficulty, the Gaussian value  $z_0$  of the dynamic exponent  $z$  can be determined by comparing the scaling of the first two terms in the denominator of  $R_0$  for small  $\omega$  and  $p$  since one expects  $\omega \sim p^z$  from the definition of  $z$  (see, e.g., [19]). First we note that for small  $\omega$ , Eq. (2.59) scales as  $\Gamma_{i\omega} \sim |\omega|^{\alpha-1}$  for  $\alpha < 1$ , whereas  $\Gamma_{i\omega} \sim 1$  for  $\alpha > 1$ :

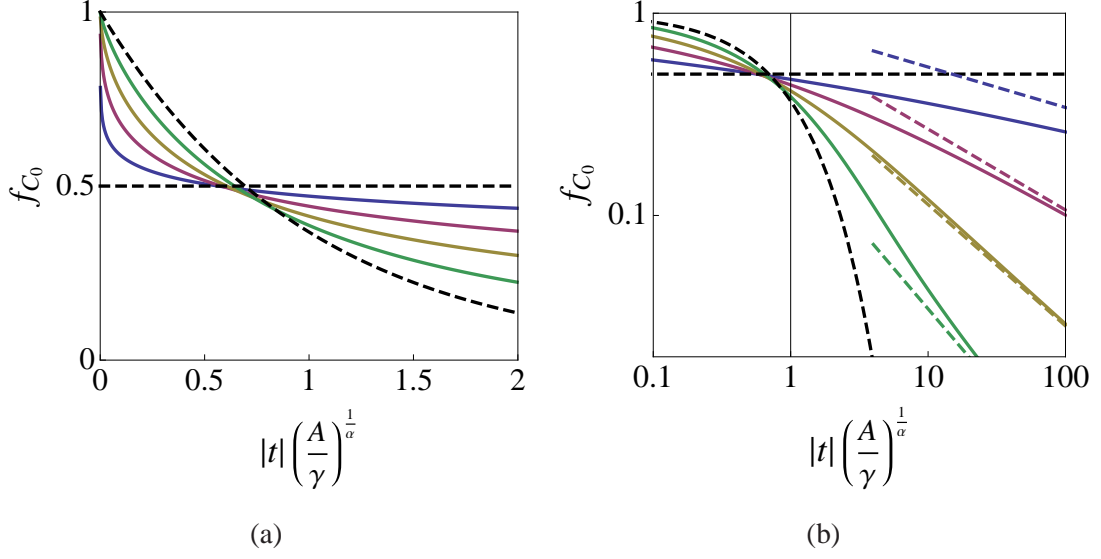


Figure 2.2: Scaling function  $AC_0$  of the Gaussian correlation  $C_0$  in equilibrium ( $T \rightarrow \infty$ ) as a function of  $u \equiv |t|(A/\gamma)^{1/\alpha}$  for various values of  $\alpha$ , with  $A = \bar{p}^2 + r$ . (a) The horizontal dashed line corresponds to the limit  $\alpha \rightarrow 0$ , whereas the other dashed line points out the purely exponential behavior  $e^{-u}$ , which is recovered for  $\alpha = 1$ . The solid lines, instead, correspond to  $\alpha = 0.2, 0.4, 0.6$ , and  $0.8$ , from bottom to top at small  $u$  and in the reverse order at large  $u$ . (b) Log-log plot of the curves shown in panel (a) compared to their corresponding leading asymptotic algebraic behavior inferred from Eq. (2.170), which are indicated as (straight) dashed lines.

in the former case the effect of the colored part of the vertex is dominant, whereas in the latter the contribution of the white noise ( $\propto \gamma_w$ ) dominates. As a result, from the scaling  $\omega \Gamma_{i\omega} \sim p^2$  one can read the Gaussian value  $z_0$  of the dynamic exponent:

$$z_0 = \begin{cases} z_0^{(\text{col})} = 2/\alpha & \text{for } \alpha < 1, \\ z_0^{(\text{w})} = 2 & \text{for } \alpha \geq 1. \end{cases} \quad (2.65)$$

A similar effect is observed in diffusion processes with colored noise, the so-called fractional Brownian motion [see Sec. 2.1.2 and [95]]. The particle's displacement is stationary and characterized by an  $\alpha$ -dependent exponent which is called *Hurst exponent* in this context.

By rescaling the momentum  $p$  and frequency  $\omega$  according to  $p \mapsto b^{-1}p$  and  $\omega \mapsto b^{-z}\omega$  with  $b$  the *scaling parameter* of the RG flow, one deduces the Gaussian scaling behavior of the response and the correlation propagator. We infer from Eq. (2.60) and Eq. (2.61) that

$$b^{-2}R_0(b^{-1}\vec{p}, b^{-z_0}\omega; r, \gamma, \gamma_w) = R_0(\vec{p}, \omega; b^2r, b^{2-\alpha z_0}\gamma, b^{2-z_0}\gamma_w), \quad (2.66)$$

with a similar expression for  $C_0$ , where the prefactor  $b^{-2}$  on the left-hand side (lhs) is replaced by  $b^{-2-z}$ . As anticipated, one can identify two asymptotically scale-invariant behaviors (the so-called Gaussian fixed-points in the parameter space) as the Gaussian critical point  $r = 0$  is approached. They correspond to  $P \equiv (\gamma_w = 0, \gamma \neq 0)$  for  $\alpha < 1$  and  $P_w \equiv (\gamma_w \neq 0, \gamma = 0)$  for  $\alpha \geq 1$ , i.e., to the cases in which either the colored or the white noise is relevant. The latter reduces to the standard Model A dynamics [19]. In order for  $P$  and  $P_w$  to be fixed points, it is necessary that the corresponding non-vanishing coupling strengths, either  $\gamma$  or  $\gamma_w$ , are constant

under renormalization which, as expected from Eq. (2.65), implies  $z = z_0^{(\text{col})} = 2/\alpha$  for  $\alpha < 1$  ( $P$ ) and  $z = z_0^{(\text{w})} = 2$  for  $\alpha \geq 1$  ( $P_w$ ).

In order for the action  $\mathcal{S}_0$  to be invariant under the momentum and frequency rescaling discussed above, one has to rescale the fields  $\phi_i$  and  $\bar{\phi}_i$  as  $\phi_i(b^{-1}\vec{p}, b^{-z_0}\omega) \mapsto b^{d_\phi} \phi_i(\vec{p}, \omega)$  and  $\bar{\phi}_i(b^{-1}\vec{p}, b^{-z_0}\omega) \mapsto b^{d_{\bar{\phi}}} \bar{\phi}_i(\vec{p}, \omega)$  where  $d_\phi$  and  $d_{\bar{\phi}}$  are the so-called scaling dimensions of the fields  $\vec{\phi}$  and  $\vec{\bar{\phi}}$ , respectively, in the  $(\vec{p}, \omega)$ -domain. (Below we shall introduce the scaling dimensions of the fields in the time-domain; in order to keep the notation as simple as possible we do not include an additional subscript to distinguish the two cases but we explain in the text which one we use in each case.) The latter take the Gaussian values

$$d_{\phi,0} = (D + 2)/2 + z_0, \quad (2.67)$$

$$d_{\bar{\phi},0} = (D + 2)/2. \quad (2.68)$$

In the white-noise case  $z_0 = 2$  we recover the standard scaling dimensions of Model A critical dynamics [19]. As far as the transformation properties of the propagators under these rescalings are concerned we have

$$b^{-2d_\phi + D + z_0} C_0(b^{-1}\vec{p}, b^{-z_0}\omega; \dots) = C_0(\vec{p}, \omega; \dots), \quad (2.69)$$

$$b^{-d_\phi - d_{\bar{\phi}} + D + z_0} R_0(b^{-1}\vec{p}, b^{-z_0}\omega; \dots) = R_0(\vec{p}, \omega; \dots), \quad (2.70)$$

where the factor  $b^{D+z_0}$  comes from the  $\delta$ -function which guarantees the conservation of momenta and frequencies. We have not specified the scaling of the parameters  $r$ ,  $\gamma$  and  $\gamma_w$  to lighten the notation. By comparing with the scaling behavior of the Gaussian response in Eq. (2.66) and of the correlation function, one confirms the Gaussian values Eq. (2.67) and Eq. (2.68) for the dimensions  $d_\phi$  and  $d_{\bar{\phi}}$ , respectively.

In Eq. (2.59) we added to the colored-noise vertex associated with Eq. (2.34) a white-noise contribution proportional to  $\gamma_w$  for the purpose of highlighting the emergence of the two distinct Gaussian fixed points  $P$  and  $P_w$ . As we shall show below such a white-noise contribution is anyhow generated under the RG flow as soon as one accounts for the effect of non-Gaussian fluctuations (i.e.,  $g \neq 0$ ) on the Gaussian fixed-point  $P = (\gamma \neq 0, \gamma_w = 0)$  with colored noise alone.

### 2.3.3 The interaction part

The interaction part of the action reads

$$\begin{aligned} \mathcal{S}_{int} = & \int \frac{d\omega}{2\pi} \frac{d\omega'}{2\pi} \frac{d\omega''}{2\pi} \frac{d^D p}{(2\pi)^D} \frac{d^D p'}{(2\pi)^D} \frac{d^D p''}{(2\pi)^D} \frac{g}{3!} \bar{\phi}(-\vec{p} - \vec{p}' - \vec{p}'', -\omega - \omega' - \omega'') \\ & \times \phi(\vec{p}, \omega) \phi(\vec{p}', \omega') \phi(\vec{p}'', \omega'') \end{aligned}$$

in the frequency and momentum domain. Under the naive scaling with Eqs. (2.65), (2.67), and (2.68) one easily obtains the scaling of the coupling constant:  $g \rightarrow b^{4-D}g$ . The upper critical dimension is thus  $D_c = 4$  independently of  $\alpha$  and the effects of fluctuations beyond mean-field can be accounted for by using a standard perturbative expansion in terms of  $\epsilon = 4 - D$ .

In the presence of the interaction  $\mathcal{S}_{int}$ , the scaling dimension of the fields and the coupling constants are altered. In addition, we shall show that the crossover value  $\alpha_c = 1$ , which separates the colored-noise-dominated case from the white-noise-dominated one, acquires a dependence on  $D$ , thus dividing the  $(\alpha, D)$ -plane (for  $N$  fixed) in two distinct regions, each one

with different scaling properties. Under a RG flow with scaling parameter  $b > 1$  the noise strengths  $\gamma$  and  $\gamma_w$  scale as

$$\gamma \mapsto b^{2-\alpha z_0+\alpha\eta_\gamma} \gamma, \quad (2.71)$$

$$\gamma_w \mapsto b^{2-z_0+\eta_w} \gamma_w, \quad (2.72)$$

which generalize the corresponding Gaussian scaling behavior of these parameters — encoded in Eq. (2.66) — via the introduction of suitable anomalous dimensions  $\eta_\gamma$  and  $\eta_w$  of  $\gamma$  and  $\gamma_w$ , respectively. These anomalous dimensions  $\eta_\gamma$  and  $\eta_w$  determine the corrections to the Gaussian value  $z_0$  of the dynamical exponent  $z$  and the crossover value  $\alpha_c$  which separates the different regions in the  $(\alpha, D)$ -plane. Indeed, let  $l$  be a length scale and  $\tau$  be a time scale. Dimensional analysis implies  $t \sim \tau$  and  $x \sim l$ . From Eq. (2.60) we infer that  $\gamma \sim \tau^\alpha/l^2$  and  $\gamma_w \sim \tau/l^2$ . Consider the case in which the colored noise dominates, which corresponds to having  $2 - \alpha z_0 + \alpha\eta_\gamma > 2 - z_0 + \eta_w$  in terms of the dimensions of the noise strengths [see (2.71) and (2.72)] with  $z_0 = 2/\alpha$ . By choosing  $\tau^\alpha = l^2\gamma$  we have  $t \sim l^{2/\alpha}\gamma^{1/\alpha}$ . Therefore, under an RG flow with  $l \mapsto bl$  ( $b > 1$ ) we deduce from (2.71) that  $t \sim b^{2/\alpha+\eta_\gamma} l^{2/\alpha}\gamma^{1/\alpha}$ . On the other hand, by noting that the dynamic exponent  $z$  is defined through  $t \rightarrow b^z t$  we can readily identify the dynamic exponent  $z = 2/\alpha + \eta_\gamma$  in terms of  $\eta_\gamma$ . In the white-noise-dominated case we choose  $\tau = l^2\gamma_w$  and a similar argument yields the white-noise result  $z = 2 + \eta_w$ . In short,

$$z = \begin{cases} 2 + \eta_w & \text{for } \alpha > \alpha_c(D, N), \\ 2/\alpha + \eta_\gamma & \text{for } \alpha < \alpha_c(D, N), \end{cases} \quad (2.73)$$

and therefore one needs to calculate  $\eta_w$  and  $\eta_\gamma$  in order to determine  $z$ .

In the presence of non-Gaussian fluctuations, the scaling dimensions  $d_\phi = d_{0,\phi} - z_0 - \eta/2$  and  $d_{\bar{\phi}} = d_{0,\bar{\phi}} - z_0 - \bar{\eta}/2$  in the  $(\vec{p}, t)$ -domain of the fields  $\phi$  and  $\bar{\phi}$ , respectively, differ from their Gaussian values by the corresponding anomalous dimensions  $\eta$  and  $\bar{\eta}$  (the extra  $-z_0$  comes from the conversion of  $d_{0,\phi}$  and  $d_{0,\bar{\phi}}$  from the frequency to the time domain). In order to determine the resulting scaling in the  $(\vec{p}, \omega)$ -domain one has to take into account the integral over time that carries a dimension  $z$  (which differs from the Gaussian value  $z_0$ ); therefore

$$\phi_i(b^{-1}\vec{p}, b^{-z}\omega) \mapsto b^{d_\phi+z-z_0} \phi_i(\vec{p}, \omega) = b^{D/2+1+z-\eta/2} \phi_i(\vec{p}, \omega), \quad (2.74)$$

$$\bar{\phi}_i(b^{-1}\vec{p}, b^{-z}\omega) \mapsto b^{d_{\bar{\phi}}+z-z_0} \bar{\phi}_i(\vec{p}, \omega) = b^{D/2+1+z-z_0-\bar{\eta}/2} \bar{\phi}_i(\vec{p}, \omega). \quad (2.75)$$

The FDT implies a relation between  $\eta_\gamma$ ,  $\eta_w$ ,  $\eta$  and  $\bar{\eta}$ , which allows one to express  $z$  in terms of the latter two. Indeed, the right-hand side (rhs) and the lhs of Eq. (2.40) should have the same scaling dimensions; therefore  $z = d_\phi - d_{\bar{\phi}}$  in terms of the dimensions of the fields in the time-domain. Using now the expressions of the field anomalous dimensions provided above, transforming into the dimensions in the frequency domain, and replacing the Gaussian values in Eqs. (2.67) and (2.68) one concludes that

$$z = z_0 + \frac{\bar{\eta} - \eta}{2}. \quad (2.76)$$

### 2.3.4 Perturbative expansion

As we explained above, one does not expect any modification of equal-time correlation functions, as they are determined by a static theory with the effective Hamiltonian  $\mathcal{H}$  in Eq. (2.2). Hence, we focus on the dynamical exponent  $z$ , the corrections to which can be obtained on the

basis of the standard perturbative method consisting in a combined expansion in the coupling constant  $g$  and in the deviation  $\epsilon = 4 - D$  from the upper critical dimensionality of the model [20, 19, 18, 96]. In performing such an expansion one also takes advantage of the fact that  $g$  will eventually be set to its fixed-point value  $g^* = \mathcal{O}(\epsilon)$ . We remind here that the inverse temperature  $\beta$  has been eliminated by a suitable redefinition of the fields and the coupling constant  $g$ . In the following we concentrate on the one-particle irreducible vertex functions [19, 96] with  $n$  external  $\phi$ -lines and  $\bar{n}$  external  $\bar{\phi}$ -lines, denoted<sup>7</sup> by

$$\mathcal{V}^{n,\bar{n}} = \mathcal{V}_0^{n,\bar{n}} + \mathcal{V}_1^{n,\bar{n}} + \mathcal{V}_2^{n,\bar{n}} + \dots \quad (2.77)$$

The subscripts indicate the order in the perturbation series. For example,  $\mathcal{V}_2^{n,\bar{n}}$  includes all terms proportional to  $g^2$ ,  $g\epsilon$  and  $\epsilon^2$ . The Feynman rules of this perturbative expansion are those associated with the statistical weight  $e^{-\mathcal{S}}$  in Eq. (2.35) and they are the same as in the white noise case [82, 19], the only difference being in the form of the Gaussian response and correlation functions. In the diagrammatic representation of the perturbation series we shall indicate the relevant propagators and vertices as depicted in Fig. 2.3. Note that the noise vertex  $\Gamma_{i\omega} + \Gamma_{i\omega}^*$  [see Fig. 2.3(d)] is diagonal in frequency space (i.e., it amounts to a multiplication by an  $\omega$ -dependent factor) whereas it is non-local in the time domain. In addition, we point out the fact that in principle the correlation function can be obtained in the frequency domain as a multiplication of two response functions by the noise vertex, which corresponds to a convolution in the time domain.

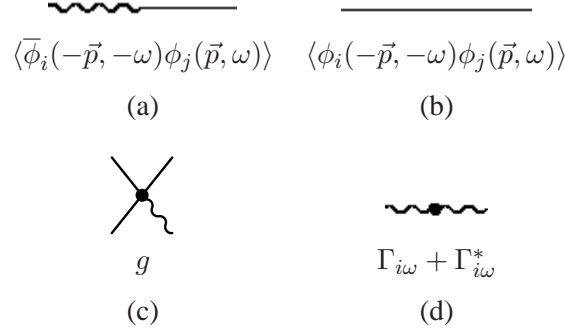


Figure 2.3: Diagrammatic elements of the perturbation theory: (a) response propagator, (b) correlation propagator, (c) interaction vertex and (d) noise vertex. The straight parts of each line are associated to fields  $\phi$ , whereas wiggled lines correspond to  $\bar{\phi}$  fields.

### Renormalization of the noise vertex.

Our interest here is to know whether the correlated noise modifies the critical behavior of the model. Within the Gaussian approximation  $z$  is given by Eq. (2.65), where we assumed that a white-noise vertex is generated under renormalization, a fact that yields two distinct fixed points  $P$  and  $P_w$ : the former is characterized by the colored noise and is stable for  $\alpha < \alpha_c \equiv 1$ , whereas the latter is characterized by the white noise, is stable for  $\alpha > \alpha_c$ , and it reduces to the standard Model A dynamics. We shall show that, on the one hand, expanding around  $P$  (with

<sup>7</sup>Our notation differs from the standard one, that is  $\Gamma^{n,\bar{n}}$  for the 1PI-vertex functions, in order to avoid confusion with the noise kernel.

$\gamma_w = 0$ ) renormalization indeed generates a supplementary white noise vertex  $\gamma_w \neq 0$  and, on the other hand, such a vertex becomes relevant at a  $D$ - and  $N$ -dependent value  $\alpha_c(D, N)$ , where  $\alpha_c(D, N)$  shows corrections to the Gaussian cross-over occurring at  $\alpha_c = 1$  for  $D < 4$ .

The first correction to the noise vertex  $\mathcal{V}_2^{0,2}$  is given by the second-order diagram depicted in Fig. 2.4 which can be conveniently written as the Fourier transform of its expression in the

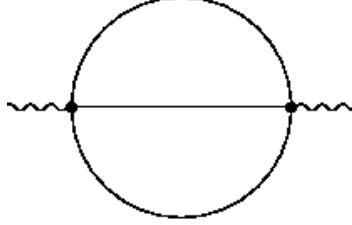


Figure 2.4: Lowest-order perturbative contribution to the noise vertex.

time and space domain

$$\begin{aligned} \mathcal{V}_2^{0,2}(\vec{q}, \sigma) &= -\frac{g^2(N+2)}{18} \int d^D x \int_{-\infty}^{+\infty} dt e^{i\vec{q}\cdot\vec{x}-i\sigma t} C_0^3(\vec{x}, t) \\ &= -\frac{g^2(N+2)}{9} \int_0^\infty dt \cos(\sigma t) \int d^D x e^{i\vec{q}\cdot\vec{x}} C_0^3(\vec{x}, t), \end{aligned} \quad (2.78)$$

where the  $N$ -dependent prefactor accounts for the combinatorics of the graph (see, e.g., [19]) and  $C_0$  is the Gaussian correlation function with  $\gamma_w = 0$ . In the last line of this equation we used the symmetry  $C(\vec{x}, t) = C(\vec{x}, -t)$ . Since we are interested in the critical dynamics, we set  $r$  to its critical value  $r_c = \mathcal{O}(g)$  (determined, e.g., by the value of  $r$  at which  $C(\vec{p} = \vec{0}, t = 0)$  diverges [19, 18, 96]). However, at the order  $g^2$  we are presently interested in, one can neglect the shift of the critical point and set  $r = 0$ . The leading behavior of the noise vertex is completely determined by the small- $q$  and small- $\sigma$  asymptotics of  $\mathcal{V}_2^{0,2}$ . We can set  $q = 0$  from the outset, while the small-frequency limit  $\sigma \rightarrow 0$  has to be considered with care since the tree-level noise vertex  $\mathcal{V}_0^{0,2}(\sigma) = 2\text{Re}\Gamma_{i\sigma}(\gamma_w = 0) = 2\gamma|\sigma|^{\alpha-1} \sin(\pi\alpha/2)$  [see Eq. (2.59)] diverges in this limit for  $\alpha < 1$ . At the end we shall see that no contribution to  $\mathcal{V}_2^{0,2}$  proportional to  $|\sigma|^{\alpha-1}$  is actually generated. In what follows we only take the limit  $\sigma \rightarrow 0$  when it becomes manifestly possible. In this formulation, divergences arise due to the singular behavior of  $C_0$  at small distances and times,  $|\vec{x}| \rightarrow 0$  and  $t \rightarrow 0$ . In order to regularize the theory, we introduce a short-distance cut-off  $\ell$ , below which the description in the continuum is no longer considered to be realistic. For example, in lattice models, the cut-off  $\ell$  is naturally identified with the lattice spacing. Analogously, a short-time cut-off is introduced in the convenient form  $\ell^z$ , which is motivated by the scaling behavior discussed above. By using, c.f., the scaling form Eq. (2.156) of the Gaussian correlation  $C_0$  influenced by the colored noise (see App. B), the second-order contribution to the regularized vertex function takes the form

$$\mathcal{V}_2^{0,2}(\vec{0}, \sigma; \ell) = -\frac{g^2 A_D (N+2)}{9} \int_{\ell^z}^\infty dt \cos(\sigma t) \int_\ell^\infty dx x^{5-2D} g_{C_0}^3(\gamma x^2/t^\alpha), \quad (2.79)$$

where  $A_D = 2\pi^{D/2}/\Gamma_E(D/2)$  is the solid angle in  $D$  dimensions.

**The Wilsonian renormalization scheme.** The Wilsonian renormalization scheme (see, e.g., [18]) amounts to a resummation of the perturbation series which is performed according to the following steps:

(I) Effective vertex functions for the ‘slow’ fluctuations are determined by performing an integration (averaging) over ‘fast’ fluctuations, within a spatial shell between  $\ell$  and  $b\ell$  and at a temporal scale between  $\ell^z$  and  $(b\ell)^z$ . As a result of this integration the effective vertex functions — and therefore the coupling constants which characterize them — acquire a dependence on the scaling parameter  $b > 1$ . To be more specific, consider the typical integral which arises in loop calculations and which can be written in the generic form

$$\mathcal{I}(\ell) = \int_{\ell^z}^{\infty} dt \int_{\ell}^{\infty} d^D x \mathcal{F}(\vec{x}, t),$$

with some integrand  $\mathcal{F}(\vec{x}, t)$ . The contribution of the integration over the fast fluctuations is then equivalent to  $\mathcal{I}(\ell) - \mathcal{I}(b\ell)$ , an expression which we shall use repeatedly below. In the limit  $b \rightarrow 1$  with  $b > 1$  one has  $\mathcal{I}(\ell) - \mathcal{I}(b\ell) = -[\partial\mathcal{I}(\ell)/\partial \ln \ell] \ln b + \mathcal{O}(\ln^2 b)$ .

(II) The effective vertex functions calculated in step (I) depend on a new cut-off  $b\ell$ . In order to recover the original cut-off  $\ell$  one rescales the coordinates and fields in the frequency and momentum domain according to

$$\begin{aligned} \vec{q} &\mapsto b^{-1}\vec{q}, \\ \sigma &\mapsto b^{-z}\sigma, \\ \phi_i &\mapsto b^{D/2+1+z-\eta/2}\phi_i, \\ \bar{\phi}_i &\mapsto b^{D/2+1+z-z_0-\bar{\eta}/2}\bar{\phi}_i. \end{aligned} \tag{2.80}$$

The resulting expression is multiplied by  $b^{-D-z}$  which accounts for the rescaling of the integration measure in the Hamiltonian.

(III) In order to study the evolution of the coupling constants under the renormalization procedure it is convenient to consider the case  $b \rightarrow 1^+$  which corresponds to an infinitely thin integration shell. In this case the evolution equations for the coupling constants are coupled differential equations that depend upon  $\alpha$  and the anomalous dimensions introduced by the rescaling in step (II). The anomalous dimensions are determined by requiring that all coupling constants have a finite asymptotic value under the RG transformation for  $b \rightarrow \infty$ .

**The flow equation of  $z$  and the crossover  $\alpha_c$ .** Applying step (I) to the noise vertex function  $\mathcal{V}_2^{0,2}$  we derive Eq. (2.79) with respect to  $\ln \ell$  and we multiply the result by  $\ln b$ . By defining [see Eq. (2.175)]

$$u^2 \mathcal{E}^{0,2}(\sigma; \gamma) = \frac{\partial \mathcal{V}_2^{0,2}(\vec{0}, \sigma; \ell)}{\partial \ln \ell} \tag{2.81}$$

with

$$u = A_D g / (2\pi)^D, \tag{2.82}$$

we find that the effective noise vertex  $\mathcal{V}_2^{0,2}(\vec{0}, \sigma \rightarrow 0; b\ell)$  for the slow fluctuations with short-time and -distance cut-offs  $b\ell$  and  $(b\ell)^z$ , respectively, is given by

$$\begin{aligned} \mathcal{V}_2^{0,2}(\vec{0}, \sigma \rightarrow 0; b\ell) &= -(\Gamma_{i\sigma \rightarrow 0} + \Gamma_{i\sigma \rightarrow 0}^*) - u^2 \mathcal{E}^{0,2}(0; \gamma) \ln b \\ &\quad + \mathcal{O}(u^2 \ln^2 b, u^3). \end{aligned} \tag{2.83}$$

For details on the calculation of  $\mathcal{E}^{0,2}(\sigma; \gamma)$  we refer to App. 2.4.3.

Clearly, the form of the effective noise vertex has changed, as the term  $\mathcal{E}^{0,2}(0; \gamma)$  generated by the non-Gaussian fluctuations has the form of a white-noise contribution, whereas the coefficient  $\gamma$  of the colored noise is not modified up to this order in perturbation theory. As a result, it is convenient to account for the contribution of a white-noise vertex from the outset, by replacing  $\Gamma_{i\sigma}$  by  $\Gamma_{i\sigma} + \gamma_w$ . This implies that the Gaussian correlation function  $C_0$  that determines the loop correction still has a scaling form but with a scaling function  $g_{C_0}$  that is now a function of two variables, see Eq. (2.163). The correction  $\mathcal{E}^{0,2}$  that is generated depends on both  $\gamma$  and  $\gamma_w$ , we denote it by  $\mathcal{E}^{0,2}(0; \gamma, \gamma_w)$  and we explicitly calculate it in Eq. (2.175).

The effective noise vertex depends on the cut-off  $bl$ . Following step (II) of the renormalization procedure we rescale the effective noise vertex as specified in Eq. (2.80). The coupling strengths of the colored and the white noise  $\gamma$  and  $\gamma_w$  become running coupling constants  $\gamma(b)$  and  $\gamma_w(b)$  and in the limit  $b \rightarrow 1$  they satisfy the set of coupled differential equations

$$\frac{\partial \gamma}{\partial \ln b} = \left[ 2 - \alpha z_0 - \frac{\alpha}{2}(\bar{\eta} - \eta) - \eta \right] \gamma + \mathcal{O}(\epsilon^3) \quad (2.84)$$

and

$$\frac{\partial \gamma_w}{\partial \ln b} = \left[ 2 - z_0 - \frac{\bar{\eta} + \eta}{2} \right] \gamma_w + \frac{z}{2} u^{*2} \mathcal{E}^{0,2}(0; \gamma, \gamma_w) + \mathcal{O}(\epsilon^3), \quad (2.85)$$

valid at the critical point.  $u^* = \mathcal{O}(\epsilon)$  is the fixed point value of the coupling constant, i.e., the value at which the effective coupling constant  $u(b)$  — obtained by applying the procedure outlined here to the 4-point function — flows for  $b \rightarrow \infty$  and  $D < 4$ . For  $D > 4$ ,  $u^* = 0$  and the scenario within the Gaussian approximation presented in Sec. 2.3.2 is not altered by the interaction. Accordingly we focus below on the case  $D < 4$ . Two additional differential equations can be written by considering how the coupling constant  $u$  in  $\mathcal{V}^{1,3}$  and the coefficient of the term  $\propto q^2$  in  $\mathcal{V}^{1,1}(\vec{q}, \dots)$  are modified by the non-Gaussian fluctuations. In particular, the requirement of an effective  $b$ -independent coefficient of  $q^2$  fixes  $\eta$  to its well-known static value [19] (see Sec. 2.3.4 for further details).

In order to determine the critical exponents we demand that the amplitude of the noise vertex in the effective Hamiltonian be constant as explained in step (III) of the renormalization procedure. Neglecting for a while the contribution of the non-Gaussian fluctuations to Eqs. (2.84) and (2.85) (which amounts to setting  $u^*$  and the anomalous dimensions to zero), one can easily solve them and recover the Gaussian picture which we anticipated in Sec. 2.3.2. Indeed,  $\gamma(b) \sim b^{2-\alpha z_0}$  whereas  $\gamma_w(b) \sim b^{2-z_0}$  as  $b \rightarrow \infty$ , which implies  $\gamma(b)/\gamma_w(b) \sim b^{(1-\alpha)z_0}$ . Independently of the value of  $z_0 > 0$ , this ratio tends to zero for  $\alpha > 1$ . The associated fixed point is characterized by a finite  $\gamma_w(b \rightarrow \infty)$  with a vanishing  $\gamma(b \rightarrow \infty)$ , i.e., the fixed point  $P_w$  introduced in Sec. 2.3.2. In order for  $\gamma_w(b)$  to stay finite, it is necessary to have  $z_0 = z_0^{(w)} = 2$  in Eq. (2.85), as expected from our previous discussion. On the contrary, for  $\alpha < 1$ ,  $\gamma(b)/\gamma_w(b) \rightarrow \infty$  for  $b \rightarrow \infty$  and the associated fixed point has a finite  $\gamma(b \rightarrow \infty)$  and a vanishing  $\gamma_w(b \rightarrow \infty)$ , corresponding to the fixed point  $P$  of Sec. 2.3.2. The former condition requires  $z_0 = z_0^{(\text{col})} = 2/\alpha$  in Eq. (2.84), consistently with the discussion therein.

Including now the effects of non-Gaussian fluctuations, the colored-noise fixed point  $P$  with  $z_0 = z_0^{(\text{col})} = 2/\alpha$  and  $\gamma(b \rightarrow \infty) \neq 0$  is characterized by a value of  $\bar{\eta}$  such that the lhs of Eq. (2.84) vanishes. This yields

$$\bar{\eta} = \bar{\eta}^{(\text{col})} \equiv \left( 1 - \frac{2}{\alpha} \right) \eta + \mathcal{O}(\epsilon^3) = \left( 1 - \frac{2}{\alpha} \right) \frac{N+2}{2(N+8)^2} \epsilon^2 + \mathcal{O}(\epsilon^3). \quad (2.86)$$

We replaced  $\eta$  by its static value given in [19, 18] since, as we shall show in Sec. 2.3.4, it is  $\alpha$ -independent. The value  $z^{(\text{col})}$  of  $z$  at this fixed point is determined via Eq. (2.76)

$$z = z^{(\text{col})} = \frac{2 - \eta}{\alpha} + \mathcal{O}(\epsilon^3) = \frac{2}{\alpha} \left[ 1 - \frac{N + 2}{4(N + 8)^2} \epsilon^2 \right] + \mathcal{O}(\epsilon^3). \quad (2.87)$$

The fixed point  $P$  is stable in the  $(\alpha, D)$ -plane (region C in Fig. 2.5) as long as the value of  $\gamma_w(b)$  determined by Eq. (2.85) at the fixed-point  $P$  with  $\bar{\eta} = \bar{\eta}^{(\text{col})}$  and  $z_0 = z_0^{(\text{col})} = 2/\alpha$  stays finite for  $b \rightarrow \infty$ . A crossover towards the fixed-point  $P_w$  in the  $(\alpha, D)$ -plane (region W in Fig. 2.5) controlled by the white noise occurs as soon as  $\gamma_w(b \rightarrow \infty) \rightarrow \infty$ . In this limit,  $\mathcal{E}^{0,2}(0; \gamma, \gamma_w \rightarrow \infty) \simeq \gamma_w \mathcal{E}_w^{0,2}$  independently of  $\gamma$  [as long as  $\gamma(b)$  remains finite, see Eq. (2.179) for details] where the constant  $\mathcal{E}_w^{0,2}$  is given in Eq. (2.180) and is such that

$$u^{*2} \mathcal{E}_w^{0,2} = \frac{N + 2}{(N + 8)^2} 3 \ln \frac{4}{3} \epsilon^2 + \mathcal{O}(\epsilon^3). \quad (2.88)$$

Thus, the equation which determines the evolution of  $\gamma_w$  at the fixed point  $P$  becomes

$$\frac{\partial \gamma_w}{\partial \ln b} = \left[ 2 - z_0^{(\text{col})} - \frac{\bar{\eta}^{(\text{col})} + \eta}{2} + \frac{z^{(\text{col})}}{2} u^{*2} \mathcal{E}_w^{0,2} \right] \gamma_w + \mathcal{O}(u^{*3}), \quad (2.89)$$

and the crossover occurs as soon as the quantity in brackets changes sign. The expression of the crossover line is readily determined by taking into account the values of  $z_0^{(\text{col})}$ ,  $\bar{\eta}^{(\text{col})}$ ,  $z^{(\text{col})}$ , and  $\mathcal{E}_w^{0,2}$  reported in Eqs. (2.86), (2.87), and (2.88):

$$\alpha_c = 1 - \frac{3}{2} \ln \frac{4}{3} \frac{N + 2}{(N + 8)^2} \epsilon^2 + \mathcal{O}(\epsilon^3). \quad (2.90)$$

For  $\alpha > \alpha_c$  (region W in Fig. 2.5),  $\gamma_w(b \rightarrow \infty) \rightarrow \infty$  and the point  $P$  is no longer a fixed point of the rescaled effective action, as the white-noise contribution becomes predominant. In order for it to become constant and therefore to determine the fixed point  $P_w$ ,  $\bar{\eta}$  in Eq. (2.85) should now take the value  $\bar{\eta}^{(\text{w})}$  such that  $\partial \gamma_w / \partial \ln b = 0$ , with  $z_0 = z_0^{(\text{w})} = 2$ . Assuming that the coefficient  $\gamma(b)$  of the colored noise vanishes asymptotically for  $b \rightarrow \infty$ , the lhs of Eq. (2.85) becomes  $-(\bar{\eta}^{(\text{w})} + \eta)/2 + (z/2) u^{*2} \mathcal{E}_w^{0,2}$ , where we used the fact that  $\mathcal{E}^{0,2}(0; \gamma = 0, \gamma_w) = \gamma_w \mathcal{E}_w^{0,2}$ . The condition that the rhs of the same equation vanishes implies

$$\bar{\eta} = \bar{\eta}^{(\text{w})} = -\eta + 2u^{*2} \mathcal{E}_w^{0,2} + \mathcal{O}(\epsilon^3) = \frac{N + 2}{(N + 8)^2} \left[ 6 \ln \frac{4}{3} - \frac{1}{2} \right] \epsilon^2 + \mathcal{O}(\epsilon^3) \quad (2.91)$$

and from Eq. (2.76),

$$z = z^{(\text{w})} = 2 + \frac{N + 2}{(N + 8)^2} \left[ 3 \ln \frac{4}{3} - \frac{1}{2} \right] \epsilon^2 + \mathcal{O}(\epsilon^3) \quad (2.92)$$

in agreement with [75, 19]. In order to verify the consistency of the assumption  $\gamma(b) \rightarrow 0$  for  $b \rightarrow \infty$  under which Eq. (2.91) has been derived, one can specialize Eq. (2.84) to the white-noise fixed point  $P_w$ , by using  $\bar{\eta}^{(\text{w})}$ ,  $z_0^{(\text{w})} = 2$ , and  $z^{(\text{w})}$  [see Eq. (2.92)] as the values of  $\bar{\eta}$ ,  $z_0$ , and  $z$ . Accordingly, the term in parenthesis in the rhs can be written as  $-2(\alpha - \alpha_c) + \mathcal{O}(\epsilon^3)$  and therefore  $\gamma(b) \sim b^{-2(\alpha - \alpha_c)}$  indeed vanishes for  $\alpha > \alpha_c$  as  $b \rightarrow \infty$ . This also proves that the white-noise fixed point  $P_w$  is stable against the perturbation of the colored noise as long as  $\alpha > \alpha_c$ , a statement which complements the one presented above about the stability of  $P$ .

Summarizing, Eq. (2.90) determines the line in the  $(\alpha, D)$ -plane which separates region W from region C: in the former, the white noise dominates and  $z = z^{(w)}$  (in agreement with [75, 19]), whereas in the latter the colored noise dominates and  $z = z^{(col)}$  is given by Eq. (2.87). Figure 2.5 illustrates this scenario for  $N = 1, 4, \infty$ .

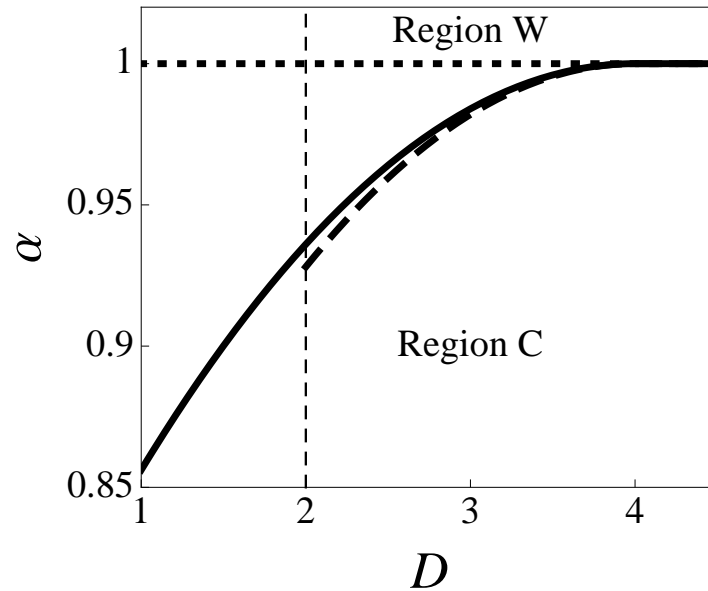


Figure 2.5: Boundary between the regions W and C of the  $(\alpha, D)$ -plane characterized, respectively, by white and colored noise. The boundary curve  $\alpha = \alpha_c(D, N)$  as a function of the spatial dimensionality  $D$  is reported here for  $N = 1$  (solid line, Ising universality class), 4 (dashed), and  $\infty$  (dotted) where the  $\mathcal{O}((4 - D)^3)$ -correction in the corresponding perturbative expression (2.90) for  $D < 4$  has been neglected. The vertical dashed line indicates the lower critical dimensionality of the model for  $N > 1$ . The coefficient of the term  $\mathcal{O}((4 - D)^2)$  in Eq. (2.90) takes its maximum value for  $N = 4$  (dashed curve) and then it decreases monotonically as a function of  $N$ , vanishing for  $N \rightarrow \infty$ . For  $D > 4$ ,  $\alpha_c$  takes the  $D$ -independent Gaussian value  $\alpha_{c,0} = 1$  (dotted line). Clearly, the dependence of the boundary curve on the dimensionality  $D$  is quantitatively rather weak.

### Renormalization of the self-energy and FDT.

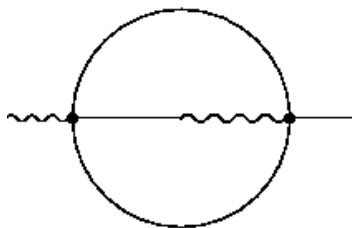


Figure 2.6: Second-order contribution to the self-energy.

The fluctuation-dissipation theorem (FDT) expressed in Eq. (2.40) is a consequence of a symmetry of the action in equilibrium [82, 92] and it has to be preserved under renormalization. Therefore, the noise vertex and the memory kernel have to be related by the FDT even beyond

the Gaussian approximation, that we analyzed in Sec. 2.3.2. Here we explicitly show that this relation is still valid when non-Gaussian corrections up to  $\mathcal{O}(\epsilon^2)$  (or, equivalently,  $\mathcal{O}(g^2)$ ) are accounted for. The first correction to the memory kernel comes from the second-order self-energy contribution

$$\mathcal{V}_2^{1,1}(\vec{q}, \sigma) = -\frac{g^2(N+2)}{6} \int_0^\infty dt \int d^D x e^{i\vec{q}\cdot\vec{x}-i\sigma t} C_0^2(\vec{x}, t) R_0(\vec{x}, t) \quad (2.93)$$

represented in Fig. 2.6. Note that  $R_0$  is causal and restricts the time integral to run over positive values only. The expansion of this expression as a power series in  $\sigma$  and  $\vec{q}$  allows one to identify the terms which contribute to the renormalization of the different parameters of the Gaussian vertex  $\mathcal{V}_0^{1,1}(\vec{q}, \sigma) = i\sigma\Gamma_{i\sigma} + q^2 + r$ . The terms which are independent of both  $\sigma$  and  $\vec{q}$  contribute to the renormalization of the parameter  $r$  (which is also modified by an  $\mathcal{O}(g)$  term not discussed here), the terms proportional to  $\sigma^0 q^2$  contribute to the renormalization of the fields and those proportional to  $i\sigma^1 q^0$  to the renormalization of the memory kernel  $\Gamma$ . First of all we observe that the FDT given in Eq. (2.40) allows us to express  $R_0$  in Eq. (2.93) as  $-\partial_t C_0$ . An integration by parts yields

$$\mathcal{V}_2^{1,1}(\vec{q}, \sigma) = -\frac{g^2(N+2)}{18} \int d^D x e^{i\vec{q}\cdot\vec{x}} \left\{ C_0^3(\vec{x}, 0) - i\sigma \int_0^\infty dt e^{-i\sigma t} C_0^3(\vec{x}, t) \right\}. \quad (2.94)$$

Hence,

$$\begin{aligned} \text{Im } \mathcal{V}_2^{1,1}(\vec{q}, \sigma) &= \sigma \frac{g^2(N+2)}{18} \text{Re} \int d^D x e^{i\vec{q}\cdot\vec{x}} \int_0^\infty dt e^{-i\sigma t} C_0^3(\vec{x}, t) \\ &= -\frac{\sigma}{2} \mathcal{V}_2^{0,2}(\vec{q}, \sigma), \end{aligned} \quad (2.95)$$

where the last equality follows from a comparison with Eq. (2.78) and shows that the FDT in the frequency domain [see Eq. (2.62)] is satisfied by the corrections  $\mathcal{O}(g^2)$ . Note that the vertex  $\mathcal{V}^{1,1}$  receives also a correction  $\mathcal{V}_1^{1,1}$  of  $\mathcal{O}(g)$  given by a tadpole diagram which, however, is a real constant and does not contribute to the imaginary part. We conclude that up to and including the second order in the coupling constant  $2 \text{Im } \mathcal{V}^{1,1}(\vec{0}, \sigma) = -\sigma \mathcal{V}^{0,2}(\vec{0}, \sigma)$ . (This proof can be readily extended to the corresponding regularized vertex functions, characterized by short- and distance cut-offs.)

### Renormalization of the self-energy: the anomalous exponent $\eta$ .

In the same spirit as before we can deduce the first correction to the static exponent  $\eta$ . It is instructive to see why the dependence upon  $\alpha$  does not affect the final result, even though the regularized expression of Eq. (2.93) does via  $C_0$  and  $R_0$ . In order to single out the contribution of  $\mathcal{V}_2^{1,1}$  to the coefficient of  $q^2$ , one expands Eq. (2.93) — suitably regularized as discussed above — up to second order in  $\vec{q}$ , finding

$$\mathcal{V}_2^{1,1}(\vec{q}, \sigma = 0; \ell) = \frac{1}{2} q^2 g^2 \frac{N+2}{6} \frac{A_D}{D} \int_{\ell z}^\infty dt \int_{\ell}^\infty dx x^{D+1} C_0^2(\vec{x}, t) R_0(\vec{x}, t) + \dots, \quad (2.96)$$

where the dots indicate all the terms which do not contribute to the field renormalization, i.e., which are not proportional to  $\sigma^0 q^2$ . In Eq. (2.96) we used the fact that, for a generic function  $f$ ,  $\int d^D x x_i x_j f(|\vec{x}|) = (\delta_{ij}/D) \int d^D x |\vec{x}|^2 f(|\vec{x}|)$ , which is valid also for the regularized integral.

As in the case of Eq. (2.94) one can take advantage of the FDT, Eq. (2.40), to express the integrand in Eq. (2.96) as a total derivative, which can be integrated to yield

$$\mathcal{V}_2^{1,1}(\vec{q}; 0; \ell) = q^2 g^2 \frac{A_D(N+2)}{36D} \int_{\ell}^{\infty} dx x^{D+1} C_0^3(\vec{x}, \ell^z) + \dots \quad (2.97)$$

We note here that even though the (full) dynamic correlation function  $C$  (and therefore its Gaussian approximation  $C_0$ ) depends on the value of  $\alpha$ , the static correlation function  $C(\vec{x}, t = 0)$  does not. This is explicitly shown for  $C_0$  in Eq. (2.155). While the limit  $\ell \rightarrow 0$  of the rhs of Eq. (2.97) cannot be explicitly taken due to the short-distance singularity of the integrand, such a limit can be taken for the correlation function, i.e.,  $C_0(\vec{x}, t = \ell^z) \simeq C_0(\vec{x}, t = 0)$  and therefore the expression of  $\mathcal{V}_2^{1,1}(\vec{q}; 0; \ell \rightarrow 0)$  becomes — as expected — independent of  $\alpha$  at the leading relevant order in  $\ell$ . Applying the same renormalization procedure as in Sec. 2.3.4, Eq. (2.97) can be used to calculate the effective vertex  $\mathcal{V}_2^{1,1}(\vec{q}; 0; b\ell)$  after having integrated out the fast fluctuations. Similarly to Eq. (2.81) one defines

$$q^2 u^2 \mathcal{E}^{1,1} + \dots = -\frac{\partial \mathcal{V}_2^{1,1}(\vec{q}; 0; \ell)}{\partial \ln \ell}, \quad (2.98)$$

For  $b \rightarrow 1$ , the resulting effective vertex is

$$\mathcal{V}_2^{1,1}(\vec{q}; 0; b\ell) = q^2 + q^2 u^2 \mathcal{E}^{1,1} \ln b + \mathcal{O}(u^2 \ln^2 b, u^3) + \dots \quad (2.99)$$

In order to recover the original cut-off  $\ell$  we rescale the fields and coupling constants according to (2.80) and we take  $b \rightarrow 1$ . The part of  $\mathcal{V}_2^{1,1}(\vec{q}; 0; \ell)$  that is proportional to  $\sigma^0 q^2$  satisfies the evolution equation

$$\frac{\partial \mathcal{V}_2^{1,1}}{\partial \ln b} = -q^2 \left[ \eta - u^{*2} \mathcal{E}^{1,1} \right] + \mathcal{O}(u^2 \ln b, u^3) + \dots \quad (2.100)$$

By demanding that the amplitude of  $\mathcal{V}_2^{1,1}$  be constant and by using the numerical value of  $\mathcal{E}^{1,1}$  calculated in Eq. (2.182) we find

$$\eta = u^{*2} \mathcal{E}^{1,1} = \frac{N+2}{2(N+8)^2} \epsilon^2 + \mathcal{O}(\epsilon^3), \quad (2.101)$$

i.e.,  $\eta$  has the same  $\alpha$ -independent value as in the static theory confirming our expectations alluded to at the beginning of Sec. 2.3.1.

### 2.3.5 Non-equilibrium dynamics

#### Preliminary remarks

In this Section we investigate the non-equilibrium dynamics assuming that the model is prepared in some initial condition at time  $t = 0$  and that it is let relax subsequently at its critical point. This problem has been studied in detail in the white-noise case [82, 85]. The analysis reveals the emergence of an interesting scaling behavior of two-time quantities, usually referred to as *aging* (see, in this context, [86, 91, 15]). More precisely, the relaxation is studied via the field-theoretical action  $\mathcal{S}$  in Eqs. (2.36) and (2.37) with  $T = 0$ , supplemented by a suitable distribution  $\mathcal{P}_{IC}$  for the initial condition at time  $t = T = 0$ . In particular, a high-temperature disordered state is modeled by a Gaussian distribution with zero mean:

$$\ln \mathcal{P}_{IC} = - \int d^D x \frac{\tau_0}{2} \phi^2(\vec{x}, t = 0) \quad (2.102)$$

The parameter  $\tau_0$  sets the inverse width of the initial distribution. Within the Gaussian approximation, the field  $\phi$  has a scaling dimension  $d_{\phi,0}$  given by Eq. (2.65) in momentum and frequency space, i.e., a dimension  $d_{\phi,0} - z_0 - D$  in the space and time domain. Using this dimension for the initial field  $\phi(\vec{x}, t = 0)$  we find that  $\tau_0 \rightarrow b^2 \tau_0$  under rescaling. Consequently, the width of the initial distribution shrinks to zero as  $b \rightarrow \infty$ , leading to a zero effective value of the initial order parameter  $\phi(\vec{x}, t = 0) = 0$  and, therefore, to a correlation function with Dirichlet boundary conditions at  $t = 0$ . In App. 2.4.4 [see Eqs. (2.187) and (2.164)] we show that the Laplace transforms of the Gaussian propagators are:

$$R_0(\vec{p}; \lambda, \kappa) = \frac{1}{(\lambda + \kappa)(\lambda \Gamma_\lambda + p^2 + r)}, \quad (2.103)$$

$$C_0(\vec{p}; \lambda, \kappa) = \frac{\Gamma_\lambda + \Gamma_\kappa}{(\lambda + \kappa)(\lambda \Gamma_\lambda + p^2 + r)(\kappa \Gamma_\kappa + p^2 + r)}, \quad (2.104)$$

where the Laplace transformed noise is  $\Gamma_\lambda = \gamma \lambda^{\alpha-1} + \gamma_w$  with  $\lambda \in \mathcal{R}_+$ . [In order to transform Eq. (2.34) for  $\alpha > 1$  one should introduce a short-time cut-off. However, as we pointed out after Eq. (2.59), this modification is not necessary as long as one is interested in the leading long-time, near critical dynamic behavior of the system. Accordingly, we shall use this form for  $\Gamma_\lambda$  irrespective of the value of  $\alpha$ .] As in the equilibrium case, the propagators have a simple analytic form in the time domain only for  $\alpha = 1$  or  $\gamma_w = 0$ . It is easy to show that the response propagator is the same in and out of equilibrium and, therefore, that it is time-translationally invariant.

The correlation function  $C_0$  can always be written as the sum of the Gaussian equilibrium correlation  $C_0^{(e)}$  and the remaining non-equilibrium contribution, which we denote by  $C_0^{(ne)}$  and which will play an important role in fixing the genuinely non-equilibrium properties of the relaxation, e.g., the non-equilibrium exponent  $\theta$  and the effective temperature. The Laplace transform  $C_0^{(e)}(\vec{p}, \lambda)$  of the equilibrium correlation function  $C_0^{(e)}(\vec{p}, t)$  can be obtained from Eq. (2.172):

$$C_0^{(e)}(\vec{p}, \lambda) = \frac{1}{p^2 + r} \frac{\Gamma_\lambda}{\lambda \Gamma_\lambda + p^2 + r}. \quad (2.105)$$

The full non-equilibrium correlator (2.104) can be expressed as

$$C_0(\vec{p}, \lambda, \kappa) = \frac{C_0^{(e)}(\vec{p}, \lambda) + C_0^{(e)}(\vec{p}, \kappa)}{\lambda + \kappa} - (p^2 + r) C_0^{(e)}(\vec{p}, \lambda) C_0^{(e)}(\vec{p}, \kappa), \quad (2.106)$$

which displays the fact that  $C_0$  is the sum of an equilibrium time-translationally invariant term and a non-stationary term. Indeed, the Laplace transform  $\mathcal{L}[F](\lambda, \kappa)$  with respect to both  $t$  and  $t'$  of any (translationally invariant) function  $F(|t-t'|)$  is given by  $\mathcal{L}[F](\lambda, \kappa) = (F_\lambda + F_\kappa)/(\lambda + \kappa)$ , which is exactly the form of the first term in Eq. (2.106) [48]. Accordingly, we can identify the non-equilibrium part  $C_0^{(ne)}$  of  $C_0$  as  $C_0^{(ne)}(\vec{p}, \lambda, \kappa) \equiv -(p^2 + r) C_0^{(e)}(\vec{p}, \lambda) C_0^{(e)}(\vec{p}, \kappa)$  which translates, by virtue of Eq. (2.172), into the non-stationary expression ( $t, t' > 0$ )

$$C_0^{(ne)}(\vec{p}; t, t') = -\frac{1}{p^2 + r} E_\alpha(-(p^2 + r)t^\alpha/\gamma) E_\alpha(-(p^2 + r)t'^\alpha/\gamma), \quad (2.107)$$

where we wrote the equilibrium Gaussian correlation function in terms of the Mittag-Leffler function, anticipated in Eq. (2.64) and discussed in App. 2.4.2.

### General non-equilibrium renormalization group analysis

The addition of the initial condition to the action modifies the scaling of the fields at the boundary  $t = 0$  compared to the one in the ‘time bulk’  $t > 0$  [82]. In addition, to the bulk renormalization a new initial time renormalization is required, which gives rise to contributions ‘located’ at the time surface (that is the hyperplane determined by the condition  $t = 0$ ). These can be absorbed by introducing a new anomalous dimension of the initial field  $\bar{\phi}_0(\vec{p}) \equiv \bar{\phi}(\vec{p}, 0)$  (see [97] for an application to surface critical phenomena). The general scaling of the initial fields in the time and momentum domain reads [cf. Eqs. (2.74) and (2.75)]

$$\begin{aligned}\phi(b^{-1}\vec{p}, t = 0) &\mapsto b^{D/2+1-\eta/2} \phi(\vec{p}, 0), \\ \bar{\phi}(b^{-1}\vec{p}, t = 0) &\mapsto b^{D/2+1-z_0-\bar{\eta}/2-\bar{\eta}_{\text{in}}/2} \bar{\phi}(\vec{p}, 0),\end{aligned}\quad (2.108)$$

where  $\bar{\eta}_{\text{in}}$  is a new exponent, with a Gaussian value  $\bar{\eta}_{\text{in},0} = 0$ . Note that the anomalous dimension of the initial response field  $\bar{\phi}(\vec{p}, 0)$  is allowed to differ by  $\bar{\eta}_{\text{in}}$  from its bulk value. In [82, 86] one can find a careful analysis for the white-noise case where it is explained why only the initial response field has to be renormalized. Here, we make the same assumption and we check its validity *a posteriori*.  $\bar{\eta}_{\text{in}}$  is related to the so-called initial-slip exponent  $\theta$  [introduced at the end of Sec. 3.2, see (2.41) and (2.42)] by [82]

$$\theta = -\bar{\eta}_{\text{in}}/(2z). \quad (2.109)$$

The analysis in [82, 86] has to be slightly modified to deal with colored noise. Our starting point is the general leading scaling behavior of the critical correlation functions  $\mathcal{G}^{n,\bar{n},\bar{n}_0}$  of  $n$  bulk fields  $\phi$ ,  $\bar{n}$  bulk response fields  $\bar{\phi}$  and  $\bar{n}_0$  initial response fields  $\bar{\phi}_0$ , evaluated at the set of points  $\{\vec{p}, t\}$  in momentum and time:

$$\mathcal{G}^{n,\bar{n},\bar{n}_0}(\{\vec{p}, t\}) \simeq b^{-\delta(n,\bar{n},\bar{n}_0)} \mathcal{G}^{n,\bar{n},\bar{n}_0}(\{b^{-1}\vec{p}, b^z t\}), \quad (2.110)$$

where  $\delta(n,\bar{n},\bar{n}_0) = -D + n(D/2 + 1 - \eta/2) + \bar{n}(D/2 + 1 - z_0 - \bar{\eta}/2) + \bar{n}_0(D/2 + 1 - z_0 - \bar{\eta}/2 - \bar{\eta}_{\text{in}}/2)$ . [In writing Eq. (2.110) and the analogous relations presented below, we always understand that the correlation functions on the lhs and rhs are characterized by the different length cut-offs  $b\ell$  and  $\ell$ , respectively.] This scaling behavior is a consequence of the scaling dimensions of the fields  $\phi$ ,  $\bar{\phi}$  and  $\bar{\phi}_0$  as functions of time and momentum [compare to Eqs. (2.74), (2.75) and (2.108)] and the dimension of the  $\delta$ -function ensuring the total momentum conservation. Note that all correlation functions with an initial field  $\phi_0 \equiv \phi(\vec{p}, 0)$  vanish [see the discussion at the end of Sec. 2.3.5]. Specifically, the two point correlation and response functions ( $\mathcal{G}^{2,0,0}$  and  $\mathcal{G}^{1,1,0}$ , respectively) scale as

$$C(\vec{p}; t, t') \simeq b^{\eta-2} C(\vec{p}/b; b^z t, b^z t'), \quad (2.111)$$

$$R(\vec{p}; t, t') \simeq b^{z_0-2+\eta/2+\bar{\eta}/2} R(\vec{p}/b; b^z t, b^z t'). \quad (2.112)$$

By choosing  $b = (t - t')^{-1/z}$  these scaling forms become

$$\begin{aligned}C(\vec{p}; t, t') &\simeq (t - t')^{(2-\eta)/z} \tilde{F}_C((t - t')^{1/z} \vec{p}, t'/t), \\ R(\vec{p}; t, t') &\simeq (t - t')^{(2-z-\eta)/z} \tilde{F}_R((t - t')^{1/z} \vec{p}, t'/t).\end{aligned}\quad (2.113)$$

In general the scaling functions  $\tilde{F}_C$  and  $\tilde{F}_R$  are not expected to have a finite, non-vanishing value for  $t' \rightarrow 0$ . In order to deduce their behavior for small  $t'$  we employ a short-distance expansion

[19] of the fields  $\phi(\vec{p}, t')$  and  $\bar{\phi}(\vec{p}, t')$  around  $t' = 0$ . However, these are not independent. Indeed, the full correlation and linear response functions verify the equations [82]

$$C(\vec{p}; t, t') = \int_0^t ds \int_0^s ds' R_0(\vec{p}; t, s) \tilde{\mathcal{V}}^{1,1}(\vec{p}, s, s') C_0(\vec{p}; t', s') \quad (2.114)$$

$$+ \int_0^{t'} ds' \int_0^{s'} ds C_0(\vec{p}; t, s) \tilde{\mathcal{V}}^{1,1}(\vec{p}, s', s) R_0(\vec{p}; t', s') \quad (2.115)$$

$$+ \int_0^t ds \int_0^{t'} ds' R_0(\vec{p}; t, s) \tilde{\mathcal{V}}^{0,2}(\vec{p}, s, s') R_0(\vec{p}; t', s') \quad (2.116)$$

and

$$R(\vec{p}; t, t') = \int_{t'}^t ds \int_{t'}^s ds' R_0(\vec{p}; t, s) \tilde{\mathcal{V}}^{1,1}(\vec{p}, s, s') R_0(\vec{p}; s', t'), \quad (2.117)$$

where  $\tilde{\mathcal{V}}^{n,\bar{n}}$  are the (not necessarily one particle irreducible in contrast to the ones introduced in Sec. 2.3.4) vertex functions with  $n$  amputated external field and  $\bar{n}$  amputated external response field legs, respectively. In writing these expressions we accounted for the causality of  $\tilde{\mathcal{V}}^{1,1}(\vec{p}, s, s') \propto \Theta(s - s')$ . After taking the derivative of Eq. (2.114) with respect to  $t'$  only the first term in the rhs survives in the limit  $t' \rightarrow 0$  [note that  $R_0(\vec{p}; s, s) = 0$  [92]]. By comparing the resulting expression with the rhs of Eq. (2.117) one notices that the equations differ only by the last factor in their integrands,  $\partial_{t'} C_0(\vec{p}; t', s')$  and  $R_0(\vec{p}; s', t')$ , respectively. We deduce that if a relation between the dimensions of the time-derivative of the initial field and the initial response field exists within the Gaussian approximation, it should be preserved when non-Gaussian fluctuations are accounted for. Let us then examine the propagators. We focus on region C where they satisfy the equation,

$$\partial_{t'} C_0(\vec{p}; t, t' \rightarrow 0) \simeq t'^{\alpha-1} \int_0^t ds \Gamma(t-s) R_0(\vec{p}; s, t' \rightarrow 0) \quad (2.118)$$

[proven in App. 2.4.4, see Eq. (2.190)]. In the early  $t'$  limit we formally expand the fields according to

$$\phi(\vec{p}, t' \rightarrow 0) \sim \varphi(t') \dot{\phi}_0(\vec{p}) \quad \text{and} \quad \bar{\phi}(\vec{p}, t' \rightarrow 0) \sim \bar{\varphi}(t') \bar{\phi}_0(\vec{p}). \quad (2.119)$$

$\phi$  is proportional to  $\dot{\phi}_0(p)$  and  $\bar{\phi}$  is proportional to  $\bar{\phi}_0(p)$  since the former vanishes while the latter is allowed to be finite for  $t' \rightarrow 0$ . We see from Eq. (2.118) that, under the rescaling  $t \rightarrow b^z t$ ,  $s \rightarrow b^z s$  and  $p \rightarrow p/b$  (leaving  $t'$  unchanged), the scaling dimensions  $d_{\dot{\phi}_0}$  and  $d_{\bar{\phi}_0}$  of  $\dot{\phi}_0$  and  $\bar{\phi}_0$ , respectively, verify

$$d_{\dot{\phi}_0} = z(1 - \alpha) + d_{\bar{\phi}_0}. \quad (2.120)$$

For  $\alpha = 1$  this reduces to the relation found in [82]. The expansion of  $\bar{\phi}$  in Eq. (2.119) can be used to calculate the correlation function  $\mathcal{G}^{1,1,0}(\vec{p}; t, t' \rightarrow 0) \sim \bar{\varphi}(t') \mathcal{G}^{1,0,1}(\vec{p}; t)$  and by matching the scaling dimensions of the lhs and rhs with the help of Eq. (2.110) we conclude that  $\bar{\varphi}(t') \sim t'^{-\theta}$  where  $\theta$  is given by Eq. (2.109). Besides, the rescaling of  $t'$  (keeping  $t$  and  $s$  unchanged) implies  $\varphi(t') \sim t'^{\alpha-\theta}$  if the scaling dimensions of the lhs and rhs in Eq. (2.118) are to match. Hence, the small- $t'$  limit of the response function is

$$R(\vec{p}; t, t' \rightarrow 0) \sim \bar{\varphi}(t') \langle \phi(-\vec{p}, t) \bar{\phi}_0(\vec{p}) \rangle \sim t'^{-\theta} \mathcal{G}^{1,0,1}(\vec{p}, t), \quad (2.121)$$

where we introduced a short-hand notation for the arguments of  $\mathcal{G}^{1,0,1}$  in which we only write the non-vanishing time  $t$ . The scaling properties of  $\mathcal{G}^{1,0,1}(\vec{p}, t)$  are given by Eq. (2.110):

$$\begin{aligned}\mathcal{G}^{1,0,1}(\vec{p}, t) &\simeq t^{-(\eta/2+\bar{\eta}/2+\bar{\eta}_{\text{in}}/2+z_0-2)/z} \mathcal{G}^{1,0,1}(t^{1/z}\vec{p}, 1) \\ &= t^{(2-\eta-z)/z+\theta} \mathcal{G}^{1,0,1}(t^{1/z}\vec{p}, 1)\end{aligned}\quad (2.122)$$

where we used the relation between anomalous and dynamic exponents, Eq. (2.76), and the relation between  $\theta$  and  $\bar{\eta}_{\text{in}}$ , Eq. (2.109). Consequently, taking Eqs. (2.113), (2.120) and (2.122) into account, we conclude that

$$R(\vec{p}; t, t' \rightarrow 0) \simeq t^{(2-z-\eta)/z} \left(\frac{t}{t'}\right)^\theta F_R(t^{1/z}\vec{p}, 0). \quad (2.123)$$

A similar analysis of the scaling behavior of the correlation, taking into account Eq. (2.120), yields

$$C(\vec{p}; t, t' \rightarrow 0) \simeq t^{(2-\eta)/z} \left(\frac{t}{t'}\right)^{\theta-\alpha} F_C(t^{1/z}\vec{p}, 0). \quad (2.124)$$

These results are used to capture the singular behavior of the scaling functions in Eq. (2.113) by writing:

$$R(\vec{p}; t, t') \simeq (t-t')^{(2-z-\eta)/z} \left(\frac{t}{t'}\right)^\theta F_R((t-t')^{1/z}\vec{p}, t'/t), \quad (2.125)$$

$$C(\vec{p}; t, t') \simeq (t-t')^{(2-\eta)/z} \left(\frac{t}{t'}\right)^{\theta-\hat{\alpha}} F_C((t-t')^{1/z}\vec{p}, t'/t), \quad (2.126)$$

with

$$\hat{\alpha} = \begin{cases} 1 & \text{for } \alpha \geq \alpha_c(D, N), \\ \alpha & \text{for } \alpha < \alpha_c(D, N), \end{cases} \quad (2.127)$$

which encompass the white noise result  $\hat{\alpha} = 1$  [82] for  $\alpha \geq \alpha_c$ . The scaling functions  $F_C$  and  $F_R$  are regular for  $t' \rightarrow 0$  and depend on  $\alpha$ . Moreover, in the RG sense they are universal functions up to an overall amplitude and the normalization of their first argument.

The emergence of  $\hat{\alpha} \neq 1$  for colored noise can be checked within the Gaussian approximation by looking at the initial-slip behavior of the propagators  $R_0$  and  $C_0$  with  $\alpha < 1$ . First of all, note that  $\theta$  takes the value  $\theta_0 = 0$  within the Gaussian theory, as one can infer by comparing the scaling form (2.125) with the expression for the non-equilibrium response  $R_0$  at criticality, which coincides with the equilibrium one in Eq. (2.63) and is invariant under time translations. Using this value  $\theta_0$  of  $\theta$  one has  $\lim_{\kappa \rightarrow \infty} \kappa C_0(\vec{p}; \lambda, \kappa) \sim \kappa^{-\alpha}$  and  $\lim_{\kappa \rightarrow \infty} \kappa R_0(\vec{p}; \lambda, \kappa) \sim \kappa^0$  from Eqs. (2.103) and (2.104), respectively.

**The initial-slip exponent  $\theta$ .** Out of equilibrium the first correction to the self energy leads to a modification of the scaling of the initial response field. The response function up to first order in the perturbative expansion reads, for zero external momentum,

$$R(\vec{0}; t, t'; \ell) = R_0(\vec{0}; t, t') + \int_{t'}^t ds R_0(\vec{0}; t, s) B_{\ell-1}(s) R_0(\vec{0}; s, t'). \quad (2.128)$$

$B_{\ell^{-1}}(s)$  stands for the ‘tadpole’ diagram represented in Fig. 2.7, which can be calculated by using standard Feynman rules in the time domain [73, 74, 79], whereas  $\ell^{-1}$  is the large-momentum cut-off introduced in order to regularize the otherwise divergent integral defining  $B_{\ell^{-1}}(s)$ :

$$B_{\ell^{-1}}(s) = -\frac{g(N+2)}{6} \int_{|\vec{p}| < \ell^{-1}} \frac{d^D p}{(2\pi)^D} C_0(\vec{p}; s, s). \quad (2.129)$$

The renormalization of the initial response field is due to the non-equilibrium part  $C_0^{(\text{ne})}$  of  $C_0$ .

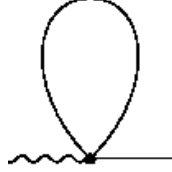


Figure 2.7: First order contribution to the non-equilibrium self-energy.

Indeed, the equilibrium part  $C_0^{(\text{e})}$  is characterized by time-translation invariance and therefore it contributes with a time-independent function of  $\vec{p}$  to  $C_0(\vec{p}; s, s)$  in Eq. (2.129). In turn, such a function results in a time-independent contribution  $B_{\ell^{-1}}^{(\text{e})}$  to  $B_{\ell^{-1}}$ , which can be thought of as due to a shift  $r \mapsto r - B_{\ell^{-1}}^{(\text{e})}$  of the mass  $r$  in the expression of the response functions  $R_0$  appearing in the rhs of Eq. (2.128), i.e., as a mass renormalization. [We recall that  $R_0(\vec{p}; t, t')$  actually depends on the two times via  $t - t'$ .] One can check that this term yields the correct first order correction to the critical exponent  $\nu$  which is the same as in the static theory.

In view of the renormalization procedure outlined in Sec. 2.3.4 we need to calculate

$$\ell^{-1} \partial_{\ell^{-1}} B_{\ell^{-1}}(t) = -\frac{u(N+2)}{6} \ell^{-4} C_0^{(\text{ne})}(|\vec{p}| = \ell^{-1}; t, t) \quad (2.130)$$

in the limit  $\ell \rightarrow 0$ , for  $r = 0$  and  $D = 4$ . By using the asymptotic expansion of the generalized Mittag-Leffler functions (2.170) and their definition, (2.169), one finds

$$E_\alpha(x) = E_{\alpha,1}(x) = \begin{cases} (-x)^{-1}/\Gamma_E(1-\alpha) & \text{for } x \rightarrow -\infty \\ E_\alpha(0) = 1 & \text{for } |x| \ll 1 \end{cases} \quad (2.131)$$

and therefore, using Eq. (2.107),

$$\ell^{-4} C_0^{(\text{ne})}(\ell^{-1}; t, t) = -\ell^{-2} E_\alpha^2(-t^\alpha/(\gamma\ell^2)) = \begin{cases} \mathcal{O}(\ell^2/t^{2\alpha}) & \text{for } \ell^{-2}t^\alpha/\gamma \gg 1, \\ \mathcal{O}(\ell^{-2}) & \text{for } \ell^{-2}t^\alpha/\gamma \ll 1. \end{cases} \quad (2.132)$$

Accordingly,  $\ell^{-1} \partial_{\ell^{-1}} B_{\ell^{-1}}(t) \rightarrow 0$  in the limit  $\ell \rightarrow 0$  for every fixed  $t > 0$ . The physical interpretation of this fact is that only the initial field is renormalized by Eq. (2.128). Indeed the rhs of Eq. (2.132) for finite  $\ell$  provides an approximation of the delta distribution restricted to  $z \in \mathbb{R}^+$ , usually denoted by  $\delta_+(z)$ :

$$(\gamma\ell^2)^{-1} E_\alpha^2(-z/(\gamma\ell^2)) \longrightarrow \frac{d(\alpha)}{2} \delta_+(z) \quad \text{for } \ell \rightarrow 0, \quad (2.133)$$

where the normalization constant  $d(\alpha)$  is given by

$$d(\alpha) = 2 \int_0^\infty dz E_\alpha^2(-z), \quad (2.134)$$

and the additional factor  $1/2$  on the rhs of Eq. (2.133) has been introduced for later convenience in order to have  $d(1) = 1$ . Taking advantage of the closed-form expressions of the Mittag-Leffler function for  $\alpha = 1, 1/2$ , and  $0$ , i.e.,  $E_1(-z) = \exp(-z)$ ,  $E_{1/2}(-z) = (2/\sqrt{\pi}) \int_z^\infty dt e^{z^2-t^2}$ , and  $E_0(-z) = 1/(1+z)$  [98], respectively, it is possible to calculate the corresponding values of the  $\alpha$ -dependent constant  $d(\alpha)$ . One finds  $d(1) = 1$ ,  $d(0) = 2$  and, after some algebra,  $d(1/2) = \sqrt{2/\pi} \ln(3 + 2\sqrt{2}) = 1.406\dots$  Hence,

$$\frac{\partial B_{\ell-1}(t)}{\partial \ln \ell^{-1}} \longrightarrow \frac{u\gamma(N+2)d(\alpha)}{12} \delta_+(t^\alpha) \quad \text{for } \ell \rightarrow 0. \quad (2.135)$$

Using this expression and the one of the zero-momentum response function  $R_0(\vec{0}; t, s) = (t-s)^{\alpha-1}/[\gamma\Gamma_E(\alpha)]$  at criticality which follows from Eq. (2.168), the derivative of the tadpole contribution to the rhs of Eq. (2.128) can be written as

$$\frac{\partial}{\partial \ln \ell^{-1}} \int_s^t ds R_0(\vec{0}; t, s) B_{\ell-1}(s) R_0(\vec{0}; s, t') = \delta_{t',0} \frac{u(N+2)}{12} \frac{d(\alpha)}{\alpha\Gamma_E(\alpha)} R_0(\vec{0}; t, t') \quad (2.136)$$

where  $\delta_{t',0} = 1$  for  $t' = 0$  and  $0$  otherwise, illustrating the fact that only the initial field is renormalized. In deriving this last equation we used the fact that  $\delta_+(t^\alpha) = \delta_+(t)/(\alpha t^{\alpha-1})$ . Altogether, the effective response function with cut-off  $b\ell$  reads

$$R(\vec{0}; t, t'; b\ell) = R_0(\vec{0}; t, t') \left[ 1 + \delta_{t',0} \frac{u(N+2)d(\alpha)}{12\alpha\Gamma_E(\alpha)} \ln b \right]. \quad (2.137)$$

In order to recover the original cut-off  $\ell$  we make use of the scaling relation (2.110) with  $t' = 0$ . By taking into account that  $\eta = \bar{\eta} = \mathcal{O}(\epsilon^2)$  we have

$$R(\vec{0}; t, 0; b\ell) \simeq b^{-2+z_0+\bar{\eta}_{\text{in}}/2} R(\vec{0}; b^z t, 0; \ell) \quad (2.138)$$

$$= R_0(\vec{0}; t, 0) b^{\bar{\eta}_{\text{in}}/2} \left[ 1 + \frac{u(N+2)d(\alpha)}{12\alpha\Gamma_E(\alpha)} \ln b \right] \quad (2.139)$$

$$= R_0(\vec{0}; t, 0) \left[ 1 + \frac{\bar{\eta}_{\text{in}}}{2} \ln b + \frac{u(N+2)d(\alpha)}{12\alpha\Gamma_E(\alpha)} \ln b \right]. \quad (2.140)$$

By requiring that the amplitude of the response function be constant at the fixed point  $u^*$  we obtain

$$\bar{\eta}_{\text{in}} = -\frac{(N+2)d(\alpha)}{(N+8)\alpha\Gamma_E(\alpha)} \epsilon + \mathcal{O}(\epsilon^2) \quad (2.141)$$

whence we find the  $\alpha$ -dependent initial slip exponent from Eq. (2.109)

$$\theta = -\frac{\alpha}{4} \bar{\eta}_{\text{in}} = \frac{(N+2)d(\alpha)}{4(N+8)\Gamma_E(\alpha)} \epsilon + \mathcal{O}(\epsilon^2). \quad (2.142)$$

In the white noise case  $\alpha = 1$  we obtain  $\theta = (N+2)\epsilon/[4(N+8)] + \mathcal{O}(\epsilon^2)$  in agreement with the first order result reported in [82]. The dependence of  $\theta$  on  $\alpha$  is shown in Fig. 2.8.  $\theta$  increases monotonically from  $\theta = 0$  at  $\alpha = 0$  to  $\theta = \theta(1)$  at  $\alpha = 1$  which is the cross-over value up to  $\mathcal{O}(\epsilon)$ .

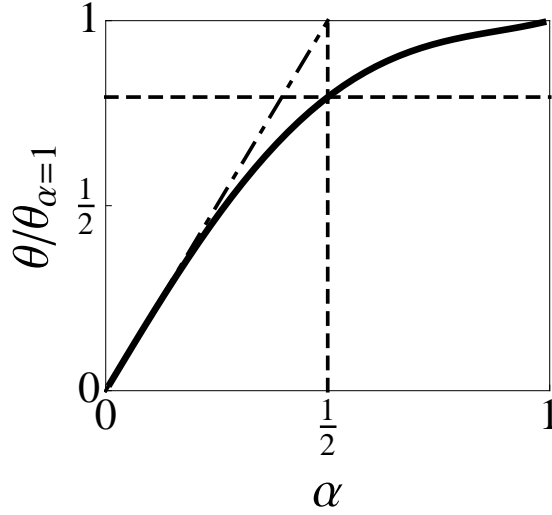


Figure 2.8: Ratio  $\theta/\theta_{\alpha=1}$  between the initial-slip exponent  $\theta$  in Eq. (2.142) and its white-noise value  $\theta_{\alpha=1}$ , as a function of  $\alpha$ , within the relevant range  $0 < \alpha \leq 1$  at the first order in the  $\epsilon$ -expansion. The dashed horizontal line indicates the value  $d(1/2)/\sqrt{\pi} = (\sqrt{2}/\pi) \ln(3+2\sqrt{2}) = 0.793\dots$  corresponding to  $\alpha = 1/2$  (vertical dashed line). The dash-dotted line points out the linear behavior  $\theta/\theta_{\alpha=1} \simeq 2\alpha$  expected for  $\alpha \rightarrow 0$ .

**Fluctuation-dissipation ratio and effective temperature.** A system which equilibrates after a certain finite relaxation time satisfies the FDT. More generally, one defines the *fluctuation-dissipation ratio* (FDR) by

$$X(\vec{p}; t, t') = \frac{\beta^{-1} R(\vec{p}; t, t')}{\partial_{t'} C(\vec{p}; t, t')}, \quad (2.143)$$

where  $\beta^{-1}$  is the temperature of the thermal bath (set to 1 in the previous analysis). In glassy and weakly driven macroscopic systems with slow dynamics — small entropy production limit — this ratio approaches a constant on asymptotic two-time regimes in which, moreover, it is independent of the observable used to define the correlation and associated linear response and admits the interpretation of an effective temperature [99, 100]. For systems with critical points, the asymptotic value

$$X^\infty = \lim_{t' \rightarrow \infty} \lim_{t \rightarrow \infty} X(\vec{0}, t, t'), \quad (2.144)$$

has been suggested to behave as a universal property [101] and, moreover, as an *effective temperature*,

$$\beta^\infty = \beta X^\infty. \quad (2.145)$$

(Note, however, that beyond the Gaussian approximation such a temperature depends upon the observable used to define it [102].) In equilibrium one has  $X^\infty = 1$  (which is just a reformulation of the FDT) and  $\beta^\infty = \beta$ . Instead,  $X^\infty \neq 1$  is a signal of an asymptotic non-equilibrium dynamics and therefore we shall focus on this quantity for the dynamics we are presently interested in.

Within the Gaussian approximation discussed in Sec. 2.3.2 the fluctuation-dissipation ratio  $X$  can be easily calculated from the expressions in Eqs. (2.63) and (2.64) [see also Eqs. (2.168) and (2.172)] for the response and correlation function, respectively, in terms of Mittag-Leffler functions:

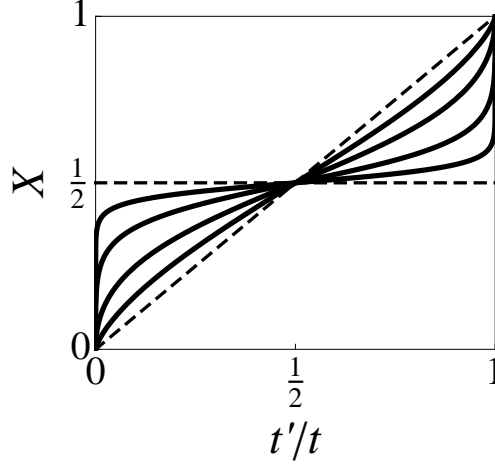


Figure 2.9: Fluctuation-dissipation ratio for the global order parameter (corresponding to  $\vec{p} = 0$ ) at criticality  $r = 0$  within the Gaussian approximation, as a function of the ratio  $0 \leq t'/t \leq 1$  for various values of  $\alpha$ . The straight horizontal and diagonal dashed lines correspond to  $\alpha = 1$  and  $\alpha = 0$ , respectively. The solid curves, instead, correspond to  $\alpha = 0.25, 0.5, 0.75$ , and  $0.9$  upon moving away from the diagonal line.

$$X^{-1}(t, t') = 1 + \left( \frac{t}{t'} - 1 \right)^{1-\alpha} \frac{E_\alpha(-At^\alpha/\gamma) E_{\alpha,\alpha}(-At'^\alpha/\gamma)}{E_{\alpha,\alpha}(-A(t-t')^\alpha/\gamma)}, \quad (2.146)$$

where we assumed  $t > t'$  and  $A \equiv p^2 + r$ . For  $A \neq 0$  (e.g., far from the critical point  $r = 0$  or at criticality with  $\vec{p} \neq 0$ ) and long and well-separated times  $t, t', t-t' \gg (\gamma/A)^{1/\alpha}$ , one can easily see from Eq. (2.170) that  $X^{-1} \rightarrow 1$ , confirming the expectation that the system equilibrates at long times, independently of the value of  $\alpha > 0$ . On the other hand, for the fluctuation of the homogeneous mode  $\vec{p} = 0$  at criticality one has  $A = 0$  and the FDR takes the simple form (originally derived in Ref. [48] for an anomalously diffusing particle)

$$X_{\vec{p}=0,\text{crit}}^{-1}(t, t') = 1 + \left( \frac{t}{t'} - 1 \right)^{1-\alpha}, \quad (2.147)$$

which is a universal scaling function of the dimensionless scaling variable  $t'/t$ , reported in Fig. 2.9 for various values of  $\alpha$ . In contrast to the white noise case  $\alpha = 1$ , in the presence of colored noise  $0 < \alpha < 1$ ,  $X_{\vec{p}=0,\text{crit}}^{-1}(t, t')$  does actually depend on  $t'/t$  and it interpolates continuously between the quasi-equilibrium regime  $t' \simeq t$ , within which  $X_{\vec{p}=0,\text{crit}} \simeq 1$ , and the non-equilibrium regime of well separated times  $t' \ll t$ , for which  $X_{\vec{p}=0,\text{crit}} \simeq 0$  as it is generically observed in the case of coarsening dynamics [93, 94, 103].

Beyond the Gaussian approximation, we can deduce an expression of the two-time dependent FDR and its limiting values from the scaling forms in Eqs. (2.125) and (2.126). First of all we note that for  $t \gg t'$  and  $\vec{p} = 0$  one has  $\partial_{t'} C \simeq t^{(2-\eta)/z+\theta-\hat{\alpha}} (\hat{\alpha} - \theta) t'^{\hat{\alpha}-\theta-1} F_C(\vec{0}, 0)$  and  $R \simeq t^{(2-\eta-z)/z} (t/t')^\theta F_R(\vec{0}, 0)$ . We thus obtain

$$X^\infty = \frac{F_R(\vec{0}, 0)}{(\hat{\alpha} - \theta) F_C(\vec{0}, 0)} \lim_{t' \rightarrow \infty} \lim_{t \rightarrow \infty} \left( \frac{t}{t'} \right)^{\hat{\alpha}-1}. \quad (2.148)$$

In the case  $\hat{\alpha} = 1$  of dominant white noise this expression renders the well-known result  $X^\infty = F_R(\vec{0}, 0)/[(1 - \theta) F_C(\vec{0}, 0)]|_{\alpha=1} \equiv X_w^\infty$  [101, 86], i.e.,  $X_w^\infty = 1/2$  within the Gaussian

approximation [104, 105, 106]. The contribution of non-Gaussian fluctuations for  $D < 4$  and up to the second order in the  $\epsilon$ -expansion have been calculated in [91], in rather good agreement with Monte Carlo simulation (see Ref. [86] for a summary). Instead, if the colored noise dominates  $\hat{\alpha} = \alpha < 1$  and therefore the long-time limit  $X^\infty$  of the FDR in Eq. (2.148) vanishes, formally corresponding to an infinite effective temperature as observed in coarsening processes. Note that this result holds at all orders in perturbation theory. Therefore,

$$X^\infty = \begin{cases} X_w^\infty & \text{for } \alpha > \alpha_c(D, N) , \\ 0 & \text{for } \alpha < \alpha_c(D, N) , \end{cases} \quad (2.149)$$

where both values do not depend on the actual value of  $\alpha$  and therefore  $X^\infty$  exhibits a discontinuity as a function of  $\alpha$  upon crossing the line  $\alpha = \alpha_c(D, N)$ . Within the Gaussian approximation one can easily check the general result (2.149) for  $X^\infty$ , on the basis of Eqs. (2.103) and (2.104). Indeed the behavior of the correlation and response functions can be determined by taking  $\lim_{\lambda \rightarrow 0} \lambda C_0(\vec{0}; \lambda, \kappa)$  and  $\lim_{\lambda \rightarrow 0} \lambda R_0(\vec{0}; \lambda, \kappa)$ , respectively, for the propagators at zero momentum and at criticality. It is then straightforward to obtain  $X_0^\infty = 1/2$  within region W and  $X_0^\infty = \lim_{\lambda \rightarrow 0} \Gamma_\kappa / \Gamma_\lambda = 0$  within region C, which confirms our general results. Apparently, this result for  $X_0^\infty$  contradicts the corresponding one  $X_0^\infty = 1$  for a freely diffusing particle in a super-Ohmic bath (corresponding to  $\alpha > 1$ ) found in [48], which our model reduces to within the Gaussian approximation. However, within the field-theoretical approach discussed here, it turns out that a super-Ohmic bath, responsible for a noise  $\Gamma$  with  $\alpha > 1$  in Eq. (2.34), is eventually controlled by the white-noise vertex and it is therefore unstable with respect to the effects of the interaction, which effectively generates such a vertex even though it was not present in the original coupling to the bath. Therefore, the white-noise result  $X_0^\infty = 1/2$  does not only apply to the cross-over line  $\alpha_c(D, N)$  but it is valid within the whole region W. On the same footing, the results discussed here suggest that, at least in higher spatial dimensions, adding interactions to a system which displays superdiffusion (corresponding to  $z < 2$ ) results quite generically in a sub-diffusive behavior ( $z > 2$ ) as expected in the case of a diffusing particle (Gaussian approximation) with interactions.

## 2.4 Appendix A

### 2.4.1 Fourier and Laplace conventions

Within the present study we define the Fourier transform and its inverse via

$$\hat{F}(\omega) = \int_{-\infty}^{\infty} dt e^{-i\omega t} F(t) , \quad (2.150)$$

and

$$F(t) = \int_{-\infty}^{\infty} \frac{d\omega}{2\pi} e^{i\omega t} \hat{F}(\omega) . \quad (2.151)$$

Instead, for every  $\lambda > 0$  the Laplace transform is defined as

$$\hat{F}_\lambda = \int_0^{\infty} dt e^{-\lambda t} F(t) . \quad (2.152)$$

In the main text we shall drop the hats, whenever this does not generate confusion.

## 2.4.2 The equilibrium propagators

### Scaling in real time

For  $\alpha = 1$  (white noise) the equilibrium propagators have a simple analytic form in the time domain [75, 82, 92]. They can be calculated by applying an inverse Fourier transform to Eqs. (2.60) and (2.61):

$$\begin{aligned} R_0(\vec{p}, t) &= \Theta(t) e^{-(p^2+r)t/\gamma_w} \\ C_0(\vec{p}, t) &= \frac{1}{p^2+r} e^{-(p^2+r)|t|/\gamma_w}. \end{aligned} \quad (2.153)$$

For general  $\alpha$  dimensional analysis suggests that the critical ( $r = 0$ ) Gaussian correlation  $C_0$  with  $\gamma_w = 0$  should scale as

$$C_0(\vec{p}, t) = p^{-2} f_{C_0}(p^2|t|^\alpha/\gamma). \quad (2.154)$$

Using Eqs. (2.59) and (2.61) the equal-time correlator is given by

$$\begin{aligned} C_0(\vec{p}, t=0) &= \int \frac{d\omega}{2\pi} C_0(\vec{p}, \omega) \\ &= \int \frac{d\omega}{2\pi} \frac{2\gamma \sin(\pi\alpha/2) |\omega|^{\alpha-1}}{\gamma^2 |\omega|^{2\alpha} + 2\gamma(p^2+r) |\omega|^\alpha \cos(\pi\alpha/2) + (p^2+r)^2} \\ &= \frac{1}{p^2+r}. \end{aligned} \quad (2.155)$$

Hence, we infer that  $f_{C_0}(0) = 1$ . Naturally, we have  $f_{C_0}(\infty) = 0$  since correlations have to vanish in the long-time limit. Applying a Fourier transform to Eq. (2.154) it is easy to show that at criticality ( $r = 0$ )

$$C_0(\vec{x}, t) = \frac{1}{|x|^{D-2}} g_{C_0}(\gamma x^2/|t|^\alpha), \quad (2.156)$$

where the function  $g_{C_0}$  reaches the asymptotic value  $g_{C_0}(\infty) = \Gamma_E(D/2 - 1)/(4\pi^{D/2})$ . In order to deduce the leading behavior for  $g_{C_0}(u)$  when  $u \rightarrow 0$  we start from the explicit expression of the noise kernel  $\Gamma_{i\omega}$  given in Eq. (2.59). After some algebra we obtain

$$g_{C_0}(u) = \int \frac{d^D p}{(2\pi)^D} \frac{d\omega}{2\pi} \frac{2u \sin(\pi\alpha/2) |\omega|^{\alpha-1} e^{i\omega + i\vec{p} \cdot \hat{z}}}{u^2 |\omega|^{2\alpha} + 2up^2 |\omega|^\alpha \cos(\pi\alpha/2) + p^4}, \quad (2.157)$$

where  $u = \gamma x^2/t^\alpha$  and  $\hat{z}$  is an arbitrary unit vector. For  $\alpha \leq 1$  we neglect the contributions of  $\mathcal{O}(u^2)$  in the denominator and we obtain

$$g_{C_0}(u \rightarrow 0) = 2u \int \frac{d\omega}{2\pi} |\omega|^{\alpha-1} e^{i\omega} \int \frac{d^D p}{(2\pi)^D} \frac{\sin(\pi\alpha/2) e^{i\vec{p} \cdot \hat{z}}}{(p^2 + u|\omega|^\alpha \cos(\pi\alpha/2))^2}. \quad (2.158)$$

The integral over  $\vec{p}$  is of  $\mathcal{O}(u \ln[u|\omega|^\alpha \cos \pi\alpha/2])$  for  $D = 4$  and the resulting integral converges for  $\alpha < 1$ ; consequently,

$$g_{C_0}(u \rightarrow 0) \sim \mathcal{O}(u \ln u). \quad (2.159)$$

By using FDT we derive

$$R_0(\vec{x}, t) = \frac{\alpha\gamma}{x^{D-4} t^{\alpha+1}} g'_{C_0}(\gamma x^2/t^\alpha) \Theta(t). \quad (2.160)$$

In the white-noise case, the scaling function  $g_{C_0}$  has the simple form

$$g_{C_0}(u) = \frac{\Gamma_E(D/2 - 1)}{4\pi^{D/2}} \left[ 1 - \frac{\Gamma_E\left(\frac{D}{2} - 1, \frac{u}{4}\right)}{\Gamma_E\left(\frac{D}{2} - 1\right)} + \mathcal{O}(\epsilon) \right], \quad (2.161)$$

with  $\Gamma_E(s, x) = \int_x^\infty dy y^{s-1} e^{-t}$ , whence we deduce for  $\alpha = 1$  and  $D = 4$

$$g_{C_0}(u \rightarrow 0) = \mathcal{O}(u). \quad (2.162)$$

For generic  $\gamma$  and  $\gamma_w$  the scaling function  $g_{C_0}$  is no longer a function of one variable. It is easy to show that

$$C_0(\vec{x}, t) = \frac{1}{|x|^{D-2}} g_{C_0}(\gamma|x|^2/|t|^\alpha, \gamma_w|x|^2/|t|). \quad (2.163)$$

Moreover, by using a similar argument as above one has for  $D = 4$

$$\lim_{t \rightarrow \infty} g_{C_0}(u, v) = \mathcal{O}((u + v) \ln u), \quad (2.164)$$

where  $u = \gamma|x|^2/t^\alpha$  and  $v = \gamma_w|x|^2/t$  vanish with  $u/v$  finite. In the opposite short-time limit in which  $u$  and  $v$  diverge with  $u/v$  finite,

$$\lim_{t \rightarrow 0} g_{C_0}(u, v) = \Gamma_E(D/2 - 1)/(4\pi^{D/2}) \quad (2.165)$$

as for the purely colored problem.

The equilibrium propagators can be written in terms of the generalized Mittag-Leffler functions  $E_{a,b}(z)$ , as discussed in App. 2.4.2.

### Generalized Mittag-Leffler functions

The Laplace transform of  $R_0(\vec{p}, t)$  is given by

$$R_0(\vec{p}, \lambda) = \frac{1}{\lambda \Gamma_\lambda + A}, \quad (2.166)$$

where we defined  $A \equiv p^2 + r$  and, in the case of colored noise,  $\Gamma_\lambda = \gamma \lambda^{\alpha-1}$ . We formally expand this expression for small  $A$ :

$$R_0(\vec{p}, \lambda) = \frac{1}{\gamma \lambda^\alpha} \frac{1}{1 + A(\gamma \lambda^\alpha)^{-1}} = \frac{1}{\gamma \lambda^\alpha} \sum_{k=0}^{\infty} \frac{(-A/\gamma)^k}{\lambda^{\alpha k}}, \quad (2.167)$$

where the terms of the form  $1/\lambda^\beta$  (with  $\text{Re } \beta > 0$ ) are recognized as the Laplace transform of  $\Theta(t)t^{\beta-1}/\Gamma_E(\beta)$ , so that Eq. (2.167) is identified as the Laplace transform of

$$\begin{aligned} R_0(\vec{p}, t) &= \Theta(t) \frac{1}{\gamma} \sum_{k=0}^{\infty} (-A/\gamma)^k \frac{t^{\alpha k + \alpha - 1}}{\Gamma_E(\alpha k + \alpha)} \\ &= \Theta(t) \frac{t^{\alpha-1}}{\gamma} E_{\alpha, \alpha}(-At^\alpha/\gamma), \end{aligned} \quad (2.168)$$

where we have introduced the generalized Mittag-Leffler function

$$E_{\alpha, \beta}(z) \equiv \sum_{k=0}^{\infty} \frac{z^k}{\Gamma_E(\alpha k + \beta)} \quad \text{with } \alpha, \beta, z \in \mathbb{C}, \text{Re}\{\alpha, \beta\} > 0. \quad (2.169)$$

Note that this function reduces to an exponential for  $\alpha = \beta = 1$ :  $E_{1,1}(z) = e^z$ , whereas for  $z \in \mathbb{R}$  [98],

$$E_{\alpha,\beta}(z \rightarrow -\infty) = - \sum_{k=1}^{k^*} \frac{1}{\Gamma_E(\beta - \alpha k)} \frac{1}{z^k} + \mathcal{O}(z^{-(k^*+1)}) . \quad (2.170)$$

The corresponding expression for the equilibrium Gaussian correlation function can be obtained from the FDT (2.11). Indeed, after integration Eq. (2.40) takes the form

$$C_0(\vec{p}, t) = C_0(\vec{p}, t = 0) - \int_0^{|t|} ds R_0(\vec{p}, s) , \quad (2.171)$$

where we used the fact that, in equilibrium,  $C(\vec{x}, t) = C(\vec{x}, -t)$ . Taking into account Eq. (2.155) and the first line of Eq. (2.168) one readily finds

$$C_0(\vec{p}, t) = \frac{1}{A} E_\alpha(-A|t|^\alpha/\gamma) , \quad (2.172)$$

where  $E_\alpha(z) \equiv E_{\alpha,1}(z)$  is the Mittag-Leffler function.

The correlation function  $C_0(\vec{p}, t)$  in Eq. (2.172) can also be expressed as the inverse Fourier transform of  $C_0(\vec{p}, \omega)$  reported in Eq. (2.61) [see also Eq. (2.59)]. After some suitable change of variables one finds the following scaling form

$$C_0(\vec{p}, t) = \frac{1}{A} f_{C_0}(A|t|^\alpha/\gamma) , \quad (2.173)$$

where

$$\begin{aligned} f_{C_0}(u) &\equiv \frac{2}{\pi} \int_0^\infty dv \cos(u^{1/\alpha}v) \frac{v^{\alpha-1} \sin(\pi\alpha/2)}{v^{2\alpha} + 2v^\alpha \cos(\pi\alpha/2) + 1} \\ &= \frac{\sin(\pi\alpha/2)}{\pi\alpha/2} \int_0^\infty dv \frac{\cos(u^{1/\alpha}v^{1/\alpha})}{v^2 + 2v \cos(\pi\alpha/2) + 1} \end{aligned} \quad (2.174)$$

is the explicit expression for the scaling function introduced in Eq. (2.154).

### 2.4.3 Calculation of $\mathcal{E}_w^{0,2}$ and $\mathcal{E}^{1,1}$

Starting from Eq. (2.79) we have for generic  $\gamma$  and  $\gamma_w$

$$\begin{aligned} u^2 \mathcal{E}^{0,2}(\sigma; \gamma, \gamma_w) &= \ell \frac{g^2 A_D (N+2)}{9} \\ &\times \left\{ z \ell^{z-1} \cos(\sigma \ell^z) \int_\ell^\infty dx x^{5-2D} g_{C_0}^3 \left( \frac{\gamma x^2}{\ell \alpha z}, \frac{\gamma_w x^2}{\ell^z} \right) \right. \\ &\left. + \int_{\ell^z}^\infty dt \cos(\sigma t) \ell^{5-2D} g_{C_0}^3 \left( \frac{\gamma \ell^2}{t^\alpha}, \frac{\gamma_w \ell^2}{t} \right) \right\} . \end{aligned} \quad (2.175)$$

The result of the integral in the first term in curly brackets is an analytic function of  $\sigma$  that admits a Taylor expansion in powers of  $\sigma^2$ , i.e.,

$$c_0 + c_2 \sigma^2 + c_4 \sigma^4 + \dots \quad (2.176)$$

with coefficients that, in principle, depend separately on  $\gamma$ ,  $\gamma_w$  and  $\ell$ . The integral in the second term in curly brackets yields, instead, a non-analytic function of  $\sigma$  that we can still express as a series:

$$d_0 + d_2\sigma^2 + \dots + d_{3\alpha-1}\sigma^{3\alpha-1} + \dots, \quad (2.177)$$

where the term  $\propto \sigma^{3\alpha-1}$  is due to the leading behavior of  $g_{C_0}^3$  for  $t \rightarrow +\infty$  [see Eq. (2.159)] which has to be subtracted for  $\alpha < 1/3$  in order to make the integral convergent at large  $t$ . If  $3\alpha - 1 > 0$  the limit  $\sigma \rightarrow 0$  can be safely taken and the white-noise vertex is renormalized by  $c_0 + d_0$ . If, on the contrary,  $3\alpha - 1 < 0$  the contribution proportional to  $\sigma^{3\alpha-1}$  is anyhow negligible (for  $\alpha > 0$ ) with respect to the term  $\gamma\sigma^{\alpha-1}$  which is already present in the tree-level vertex. Therefore, there is no renormalization of the colored-noise vertex and we can focus on the limit  $\gamma_w \gg \gamma$ , i.e., on the correction to the white-noise vertex only. Since we calculate evolution equations up to order  $\epsilon^2$  we simply need to evaluate Eq. (2.175) in  $D = 4$ . We obtain

$$\begin{aligned} u^2 \mathcal{E}^{0,2}(0; \gamma, \gamma_w) &= \ell \frac{g^2 A_D (N+2)}{9} \\ &\times \left\{ z \ell^{z-1} \int_{\ell}^{\infty} dx x^{-3} g_{C_0}^3 \left( \frac{\gamma x^2}{\ell^{\alpha z}}, \frac{\gamma_w x^2}{\ell z} \right) \right. \\ &\left. + \int_{\ell^z}^{\infty} dt \ell^{-3} g_{C_0}^3 \left( \frac{\gamma \ell^2}{t^{\alpha}}, \frac{\gamma_w \ell^2}{t} \right) \right\}. \end{aligned} \quad (2.178)$$

We are interested in the  $\alpha \rightarrow \alpha_c$  limit in which  $\gamma_w \rightarrow \infty$  and  $z = 2 + \mathcal{O}(\epsilon^2)$ . By first using  $x \mapsto x\ell/\sqrt{\gamma_w}$  and  $t \mapsto \gamma_w \ell^2/x^2$  we transform the two-variable scaling function into the one-variable white-noise one. Using then Eq. (2.161) and  $A_4 = 2\pi^2$  we obtain the second and third line below.

$$\begin{aligned} u^2 \mathcal{E}^{0,2}(0; \gamma, \gamma_w) &= \frac{2\gamma_w g^2 A_D (N+2)}{9} \left[ \int_{\sqrt{\gamma_w}}^{\infty} dx x^{-3} g_{C_0}^3(0, x^2) \right. \\ &\quad \left. + \int_0^{\sqrt{\gamma_w}} dx x^{-3} g_{C_0}^3(0, x^2) \right] \\ &= \frac{2\gamma_w u^2 (N+2)}{9} \int_0^{\infty} dx \left[ 1 - e^{-x^2/4} \right]^3 / x^3 \\ &= \frac{\gamma_w u^2 (N+2)}{12} \ln \frac{4}{3}. \end{aligned} \quad (2.179)$$

Therefore, at the critical point, using the Wilson-Fisher fixed point value  $u^* = 6\epsilon/(N+8) + \mathcal{O}(\epsilon^2)$  [19], we find

$$u^2 \mathcal{E}^{0,2}(0; \gamma, \gamma_w) \rightarrow u^{*2} \gamma_w \mathcal{E}_w^{0,2} = \gamma_w \frac{3(N+2)}{(N+8)^2} \ln \frac{4}{3} \epsilon^2 + \mathcal{O}(\epsilon^3). \quad (2.180)$$

We now compute  $\mathcal{E}^{1,1}$  in  $D = 4$ . We start from Eqs. (2.97) and (2.98). Using Eqs. (2.187) and (2.165) in the limit  $\ell \rightarrow 0$  we obtain

$$\begin{aligned} u^2 \mathcal{E}^{1,1}(0; \gamma, \gamma_w) &= \frac{g^2 A_4 (N+2) \pi}{144} \frac{-\partial}{\partial \ln \ell} \int_{\ell}^{\infty} \frac{dx}{x} \frac{1}{(2\pi)^6} \\ &= \frac{u^2 (N+2)}{72}. \end{aligned} \quad (2.181)$$

Note that the term coming from the differentiation of  $C_0(\vec{x}, \ell^z)$  in Eq. (2.97) with respect to  $\ln \ell$  vanishes in the limit  $\ell \rightarrow 0$  [use Eq. (2.156)]. At the critical point we obtain

$$u^{*2} \mathcal{E}^{1,1} = \frac{u^{*2}(N+2)}{72} = \frac{N+2}{2(N+8)^2} \epsilon^2 + \mathcal{O}(\epsilon^3). \quad (2.182)$$

#### 2.4.4 Non-equilibrium propagators

For  $\alpha = 1$  the Gaussian non-equilibrium propagators read in the momentum and time domain

$$C_0(\vec{p}; t, s) = \frac{1}{p^2 + r} \left[ e^{-(p^2+r)|t-s|/\gamma_w} - e^{-(p^2+r)(t+s)/\gamma_w} \right], \quad (2.183)$$

$$R_0(\vec{p}; t, s) = \Theta(t-s) e^{-(p^2+r)(t-s)/\gamma_w}. \quad (2.184)$$

For generic  $\alpha$ , however, analogously compact expressions are not available and our analysis proceeds using Laplace transforms. In order to determine the response function  $R_0$  — consistently with the Gaussian approximation — we start with the linearized version of the Langevin equation (2.3) in the presence of an external perturbation  $\vec{h}$ :

$$\int_0^t dt' \Gamma(t-t') \partial_{t'} \vec{\phi}(\vec{x}, t') + (r - \nabla^2) \vec{\phi}(\vec{x}, t') = \vec{\zeta}(\vec{x}, t) + \vec{h}(\vec{x}, t) \quad (2.185)$$

Calculating the expectation value of both sides with respect to the distribution of the noise eliminates the vanishing average  $\langle \vec{\zeta} \rangle$ . The Laplace transform yields

$$(\lambda \Gamma_\lambda + p^2 + r) \langle \vec{\phi}_\lambda(\vec{p}) \rangle_h = \vec{h}_\lambda(\vec{p}) \quad (2.186)$$

in momentum space where we used the Dirichlet boundary condition  $\phi(\vec{x}, t=0) = 0$  [see discussion at the beginning of Sec. 2.3.5]. Note that the expectation value of the order parameter depends on  $h$ . The response propagator in the Laplace domain is given by

$$\begin{aligned} R_0(\vec{p}; \lambda, \kappa) \delta_{ij} &= \frac{\delta \langle \phi_{i,\lambda}(\vec{p}) \rangle_h}{\delta h_{j,\kappa}} \Big|_{\vec{h}=\vec{0}} = \frac{1}{\lambda \Gamma_\lambda + p^2 + r} \frac{\delta h_{i,\lambda}}{\delta h_{j,\kappa}} \\ &= \frac{1}{(\lambda + \kappa)(\lambda \Gamma_\lambda + p^2 + r)} \delta_{ij}. \end{aligned} \quad (2.187)$$

The last equality follows from the fact that  $\delta h_i(t)/\delta h_j(s) = \delta_{ij} \delta(t-s)$  as a function of time translates into  $\delta_{ij}/(\lambda + \kappa)$  in Laplace space, given that  $\int_0^\infty dt ds e^{-\lambda t - \kappa s} \delta(t-s) = 1/(\lambda + \kappa)$ .

In order to deduce the correlation propagator we start directly from Eq. (2.185) with  $\vec{h} = 0$  and we consider its Laplace transform:

$$\vec{\phi}_\lambda(\vec{p}) = \frac{\vec{\zeta}_\lambda}{\lambda \Gamma_\lambda + p^2 + r}, \quad (2.188)$$

which yields

$$\begin{aligned} C_0(\vec{p}; \lambda, \kappa) \delta_{ij} &= \langle \phi_{i,\lambda}(\vec{p}) \phi_{j,\kappa}(-\vec{p}) \rangle = \frac{\langle \zeta_{i,\lambda} \zeta_{j,\kappa} \rangle}{(\lambda \Gamma_\lambda + p^2 + r)(\kappa \Gamma_\kappa + p^2 + r)} \\ &= \frac{\Gamma_\lambda + \Gamma_\kappa}{(\lambda + \kappa)(\lambda \Gamma_\lambda + p^2 + r)(\kappa \Gamma_\kappa + p^2 + r)} \delta_{ij}. \end{aligned} \quad (2.189)$$

In the last line we used the fact that  $\int_0^\infty dt ds e^{-\lambda t - \kappa s} \Gamma(t-s) = (\Gamma_\lambda + \Gamma_\kappa)/(\lambda + \kappa)$ . The propagators verify an ‘initial time FDT’. We see that for  $\alpha < 1$   $\lim_{\kappa \rightarrow \infty} \kappa R_0(\vec{p}; \lambda, \kappa) = R_0(\vec{p}, \lambda)$  and  $\lim_{\kappa \rightarrow \infty} \kappa^2 C_0(\vec{p}; \lambda, \kappa) = \lim_{\kappa \rightarrow \infty} \kappa^{1-\alpha} \Gamma_\lambda R_0(\vec{p}, \lambda)$ , with  $R_0(\vec{p}, \lambda) = 1/(\lambda \Gamma_\lambda + p^2 + r)$ . In the time domain, the second identity reads

$$\partial_{t'} C_0(\vec{p}; t, t' \rightarrow 0) \sim t'^{\alpha-1} \int_0^t ds \Gamma(t-s) R_0(\vec{p}; s, t' \rightarrow 0) . \quad (2.190)$$

To derive this equation we used the convolution theorem for the Laplace transform  $\mathcal{L}$ , that is

$$\mathcal{L} \left[ \int_0^t dt' f(t-t') g(t') \right] (\lambda) = \mathcal{L}[f](\lambda) \mathcal{L}[g](\lambda) . \quad (2.191)$$

In order to deduce the scaling of Eq. (2.190) with respect to  $t'$  one observes that if  $\lambda \mathcal{L}[f(t)](\lambda) \sim \lambda^\alpha$  for  $\lambda \rightarrow \infty$  then  $f(t) \sim t^{-\alpha}$  for  $t \rightarrow 0$ .

---

## Out of equilibrium quantum Brownian motion

---

*“Well, our friend Dirac, too, has a religion, and its guiding principle is: God does not exist and Dirac is His prophet.”*  
Wolfgang Pauli

Quantum Brownian motion has been the starting point for the understanding of more complex dissipative quantum systems [50]. Applications to quantum tunnel junctions [107], dissipative two-state systems [108] and reaction-rate theory [109] are just a few among many. In its simplest form, as proposed in the founding papers [110, 111, 9], the environment induced dissipation is modeled by an ensemble of quantum harmonic oscillators linearly coupled to the particle of interest. So far, in most studies of the dissipative dynamics of a harmonically confined [111, 112] or a free [8, 113] quantum particle, the quantity of interest has been the reduced density matrix that is obtained by tracing away the bath degrees of freedom in the density matrix of the coupled system. For generic initial conditions this quantity has been obtained with the help of functional integral methods [8, 114]. An alternative simpler, though in general only approximate, description of the reduced density matrix is given by a master equation. For factorizing initial conditions [115] and thermalized initial conditions [116] an exact master equation can be obtained. However, it is also known that there cannot be a master equation – in the form of a partial differential equation local in time – for arbitrary initial conditions [116]. The alternative quantum Langevin approach [117] extensively used in quantum optics [118] is not sufficiently powerful either, for quite the same reason: only a few special initial conditions can be successfully treated within this approach and the quantum noise statistics are not tractable in the generic case.

In the following I show how to generalize the path integral formalism found in [8] such that generic Gaussian initial conditions can be treated. With the help of a *generating functional* all non-equilibrium correlation functions will be derived.

### 3.1 What is Quantum Brownian motion?

In the previous chapter I have discussed aspects of critical dynamics in the presence of colored – time correlated – noise. I have shown that such noise produced by non-Markovian environments leads to novel critical dynamics for second-order phase transitions. In general one may say that the dynamics of a collective variable, i.e. a field, coupled to a thermodynamic environment has not yielded yet to the efforts of the physicists which would lead to a full understanding of these dynamics and it is likely that some surprises might still be ahead of us. The case of a single particle coupled to an environment is on the other hand very well understood. The particle’s dynamics are described by a Langevin equation and if this Langevin equation is solvable without the stochastic term it is usually also solvable in presence of the noise. In this sense the problem may become more difficult when the bath is present, but no fundamentally new physics arise. For instance, the onset of deterministic chaos dynamics does not depend on whether the particle in question is coupled to a bath or not – as long as this coupling is linear, which is an extremely well approximation for many situations<sup>1</sup>. Another example is the escape rate of an activated particle confined to a well potential. Of course, it is known that the color of the noise has some impact on the well-known Arrhenius formula [54], but still the noise statistics do not fundamentally change the physics. It goes without saying that I do not imply here that such systems are not interesting. On the contrary, in order to understand many effects in nature, and in biology in particular, one needs precise formulae which reflect a realistic description of the stochastic environment. However, even the most ardent fan of classical one-particle dynamics cannot deny that the thermal quantum world behaves slightly differently. One of the most striking single particle phenomena is quantum tunneling and the Heisenberg uncertainty relation. Both of these quantum phenomena lead to far reaching consequences when combined with dissipative dynamics. Let me briefly deviate from the main subject and talk first about quantum tunneling. A particle confined to a double-well potential can tunnel from one potential well through the potential barrier to the other one and back. This process relies on quantum coherence and therefore allows for quantum superpositions of the two single potential well states such that Rabi oscillations between the two wells are observed. It is essentially a zero-temperature process and thus fundamentally different from the activated hopping over a potential barrier. While thermally activated processes are usually enhanced by a growing temperature or an increase of the particle-bath coupling (i.e. by the energy exchange rate between the particle and the environment), the opposite is true for quantum tunneling processes. Indeed, at zero temperature the quantum bath can actually totally suppress the quantum tunneling since it destroys the quantum coherence. This phenomenon has been formulated in many different ways [121, 122, 123, 9, 108]. If we come back to the particle in a single well the escape rate due to tunneling drops to zero when the coupling to the bath increases. On the other hand, upon increasing the temperature the tunneling rate grows [124, 50]. More importantly, the typical temperature which separates the quantum from the classical regime is lowered by an increasing coupling to the bath. The environment thus renders the system more classical and eventually destroys all quantum coherence, i.e. the quantum tunneling at absolute zero.

It is probably true for any introduction to quantum dissipation that it is a sign of lack of taste if the spin-boson model remains unmentioned in this context. The double-well system is essentially universal. In the 1980s Leggett et. al. [108] considered the so-called dissipative two-level system or spin-boson system which arises naturally from the dissipative particle in a

---

<sup>1</sup>Note however, that dissipation does not always has a “stabilizing” effect due to damping. In magneto-hydrodynamics a finite resistance can trigger instabilities [119, 120].

double-well system in the limit of a small tunneling rate (i.e. a neat separation of the two wells). All the parameters can then be combined into two variables, the tunneling matrix element  $h$  and the dissipative coupling constant to the bath, usually called  $\alpha$ . The two-level system is conveniently described by a single spin, the  $z$ -component of which is linearly coupled to the quantum bath. The tunneling rate is described by the term  $h\sigma_x$  in the Hamiltonian which flips between the two  $z$ -spin states. In the absence of dissipation the spin undergoes Rabi oscillations between the two  $z$ -states with a frequency  $h$ . One might guess that these coherent oscillations are gradually destroyed when the spin-bath coupling is switched on. However, not only is coherence destroyed, but tunneling itself (in the case of an Ohmic bath), i.e. for  $\alpha > 1$  the spin remains localized in one of the two states. This well-known localization transition shares the features of the Kosterlitz-Thouless transition and it is closely related to the phase transitions found in the anisotropic Kondo model [108] and the long-range interacting classical Ising chain [125].

Let me come back to the second genuine quantum feature I mentioned: The Heisenberg uncertainty relation whose consequences are most far-reaching. When Einstein combined in his ingenious approach classical thermodynamics with statistical methods, he found what is known as the Einstein relation, namely that the diffusion is proportional to the temperature. This is expressed by the classical FDT which links the linear response to the correlation function *via* the proportionality constant  $\beta^{-1}$ . Yet another way of stating this (for today's mind) trivial fact is the equipartition theorem. If we model the environment by a large set of independent harmonic oscillators, where each one has a different frequency, equipartition states that each mode will acquire the same energy on average. In the quantum world equipartition is however not satisfied. Since the work by M. Planck on the thermal black body radiation another energy partition arises, characterized by the frequency dependent factor  $\coth \hbar\beta\omega$ . This term always arises for a set of quantum harmonic oscillators at then temperature  $\beta$  and we will encounter it on numerous occasions during the next section. For high temperatures, the quantum partition reduces to classical equipartition, which is  $\omega$ -independent. However, when the temperature is lowered, the energy of the bath modes does not tend to zero as one might expect by extrapolating the classical law; we rather have  $\coth[\hbar\beta\omega/2] \rightarrow 1$  for large  $\beta$ . This simple statement leads to a very important property of a quantum bath: It fluctuates at zero temperature and these quantum fluctuation can lead to diffusion or suppress – as we have seen – quantum coherence. Interestingly enough, pure quantum diffusion at zero temperature is much slower than classical diffusion, i.e. one can show that the mean squared displacement grows with  $\log t$  [see [8] and next paragraph].

How does one usually model quantum Brownian motion? The environment is almost always modeled by an ensemble of harmonic oscillators and it is coupled linearly to the particle. However, important exceptions do exist. In some applications, the fundamental noise is not caused by phonons but by spins, one then needs a spin bath, which is far more difficult to deal with than a quantum harmonic oscillator bath, but which leads to richer physics [126]. Also, many articles deal with baths of two-level systems in order to model decoherence [127, 128, 129]. The analysis of the physical effects of quantum baths which are more complicated than the standard quantum harmonic oscillator environment would go beyond the scope of the present chapter. In chapter 4, however, we will study heavily entangled quantum baths formed by one-dimensional quantum liquids. Here, let us assume that the bath can be modeled by harmonic oscillators. Then the fundamental Hamiltonian of quantum Brownian motion reads  $\mathcal{H} = \mathcal{H}_S + \mathcal{H}_B + \mathcal{H}_{SB}$ ,

with

$$\mathcal{H}_S[\hat{q}, \hat{p}] = \frac{\hat{p}^2}{2M} + V(\hat{q}; t), \quad (3.1)$$

$$\mathcal{H}_B[\{\hat{x}_n, \hat{p}_n\}] = \sum_{n=1}^{\infty} \frac{\hat{p}_n^2}{2m_n} + \frac{m_n \omega_n^2}{2} \hat{x}_n^2, \quad (3.2)$$

$$\mathcal{H}_{SB}[\{\hat{x}_n\}, \hat{q}] = -\hat{q} \sum_{n=1}^{\infty} c_n \hat{x}_n + \hat{q}^2 \sum_{n=1}^{\infty} \frac{c_n^2}{2m_n \omega_n^2}. \quad (3.3)$$

One may convince oneself that  $\mathcal{H}$  indeed models dissipation. By using the Heisenberg equations of motion for the particle and the bath one arrives at the reduced equation of motion of the particle by eliminating the bath's degrees of freedom. The result can be written in the form of a quantum Langevin equation

$$M\ddot{\hat{q}}(t) + \partial_t M \int_0^t ds \gamma(t-s) \hat{q}(s) + \frac{dV(\hat{q}, t)}{d\hat{q}} = \hat{\xi}(t), \quad (3.4)$$

with the damping kernel

$$\gamma(t) = \frac{1}{M} \sum_n \frac{c_n^2}{m_n \omega_n^2} \cos(\omega_n t) \quad (3.5)$$

and the quantum stochastic force operator

$$\hat{\xi}(t) = \sum_n c_n \left[ \left( \hat{q}(0) + \frac{c_n}{m_n \omega_n^2} \hat{x}_n(0) \right) \cos \omega_n t + \frac{\hat{p}_n(0)}{m_n \omega_n} \sin \omega_n t \right]. \quad (3.6)$$

The Langevin force becomes stochastic *via* its dependence on the initial condition of the bath *and* the particle. It is thus in general necessary to specify the initial state of the full particle-bath system. To put it in other words: One needs to specify the experimental preparation procedure. Several possibilities have been studied in the literature. One common initial state is the so-called factorized initial state, where the bath and the particle are initially uncorrelated. While such an initial state leads to many simplifications in concrete calculations, its physical content is not so clear. In many experiments it is most uncommon to “decouple” the particle from its environment at some time. Moreover, when instantly coupled to the particle at  $t > 0$  the system undergoes a quench since the total energy increases due to the supplement interaction energy. From a physical point of view the factorizing initial state is hence most unusual.

On the other hand, equilibrium can be described by setting the initial state of the particle-bath system to its canonical Boltzmann weight  $e^{-\beta \mathcal{H}}$ . Again, I insist that such an initial state is different from the factorizing “equilibrium” state  $e^{-\beta \mathcal{H}_S} \otimes e^{-\beta \mathcal{H}_B}$  which has a lower energy and entropy. From now on I will set the potential  $V(q, t)$  equal to the harmonic oscillator potential  $M\Omega^2 q^2/2$  for pedagogical reasons. The canonical equilibrium initial state is a mixed state and it is therefore described by a density matrix  $\hat{\rho}_0$ . For an equilibrium preparation  $\hat{\rho}_0$  is given by

$$\hat{\rho}_0 = \exp \left[ -\beta \frac{\hat{p}^2(0)}{2M} - \beta \frac{M}{2} \Omega^2 \hat{q}^2(0) - \beta \sum_{n=1}^{\infty} \frac{\hat{p}_n^2}{2m_n} - \beta \frac{m_n \omega_n^2}{2} \left( \hat{x}_n - \frac{c_n}{m_n \omega_n^2} \hat{q}(0) \right)^2 \right], \quad (3.7)$$

where I completed the square with the counterterm. The statistical properties of the random force  $\hat{\xi}(t)$  then follow immediately:  $\hat{\xi}(t)$  is a stationary operator valued Gaussian random variable with  $\langle \hat{\xi}(t) \rangle = 0$  and

$$\left\langle \frac{1}{2} \left[ \hat{\xi}(t)\hat{\xi}(s) + \hat{\xi}(s)\hat{\xi}(t) \right] \right\rangle = \frac{\hbar}{2} \sum_n \frac{c_n^2}{m_n \omega_n} \cos \omega_n(t-s) \coth[\hbar \omega_n \beta / 2]. \quad (3.8)$$

Note the appearance of the typical  $\coth[\hbar \omega \beta / 2]$  characteristic for an oscillator bath. One should bear in mind that  $\xi$  is operator-valued; it has thus a non vanishing commutator:

$$[\hat{\xi}(t), \hat{\xi}(s)] = -i\hbar \sum_n \frac{c_n^2}{m_n \omega_n} \sin \omega_n(t-s). \quad (3.9)$$

The quantum Langevin equation is an operator equation which acts on the full Hilbert space spanned by the bath and the particle states. The dynamics thus lead always to an entanglement between the particle and the oscillators. By using the equation of motion 3.4 one can show together with the above noise commutator that  $\hat{q}(t)$  and  $\hat{p}(t)$  satisfy at all times the Heisenberg uncertainty relation, as required. This point is crucial: If one sets the commutator (3.9) to zero the Heisenberg uncertainty relation – however fundamental – would be violated for the particle (and moreover, for the bath, too). Consequently, the quantum bath is not only a matter of statistics. One *cannot* replace  $\hat{\xi}(t)$  by a  $c$ -valued Gaussian noise with the same statistics as  $\hat{\xi}$ , since an approximation of this type clearly would not satisfy the commutator properties of position and conjugate momentum. As a corollary it would violate the uncertainty relation and thus fundamental quantum mechanics.

Let us now briefly discuss the equilibrium static properties that come with Eq. (3.4). The usual strategy in order to find the reduced dynamics for the particle is to integrate (trace) out the bath degrees of freedom in the initial density matrix  $\hat{\rho}_0$ . When the theory is Gaussian and when one is interested only in static properties, it is however easier to first introduce the variances  $\langle \hat{q}^2 \rangle$  and  $\langle \hat{p}^2 \rangle$ . The reduced initial density matrix then takes necessarily the following form in the position basis:

$$\rho_R(x, y) = \frac{1}{\sqrt{2\pi \langle \hat{q}^2 \rangle}} \exp \left[ -\frac{(x+y)^2}{8 \langle \hat{q}^2 \rangle} - \frac{\langle \hat{p}^2 \rangle}{2\hbar^2} (x-y)^2 \right]. \quad (3.10)$$

There is indeed a very elegant way of deriving Eq. (3.10). Let us start from the average

$$\langle e^{-iy\hat{p}(t)} e^{ir\hat{q}(t)} \rangle = \text{Tr} \left[ e^{-iy\hat{p}} e^{ir\hat{q}} \hat{\rho}(t) \right] = \int dx' \rho(x' + y, x') e^{irx'}, \quad (3.11)$$

where  $\rho(x' + y, x')$  is the matrix element of  $\hat{\rho}$  in position space. With the help of the Baker-Campbell-Hausdorff formula we find

$$\rho_{y,x}(t) = \int dr e^{-\frac{i}{2}r(x+y)} \langle e^{-i(y-x)\hat{p}(t) + ir\hat{q}(t)} \rangle. \quad (3.12)$$

On the other hand, we can evaluate the rhs of (3.12) in the path integral formalism where the operators  $\hat{q}$  and  $\hat{p}$  are replaced by  $c$ -numbers  $q$  and  $p$ . Moreover, we know that  $q$  and  $p$  are – as soon as the initial condition is Gaussian – Gaussian random variables for all  $t$  so that

$$\begin{aligned} \rho_{y,x}(t) &= \int dr e^{-\frac{i}{2}r(x+y)} \langle e^{-i(y-x)\hat{p}(t) + ir\hat{q}(t)} \rangle \\ &= \int dr e^{-\frac{i}{2}r(x+y)} e^{-\frac{1}{2}(y-x)^2 \langle \hat{p}^2(t) \rangle - \frac{1}{2}r^2 \langle \hat{q}^2(t) \rangle + r(y-x) \langle [\hat{q}(t), \hat{p}(t)]_+ \rangle}, \end{aligned} \quad (3.13)$$

where  $\langle [\hat{q}(t), \hat{p}(t)]_+ \rangle = \langle [\hat{q}(t)\hat{p}(t) + \hat{p}(t)\hat{q}(t)] \rangle / 2$  is the symmetrized position-momentum equal time correlator and we have  $\langle [\hat{q}(t), \hat{p}(t)]_+ \rangle = 0$  due to symmetry reasons [8]. For simplicity we assumed  $\langle \hat{q} \rangle = 0$  and  $\langle \hat{p} \rangle = 0$ , but everything that follows can be easily generalized to the case where  $\hat{q}$  and  $\hat{p}$  are not centered at zero. The final integral over  $r$  then gives back Eq. (3.10).

From the Langevin equation (3.4) we find in the Laplace domain

$$M\tilde{q}(z) = \frac{\tilde{\xi}(z)}{z^2 + z\tilde{\gamma}(z) + \Omega^2}, \quad (3.14)$$

so that the linear response function reads

$$\tilde{\mathcal{R}}(z) = \frac{M^{-1}}{z^2 + z\tilde{\gamma}(z) + \Omega^2}. \quad (3.15)$$

We now use the quantum mechanical version of the fluctuation-dissipation theorem,

$$\mathcal{C}^{1\text{eq}}(\omega) = \hbar \coth[\hbar\omega\beta/2] \text{Im } \mathcal{R}(\omega), \quad (3.16)$$

with  $\mathcal{C}^{1\text{eq}}(\omega)$  the one-time stationary equilibrium correlation function in the Fourier domain. The trick is now to use the causality of the response function which implies  $\tilde{\mathcal{R}}(z) = \mathcal{R}(i\omega)$ . Together with the formula  $\sum_k \omega / (\omega^2 + \nu_k^2) = (\beta\hbar/2) \coth[\hbar\omega\beta/2]$  with  $\nu_k = 2\pi k / \hbar\beta$  the bosonic Matsubara frequencies I can recast the correlator as

$$\mathcal{C}^{1\text{eq}}(\omega) = \frac{1}{\beta} \sum_k \frac{i\omega}{\omega^2 + \nu_k^2} \left[ \tilde{\mathcal{R}}(i\omega) - \tilde{\mathcal{R}}(-i\omega) \right]. \quad (3.17)$$

By using an appropriate contour integration one finally finds the equal-time correlator, which in the case of thermal equilibrium does not depend on time at all,

$$\langle \hat{q}^2 \rangle = \frac{1}{M\beta} \sum_k \frac{1}{\nu_k^2 + |\nu_k| \tilde{\gamma}(|\nu_k|) + \Omega^2}. \quad (3.18)$$

By the same method we get

$$\langle \hat{p}^2 \rangle = \frac{M}{\beta} \sum_k \frac{\omega_0^2 + |\nu_k| \tilde{\gamma}(|\nu_k|)}{\nu_k^2 + |\nu_k| \tilde{\gamma}(|\nu_k|) + \Omega^2}. \quad (3.19)$$

Let us go back to the density matrix (3.10). Note that in the general non-equilibrium case the equal-time correlators are time dependent. As in the case of a non-dissipative single harmonic oscillator one can now make use of Mehler's formula for the Hermite polynomials. It is convenient to define the real variable

$$A = \langle \hat{p}^2(t) \rangle - \frac{1}{\langle \hat{q}^2(t) \rangle} \left( \frac{1}{4} + \langle [\hat{q}(t), \hat{p}(t)]_+ \rangle^2 \right) \quad (3.20)$$

and the complex variable

$$B = \langle \hat{p}^2(t) \rangle + \frac{1}{\langle \hat{q}^2(t) \rangle} \left( \frac{1}{2} - i \langle [\hat{q}(t), \hat{p}(t)]_+ \rangle \right)^2, \quad (3.21)$$

(Again, note that we assume a more general initial condition for which  $\mathcal{C}_{xp} \neq 0$  possibly) then the reduced density matrix can be recast as

$$\rho_{x,y}(t) = \frac{1}{\sqrt{2\pi\langle\hat{q}^2(t)\rangle}} e^{Axy - \frac{B}{2}x^2 - \frac{B^*}{2}y^2}. \quad (3.22)$$

By virtue of Mehler's formula we find

$$\rho_{x,y}(t) = \frac{\sqrt{1-u^2}}{2v'\langle\hat{q}^2(t)\rangle} \sum_0^\infty u^n \phi_n(x) \phi_n^*(y), \quad (3.23)$$

with the ‘‘eigenstates’’

$$\phi_n(x) = \frac{v'^{1/4}}{\sqrt{2^n n! \sqrt{\pi}}} H_n(\sqrt{v'}x) e^{-vx^2/2}. \quad (3.24)$$

$H_n(z)$  is the  $n$ -th Hermite polynomial,

$$A = \frac{2u}{1-u^2}v', \quad (3.25)$$

$$v = B - \frac{2u^2}{1-u^2}v' \quad (3.26)$$

and  $v' = \text{Re } v$ . Note that  $v$  is complex while  $u$  is real. The solution to (3.25) and (3.26) are found to be

$$u = \frac{\sqrt{B'+A} - \sqrt{B'-A}}{\sqrt{B'+A} + \sqrt{B'-A}} \quad \text{and} \quad v' = \sqrt{B'^2 - A^2}, \quad (3.27)$$

where  $B' = \text{Re } B$  is the real part of  $B$ . This representation of the reduced density matrix has been used in [25].

### 3.1.1 Some equilibrium results for Ohmic dissipation

Let me rewrite the formulae (3.18) and (3.19) for Ohmic dissipation. It is important to specify the cutoff procedure in order to remove unphysical divergences. For instance, in the Drude model the damping kernel has a short-time memory such that  $\gamma(t) = \gamma\omega_D e^{-\omega_D t}$ . With this regularized theory we have  $\tilde{\gamma}(z) = \omega_D/(\omega_D + z)$  and therefore in equilibrium

$$\langle\hat{q}^2\rangle = \frac{1}{M\beta} \sum \frac{1}{\nu_n^2 + |\nu_n|\omega_D/(\omega_D + |\nu_n|) + \Omega^2}, \quad (3.28)$$

and

$$\langle\hat{p}^2\rangle = \frac{M}{\beta} \sum_k \frac{\Omega^2 + \gamma|\nu_n|\omega_D/(\omega_D + |\nu_n|)}{\nu_n^2 + |\nu_n|\omega_D/(\omega_D + |\nu_n|) + \Omega^2}. \quad (3.29)$$

There are two interesting questions related to the equilibrium widths (3.28) and (3.29). First one can study their dependence on the bath temperature. This is plotted in Fig. 3.1. It is interesting to note that the position width decreases with increasing particle-bath coupling  $\gamma$  while the position width increases such that Heisenberg's uncertainty relation is ensured. In the next figure (Fig. 3.2) I plot the product  $4\langle\hat{q}^2\rangle\langle\hat{p}^2\rangle/\hbar^2$ , which grows with increasing  $\gamma$ . Note that  $4\langle\hat{q}^2\rangle\langle\hat{p}^2\rangle/\hbar^2$  is exactly equal to one for zero temperature and zero particle-bath coupling.

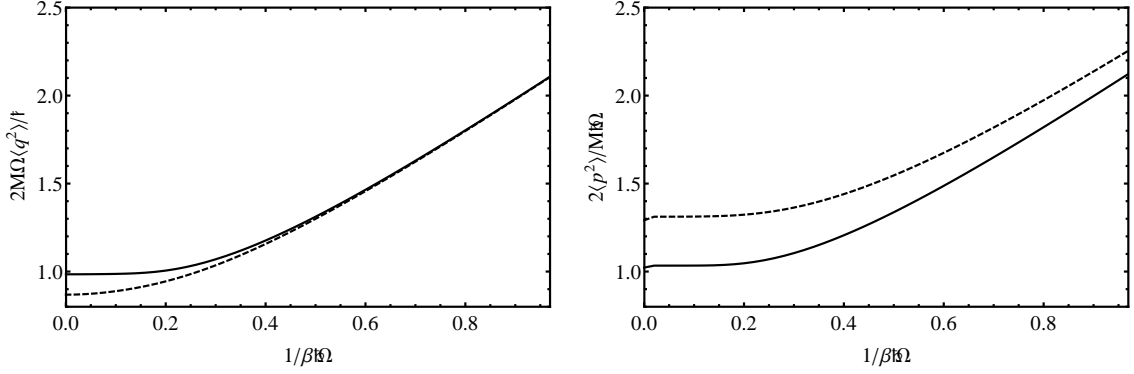


Figure 3.1: Temperature dependence of the position and momentum correlations.  $2M\Omega\langle\hat{q}^2\rangle/\hbar$  (left) and  $2\langle\hat{p}^2\rangle/(M\Omega\hbar)$  (right) is plotted for the Drude model, with  $\omega_D/\Omega = 1.0$ , versus  $1/\beta\hbar\Omega$ . The dashed line corresponds to  $\gamma/\Omega = 1.0$  whereas the solid line corresponds to  $\gamma/\Omega = 0.1$ .

While the Heisenberg uncertainty relation forbids that  $4\langle\hat{q}^2\rangle\langle\hat{p}^2\rangle/\hbar^2 < 1$ , the environment is perfectly allowed to excite the particle such that the width product increases. Indeed, if we reason naively in terms of the undamped oscillator eigenstates, a zero temperature behaviour as depicted in Fig. 3.2 implies that the particle is not only in its ground state but has a finite probability to be in its excited state. Let us put this reasoning on a more quantitative basis. In the last subsection I have shown that the reduced density matrix of the damped harmonic oscillator can be diagonalized in terms of stretched Hermite functions [see (3.23) and (3.24)]. Standard thermodynamics always assumes that the interaction energy between the system and its environment has to go to zero if the system is expected to be described by the canonical density matrix. Obviously this is not the case, here. Indeed, for  $\beta \rightarrow \infty$  and  $\gamma = 0$  we have  $u = 0$  as expected; however for  $\gamma/\Omega = 0.1$  we find by using  $\langle\hat{q}(t)\hat{p}(t) + \hat{p}(t)\hat{q}(t)\rangle(t) = 0$  [8]  $u \approx 0.00166$  and for  $\gamma/\Omega = 1.0$  we find  $u \approx 0.287$ . Therefore, there exists a non-zero probability to find the particle in an excited state. Such a behaviour is caused by the entanglement between the bath and the particle which does not vanish even at zero temperature. Due to the entanglement the naive reasoning in terms of pure particle eigenfunctions breaks down: The particle is not in its groundstate because it does not have any groundstate itself; only an entangled state depending on bath degrees of freedom can be the groundstate of the whole particle-bath system.

The diagonal representation of the reduced density matrix (3.23) is very useful when quantities such as the purity or the van Neumann entropy of  $\hat{\rho}$  are searched for. To cite an example, it is straightforward to monitor the decoherence of a superposition of two displaced Gaussians with this formula. It is also interesting to study the decoherence intensity as a function of bath characteristics.

At last, let me briefly discuss the subdiffusive behaviour of an untrapped Brownian particle. The equilibrium position correlation function is given in Eq. (3.170) or in [8]. When the external potential is switched off, i.e.  $\Omega \rightarrow 0$ , the particle undergoes free quantum Brownian motion. One of the fundamental questions one may ask concerns its diffusion behaviour when quantum effects dominate, i.e. when temperature is very low. As has been shown [8] for an Ohmic bath by performing a large-time analysis of Eq. (3.170) that the displacement function at zero

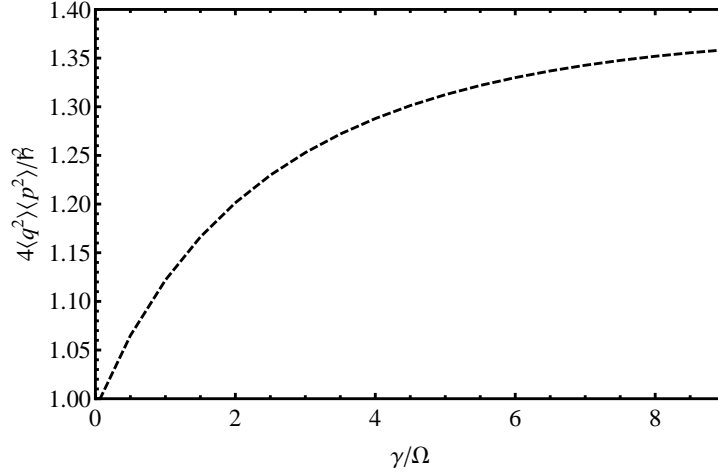


Figure 3.2:  $4\langle\dot{q}^2\rangle\langle\dot{p}^2\rangle/\hbar^2$  versus  $\gamma/\Omega$  for the Drude model with  $\omega_D/\Omega = 1.0$  at zero temperature.

temperature has the behaviour

$$\mathcal{Q}_F(t) \equiv \langle(\hat{q}(t) - \hat{q}(0))^2\rangle \simeq \frac{2\hbar}{\pi M\gamma} \log(\gamma t) \quad (3.30)$$

for  $\gamma t \rightarrow \infty$ . Note that the correlation function is formally infinite since free Brownian motion is not bounded. Only when the mean displacement is considered can one obtain a finite quantity which describes the diffusion law of the particle. For super-Ohmic and sub-Ohmic baths, too, behaviours which differ from the classical (fractional) diffusion laws are observed. For sub-Ohmic baths with a spectral density [see Eq. 3.133]  $S(\omega) \simeq \omega^\alpha$  with  $\alpha < 1$  the displacement function is bounded (at zero temperature) since the friction force exceeds the stochastic accelerating force of the bath. The particle is thus “trapped” in this case. The Ohmic  $\alpha = 1$  case is discussed above. For  $1 < \alpha < 3, \alpha \neq 2$  the displacement function behaves as  $\mathcal{Q}_F(t) \sim t^{\alpha-1}$ . For the special case  $\alpha = 2$  one has  $\mathcal{Q}_F(t) \sim t/\log^2(t)$ . The case  $\alpha = 3$  corresponds to a three dimensional (Ohmic) phonon bath such that the zero-temperature quantum diffusion for  $\alpha = 3$  and  $\alpha = 1$  are alike. The derivation of these diffusion laws can be found in [130].

The denominator of Eq. (3.30) shows the same viscosity coefficient  $M\gamma$  as the high temperature classical case which is governed by the standard diffusion coefficient  $D = \beta^{-1}/M\gamma$ . While thermal fluctuations have an effect on the particle displacement which linearly scales with temperature, the same “accelerating” effect of a pure quantum bath (i.e.  $\beta \rightarrow \infty$ ) is strongly suppressed (since at scales as the logarithm of the bath strength).

### 3.1.2 Other important dissipative quantum systems

Throughout this manuscript I will not talk anymore about quantum tunneling and dissipation. Due to the great importance of this topic I would like to present some basic notions of the dissipative effects on tunneling in this short subsection. The analysis of particle in a double-well and coupled to a bosonic quantum bath has been studied in [122, 123, 9, 108, 124]. All these studies concluded that coherence is gradually destroyed by the quantum bath. Hence, above a certain threshold value quantum coherence is totally suppressed and tunneling does not occur anymore. In this case, the particle is localized in one of the two potential wells.

As shown in [108] the double-well problem can be well approximated by the so called spin-boson Hamiltonian, where the particle position can only take two values,  $\pm 1$ , depending on whether it is found in the right or the left potential well. Within this approximation, the particle thus behaves as an effective two-state system and it can be described by a quantum spin  $\vec{s} = \frac{1}{2}(\sigma^x, \sigma^y, \sigma^z)$ . The tunneling is directly introduced *via* a tunneling matrix element  $h$ . The spin-boson Hamiltonian then reads

$$\hat{\mathcal{H}}_{\text{SB}} = \frac{\epsilon}{2}\sigma^z + \frac{h}{2}\sigma^x + \sum_i \lambda_i (a_i^\dagger + a_i)\sigma^z + \sum_i \hbar\omega_i a_i^\dagger a_i. \quad (3.31)$$

The two potential wells have an energy difference modeled by the detuning parameter  $\epsilon$ . The spin-boson model is probably the paradigm model of quantum dissipation, very much as the Ising model for statistical physics or the Hubbard model in condensed matter physics. In the best tradition of its “brothers”, the spin-boson Hamiltonian cannot be integrated for a general bath spectral density, despite its apparent simplicity. There are in general two ways of approaching the problem. Either one considers Eq. (3.31) as a well-defined approximation of the double-well problem; in this case one can carry over results obtained in the latter formalism to the former and vice-versa. However, since the review by Legget et al. [108] the spin-boson problem has been considered as an independent problem. In this context the close relationship between Eq. (3.31) and the anisotropic Kondo problem [108] and the long-range classical Ising chain [125, 72, 131, 132] has been realized and extensively studied. The mapping to the classical long-range Ising chain led to renormalization group equations of the spin-boson system which complemented the non-interacting-blip-approximation [108] used for describing its dynamics. All these studies concluded that a localization transition takes place if the spin is coupled to an Ohmic bath.

However, many aspects of the spin-boson model are not yet understood. Most of the recent studies focus on the quantum phase transition of the spin boson model for sub-Ohmic bath spectral densities. It has been argued that the sub-Ohmic spin-boson model violates the quantum-classical mapping [132], a claim which could not be upheld afterwards [133]. However, it seems certain that the system undergoes a second order phase transition at some critical bath strength which depends on  $h$  and the bath cutoff frequency. Recently this picture has been confirmed by using a variational ansatz [134] for the groundstate wavefunction.

### 3.2 The Hamiltonian of a quantum Brownian particle

We study the evolution of a particle of mass  $M$  evolving in a (possibly time-dependent) potential  $V(\hat{q}; t)$  where  $\hat{q}$  is the position operator. The Brownian motion stems from its interaction with a quantum heat bath which is usually modeled by an infinite set of harmonic oscillators linearly coupled to the position operator  $\hat{q}$ . The full system is then described by the Hamiltonian  $\hat{\mathcal{H}} = \hat{\mathcal{H}}_S + \hat{\mathcal{H}}_B + \hat{\mathcal{H}}_{SB}$ , with

$$\hat{\mathcal{H}}_S[\hat{q}, \hat{p}] = \frac{\hat{p}^2}{2M} + V(\hat{q}; t) - H(t)\hat{q}, \quad (3.32)$$

$$\hat{\mathcal{H}}_B[\{\hat{x}_n, \hat{p}_n\}] = \sum_{n=1}^{\infty} \frac{\hat{p}_n^2}{2m_n} + \frac{m_n\omega_n^2}{2}\hat{x}_n^2, \quad (3.33)$$

$$\hat{\mathcal{H}}_{SB}[\{\hat{x}_n\}, \hat{q}] = -\hat{q} \sum_{n=1}^{\infty} c_n \hat{x}_n + \hat{q}^2 \sum_{n=1}^{\infty} \frac{c_n^2}{2m_n\omega_n^2}. \quad (3.34)$$

$\hat{p}$  is the momentum operator of the particle. In contrast to Eq. (3.1) we introduced in the rhs of Eq. (3.32) a time-dependent source  $H(t)$ , a c-number, that couples linearly to the particle's position  $\hat{q}$ . This source term will be important for the derivation of the generating functional in the following.  $\hat{x}_n$  and  $\hat{p}_n$  are the position and momentum operators of the  $n$ -th harmonic oscillator, with mass and frequency  $m_n$  and  $\omega_n$ , respectively.  $c_n$  is the coupling strength between the particle and the  $n$ -th oscillator's position. The last term in Eq. (3.34) compensates for the bath-induced renormalization of the potential. Indeed, the sum of Eqs. (3.33) and (3.34) can be rewritten as

$$\hat{\mathcal{H}}_B + \hat{\mathcal{H}}_{SB} = \sum_{n=1}^{\infty} \frac{\hat{p}_n^2}{2m_n} + \frac{m_n \omega_n^2}{2} \left[ \hat{x}_n - \frac{c_n}{m_n \omega_n^2} \hat{q} \right]^2, \quad (3.35)$$

which shows the absence of any drift force induced by the bath and ensures that  $V(\hat{q}, t)$  corresponds to the physical potential right from the start. The model Hamiltonian Eqs. (3.33)-(3.34) has been widely used in the literature as a generic model for the dissipative dynamics of a quantum particle [9, 8, 50].

In the Heisenberg representation the time evolution of all possible observables  $\hat{A}$  is governed by

$$\begin{aligned} \hat{A}(t) &= \left[ \hat{\mathcal{T}} \exp \left( -\frac{i}{\hbar} \int_0^t dt' \hat{\mathcal{H}}(t') \right) \right]^\dagger \hat{A} \\ &\times \left[ \hat{\mathcal{T}} \exp \left( -\frac{i}{\hbar} \int_0^t dt' \hat{\mathcal{H}}(t') \right) \right], \end{aligned} \quad (3.36)$$

with  $\hat{\mathcal{T}}$  the time-ordering operator. By introducing the density matrix of the initial state  $\hat{\rho}_0$  the  $N$ -time average of a set  $\{\hat{A}_i\}$  of  $N$  operators, is

$$\begin{aligned} \langle \hat{A}_N(t_N) \hat{A}_{N-1}(t_{N-1}) \cdots \hat{A}_1(t_1) \rangle &= \\ \text{Tr} \left[ \hat{A}_N(t_N) \cdots \hat{A}_1(t_1) \hat{\rho}_0 \right], \end{aligned} \quad (3.37)$$

where we took the product of the  $\hat{A}_i$ s to be time ordered (with  $t_N \geq t_{N-1} \geq \dots \geq t_1$ ) so that we can more easily make the connection between Eq. (3.37) and its path integral representation. We assumed that  $\text{Tr} \hat{\rho}_0$  is normalized to one. Note that for a generic initial matrix  $\hat{\rho}_0$  this, as well as any other, correlation function is not necessarily stationary, i.e., it may depend on the  $N$  times explicitly.

In all cases the model has to be supplemented by information on the initial condition of the coupled system. These are incorporated in the initial density matrix  $\hat{\rho}_0$ . *Equilibrium dynamics* can be studied by choosing  $\hat{\rho}_0$  to be the Boltzmann weight, that is

$$\hat{\rho}_0 = \exp(-\beta \hat{\mathcal{H}}), \quad (3.38)$$

where  $\hat{\mathcal{H}}$  is the *full coupled* Hamiltonian and the normalization constant has been ignored. This truly equilibrium density matrix has to be distinguished from  $\hat{\rho}_0 = e^{-\beta \hat{\mathcal{H}}_S} \otimes e^{-\beta \hat{\mathcal{H}}_B}$ , a case in which each component of the “universe” (the whole particle–bath system) is in equilibrium on its own at the same temperature. This subtle point is often overlooked in the literature.

*Non equilibrium dynamics* can be studied whenever the initial density matrix is not of the form in Eq. (3.38). The simplest choice is an initial product state for which the initial density matrix factorizes into two contributions  $\hat{\rho}_{S0}$  and  $\hat{\rho}_{B0}$  which solely depend on particle and bath variables, respectively:

$$\hat{\rho}_0 = \hat{\rho}_{S0} \otimes \hat{\rho}_{B0}. \quad (3.39)$$

Brownian motion [135, 50] as well as the dynamics of more complex macroscopic systems [136, 137, 138, 139, 140, 141, 142, 92, 143] with a factorized initial density matrix have been studied in a variety of physical situations. However, in many cases it is not appropriate to assume Eq. (3.39) since one has no command over the bath and it is impossible to “switch it on and off” at will. In addition, with recent developments in cold atom experiments (see chapter 4), new classes of initial conditions become of relevance.

The first one covers all situations in which the particle is in equilibrium in a potential and either it is released or the potential is suddenly modified at  $t = 0$ . In this case Eq. (3.38) holds with  $\hat{\mathcal{H}}$  replaced by  $\hat{\mathcal{H}}_0$  ( $\neq \hat{\mathcal{H}}$ ) describing the initial state.

The second class concerns all situations in which the position of the free particle is measured at  $t = 0$ . This procedure projects the initial density matrix onto the quantum states of the measurement outcome. We focus on the case where no quantum quench is performed in addition to the position measurement so that  $\hat{\mathcal{H}}_0 = \hat{\mathcal{H}}$ . If the position is exactly determined at  $t = 0$  the initial density matrix is

$$\hat{\rho}_0 = \hat{\Pi}(q) e^{-\beta \hat{\mathcal{H}}} \hat{\Pi}(q) \quad \text{with} \quad \hat{\Pi}(q) = |q\rangle\langle q| \quad (3.40)$$

the projection operator onto the state  $|q\rangle$ . If, instead, we take the measured position of the particle to be Gaussian distributed around  $q_m$  the projection operator takes the form

$$\hat{\Pi}(q_m) = \int dq e^{-\frac{(q-q_m)^2}{4\Delta^2}} |q\rangle\langle q|, \quad (3.41)$$

where  $\Delta$  measures the uncertainty of the particle’s position at  $t = 0$ . Once again we neglected the irrelevant normalization factor.

A third important class of initial conditions are the factorized density operators, see Eq. (3.39), in which the initial state of the system is a pure state. Since any state can be expanded in terms of displaced Gaussians (or *coherent states*) it suffices to consider initial states of the form

$$\hat{\rho}_{S0} = |\psi\rangle\langle\varphi|, \quad (3.42)$$

where

$$\psi(q) = e^{-\frac{(q-q_m)^2}{4\Delta^2}} \quad \text{and} \quad \varphi(q') = e^{-\frac{(q'-q'_m)^2}{4\Delta'^2}}, \quad (3.43)$$

to cover the whole class of initially factorized pure states.

In this article we derive a generating functional that allows us to obtain the  $N$ -time correlators for these types of initial conditions. We are mainly interested in the evolution and averages of the *particle’s position observables* for which  $\hat{A} = A[\hat{q}]$  with some function  $A$  depending on the position  $\hat{q}$  of the particle. Note that due to the coupling of the bath to the particle’s position the momentum dynamics follow from the Heisenberg equation  $M\partial_t\hat{q} = \hat{p}$ . Therefore, by focusing on the particle position operator we simultaneously describe the dynamics of the particle’s momentum. While in [8] the authors derived an explicit expression for the equilibrium correlation functions the generating functional will allow us to go beyond the equilibrium case.

### 3.3 The non-equilibrium generating functional

This part of my thesis is central since many of its results and formulae will be reused in part 4 which focuses on impurity dynamics. It can be read as a junction section which belongs both to part 3 and to part 4.

This section will generalize the path integral formalism in [8] to the language of *generating functionals* commonly used in quantum field theory. We will use the Schwinger-Keldysh formalism [111, 144] which is particularly well suited for our purposes. A simple alternative approach based on the quantum Langevin equation has been discussed in the introductory section 3.1. From the generating functional we will easily deduce the *non-equilibrium correlation functions* for generic non-factorizing Gaussian initial conditions (for a stochastic description of open quantum systems *via* a generating functional, see [145]) that *cannot* be obtained within the density matrix formalism. We will use this technique to treat two problems: the relaxation dynamics of a particle confined in a harmonic potential after a position measurement performed at the “initial time” and the relaxation dynamics of a particle after an abrupt change in the parameters of the confining potential.

More precisely, this chapter is organized as follows. In Sec. 3.3 we employ path integral methods to derive the generating functional of out of equilibrium correlations. Our results cover both factorized and non-factorized Gaussian initial conditions as well as the effects of an initial position measurement performed on the particle. In Sec. 3.4 we study the equilibration processes after an initial position measurement and after a quench in the harmonic potential and we derive the equilibration times for low and high bath temperatures.

Note that my work goes beyond the analysis in [8] where explicit expressions for equilibrium correlation functions were given. More precisely, I will derive a functional of two time-dependent sources  $\mathcal{J}[F, G]$  such that the two-time correlation is given by

$$\langle \hat{q}(t)\hat{q}(t') \rangle = \frac{\hbar}{i} \frac{\delta}{\delta G(t)} \frac{\hbar}{i} \left[ \frac{\delta}{\delta G(t')} + \frac{\delta}{2\delta F(t')} \right] e^{\mathcal{J}[F, G]} \Big|_{F, G=0} \quad (3.44)$$

and similarly for higher order correlations.

Then I will obtain the path integral formulation of the generating functional by making use of the coherent states of the bath variables  $\{|\xi_{n,f}\rangle\}$  which are defined in App. 3.5.1. The ensuing functional integration includes paths over particle and bath variables. Since we are not interested in the degrees of freedom of the bath, we average over all bath variables to find a “reduced action” that only depends on the particle variables. In the special cases discussed below (e.g., harmonic potential) the remaining path-integrals can also be performed and the functional  $\mathcal{J}$  can be fully determined. In this section we sketch all steps in the derivation. Further technical details are reported in App. 3.5.1. The reader who is not interested in these technical details can jump directly to Eq. (3.87) where its rather lengthy final expression is given.

As a preview let be briefly discuss in what way the results in this section on non equilibrium correlation functions in quantum Brownian motion will be of use in part 4: Non equilibrium correlation functions have been recently observed in cold atoms experiments on the dynamics of an *impurity* atom moving in a one dimensional (1D) quantum liquid [146, 147, 148]. Both the impurity and the quantum liquid are confined in an optical harmonic trap so that the impurity motion resembles the dynamics of a damped quantum harmonic oscillator. In Sec. 4.4 I apply the formalism developed here to impurity motion in a 1D quantum gas described by the Luttinger theory. In Sec. 4.4 a simplified modeling of the experiment in which polaronic effects [149, 150] as well as the possible renormalization of the external potential [146] are neglected. These subtle effects will be analyzed in the subsequent Section 4.6. The Luttinger liquid will turn out to behave as an exotic quantum bath of harmonic oscillators with a highly *non Ohmic spectral density* and non-linearly coupled to the particle, see also Peotta et al. [151, 151]. This is shown to lead to the curious behavior that the oscillator frequency can *increase* upon

increasing the coupling constant between the “bath” and the impurity in strong contrast to the behavior of an Ohmic damped oscillator.

### 3.3.1 The density matrix

In the following we will use the product states  $|q, \{\xi_n\}\rangle \equiv |q\rangle|\{\xi_n\}\rangle$  between the particle and the bath eigenstates.  $|q\rangle$  is the particle position eigenstate and  $|\{\xi_n\}\rangle$  is a coherent state of the oscillators. If we define the oscillator creation and annihilation operators through

$$\hat{a}_n^\dagger = \sqrt{\frac{m_n\omega_n}{2\hbar}} \left[ \hat{q}_n - \frac{i}{m_n\omega_n} \hat{p}_n \right], \quad (3.45)$$

$$\hat{a}_n = \sqrt{\frac{m_n\omega_n}{2\hbar}} \left[ \hat{q}_n + \frac{i}{m_n\omega_n} \hat{p}_n \right], \quad (3.46)$$

we have by definition  $\hat{a}_n|\{\xi_n\}\rangle = \xi_n|\{\xi_n\}\rangle$ . In terms of these product states the matrix elements of the time evolution operator read

$$\begin{aligned} \mathcal{K}(q_f, \{\xi_{n,f}\}; q_i, \{\xi_{n,i}\}; t) \equiv \\ \langle q_f, \{\xi_{n,f}\} | \hat{\mathcal{T}} e^{-\frac{i}{\hbar} \int_0^t dt' \hat{\mathcal{H}}(t')} | q_i, \{\xi_{n,i}\} \rangle \end{aligned} \quad (3.47)$$

and of its Hermitian conjugate

$$\begin{aligned} \mathcal{K}^*(q'_f, \{\xi'_{n,f}\}; q'_i, \{\xi'_{n,i}\}; t) \equiv \\ \langle q'_i, \{\xi'_{n,i}\} | \hat{\mathcal{T}}^\dagger e^{\frac{i}{\hbar} \int_0^t dt' \hat{\mathcal{H}}(t')} | q'_f, \{\xi'_{n,f}\} \rangle. \end{aligned} \quad (3.48)$$

$\hat{\mathcal{T}}^\dagger$  is the anti-chronological time ordering operator. The elements of the time-dependent density matrix,  $\hat{\rho}(t) \equiv \mathcal{K}\hat{\rho}_0\mathcal{K}^*$ , are given by

$$\begin{aligned} \mathcal{W}(q_f, \{\xi_{n,f}\}; q'_f, \{\xi'_{n,f}\}; t) \equiv \langle q_f, \{\xi_{n,f}\} | \hat{\rho}(t) | q'_f, \{\xi'_{n,f}\} \rangle \\ = \int dq_i dq'_i d\xi_i d\xi'_i \mathcal{K}(q_f, \{\xi_{n,f}\}; q_i, \{\xi_{n,i}\}; t) \\ \times \mathcal{W}(q_i, \{\xi_{n,i}\}; q'_i, \{\xi'_{n,i}\}) \mathcal{K}^*(q'_f, \{\xi'_{n,f}\}; q'_i, \{\xi'_{n,i}\}; t), \end{aligned} \quad (3.49)$$

where the matrix elements of the initial density matrix have been denoted by

$$\mathcal{W}(q_i, \{\xi_{n,i}\}; q'_i, \{\xi'_{n,i}\}) = \langle q_i, \{\xi_{n,i}\} | \hat{\rho}_0 | q'_i, \{\xi'_{n,i}\} \rangle \quad (3.50)$$

and we used the short-hand notation

$$d\xi_i = \prod_{n=1}^{\infty} e^{-\xi_{n,i}^* \xi_{n,i}} d\xi_{n,i}^* d\xi_{n,i}. \quad (3.51)$$

The path integral representations of  $\mathcal{K}$  and  $\mathcal{K}^*$  are

$$\begin{aligned} \mathcal{K}(q_f, \{\xi_{n,f}\}; q_i, \{\xi_{n,i}\}; t) &= \int \mathcal{D}q^+ \mathcal{D}\xi^+ e^{\frac{i}{\hbar} \mathcal{S}[q^+, \{\xi_n^+\}]}, \\ \mathcal{K}^*(q'_f, \{\xi'_{n,f}\}; q'_i, \{\xi'_{n,i}\}; t) &= \int \mathcal{D}q^- \mathcal{D}\xi^- e^{-\frac{i}{\hbar} \mathcal{S}^*[q^-, \{\xi_n^-\}]}, \end{aligned}$$

where we made clear with the superscripts  $+$  and  $-$  which paths belong to  $\mathcal{K}$  and  $\mathcal{K}^*$ , respectively. The functional integration measures are defined in App. 3.5.1.

### 3.3.2 Reduced density matrix for a system initially coupled to an equilibrium bath

The time-dependent density matrix in Eq. (3.49) still contains information about the degrees of freedom of the bath which we are not interested in. Therefore, we average (trace) over all the bath variables to find a reduced density matrix that depends only on the particle variables and the external sources.

We are interested in a system that is initially coupled to an equilibrium bath. Therefore,

$$\hat{\mathcal{H}}_{B0} = \hat{\mathcal{H}}_B, \quad \hat{\mathcal{H}}_{SB0} = \hat{\mathcal{H}}_{SB}, \quad (3.52)$$

where all initial Hamiltonians are labeled with a subscript  $_0$ . At this point it is not necessary to make  $\hat{\mathcal{H}}_{S0}$  explicit since this term involves only particle variables that are not affected by the trace over the bath variables. The matrix element of the initial density operator Eq. (3.50) in Eq. (3.49) can be represented by an imaginary time path integral

$$\mathcal{W}(q_i, \{\xi_{n,i}\}; q'_i, \{\xi'_{n,i}\}) = \int \mathcal{D}q^0 \mathcal{D}\xi^0 e^{-\frac{1}{\hbar} \mathcal{S}_0[q^0, \{\xi_n^0\}]},$$

where the initial action  $\mathcal{S}_0$  is in general different from  $\mathcal{S}$  reflecting the fact that  $\hat{\mathcal{H}}_0 \neq \hat{\mathcal{H}}$ . The reduced density matrix can now be recast as

$$\begin{aligned} \mathcal{W}(q_f; q'_f; t) &\equiv \int dq_i dq'_i \mathcal{D}q^0 \mathcal{D}q^+ \mathcal{D}q^- \\ &\times e^{\frac{i}{\hbar} \mathcal{S}_S[q^+] - \frac{i}{\hbar} \mathcal{S}_S[q^-] - \frac{1}{\hbar} \mathcal{S}_{S0}[q^0]} \mathcal{F}[q^+, q^-, q^0], \end{aligned}$$

where  $\mathcal{F}[q^+, q^-, q^0]$  is the ‘‘influence functional’’ that depends only on the particle variables, as also do  $\mathcal{S}_S$  and  $\mathcal{S}_{S0}$ . The path integral runs over all paths with

$$\begin{aligned} q^+(t) &= q_f, \quad q^+(0) = q_i, \quad q^-(t) = q'_f, \\ q^-(0) &= q'_i, \quad q^0(\beta\hbar) = q^-(0), \quad q^0(0) = q^+(0), \end{aligned}$$

which is the reason for the name ‘‘closed-time path integral’’. It is convenient to introduce the linear combinations

$$x = (q^+ + q^-)/2 \quad \text{and} \quad \bar{x} = q^+ - q^-. \quad (3.53)$$

The calculation of  $\mathcal{F}$  can be found in App. 3.5.1 or in [8]; the result reads

$$\mathcal{F}[x, \bar{x}, q^0] = e^{\frac{i}{\hbar} \Phi[x, \bar{x}, q^0]}, \quad (3.54)$$

with

$$\begin{aligned} \Phi[x, \bar{x}, q^0] &= \frac{i}{2} \int_0^{\beta\hbar} d\tau d\sigma k(\tau - \sigma) q^0(\tau) q^0(\sigma) \\ &+ \int_0^{\beta\hbar} d\tau \int_0^t ds K^*(s - i\tau) q^0(\tau) \bar{x}(s) \\ &- \frac{i}{2} \int_0^t ds du K_R(s - u) \bar{x}(s) \bar{x}(u) \\ &- M \int_0^t ds \bar{x}(s) \frac{d}{ds} \int_0^s du \gamma(s - u) x(u). \end{aligned} \quad (3.55)$$

The kernels  $K(\theta)$ ,  $\gamma(t)$  and  $k(t)$  are defined in Eqs. (3.134), (3.145) and (3.146), respectively.  $K_R$  denotes the real part of  $K$ . Note that  $\Phi[x, \bar{x}, q^0]$  depends on the fixed “end-points”  $t$  and  $\beta\hbar$  of the closed-time path.

Expected values evaluated at different times are now expressed in terms of a path-integral over  $q^0$ ,  $x$  and  $\bar{x}$  with an effective action  $\Sigma$ ,

$$\langle \dots \rangle = \int dx_f dx_i d\bar{x}_i \int' \mathcal{D}x \mathcal{D}\bar{x} \mathcal{D}q^0 \dots e^{\frac{i}{\hbar} \Sigma[x, \bar{x}, q^0]}, \quad (3.56)$$

where  $\Sigma[x, \bar{x}, q^0]$  is given by

$$\begin{aligned} \Sigma[x, \bar{x}, q^0] &= \\ & \Phi[x, \bar{x}, q^0] + i\mathcal{S}_{S_0}[q^0] + \mathcal{S}_S[x + \bar{x}/2] - \mathcal{S}_S[x - \bar{x}/2] \\ &= \Phi[x, \bar{x}, q^0] + i \int_0^{\beta\hbar} d\tau \left[ \frac{M_0}{2} (\dot{q}^0)^2 + V_0(q^0) \right] \\ &+ \int_0^t ds \left[ M\dot{x}\dot{x} - V_H\left(x + \frac{\bar{x}}{2}; s\right) + V_{H'}\left(x - \frac{\bar{x}}{2}; s\right) \right]. \end{aligned} \quad (3.57)$$

We introduced the initial mass  $M_0$  of the particle and the initial potential  $V_0$  that are in general different from the “bulk” mass  $M$  and potential  $V$ . This allows for quenches in these parameters. Note that the case in which the initial state is a pure state [e.g. Eq. (3.42)] can be easily recovered by setting  $M_0 = 0$  and  $V_0 = 0$  or, equivalently, by noting that the path  $q^0$  shrinks identically to zero (since there is no initial Hamiltonian for this simple type of initial condition).

The superscripts in the path integral in Eq. (3.56) remind us of the constraint that the paths are subject to. One has

$$\begin{aligned} x(0) &= x_i, \quad \bar{x}(0) = \bar{x}_i, \\ x(t) &= x_f, \quad q^0(0) = q^+(0) = x_i + \frac{\bar{x}_i}{2}, \\ \bar{x}(t) &= 0, \quad q^0(\beta\hbar) = q^-(0) = x_i - \frac{\bar{x}_i}{2}. \end{aligned} \quad (3.58)$$

Note that due to the periodic boundary conditions of the trace  $\bar{x}_f = q^+(t) - q^-(t) = 0$ .

### 3.3.3 Generic Gaussian initial conditions

It is very easy to include the change of  $\Phi[x, \bar{x}, q^0]$  induced by the initial position measurement in Eq. (3.40). By using the explicit Gaussian form of the projector  $\hat{\Pi}(q_m)$  [see Eq. (3.41)] the dependence on the initial measurement can be simply incorporated in  $\Sigma[x, \bar{x}, q^0]$  by an additional term of the form

$$\begin{aligned} & \frac{i\hbar}{4\Delta^2} \left[ \left(x_i + \frac{\bar{x}_i}{2} - q_m\right)^2 + \left(x_i - \frac{\bar{x}_i}{2} - q_m\right)^2 \right] \\ &= \frac{i\hbar}{2\Delta^2} \left[ (x_i - q_m)^2 + \frac{\bar{x}_i^2}{4} \right]. \end{aligned} \quad (3.59)$$

In the limit of strong uncertainty  $\Delta \rightarrow \infty$  the effect of the initial measurement is blurred.

In order to recover the case where the initial state of the system is pure and decouples from the environment [which corresponds to the factorized initial density matrix with  $\hat{\rho}_{S_0}$  given by

Eq. (3.42)] the action in Eq. (3.57) has to be supplemented by

$$\begin{aligned} & \frac{i\hbar}{4\Delta^2} \left[ \left( x_i + \frac{\bar{x}_i}{2} - q_m \right)^2 + \left( x_i - \frac{\bar{x}_i}{2} - q'_m \right)^2 \right] \\ & = \frac{i\hbar}{2\Delta^2} \left[ x_i^2 + \frac{\bar{x}_i^2}{4} + x_m^2 + \frac{\bar{x}_m^2}{4} - 2x_m x_i - \frac{1}{2} \bar{x}_m \bar{x}_i \right], \end{aligned} \quad (3.60)$$

with the notation

$$x_m = (q_m + q'_m)/2 \quad \text{and} \quad \bar{x}_m = (q_m - q'_m). \quad (3.61)$$

Since Eq. (3.59) is a special case of Eq. (3.60) corresponding to  $q_m = q'_m$  (or  $x_m = q_m$  and  $\bar{x}_m = 0$ ) we will work with the latter in the following. The relevant cases can then be selected by taking simple limits.

In the following expressions we will write only the terms that depend on  $x_i$  or  $\bar{x}_i$  since the ones depending on  $x_m$  and  $\bar{x}_m$  contribute only to an overall constant.

### 3.3.4 The sources

The source term appears as  $\int dt' H(t') q^+(t')$  in  $\mathcal{K}$  [see Eq. (3.47)] and as  $-\int dt' H(t') q^-(t')$  in  $\mathcal{K}^*$  [see Eq. (3.48)]. For convenience, we distinguished the function existing on the positive running branch of the closed time contour, which we still call  $H(t)$ , from the one existing on the negative running branch of the same contour, which we call  $H'(t)$ . This implies that the potentials in Eq. (3.57) are given by  $V_H(y) = V(y) - Hy$  and  $V_{H'}(y) = V(y) - H'y$ .

After the transformation of variables in Eq. (3.53) we obtain two external time-dependent sources  $F(s) = [H(s) + H'(s)]/2$  and  $G(s) = [H(s) - H'(s)]$  which couple linearly to the variables  $\bar{x}(s)$  and  $x(s)$ , respectively. All correlation functions can be computed from the generating functional  $\mathcal{J}[F, G]$  as derivatives of  $\mathcal{J}$  with respect to  $F$  or  $G$  evaluated at  $F = G = 0$ . A physical force is represented by  $H(s) = H'(s)$ , that is by  $F(s) \neq 0$  and  $G(s) = 0$ . Therefore, the linear response of the mean value Eq. (3.56) to an external force can be obtained for  $F(s) \neq 0$ .

The generating functional, that is to say, the trace over the reduced density matrix in the presence of the external sources reads

$$e^{\mathcal{J}[F, G]} \sim \int dx_i d\bar{x}_i dx_f \int' \mathcal{D}x \mathcal{D}\bar{x} \mathcal{D}q^0 e^{\frac{i}{\hbar} \Sigma[x, \bar{x}, q^0, x_i, x_f, \bar{x}_i]},$$

where the path integral is subject to the constraints in Eqs. (3.58). The overall normalization factor depends on  $t$ ,  $\beta$  and all parameters in the model but not on the fields. We can now write

$$\langle \hat{q}(t) \rangle = \frac{\hbar}{i} \frac{\delta}{\delta G(t)} e^{\mathcal{J}[F, G]} \Big|_{F=0, G=0} \quad (3.62)$$

and

$$\langle \hat{q}(t) \hat{q}(t') \rangle = \frac{\hbar}{i} \frac{\delta}{\delta G(t)} \frac{\hbar}{i} \left[ \frac{\delta}{\delta G(t')} + \frac{\delta}{2\delta F(t')} \right] e^{\mathcal{J}[F, G]} \Big|_{F, G=0} \quad (3.63)$$

and all other correlation functions can be obtained in a similar way by noting that  $q^+(t) = q_f = x_f$  and  $q^-(t') = x(t) + \bar{x}(t)/2$ . At this point it has become obvious why two sources are needed in order to obtain all non-equilibrium correlation functions.

### 3.3.5 The harmonic case

To go further we restrict ourselves to the study of a quantum Brownian particle in a harmonic potential for which

$$-V(x + \bar{x}/2; s) + V(x - \bar{x}/2; s) = -M\Omega^2 x\bar{x} \quad (3.64)$$

and

$$V_0(q^0) = \frac{1}{2}M_0\Omega_0^2(q^0)^2. \quad (3.65)$$

The choice of a quadratic potential renders the problem analytically solvable. The generating functional can be calculated by simply evaluating the action on its minimal action path (over the initial condition branch and the time-dependent branches) as Gaussian fluctuations yield only pre-factors that are independent of the sources and can be determined at the end of the calculation from the normalization of the density matrix. Note that, although both initial and bulk potentials are harmonic, they are not necessarily the same thus allowing for the study of quantum quenches.

### 3.3.6 Integration over the initial condition

We first treat the contribution of the initial condition path  $q^0$  in Eq. (3.57). The equation of motion for  $q^0$  can be easily obtained from Eq. (3.57):

$$\begin{aligned} M_0\ddot{q}^0(\tau) - \int_0^{\beta\hbar} d\sigma k(\tau - \sigma)q^0(\sigma) - M_0\Omega_0^2 q^0(\tau) \\ = -i \int_0^t ds K^*(s - i\tau)\bar{x}(s), \end{aligned} \quad (3.66)$$

with the fixed end-points  $q^0(0) = q_i^+$  and  $q^0(\beta\hbar) = q_i^-$ . As the  $q^0$  path is part of the whole closed-time path it implicitly depends on the fixed end-time  $t$  as well. In [8] one can find a detailed analysis of this equation of motion which uses a Fourier expansion of the path  $q^0(\tau)$  on the interval  $[0, \beta\hbar]$ . By using the results found therein we obtain

$$\begin{aligned} \Sigma[x, \bar{x}, x_i, x_f, \bar{x}_i] = & \frac{i}{2M_0} \int_0^t dsdu R'(s, u)\bar{x}(s)\bar{x}(u) + iM_0 \left[ \frac{1}{2\Lambda}x_i^2 + \frac{\Xi}{2}\bar{x}_i^2 \right] \\ & + \frac{i\hbar}{2\Delta^2} \left[ x_i^2 + \frac{\bar{x}_i^2}{4} - 2x_mx_i - \frac{1}{2}\bar{x}_m\bar{x}_i \right] \\ & + \int_0^t ds M \left[ \dot{x}\dot{x} - \Omega^2\bar{x}x + \frac{1}{M}\bar{F}(s)\bar{x}(s) + \right. \\ & \left. \frac{1}{M}G(s)x(s) - \bar{x}(s)\frac{d}{ds} \int_0^s du\gamma(s-u)x(u) \right]. \end{aligned} \quad (3.67)$$

We introduced the complex ‘‘force’’

$$\bar{F}(s) = F(s) + x_iC_1(s) - i\bar{x}_iC_2(s), \quad (3.68)$$

with the functions  $C_1$  and  $C_2$

$$\begin{aligned} C_1(s) &= \frac{1}{\beta\hbar\Lambda} \sum_{k=-\infty}^{\infty} u_k g_k(s) , \\ C_2(s) &= \frac{1}{\beta\hbar} \sum_{k=-\infty}^{\infty} u_k \nu_k f_k(s) . \end{aligned} \quad (3.69)$$

The constants  $\Lambda$  and  $\Xi$  are given by

$$\Lambda = \frac{1}{\beta\hbar} \sum_{k=-\infty}^{\infty} u_k \quad \text{and} \quad \Xi = \frac{1}{\beta\hbar} \sum_{k=-\infty}^{\infty} u_k (\Omega_0^2 + \zeta_k) , \quad (3.70)$$

with  $u_k = (\Omega_0^2 + \nu_k^2 + \zeta_k)^{-1}$ ,  $\nu_k = 2\pi k/\beta\hbar$ ,  $\zeta_k = [M\gamma(0) - g_k(0)]/M_0$  [for the definition of  $\gamma(t)$  see Eq. (3.75) below] and

$$g_k(s) = \int_0^\infty \frac{d\omega}{\pi} S(\omega) \frac{2\omega}{\omega^2 + \nu_k^2} \cos(\omega s) , \quad (3.71)$$

$$f_k(s) = \int_0^\infty \frac{d\omega}{\pi} S(\omega) \frac{2\nu_k}{\omega^2 + \nu_k^2} \sin(\omega s) , \quad (3.72)$$

where  $S(\omega)$  is the spectral density of the bath. The two-time function  $R'$  reads

$$\begin{aligned} R'(s, u) &= R(s, u) + M_0 K_R(s - u) , \\ R(s, u) &= -\Lambda C_1(s) C_1(u) + \frac{1}{\beta\hbar} \sum_{k=-\infty}^{\infty} u_k [g_k(s) g_k(u) - f_k(s) f_k(u)] , \end{aligned} \quad (3.73)$$

with

$$K_R(s - u) = \frac{1}{\beta\hbar} \sum_k g_k(s - u) \quad (3.74)$$

the real part of the kernel  $K$ . The time-dependent bath kernel  $\gamma(s)$  is given by [see Eq. (3.145)]

$$\gamma(s) = \frac{2}{M} \int_0^\infty \frac{d\omega}{\pi} \frac{S(\omega)}{\omega} \cos(\omega s) . \quad (3.75)$$

The functions  $C_1$  and  $C_2$  as well as the kernel  $R(s, u)$  are not to be confused with the correlation functions and the linear response function that will be denoted by  $\mathcal{C}$  and  $\mathcal{R}$ , respectively.

### 3.3.7 Real time minimal action paths with external sources

The equations of motion for  $x(s)$  and  $\bar{x}(s)$  read

$$\begin{aligned} \ddot{x}(s) + \frac{d}{ds} \int_0^s du \gamma(s - u) x(u) + \Omega^2 x(s) \\ = \frac{\bar{F}(s)}{M} + \frac{i}{MM_0} \int_0^t du R'(s, u) \bar{x}(u) , \end{aligned} \quad (3.76)$$

$$\ddot{\bar{x}}(s) - \frac{d}{ds} \int_s^t du \gamma(u - s) \bar{x}(u) + \Omega^2 \bar{x}(s) = \frac{G(s)}{M} . \quad (3.77)$$

The action  $\Sigma$  evaluated along the minimal action paths can be determined by inserting the solutions to Eqs. (3.76) and (3.77) into Eq. (3.67). However, the authors of [8] noted a simplification of the calculation which can be generalized to our case where the source  $G(s)$  is also present (in [8] no external source for  $\bar{x}$  was used). The idea is the following. After a partial integration in the second line of Eq. (3.67) the action  $\Sigma$  takes the form

$$\begin{aligned} \Sigma[x, \bar{x}, x_i, x_f, \bar{x}_i] = & \\ & -M\bar{x}_i\dot{x}_i - \frac{i}{2M_0} \int_0^t ds du R'(s, u)\bar{x}(s)\bar{x}(u) \\ & + \int_0^t ds G(s)x(s) + \text{border}(x_i, x_f, \bar{x}_i) \end{aligned} \quad (3.78)$$

when evaluated along the minimal action paths determined by Eqs. (3.76) and (3.77), where we used the boundary condition  $\bar{x}_f = 0$ . Here,  $\text{border}(x_i, x_f, \bar{x}_i)$  stands for all border terms in Eq. (3.67).

On the other hand, one can split the force Eq. (3.68) into its real and imaginary parts  $\bar{F}(s) = \bar{F}_R(s) + i\bar{F}_I(s)$ . Then, the minimal action path  $x(s)$  splits into  $x(s) = x_R(s) + ix_I(s)$ , where  $x_I(s)$  satisfies the boundary conditions  $x_I(0) = x_I(t) = 0$ . The trick is to show now that one can simply focus on the real part  $x_R(s)$  of the minimal action path in order to obtain the complete stationary phase action. Indeed, if we evaluate the action Eq. (3.67) only along the minimal  $x_R(s)$  and  $\bar{x}(s)$  we obtain

$$\begin{aligned} \Sigma[x_R, \bar{x}, x_i, x_f, \bar{x}_i] = & -M\bar{x}_i\dot{x}_{R,i} + \int_0^t ds G(s)x_R(s) \\ & + \int_0^t ds \bar{x}(s) \left[ \bar{F}_I(s) + \frac{i}{2M_0} \int_0^t du R'(s, u)\bar{x}(u) \right] \\ & + \text{border}(x_i, x_f, \bar{x}_i), \end{aligned} \quad (3.79)$$

where we used the fact that  $x_R(s)$  satisfies the real part of Eq. (3.76). We now want to show that Eqs. (3.79) and (3.78) are indeed equal. With the help of the imaginary part of Eq. (3.76) and the equation of motion (3.77) we can easily prove by integration by parts that

$$\begin{aligned} \int_0^t ds \bar{x}(s) \left[ \bar{F}_I(s) + \frac{1}{M_0} \int_0^t du R'(s, u)\bar{x}(u) \right] \\ = -M\bar{x}_i\dot{x}_{I,i} + \int_0^t ds G(s)x_I(s), \end{aligned}$$

and by using this identity in Eq. (3.79) we recover Eq. (3.78). Therefore, the right-hand-side (rhs) of Eq. (3.78) and the rhs of Eq. (3.79) coincide. It is sufficient to evaluate the action Eq. (3.67) along the real component  $x_R(s)$  that satisfies a much simpler equation than  $x(s)$ .

In terms of the end points  $x_i, x_f$  and  $\bar{x}_i$ , the solutions to the real parts of Eqs. (3.76) and (3.77) read

$$\begin{aligned} x_R(s) = & \frac{\mathcal{G}_+(s)}{\mathcal{G}_+(t)} x_f + \left[ \dot{\mathcal{G}}_+(s) - \frac{\mathcal{G}_+(s)}{\mathcal{G}_+(t)} \dot{\mathcal{G}}_+(t) \right] x_i \\ & + \frac{1}{M} \int_0^s du \mathcal{G}_+(s-u) \bar{F}_R(u) \\ & - \frac{1}{M} \frac{\mathcal{G}_+(s)}{\mathcal{G}_+(t)} \int_0^t du \mathcal{G}_+(t-u) \bar{F}_R(u) \end{aligned} \quad (3.80)$$

and

$$\begin{aligned}\bar{x}(s) &= \frac{\mathcal{G}_+(t-s)}{\mathcal{G}_+(t)}\bar{x}_i + \frac{1}{M} \int_s^t du \mathcal{G}_+(u-s)G(u) \\ &\quad - \frac{1}{M} \frac{\mathcal{G}_+(t-s)}{\mathcal{G}_+(t)} \int_0^t du \mathcal{G}_+(u)G(u),\end{aligned}\quad (3.81)$$

where  $\mathcal{G}_+(t)$  is a propagator that in Laplace-transform reads

$$\tilde{\mathcal{G}}_+(\lambda) = \frac{1}{\lambda^2 + \lambda\tilde{\gamma}(\lambda) + \Omega^2}. \quad (3.82)$$

From Eq. (3.80) we immediately find, by using the boundary conditions  $\mathcal{G}_+(0) = 0$ ,  $\dot{\mathcal{G}}_+(0) = 1$  and  $\ddot{\mathcal{G}}_+(0) = 0$ ,

$$\begin{aligned}\dot{x}_{R,i} &= \frac{1}{\mathcal{G}_+(t)}x_f - \frac{\dot{\mathcal{G}}_+(t)}{\mathcal{G}_+(t)}x_i \\ &\quad - \frac{1}{\mathcal{G}_+(t)}\frac{1}{M} \int_0^t du \mathcal{G}_+(t-u)\bar{F}_R(u).\end{aligned}\quad (3.83)$$

Inserting the solutions to Eqs. (3.80) and (3.81), and Eq. (3.83) into Eq. (3.79) we find an effective action  $\Sigma[x_i, x_f, \bar{x}_i]$  that depends only on the end-points,  $x_i, x_f$  and  $\bar{x}_i$ , and the external sources  $F$  and  $G$ :

$$\begin{aligned}\Sigma[x_i, x_f, \bar{x}_i] &= \\ &- \frac{iM_0}{\epsilon^2}x_ix_m - \frac{iM_0}{4\epsilon^2}\bar{x}_i\bar{x}_m - M\bar{x}_ix_f\frac{1}{\mathcal{G}_+(t)} + M\bar{x}_ix_i\frac{\dot{\mathcal{G}}_+(t)}{\mathcal{G}_+(t)} + \frac{\bar{x}_i}{\mathcal{G}_+(t)} \int_0^t du \mathcal{G}_+(t-u)\bar{F}_R(u) \\ &- i\bar{x}_i \int_0^t ds C_2(s)\bar{x}(s) + \frac{iM_0}{2} \left( \frac{x_i^2}{\Lambda'} + \Xi'\bar{x}_i^2 \right) + \frac{i}{2M_0} \int_0^t dsdu R'(s,u)\bar{x}(s)\bar{x}(u) \\ &+ x_f \int_0^t ds \frac{\mathcal{G}_+(s)}{\mathcal{G}_+(t)}G(s) \\ &+ x_i \int_0^t ds G(s) \left[ \frac{\dot{\mathcal{G}}_+(s)}{\mathcal{G}_+(t)} - \frac{\mathcal{G}_+(s)}{\mathcal{G}_+(t)}\frac{\dot{\mathcal{G}}_+(t)}{\mathcal{G}_+(t)} \right] + \frac{1}{M} \int_0^t ds \int_0^s du \mathcal{G}_+(s-u)G(s)\bar{F}_R(u) \\ &- \frac{1}{M} \int_0^t dsdu \frac{\mathcal{G}_+(t-u)}{\mathcal{G}_+(t)}\mathcal{G}_+(s)G(s)\bar{F}_R(u),\end{aligned}\quad (3.84)$$

with

$$\frac{1}{\Lambda'} \equiv \frac{1}{\Lambda} + \frac{1}{\epsilon^2}, \quad \Xi' \equiv \Xi + \frac{1}{4\epsilon^2} \quad \text{and} \quad \epsilon^2 \equiv \frac{M_0\Delta^2}{\hbar}. \quad (3.85)$$

For the sake of a clear presentation we have not replaced  $\bar{x}(s)$  and  $\bar{F}_R$  by their corresponding expressions in terms of the end-points yet.

### 3.3.8 Integration over the end-points

In order to find the final expression for  $\mathcal{J}[F, G]$  we still have to integrate over the end-points  $x_i, x_f$  and  $\bar{x}_i$ . Since the exponent  $\Sigma[x_i, x_f, \bar{x}_i]$  is linear in  $x_f$  the integration over this variable generates a  $\delta$ -function of the form

$$\delta \left[ \bar{x}_i - \frac{1}{M} \int_0^t ds \mathcal{G}_+(s)G(s) \right], \quad (3.86)$$

up to a factor not depending on the end-points which, in combination with the integration over  $\bar{x}_i$ , enforces a substitution of  $\bar{x}_i$  by  $\frac{1}{M} \int_0^t ds \mathcal{G}_+(s)G(s)$  and  $\bar{x}(s)$  by  $\frac{1}{M} \int_s^t du \mathcal{G}_+(u-s)G(u)$  [the first and the third terms of the rhs of Eq. (3.81) cancel]. Moreover, after the integration over  $\bar{x}_i$  the fifth and the last terms of the rhs of Eq. (3.84) cancel, too. Finally, the Gaussian integral over  $x_i$  yields

$$\begin{aligned}
 \mathcal{J}[F, G] = & \\
 & - \frac{\Lambda'}{2\hbar M_0} \left( \int_0^t ds G(s) \dot{\mathcal{G}}_+(s) \right)^2 + \frac{M_0}{4\hbar\epsilon^2 M} \bar{x}_m \int_0^t ds \mathcal{G}_+(s)G(s) \\
 & - \frac{\Lambda'}{\hbar M M_0} \int_0^t ds G(s) \dot{\mathcal{G}}_+(s) \int_0^{s'} ds' \int_0^{s'} du' \mathcal{G}_+(s'-u') C_1(u') G(s') \\
 & - \frac{\Xi' M_0}{2\hbar M^2} \left( \int_0^t ds G(s) \mathcal{G}_+(s) \right)^2 + \frac{i}{\hbar M} \int_0^t ds \int_0^s du \mathcal{G}_+(s-u) G(s) F(u) \\
 & + \frac{1}{\hbar M^2} \int_0^t ds \mathcal{G}_+(s) G(s) \int_0^t ds' \int_{s'}^t du' \mathcal{G}_+(u'-s') C_2(s') G(u') \\
 & + \frac{i\Lambda'}{\hbar\epsilon^2} x_m \left[ \int_0^t ds G(s) \dot{\mathcal{G}}_+(s) + \frac{1}{M} \int_0^t ds \int_0^s du \mathcal{G}_+(s-u) G(s) C_1(u) \right] \\
 & - \frac{1}{2\hbar M^2 M_0} \int_0^t ds \int_0^t ds' \int_s^t du \int_{s'}^t du' \mathcal{G}_+(u-s) R''(s, s') \mathcal{G}_+(u'-s') G(u) G(u') .
 \end{aligned} \tag{3.87}$$

Here we introduced the kernel

$$R''(s, s') = \Lambda' C_1(s) C_1(s') + R'(s, s') , \tag{3.88}$$

where we used Eq. (3.139). Equation (3.87) is the central result of the first part of this paper. It allows us to derive all non-equilibrium correlation functions in a systematic way. Direct applications of this method will be presented in Secs. 3.4 and 4.4.

### 3.3.9 The correlation function

The two-time correlation function Eq. (3.63) has two contributions,

$$\begin{aligned}
 \langle \hat{q}(t) \hat{q}(t') \rangle &= \frac{1}{2} \langle [\hat{q}(t), \hat{q}(t')]_+ \rangle + \frac{1}{2} \langle [\hat{q}(t), \hat{q}(t')]_- \rangle \\
 &= \mathcal{C}(t, t') + i\mathcal{A}(t - t') .
 \end{aligned} \tag{3.89}$$

The first term, the average of the anti-commutator or symmetrized contribution, is real and the second one, the average of the commutator or anti-symmetrized contribution, is imaginary and proportional to the linear response function,  $\mathcal{R}(t, t')$ , as shown by the Kubo formula. For

generic Gaussian initial conditions, Eq. (3.41), one finds

$$\begin{aligned}
 \mathcal{C}(t, t') = & \\
 & \frac{\Lambda' \hbar}{M_0} \left[ \dot{\mathcal{G}}_+(t) \dot{\mathcal{G}}_+(t') + \frac{\dot{\mathcal{G}}_+(t)}{M} \int_0^{t'} du \mathcal{G}_+(t' - u) C_1(u) + \frac{1}{M} \dot{\mathcal{G}}_+(t') \int_0^t du \mathcal{G}_+(t - u) C_1(u) \right] \\
 & + \frac{\hbar \Xi' M_0}{M^2} \mathcal{G}_+(t) \mathcal{G}_+(t') - \frac{\hbar}{M^2} \left[ \mathcal{G}_+(t) \int_0^{t'} \mathcal{G}_+(t' - u) C_2(u) + \mathcal{G}_+(t') \int_0^t \mathcal{G}_+(t - u) C_2(u) \right] \\
 & + \frac{\Lambda'^2}{\epsilon^4} x_m^2 \left[ \dot{\mathcal{G}}_+(t) + \frac{1}{M} \int_0^t du \mathcal{G}_+(t - u) C_1(u) \right] \left[ \dot{\mathcal{G}}_+(t') + \frac{1}{M} \int_0^{t'} du \mathcal{G}_+(t' - u) C_1(u) \right] \\
 & - \frac{M_0^2}{16\epsilon^4 M^2} \bar{x}_m^2 \mathcal{G}_+(t) \mathcal{G}_+(t') + \frac{\hbar}{M^2 M_0} \int_0^t du \int_0^{t'} du' \mathcal{G}_+(t - u) R''(u, u') \mathcal{G}_+(t' - u').
 \end{aligned} \tag{3.90}$$

To represent a pure initial condition that is initially decoupled from the bath, as in Eq. (3.42), we set  $M = M_0$ ,  $\Lambda' = \epsilon^2$  and  $\Xi' = 1/4\epsilon^2$  as well as  $C_1(s) = 0$ ,  $C_2(s) = 0$  and  $R''(u, u') = MK(u - u')$ . A non-factorized initial state with – say – an initial position measurement of “width”  $\epsilon$  is obtained with  $x_m = q_m$  and  $\bar{x}_m = 0$ . In the classical case the non equilibrium correlator of a Brownian particle is given by Eq. (3.153).

### 3.4 Non equilibrium dynamics after quantum quenches.

Quenches from a high temperature initial state have been extensively studied in the literature. They correspond to the case of a factorizing density matrix as in Eq. (3.39). In this section we will study the non-equilibrium dynamics of a quantum Brownian particle after quenches from different initial states. As already mentioned in the introduction, there are two experimental scenarios that are of interest to us. In the first one the initial position of a Brownian particle trapped by a harmonic potential is measured at  $t = 0$ . We will study this case in the first part of this section by focusing on the two-time correlation function. The second scenario consists in a quench of the trapping potential, which in the case of a harmonic potential corresponds to an abrupt change in the trapping frequency. Such a quench will be studied in the second part of this section. In both cases, we will derive the asymptotic equilibration behavior of the system in the presence of Ohmic dissipation.

#### 3.4.1 A particle in a harmonic potential with an initial position measurement

The general results in Sec. 3.3 are here specialized to the case of a particle trapped in a harmonic potential, on which a position measurement is performed at  $t = 0$ . As we work with the same particle initially and subsequently,  $M_0 = M$ , while  $\Omega_0 = \Omega > 0$ . At  $t = 0$  a measurement of the particle position is performed with outcome  $q_m = 0$  and uncertainty  $\Delta$ . The initial density matrix is given by Eq. (3.40). Note that the particle is permanently coupled to the bath, hence the initial density matrix does not factorize. Thus, our starting point is the general expression Eq. (3.90) with  $M = M_0$ ,  $\Omega = \Omega_0$  and  $x_m = \bar{x}_m = 0$ . The Laplace transform of the correlator

reads

$$\begin{aligned} \tilde{C}(\lambda, \kappa) = & \frac{\hbar}{M} \tilde{\mathcal{G}}_+(\lambda) \tilde{\mathcal{G}}_+(\kappa) \left\{ \Lambda' \lambda \kappa + \frac{\Lambda'}{M} \lambda \tilde{C}_1(\kappa) + \frac{\Lambda'}{M} \kappa \tilde{C}_1(\lambda) + \frac{\Xi' M_0^2}{M^2} \right. \\ & \left. - \frac{1}{M} \tilde{C}_2(\lambda) - \frac{1}{M} \tilde{C}_2(\kappa) + \frac{1}{M^2} \tilde{R}''(\lambda, \kappa) \right\}, \end{aligned} \quad (3.91)$$

an expression that can be simplified by using the method explained in App. 3.5.3.

Introducing the function  $\tilde{h}_k(\lambda) = \tilde{g}_k(\lambda)/M + \lambda$ , Eq. (3.91) can be written as

$$\begin{aligned} \tilde{C}(\lambda, \kappa) = & \frac{\hbar}{M} \tilde{\mathcal{G}}_+(\lambda) \tilde{\mathcal{G}}_+(\kappa) \frac{(\Lambda' - \Lambda)}{(\beta \hbar \Lambda)^2} \sum_{k, k'} u_k u_{k'} \tilde{h}_k(\lambda) \tilde{h}_{k'}(\kappa) \\ & + \frac{\hbar}{4M\epsilon^2} \tilde{\mathcal{G}}_+(\lambda) \tilde{\mathcal{G}}_+(\kappa) + \frac{\tilde{C}^{1\text{eq}}(\lambda) + \tilde{C}^{1\text{eq}}(\kappa)}{\lambda + \kappa}, \end{aligned} \quad (3.92)$$

with the equilibrium correlation function  $\tilde{C}^{1\text{eq}}(\lambda)$  in the Laplace domain defined in Eq. (3.170). In App. 3.5.3 it is shown that  $\tilde{h}_k(\lambda)$  can be written in terms of  $\tilde{\mathcal{G}}_+^{-1}(\lambda)$  and  $\tilde{\mathcal{G}}_+^{-1}(|\nu_k|)$  [see Eq. (3.169)]. For  $\Omega = \Omega_0$  we use the fact that  $u_k = \tilde{\mathcal{G}}_+(|\nu_k|)$  and we find from the definition of the equilibrium correlator

$$\tilde{C}^{1\text{eq}}(\lambda) = \frac{1}{\beta M} \sum_k \frac{\lambda}{\nu_k^2 - \lambda^2} \left[ \tilde{\mathcal{G}}_+(\lambda) - \tilde{\mathcal{G}}_+(|\nu_k|) \right], \quad (3.93)$$

which is derived in App. 3.5.3 [see Eq. (3.170)], that the desired non equilibrium correlation function of a quantum Brownian particle with initial position measurement reads

$$\begin{aligned} \tilde{C}(\lambda, \kappa) = & \frac{M}{\hbar} \frac{\Lambda' - \Lambda}{\Lambda^2} \tilde{C}^{1\text{eq}}(\lambda) \tilde{C}^{1\text{eq}}(\kappa) + \frac{\hbar}{4M\epsilon^2} \tilde{\mathcal{G}}_+(\lambda) \tilde{\mathcal{G}}_+(\kappa) \\ & + \frac{\tilde{C}^{1\text{eq}}(\lambda) + \tilde{C}^{1\text{eq}}(\kappa)}{\lambda + \kappa}. \end{aligned} \quad (3.94)$$

The classical correlator for an initial position measurement with outcome  $q^0 = 0$  and uncertainty  $\Delta$  can be obtained from Eq. (3.158) by replacing  $\langle q^{02} \rangle$  by  $\Delta^2$ . The initial momentum is not measured and it is therefore distributed according to the Boltzmann-law with  $\langle v_0^2 \rangle = (\beta M)^{-1}$ . In the limit of a sharp position measurement ( $\Delta \rightarrow 0$ ) the classical correlator of an equilibrium particle reads  $\tilde{C}^{\text{eq}}(\lambda, \kappa) = \beta M \Omega^2 \tilde{C}^{1\text{eq}}(\lambda) \tilde{C}^{1\text{eq}}(\kappa)$ . As to the quantum correlator, we note that  $\Lambda' = 0$  for  $\Delta \rightarrow 0$  and the sum of the first and the third term in the rhs of Eq. (3.94) yields  $\tilde{C}^{\text{eq}}(\lambda, \kappa) = M/(\hbar \Lambda) \tilde{C}^{1\text{eq}}(\lambda) \tilde{C}^{1\text{eq}}(\kappa)$  which already has the form of its classical counterpart. It is easy to show that in the high temperature limit  $\beta \hbar \ll |\Omega^2 - \gamma^2/4|$  the two expressions coincide exactly. The role of the second term in the rhs of Eq. (3.94) remains to be discussed: it describes the initial momentum due to Heisenberg's uncertainty relation. Consequently, it diverges when the initial position measurement becomes sharp unless one considers that  $\hbar/(M\epsilon^2) = \hbar^2/(M^2\Delta^2) \rightarrow 0$  even though  $\Delta \rightarrow 0$ . More precisely, when  $\beta \hbar |\Omega^2 - \gamma^2/4|^{1/2} \ll 1$  we have  $\mathcal{C}^{1\text{eq}} \sim 1/(\beta M \Omega^2)$  and  $\mathcal{G}_+ \sim 1/\Omega$ . In order for the second term of the rhs of Eq. (3.94) to be small compared to the other terms the condition  $\Delta \gg \lambda_T$  must hold, with  $\lambda_T = \sqrt{\beta \hbar^2/(2\pi M)}$  the *thermal de Broglie-wavelength* of the particle. Only then can one speak of a classical particle: the condition  $\beta \hbar |\Omega^2 - \gamma^2/4|^{1/2} \ll 1$  that properly defines the *high temperature regime* is *not sufficient*. One also has to take the *macroscopic measurement limit* defined through  $\Delta \gg \lambda_T$ .

In the real time domain the quantum correlation function is

$$\begin{aligned} \mathcal{C}(t, t') &= \frac{M}{\hbar} \frac{\Lambda' - \Lambda}{\Lambda^2} \mathcal{C}^{1\text{eq}}(t') \mathcal{C}^{1\text{eq}}(t) \\ &\quad + \frac{\hbar}{4M\epsilon^2} \mathcal{G}_+(t) \mathcal{G}_+(t') + \mathcal{C}^{1\text{eq}}(|t - t'|), \end{aligned} \quad (3.95)$$

where  $\mathcal{C}^{1\text{eq}}(t)$  is the real time equilibrium correlation function. This result applies to any kind of spectral density of the bath. We will use the correlation function Eq. (3.95) in Sec. 4.4 to study the non equilibrium dynamics of an impurity in a Luttinger liquid bath for which a specific spectral density of the bath applies.

We are interested in the equilibration behavior of Eq. (3.95) in the presence of Ohmic dissipation for which the spectral density behaves as  $S(\omega) \sim \gamma\omega$  for small  $\omega$ , with  $\gamma$  playing the role of a friction coefficient [for more details see App. 3.5.4]. It is of special interest to study the strong quantum regime  $\beta\hbar \gg |\Omega^2 - \gamma^2/4|^{-1/2}$ . By using the long-time limits Eq. (3.179) and Eq. (3.180) presented in App. 3.5.4 valid for  $t \gg \gamma^{-1}$  we find that the propagator  $\mathcal{G}_+(t)$  exponentially approaches zero whereas the equilibrium correlation function  $\mathcal{C}^{1\text{eq}}(t)$  relaxes with a power law  $\sim t^{-2}$  for  $t \rightarrow \infty$ . In the long-time limit the correlator Eq. (3.95) thus relaxes as fast as the squared equilibrium correlation function. Therefore, for  $\beta\hbar \gg |\Omega^2 - \gamma^2/4|^{-1/2}$ :

$$\mathcal{C}(t, t') = \mathcal{C}^{1\text{eq}}(|t - t'|) + \mathcal{O}[(tt')^{-2}] \quad (3.96)$$

when  $t, t' \gg \gamma^{-1}$ , and the equilibrium function  $\mathcal{C}^{1\text{eq}}(|t - t'|) = \mathcal{C}^{\text{eq}}(t, t')$  is asymptotically approached during the algebraic relaxation of the non-equilibrium terms. Consequently, care has to be taken in experiments when an equilibrium system is desired at very low temperatures after an initial position measurement. The relaxation of the system is slow independently of the dissipation strength  $\gamma$ . At high temperatures  $\beta\hbar \ll |\Omega^2 - \gamma^2/4|^{-1/2}$  the relaxation is of order  $\mathcal{O}(e^{-\gamma t})$  [see the discussion in App. 3.5.4] and therefore exponential as in the classical limit.

### 3.4.2 Quantum quench in the confining potential.

In this section we desire to gain insight into the equilibration process of a quantum Brownian particle after an abrupt change in the trapping frequency. At  $t < 0$  the particle is confined in a harmonic potential with frequency  $\Omega_0 > 0$ . At  $t = 0$  the experimentalist abruptly changes the strength of the harmonic potential resulting in a higher or lower trapping frequency. We do not consider an initial position measurement since we assume that the particle is already localized by the initial harmonic trap. Hence we set  $\Lambda' = \Lambda$ ,  $\Xi' = \Xi$ ,  $x_m = \bar{x}_m = 0$  and  $\epsilon \rightarrow \infty$ . By starting from Eq. (3.91) and by using Eq. (3.73) it is straightforward to show with the methods employed in App. 3.5.3 that the correlator in the Laplace domain reads

$$\tilde{\mathcal{C}}(\lambda, \kappa) = \frac{\hbar}{M} \frac{\tilde{\mathcal{G}}_+(\lambda) \tilde{\mathcal{G}}_+(\kappa)}{\tilde{\mathcal{G}}_+(\lambda) \tilde{\mathcal{G}}_+(\kappa)} \frac{1}{\lambda + \kappa} \left[ \tilde{\mathcal{C}}_0^{1\text{eq}}(\lambda) + \tilde{\mathcal{C}}_0^{1\text{eq}}(\kappa) \right], \quad (3.97)$$

where  $\tilde{\mathcal{G}}_+^0(\lambda) = 1/[\lambda^2 + \lambda\tilde{\gamma}(\lambda) + \Omega_0^2]$  is the propagator with initial frequency  $\Omega_0$ , and

$$\tilde{\mathcal{C}}_0^{1\text{eq}}(\lambda) = \frac{1}{\beta M} \sum_k \frac{\lambda}{\nu_k^2 - \lambda^2} \left[ \tilde{\mathcal{G}}_+^0(\lambda) - \tilde{\mathcal{G}}_+^0(|\nu_k|) \right] \quad (3.98)$$

is the equilibrium correlation function of a particle in a harmonic potential with frequency  $\Omega_0$  [see Eq. (3.170)]. The structure of Eq. (3.97) is very different from the classical counterpart

Eq. (3.157). Still, by using the high temperature approximation  $\tilde{\mathcal{C}}_0^{1\text{eq}}(\lambda) \simeq - [\tilde{\mathcal{G}}_+(\lambda) - 1/\Omega_0^2] / \lambda$  [see the end of the discussion in App. 3.5.4] one recovers the classical expression Eq. (3.153).

The equilibration time for Ohmic dissipation in the strong quantum regime  $\beta\hbar \gg |\Omega^2 - \gamma^2/4|^{-1/2}$  can be found in the following way. Note first that when  $\tilde{\mathcal{C}}_0^{1\text{eq}}(\lambda)$  is multiplied by  $\tilde{\mathcal{G}}_+(\lambda)/\tilde{\mathcal{G}}_+^0(\lambda)$  one obtains a new function that we call  $\tilde{\mathcal{C}}'$ :

$$\tilde{\mathcal{C}}'(\lambda) = \frac{1}{\beta M} \sum_k \frac{\lambda}{\nu_k^2 - \lambda^2} \left[ \tilde{\mathcal{G}}_+(\lambda) - \frac{\tilde{\mathcal{G}}_+(\lambda)\tilde{\mathcal{G}}_+^0(|\nu_k|)}{\tilde{\mathcal{G}}_+^0(\lambda)\tilde{\mathcal{G}}_+(|\nu_k|)} \tilde{\mathcal{G}}_+(|\nu_k|) \right]. \quad (3.99)$$

Second, we observe that the Laplace transform of  $(\partial_t + \partial_{t'})f(t, t')$  is equal to  $(\lambda + \kappa)\tilde{f}(\lambda, \kappa) - \tilde{f}(t=0; \kappa) - \tilde{f}(\lambda; t'=0)$  where  $\tilde{f}(\lambda, \kappa)$  is the Laplace transform of the generic function  $f(t, t')$  with respect to both  $t$  and  $t'$  while  $\tilde{f}(\lambda; t'=0)$  [ $\tilde{f}(t=0; \kappa)$ ] is the Laplace transform of  $f(t, t'=0)$  [ $f(t=0, t')$ ] with respect to  $t$  ( $t'$ ). Now, by choosing  $f(t, t') = \mathcal{C}(t, t')$  we find for the correlation function Eq. (3.97) in the time domain

$$\begin{aligned} (\partial_t + \partial_{t'})\mathcal{C}(t, t') &= \mathcal{C}'(t) [1 + (\Omega^2 - \Omega_0^2)\mathcal{G}_+(t')] \\ &\quad + \mathcal{C}'(t') [1 + (\Omega^2 - \Omega_0^2)\mathcal{G}_+(t)] \\ &\quad - \mathcal{C}(t, 0) - \mathcal{C}(0, t'). \end{aligned} \quad (3.100)$$

From Eq. (3.97) we easily find the expression of the Laplace transform of  $\mathcal{C}(t, t'=0)$  by multiplying  $\tilde{\mathcal{C}}(\lambda, \kappa)$  by  $\kappa$  and by taking the limit  $k \rightarrow \infty$ :

$$\tilde{\mathcal{C}}(\lambda; t'=0) = \tilde{\mathcal{C}}_0^{1\text{eq}}(\lambda) [1 + (\Omega^2 - \Omega_0^2)\tilde{\mathcal{G}}_+(\lambda)] = \tilde{\mathcal{C}}'(\lambda). \quad (3.101)$$

Accordingly, Eq. (3.100) simplifies to

$$(\partial_t + \partial_{t'})\mathcal{C}(t, t') = \mathcal{C}'(t)(\Omega^2 - \Omega_0^2)\mathcal{G}_+(t') + \mathcal{C}'(t')(\Omega^2 - \Omega_0^2)\mathcal{G}_+(t). \quad (3.102)$$

Finally, it is clear that  $(\partial_t + \partial_{t'})\mathcal{C}(t, t') = 0$  when  $\mathcal{C}(t, t') = \mathcal{C}^{\text{eq}}(t, t') = \mathcal{C}^{1\text{eq}}(|t - t'|)$  so that the terms of the rhs of Eq. (3.102) can be understood as the derivative of the non equilibrium part of  $\mathcal{C}(t, t')$ . In combination with the results of the discussion in App. 3.5.4 the equilibration behavior of the correlator at low temperatures after a quench in the trapping potential can be summarized as follows [by noting that the asymptotic long-time behavior of  $\mathcal{C}'(t)$  and  $\mathcal{C}^{1\text{eq}}(t)$  are identical]:

$$\mathcal{C}(t, t') = \mathcal{C}^{1\text{eq}}(|t - t'|) + \mathcal{O} \left[ e^{-\gamma t/2}/t' + e^{-\gamma t'/2}/t \right] \quad (3.103)$$

for  $t, t' \gg \gamma^{-1}$ . Consequently, the non equilibrium contributions are exponentially suppressed which leads to a faster equilibration than the one found after an initial position measurement.

At high temperatures the relaxation of  $\mathcal{C}'(t)$  and  $\mathcal{C}^{1\text{eq}}(t)$  are both exponential of  $\mathcal{O}(e^{-\gamma t/2})$  so that in the high temperature regime  $\mathcal{C}(t, t') = \mathcal{C}^{1\text{eq}}(|t - t'|) + \mathcal{O} \left[ e^{-\gamma(t+t')/2} \right]$  in sharp contrast with the algebraic relaxation found in Sec. 3.4.1.

## 3.5 Appendix B

### 3.5.1 Coherent state path integral formulation

In this Appendix we detail the derivation of a path-integral representation of the generating functional of the multi-time correlation functions of a quantum particle in contact with a generic quantum bath made of an ensemble of harmonic oscillators.

The terms in the Hamiltonian of the dissipative quantum Brownian particle that depend on the bath variables, Eqs. (3.33) and (3.34), can be rewritten in terms of creation and annihilation operators of the bath oscillators in view of a later use of coherent states. One defines the creator and the annihilator of the  $n$ -th oscillator mode by

$$\hat{a}_n^\dagger = \sqrt{\frac{m_n \omega_n}{2\hbar}} \left[ \hat{x}_n - \frac{i}{m_n \omega_n} \hat{p}_n \right], \quad (3.104)$$

$$\hat{a}_n = \sqrt{\frac{m_n \omega_n}{2\hbar}} \left[ \hat{x}_n + \frac{i}{m_n \omega_n} \hat{p}_n \right]. \quad (3.105)$$

The operators  $\hat{a}_n$  and  $\hat{a}_n^\dagger$  satisfy the bosonic commutation relations  $[\hat{a}_n^\dagger, \hat{a}_m] = \delta_{n,m}$  and  $[\hat{a}_n^\dagger, \hat{a}_m^\dagger] = [\hat{a}_n, \hat{a}_m] = 0$ . Equations (3.33) and (3.34) read in terms of the  $\hat{a}_n^\dagger$  and  $\hat{a}_n$

$$\hat{\mathcal{H}}_B = \sum_{n=1}^{\infty} \hbar \omega_n \hat{a}_n^\dagger \hat{a}_n, \quad (3.106)$$

$$\hat{\mathcal{H}}_{SB} = \sum_{n=1}^{\infty} g_n \hat{q} (\hat{a}_n^\dagger + \hat{a}_n). \quad (3.107)$$

Here we introduced the notation  $g_n \equiv \sqrt{\hbar c_n^2 / 2m_n \omega_n}$ .

We introduce the coherent states of the harmonic oscillators, which are particularly suitable when dealing with the bosonic ladder operators in Eq. (3.104),

$$|\xi\rangle = e^{\xi \hat{a}^\dagger} |0\rangle, \quad \langle \xi| = \langle 0| e^{\xi^* \hat{a}}, \quad (3.108)$$

where  $\xi$  is a complex number and  $\xi^*$  its complex conjugate.  $\hat{a}^\dagger$  and  $\hat{a}$  stand for the creation and annihilation operator of each harmonic oscillator. The coherent states are eigenstates of the annihilation operator, that is

$$\hat{a}|\xi\rangle = \xi|\xi\rangle, \quad \langle \xi|\hat{a}^\dagger = \langle \xi|\xi^*, \quad (3.109)$$

with the properties

$$\langle \xi|\zeta\rangle = e^{\xi^* \zeta} \quad \text{and} \quad \mathbb{1}' = \int d\xi^* d\xi e^{-\xi^* \xi} |\xi\rangle \langle \xi|, \quad (3.110)$$

where  $\mathbb{1}'$  denotes the unity matrix of one oscillator. Hence, the unity matrix of the whole particle–bath system  $\mathbb{1}$  can be written in terms of the product states  $|q, \{\xi_n\}\rangle$  as

$$\mathbb{1} = \int dq \int \prod_n \left\{ d\xi_n^* d\xi_n e^{-\xi_n^* \xi_n} \right\} |q, \{\xi_n\}\rangle \langle q, \{\xi_n\}|. \quad (3.111)$$

The trace of any observable  $\hat{B}$  that depends on the particle and the bath operators can be expressed as

$$\text{Tr} \hat{B} = \int dq \int \prod_n \left\{ d\xi_n^* d\xi_n e^{-\xi_n^* \xi_n} \right\} \langle q, \{\xi_n\} | \hat{B} | q, \{\xi_n\} \rangle. \quad (3.112)$$

The generating functional can now be obtained by supplementing the potential  $V(\hat{q}; s)$  in Eq. (3.32) by a linear term  $-H(s)\hat{q}$  where  $H(s)$  is a  $c$ -number function that plays the role

of an external source. To be more explicit, we introduce two distinct sources  $H(s)$  and  $H'(s)$  in the potential  $V$  for the time evolution operator

$$\begin{aligned} \mathcal{K}(q_f, \{\xi_{n,f}\}; q_i, \{\xi_{n,i}\}; t) &\equiv \\ &\langle q_f, \{\xi_{n,f}\} | \hat{\mathcal{T}} e^{-\frac{i}{\hbar} \int_0^t dt' \mathcal{H}(t')} | q_i, \{\xi_{n,i}\} \rangle \end{aligned} \quad (3.113)$$

and its Hermitian conjugate

$$\begin{aligned} \mathcal{K}^*(q'_f, \{\xi'_{n,f}\}; q'_i, \{\xi'_{n,i}\}; t) &\equiv \\ &\langle q'_i, \{\xi'_{n,i}\} | \hat{\mathcal{T}}^\dagger e^{\frac{i}{\hbar} \int_0^t dt' \mathcal{H}(t')} | q'_f, \{\xi'_{n,f}\} \rangle, \end{aligned} \quad (3.114)$$

respectively.  $\hat{\mathcal{T}}^\dagger$  is the anti-chronological time ordering operator. In the following we will use the shorthand notation  $d\xi_i = \prod_{n=1}^{\infty} e^{-\xi_{n,i}^* \xi_{n,i}} d\xi_{n,i}^* d\xi_{n,i}$ . All correlation functions of the position  $\hat{q}$  can be obtained by taking the corresponding variations of the trace of the *time-dependent* density matrix  $\hat{\rho}(t) \equiv \hat{\mathcal{K}} \hat{\rho}_0 \hat{\mathcal{K}}^*$ , Eq. (3.49), with respect to  $H(s)$  and  $H'(s)$ . The matrix elements of  $\hat{\rho}(t) \equiv \hat{\mathcal{K}} \hat{\rho}_0 \hat{\mathcal{K}}^*$  are given by

$$\mathcal{W}(q_f, \{\xi_{n,f}\}; q'_f, \{\xi'_{n,f}\}; t) = \langle q_f, \{\xi_{n,f}\} | \hat{\rho}(t) | q'_f, \{\xi'_{n,f}\} \rangle, \quad (3.115)$$

$$\mathcal{W}(q_i, \{\xi_{n,i}\}; q'_i, \{\xi'_{n,i}\}) = \langle q_i, \{\xi_{n,i}\} | \hat{\rho}_0 | q'_i, \{\xi'_{n,i}\} \rangle. \quad (3.116)$$

The path integral representation of  $\mathcal{K}$  and  $\mathcal{K}^*$  are found by using standard methods:

$$\begin{aligned} \mathcal{K}(q_f, \{\xi_{n,f}\}; q_i, \{\xi_{n,i}\}; t) &= \int \mathcal{D}q^+ \mathcal{D}\xi^+ \\ &\times \exp\left(\frac{i}{\hbar} \mathcal{S}[q^+, \{\xi_n^+\}]\right) \end{aligned} \quad (3.117)$$

$$\begin{aligned} \mathcal{K}^*(q'_f, \{\xi'_{n,f}\}; q'_i, \{\xi'_{n,i}\}; t') &= \int \mathcal{D}q^- \mathcal{D}\xi^- \\ &\times \exp\left(-\frac{i}{\hbar} \mathcal{S}^*[q^-, \{\xi_n^-\}]\right), \end{aligned} \quad (3.118)$$

where we make clear by the superscripts  $+$  and  $-$  which path belongs to  $\mathcal{K}$  and which to  $\mathcal{K}^*$ , respectively. The real time interval  $[0, t]$  has been discretized into  $T \in \mathbb{N}$  steps of length  $\Delta t$  with  $t = \Delta t T$ . The functional integration measures are defined as  $\mathcal{D}q = \prod_{j=1}^{T-1} dq_j$  with  $q_j \equiv q(j\Delta t)$ . The terms contributing to the total action,  $\mathcal{S}[q, \xi_n] = \mathcal{S}_S[q] + \mathcal{S}_B[\xi_n] + \mathcal{S}_{SB}[q, \xi_n]$  introduced in Eqs. (3.117) and (3.118), read in discretized form

$$\begin{aligned} \mathcal{S}_S[q] &= \sum_{j=1}^T \Delta t \left[ \frac{M}{2} \left( \frac{q_j - q_{j-1}}{\Delta t} \right)^2 - V(q_j; j\Delta t) \right. \\ &\left. + H(j\Delta t) q_j \right], \end{aligned} \quad (3.119)$$

$$\begin{aligned} \mathcal{S}_B[\xi_n] + \mathcal{S}_{SB}[q, \xi_n] &= i\hbar \sum_{j=1}^{T-1} \xi_{n,j}^* (\xi_{n,j} - \xi_{n,j-1}) \\ &+ \Delta t \sum_{j=1}^T [\hbar\omega \xi_{n,j}^* \xi_{n,j-1} + g_n q_j (\xi_{n,j}^* + \xi_{n,j-1})]. \end{aligned} \quad (3.120)$$

The reduced density matrix depends only on the particle variables and the external sources,

$$\begin{aligned} \mathcal{W}(q_f; q'_f; t) &\equiv \int dq_i dq'_i d\xi_i d\xi'_i d\xi_f \mathcal{K}(q_f, \{\xi_{n,f}\}; q_i, \{\xi_{n,i}\}; t) \\ &\times \mathcal{W}(q_i, \{\xi_{n,i}\}; q'_i, \{\xi'_{n,i}\}) \mathcal{K}^*(q'_f, \{\xi_{n,f}\}; q'_i, \{\xi'_{n,i}\}; t). \end{aligned} \quad (3.121)$$

In Eqs. (3.117) and (3.118) we omitted normalization factors that do not depend on the bath nor on the particle variables. Note that the integral runs only over bath and particle variables with an index between 1 and  $T - 1$  since  $q_0 = q_i$ ,  $q_T = q_f$  (and analogously for the bath variables) are fixed for  $\mathcal{K}$  and  $q_0 = q'_f$ ,  $q_T = q'_i$  (and analogously for the bath variables) are fixed for  $\mathcal{K}^*$ .

The path integral description of  $\hat{\rho}_0$  is obtained by dividing the imaginary time interval  $[0, \beta\hbar]$  into  $T$  time steps. Consequently, by using  $\hat{\rho} = e^{-\beta\hat{H}_0}$  we find

$$\begin{aligned} \mathcal{W}(q'_i, \{\xi'_{n,i}\}; q_i, \{\xi_{n,i}\}) &= \\ &\int \mathcal{D}q^0 \prod_n \left\{ \mathcal{D}\xi_n^0 \exp\left(-\frac{1}{\hbar} \mathcal{S}_0[q^0, \xi_n^0]\right) \right\}, \end{aligned} \quad (3.122)$$

where  $\mathcal{S}_0[q, \xi_n] = \mathcal{S}_{0S}[q] + \mathcal{S}_{0B}[\xi_n] + \mathcal{S}_{0SB}[q, \xi_n]$  with

$$\begin{aligned} \mathcal{S}_{0B}[\xi_n] + \mathcal{S}_{0SB}[q, \xi_n] &= \hbar \sum_{j=1}^{T-1} \xi_{n,j}^* (\xi_{n,j} - \xi_{n,j-1}) \\ &+ \Delta t' \sum_{j=1}^T [\hbar\omega \xi_{n,j}^* \xi_{n,j-1} + g_n q_j (\xi_{n,j}^* + \xi_{n,j-1})]. \end{aligned} \quad (3.123)$$

We introduced the imaginary time path step  $\Delta t' = \beta\hbar/T$ .

### Integration over the bath variables

The influence functional in discretized form reads

$$\begin{aligned} \mathcal{F}[\{q_j\}] &= \\ &\prod_n \int \prod_{j=1}^{3T} d\xi_{n,j} d\xi_{n,j}^* e^{-\sum_{j,j'=1}^{3T} \xi_{n,j}^* K^{-1}(j,j') \xi_{n,j'}} \\ &e^{\frac{i}{\hbar} g_n \sum_{j=1}^T \Delta t q_j (\xi_{n,j} + \xi_{n,j}^*)} \\ &\times e^{-\frac{i}{\hbar} g_n \sum_{j=T+1}^{2T} \Delta t' q_j (\xi_{n,j} + \xi_{n,j}^*) - \frac{i}{\hbar} g_n \sum_{j=2T+1}^{3T} \Delta t q_j (\xi_{n,j} + \xi_{n,j}^*)}, \end{aligned} \quad (3.124)$$

which depends on the correlation matrix

$$K^{-1} = \begin{pmatrix} 1 & 0 & 0 & \cdots & -k_1 \\ -k_2 & 1 & 0 & \cdots & 0 \\ 0 & -k_3 & 1 & \cdots & 0 \\ 0 & 0 & -k_4 & 1 & \cdots & 0 \\ \vdots & & & & & \\ 0 & 0 & \cdots & -k_{3T} & 1 \end{pmatrix}, \quad (3.125)$$

with  $k_j = 1 + i\Delta t\omega$  for  $j \leq T$ ,  $k_j = 1 - i\Delta t\omega$  for  $j \geq 2T$  and  $k_j = 1 - \Delta t'\omega$  for  $T < j \leq 2T$ . Note that in this notation there are  $3T$  time steps in Eq. (3.124) and  $q_j = q_j^+$  for  $j \leq T$ ,  $q_j = q_j^0$  for  $T < j \leq 2T$  and  $q_j = q_j^-$  for  $j > 2T$  is understood with an analogous notation for the  $\xi_{n,j}$ .

The part of the action that depends only on the particle variables  $\mathcal{S}_S$  can be found by combining the relevant contributions in Eqs. (3.117), (3.118) and (3.122),

$$\begin{aligned} \frac{i}{\hbar} \tilde{\mathcal{S}}_S(\{q_j\}) &= \frac{i}{\hbar} \mathcal{S}_S(\{q_j\}_{j=1}^T) - \frac{i}{\hbar} \mathcal{S}_S(\{q_j\}_{j=2T+1}^{3T}) \\ &\quad - \frac{i}{\hbar} \mathcal{S}_{0S}(\{q_j\}_{j=T+1}^{2T}). \end{aligned} \quad (3.126)$$

Note that the exponential factors that stem from the bath integration measure Eq. (3.51) exactly combine with the sums in the actions (3.119) and (3.123). The elements  $K(j, j')$  of the matrix  $K$  are easily found:

$$K(j, j') = \frac{1}{1 - k_1 \cdots k_{3T}} \begin{cases} 1 & \text{for } j = j' \\ \prod_{l=j'+1}^j k_l & \text{for } j > j' \\ \frac{k_1 \cdots k_{3T}}{\prod_{l=j+1}^{j'} k_l} & \text{for } j < j'. \end{cases} \quad (3.127)$$

The Gaussian integral in Eq. (3.124) is now readily done. Explicit expressions of Eq. (3.127) in the continuum limit  $T \rightarrow \infty$  are easily obtained: for instance, when  $j, j' < T$ ,  $K(j, j')$  couples to two  $q^+$  fields and is given by

$$K(j, j') = \frac{1}{1 - e^{-\beta\hbar\omega}} \begin{cases} e^{i\omega\Delta t(j-j')} & \text{for } j' < j \leq T \\ e^{-\beta\hbar\omega + i\omega\Delta t(j-j')} & \text{for } j < j' \leq T. \end{cases} \quad (3.128)$$

Note that under the sum over  $j$  and  $j'$  only its symmetrized version occurs. By reintroducing the fields  $q^+$ ,  $q^-$  and  $q^0$  we find [8]

$$\mathcal{F}[q^+, q^-, q^0] = \exp\left(-\frac{1}{\hbar} \Phi[q^+, q^-, q^0]\right), \quad (3.129)$$

where the exponent reads

$$\begin{aligned} \Phi[q^+, q^-, q^0] &= \\ &- \int_0^{\beta\hbar} d\tau \int_0^\tau d\sigma K(-i\tau + i\sigma) q^0(\tau) q^0(\sigma) + \int_0^{\beta\hbar} d\tau \frac{\mu}{2} q^{02}(\tau) \\ &- i \int_0^{\beta\hbar} d\tau \int_0^t ds K^*(s - i\tau) q^0(\tau) [q^+(s) - q^-(s)] \\ &+ \int_0^t dt \int_0^s du [q^+(s) - q^-(s)] [K(s - u) q^+(u) \\ &- K^*(s - u) q^-(u)] \\ &+ i \int_0^t ds \frac{\mu}{2} [q^{+2}(s) - q^{-2}(s)]. \end{aligned} \quad (3.130)$$

The kernel  $K$  reads for complex times  $\theta = s - i\tau$ ,  $0 \leq \tau \leq \beta\hbar$

$$K(\theta) = \sum_n \frac{g_n^2}{\hbar} \frac{\cosh[\omega_n(\beta\hbar/2 - i\theta)]}{\sinh[\omega_n\beta\hbar/2]}, \quad (3.131)$$

and the constant  $\mu$  is given by

$$\mu = 2 \sum_n^{\infty} \frac{g_n^2}{\hbar \omega_n}. \quad (3.132)$$

Note that for a fermionic bath the only difference lies in the boundary conditions enforced by the trace operation: for fermions anti-periodic boundary conditions apply in contrast to periodic boundary conditions for bosons. This difference is incorporated by replacing  $-k_1$  by  $k_1$  in Eq. (3.125). The analysis for bosons can then be repeated, leading to a fermionic bath kernel where the  $\sinh$  in the denominator of Eq. (3.131) is replaced by a  $\cosh$ . Note that the numerator does not change since two minus signs arise, one due to the anticommutation relation of the fields when passing from a  $\int_0^{\beta\hbar} d\tau d\sigma$ -integral to a  $\int_0^{\beta\hbar} d\tau \int_0^{\tau} d\sigma$ -integral, and a second one due to  $k_1 \mapsto -k_1$ .

The environment can be regarded as a proper heat bath only if the spectrum of the harmonic oscillators becomes quasi-continuous. Accordingly, we introduce the spectral density of the bath through (the  $\pi i$  is a mere convention)

$$S(\omega) = \pi \sum_n \frac{g_n^2}{\hbar} \delta(\omega - \omega_n) = \pi \sum_n \frac{c_n^2}{2m_n \omega_n} \delta(\omega - \omega_n). \quad (3.133)$$

Then the kernel  $K(\theta)$  and the constant  $\mu$  are rewritten in terms of the spectral density

$$K(\theta) = \int_0^{\infty} \frac{d\omega}{\pi} S(\omega) \frac{\cosh[\omega(\beta\hbar/2 - i\theta)]}{\sinh[\omega\beta\hbar/2]} \quad (3.134)$$

and

$$\mu = 2 \int_0^{\infty} \frac{d\omega}{\pi} \frac{S(\omega)}{\omega}. \quad (3.135)$$

The real and the imaginary parts of the kernel  $K(\theta) = K_R(\theta) + iK_I(\theta)$  are found to be

$$K_R(s - i\tau) = \int_0^{\infty} \frac{d\omega}{\pi} S(\omega) \frac{\cosh[\omega(\beta\hbar/2 - \tau)]}{\sinh[\omega\beta\hbar/2]} \cos(\omega s) \quad (3.136)$$

$$K_I(s - i\tau) = - \int_0^{\infty} \frac{d\omega}{\pi} S(\omega) \frac{\sinh[\omega(\beta\hbar/2 - \tau)]}{\sinh[\omega\beta\hbar/2]} \sin(\omega s). \quad (3.137)$$

The imaginary time argument  $\tau$  varies in the interval  $[0, \beta\hbar]$  so that it is convenient to introduce the Fourier series of  $K(s - i\tau)$  with respect to  $\tau$ . Introducing the Matsubara frequencies

$$\nu_k = \frac{2\pi k}{\beta\hbar} \quad (3.138)$$

we find

$$K_R(s - i\tau) = \frac{1}{\beta\hbar} \sum_{k=-\infty}^{\infty} g_k(s) e^{i\nu_k \tau} \quad (3.139)$$

and

$$K_I(s - i\tau) = \frac{i}{\beta\hbar} \sum_{k=-\infty}^{\infty} f_k(s) e^{i\nu_k \tau}, \quad (3.140)$$

where the functions  $g_k$  and  $f_k$  are defined through

$$g_k(s) = \int_0^\infty \frac{d\omega}{\pi} S(\omega) \frac{2\omega}{\omega^2 + \nu_k^2} \cos(\omega s) \quad (3.141)$$

and

$$f_k(s) = \int_0^\infty \frac{d\omega}{\pi} S(\omega) \frac{2\nu_k}{\omega^2 + \nu_k^2} \sin(\omega s) . \quad (3.142)$$

In the following we will express most quantities in terms of the functions  $g_k$  and  $f_k$ . For real times the real and the imaginary parts of the kernel (3.134) read [see Eqs. (3.139) and (3.140)]

$$K_R(s) = \int_0^\infty \frac{d\omega}{\pi} S(\omega) \coth(\beta\hbar\omega/2) \cos(\omega s) \quad (3.143)$$

and

$$K_I(s) = - \int_0^\infty \frac{d\omega}{\pi} S(\omega) \sin(\omega s) . \quad (3.144)$$

We now eliminate the local terms in Eq. (3.130). We define the two new kernels

$$\gamma(s) = \frac{2}{M} \int_0^\infty \frac{d\omega}{\pi} \frac{S(\omega)}{\omega} \cos(\omega s) \quad (3.145)$$

and

$$k(\tau) = \frac{M_0}{\beta\hbar} \sum_{k=-\infty}^{\infty} \zeta_k e^{i\nu_k\tau} , \quad (3.146)$$

where  $\zeta_k$  is defined by

$$\begin{aligned} \zeta_k &= \frac{1}{M_0} [\mu - g_k(0)] \\ &= \frac{1}{M_0} \int_0^\infty \frac{d\omega}{\pi} \frac{S(\omega)}{\omega} \frac{2\nu_k^2}{\omega^2 + \nu_k^2} . \end{aligned} \quad (3.147)$$

The latter kernel is related to  $K_R(-i\tau)$  via

$$\begin{aligned} & - \int_0^{\hbar\beta} d\tau \int_0^\tau d\sigma K_R(-i\tau + i\sigma) f(\tau, \sigma) = \\ & - \frac{\mu}{2} \int_0^{\hbar\beta} d\tau f(\tau, \tau) + \frac{1}{2} \int_0^{\hbar\beta} d\tau d\sigma k(\tau - \sigma) f(\tau, \sigma) , \end{aligned} \quad (3.148)$$

with a generic function  $f$ . In terms of the kernels  $\gamma(s)$ ,  $k(\tau)$ ,  $K^*(s - i\tau)$ ,  $K_R(s - u)$  and the linear combinations

$$x = (q^+ + q^-)/2 \quad \text{and} \quad \bar{x} = q^+ - q^- \quad (3.149)$$

the exponent of the influence functional reads

$$\begin{aligned}
 \Phi[x, \bar{x}, q^0] &= \frac{1}{2} \int_0^{\beta\hbar} d\tau d\sigma k(\tau - \sigma) q^0(\tau) q^0(\sigma) \\
 &\quad - i \int_0^{\beta\hbar} d\tau \int_0^t ds K^*(s - i\tau) q^0(\tau) \bar{x}(s) \\
 &\quad + \frac{1}{2} \int_0^t ds du K_R(s - u) \bar{x}(s) \bar{x}(u) \\
 &\quad + iM \int_0^t ds \bar{x}(s) \frac{d}{ds} \int_0^s du \gamma(s - u) \dot{x}(u) .
 \end{aligned} \tag{3.150}$$

Details of the derivation of Eq. (3.150) can be found in the thorough analysis in [8].

### 3.5.2 Classical Brownian particle in a harmonic potential: Initial position measurement and quenches in the trapping potential

This part is meant to be a reminder on classical stochastic motion induced by generic baths. None of the results presented herein are new but they are useful to be confronted with the quantum results discussed in the body of the paper.

The classical Brownian motion of a particle confined in a harmonic potential can be described by the *Langevin equation*

$$\ddot{q}(t) + \int_0^t ds \gamma(t - s) \dot{q}(s) + \Omega^2 q(t) = \xi(t) , \tag{3.151}$$

where  $\xi$  is a zero mean Gaussian noise<sup>2</sup> with correlation  $\langle \xi(t) \xi(s) \rangle = \frac{1}{M\beta} \gamma(|t - s|)$  and with  $\gamma(t)$  given in Eq. (3.75) [50]. In the Laplace transform formulation, the solution to Eq. (3.151) reads

$$\tilde{q}(\lambda) = \tilde{\mathcal{G}}_+(\lambda) \left[ \tilde{\xi}(\lambda) + v_0 + (\lambda + \tilde{\gamma}(\lambda)) q^0 \right] , \tag{3.152}$$

where we used  $\tilde{\mathcal{G}}_+$  defined in Eq. (3.82) and we introduced the initial conditions  $q(0) = q^0$  and  $\dot{q}(0) = v_0$ . The correlation function is now easily computed and it reads

$$\begin{aligned}
 \tilde{C}(\lambda, \kappa) &= \langle \tilde{q}(\lambda) \tilde{q}(\kappa) \rangle = \frac{1}{\beta M} \frac{\tilde{\gamma}(\lambda) + \tilde{\gamma}(\kappa)}{\lambda + \kappa} \tilde{\mathcal{G}}_+(\lambda) \tilde{\mathcal{G}}_+(\kappa) \\
 &\quad + \tilde{\mathcal{G}}_+(\lambda) \tilde{\mathcal{G}}_+(\kappa) \left[ v_0^2 + (\lambda + \tilde{\gamma}(\lambda)) (\kappa + \tilde{\gamma}(\kappa)) q^{02} \right] \\
 &\quad + \tilde{\mathcal{G}}_+(\lambda) \tilde{\mathcal{G}}_+(\kappa) v_0 q^0 [\lambda + \tilde{\gamma}(\lambda) + \kappa + \tilde{\gamma}(\kappa)] ,
 \end{aligned} \tag{3.153}$$

where we used the fact that the Laplace transform of  $\gamma(|t - s|)$  with respect to  $t$  and  $s$  is given by  $[\tilde{\gamma}(\lambda) + \tilde{\gamma}(\kappa)]/(\lambda + \kappa)$ . The initial values  $q^0$  and  $v_0$  can be sharp or drawn from a probability distribution which is typically of the Maxwell-Boltzmann type, that is

$$P[q^0, v_0] = \frac{\beta M_0 \Omega_0}{2\pi} \exp \left[ -\beta \left( \frac{M_0}{2} v_0^2 + \frac{M_0}{2} \Omega_0^2 q^{02} \right) \right] , \tag{3.154}$$

<sup>2</sup>The underlying probability distribution is of the (Gaussian) Boltzmann-Gibbs type  $\exp(-\beta\mathcal{H})$  with  $\mathcal{H}$  the *full coupled* Hamiltonian of the particle-bath system. Equation (3.151) thus describes the case where the harmonic oscillator bath and the particle are initially *coupled* as in the quantum case studied in the present work. This subtle point is often overlooked. For more details see p. 21-23 in [50].

where  $\Omega_0$  is the frequency of the initial trapping potential and  $M_0$  is the initial mass. From Eq. (3.154) we easily derive

$$\langle q^{02} \rangle = (\beta M_0 \Omega_0^2)^{-1} \quad \text{and} \quad \langle v_0^2 \rangle = (\beta M_0)^{-1}. \quad (3.155)$$

As long as  $\Omega_0 = \Omega$  and  $M = M_0$  the correlation function can be rewritten as

$$\begin{aligned} \tilde{\mathcal{C}}^{\text{eq}}(\lambda, \kappa) &= \frac{\tilde{\mathcal{C}}^{\text{1eq}}(\lambda) + \tilde{\mathcal{C}}^{\text{1eq}}(\kappa)}{\lambda + \kappa} \quad \text{with} \\ \mathcal{C}^{\text{1eq}}(\lambda) &\equiv \frac{1}{\beta M \Omega^2} \frac{\tilde{\gamma}(\lambda) + \lambda}{\lambda^2 + \tilde{\gamma}(\lambda) + \Omega^2}, \end{aligned} \quad (3.156)$$

which is the equilibrium correlation function.

The non equilibrium correlation can be recast in the form

$$\begin{aligned} \tilde{\mathcal{C}}(\lambda, \kappa) &= \frac{\tilde{\mathcal{C}}^{\text{1eq}}(\lambda) + \tilde{\mathcal{C}}^{\text{1eq}}(\kappa)}{\lambda + \kappa} + \tilde{\mathcal{G}}_+(\lambda) \tilde{\mathcal{G}}_+(\kappa) \left[ v_0^2 - \frac{1}{\beta M} \right] \\ &\quad + \beta M \Omega^2 \tilde{\mathcal{C}}^{\text{1eq}}(\lambda) \tilde{\mathcal{C}}^{\text{1eq}}(\kappa) \left[ \beta M \Omega^2 q^{02} - 1 \right] \\ &\quad + \tilde{\mathcal{G}}_+(\lambda) \tilde{\mathcal{G}}_+(\kappa) v_0 q^0 \left[ \lambda + \tilde{\gamma}(\lambda) + \kappa + \tilde{\gamma}(\kappa) \right]. \end{aligned} \quad (3.157)$$

In many cases  $q^0$  and  $v_0$  are uncorrelated random variables. Then Eq. (3.157) transforms into

$$\begin{aligned} \tilde{\mathcal{C}}(\lambda, \kappa) &= \frac{\tilde{\mathcal{C}}^{\text{1eq}}(\lambda) + \tilde{\mathcal{C}}^{\text{1eq}}(\kappa)}{\lambda + \kappa} + \tilde{\mathcal{G}}_+(\lambda) \tilde{\mathcal{G}}_+(\kappa) \left[ \langle v_0^2 \rangle - \frac{1}{\beta M} \right] \\ &\quad + \beta M \Omega^2 \tilde{\mathcal{C}}^{\text{1eq}}(\lambda) \tilde{\mathcal{C}}^{\text{1eq}}(\kappa) \left[ \beta M \Omega^2 \langle q^{02} \rangle - 1 \right]. \end{aligned} \quad (3.158)$$

### 3.5.3 The equilibrium initial condition

In this Appendix we use Eq. (3.87) in the particular case of an equilibrium initial condition and a subsequent evolution still in equilibrium. We show how to derive the equilibrium correlation function and we prove that the fluctuation-dissipation theorem (FDT) is satisfied without imposing time-translational invariance (TTI) as has been done before in the literature [8].

#### The fluctuation-dissipation theorem

The linear response is easily found by noting that the external source  $F(s)$  represents a physical drift force. Therefore, by calculating

$$\langle \hat{q}(t) \rangle = \frac{\hbar}{i} \frac{\delta}{\delta G(t)} \exp(\mathcal{J}[F, G])|_{G \equiv 0} = \int_0^t ds \mathcal{R}(t-s) F(s) \quad (3.159)$$

for  $F \neq 0$  one finds the response function  $\mathcal{R}(t)$  with respect to the external force  $F(t)$ . We set  $\epsilon \rightarrow \infty$  which corresponds to the absence of any initial measurement. By using Eq. (3.87) we obtain

$$\mathcal{R}(t) = \frac{1}{M} \mathcal{G}_+(t) \quad \text{and} \quad \tilde{\mathcal{R}}(\lambda) = \frac{1}{M} \frac{1}{\Omega^2 + \lambda \tilde{\gamma}(\lambda) + \lambda^2}, \quad (3.160)$$

in the time and Laplace transform domains, respectively. These expressions are independent of the initial condition. Therefore, the response function is the same in and out of equilibrium.

Moreover, it is equal to the response function of a classical Brownian particle [21] if it is coupled to a bath with the same friction kernel  $\gamma$ .

We will confirm the validity of the FDT when the system is in equilibrium. We choose the initial Hamiltonian to be equal to the “bulk” one, that is

$$\Omega = \Omega_0 \quad \text{and} \quad M = M_0, \quad (3.161)$$

so that the initial density matrix is equal to the Boltzmann weight  $\exp(-\beta\mathcal{H})$  with the terms contributing to  $\mathcal{H}$  given in Eqs. (3.32), (3.33) and (3.34). The initial state is not perturbed by any measurement, so we take  $\epsilon \rightarrow \infty$  which implies  $\Lambda' = \Lambda$  and  $\Xi' = \Xi$ . From Eq. (3.90) we find the equilibrium correlation function  $\mathcal{C}^{\text{eq}}(t, t')$  which in the Laplace transform version reads

$$\begin{aligned} \tilde{\mathcal{C}}^{\text{eq}}(\lambda, \kappa) = & \frac{\hbar}{M} \tilde{\mathcal{G}}_+(\lambda) \tilde{\mathcal{G}}_+(\kappa) \left\{ \Lambda \lambda \kappa + \frac{\Lambda}{M} \lambda \tilde{\mathcal{C}}_1(\kappa) \right. \\ & \left. + \frac{\Lambda}{M} \kappa \tilde{\mathcal{C}}_1(\lambda) + \Xi - \frac{1}{M} \tilde{\mathcal{C}}_2(\lambda) - \frac{1}{M} \tilde{\mathcal{C}}_2(\kappa) + \frac{1}{M^2} \tilde{R}''(\lambda, \kappa) \right\}. \end{aligned} \quad (3.162)$$

This expression can be greatly simplified. We first note that from the definitions of  $g_k$  and  $f_k$  in Eqs. (3.141) and (3.142) it follows that

$$\dot{f}_k(s) = \nu_k g_k(s), \quad \tilde{f}_k(\lambda) = \frac{\nu_k}{\lambda} \tilde{g}_k(\lambda), \quad (3.163)$$

where we used  $f_k(0) = 0$ . The Laplace transform of the kernel

$$\begin{aligned} R''(s, s') = & \frac{1}{\beta\hbar} \sum_k u_k [g_k(s)g_k(s') \\ & - f_k(s)f_k(s')] + M_0 K_R(s - s') \end{aligned} \quad (3.164)$$

[see Eq. (3.88) and (3.73) for  $\Lambda = \Lambda'$ ] can now be written as

$$\begin{aligned} \tilde{R}''(\lambda, \kappa) = & \frac{1}{\beta\hbar} \sum_k u_k \left( 1 - \frac{\nu_k^2}{\lambda\kappa} \right) \tilde{g}_k(\lambda) \tilde{g}_k(\kappa) \\ & + \frac{M}{\beta\hbar} \sum_k \frac{\tilde{g}_k(\lambda) + \tilde{g}_k(\kappa)}{\lambda + \kappa} \end{aligned} \quad (3.165)$$

and by defining  $\tilde{h}_k(\lambda) = \tilde{g}_k(\lambda)/M + \lambda$  we find that the expression in the curly brackets in the rhs of Eq. (3.162) can be recast as

$$\frac{1}{\beta\hbar} \sum_k u_k \left( 1 - \frac{\nu_k^2}{\lambda\kappa} \right) \tilde{h}_k(\lambda) \tilde{h}_k(\kappa) + \frac{1}{\beta\hbar} \sum_k \frac{\tilde{h}_k(\lambda) + \tilde{h}_k(\kappa)}{\lambda + \kappa}, \quad (3.166)$$

where we used Eqs. (3.69) and (3.70). By combining the expression for the Laplace transform of the cosine  $\int_0^\infty dt e^{-\lambda t} \cos(\omega t) = \lambda/(\lambda^2 + \omega^2)$  with Eqs. (3.145) and (3.141) we obtain

$$\frac{1}{M} \tilde{g}_k(\lambda) = \frac{\lambda}{\nu_k^2 - \lambda^2} (|\nu_k| \tilde{\gamma}(|\nu_k|) - \lambda \tilde{\gamma}(\lambda)). \quad (3.167)$$

By using instead Eqs. (3.145) and (3.147) we derive

$$\zeta_k = |\nu_k| \tilde{\gamma}(|\nu_k|). \quad (3.168)$$

The kernel  $\tilde{\gamma}$  can be eliminated in favor of  $\tilde{\mathcal{G}}_+$  through Eq. (3.82) which yields

$$\tilde{h}_k(\lambda) = \frac{\lambda}{\nu_k^2 - \lambda^2} \left[ \tilde{\mathcal{G}}_+^{-1}(|\nu_k|) - \tilde{\mathcal{G}}_+^{-1}(\lambda) \right]. \quad (3.169)$$

This expression can now be inserted via Eq. (3.166) into Eq. (3.162) to find the equilibrium correlator. Note that, for  $\Omega_0 = \Omega$  we have  $\tilde{\mathcal{G}}_+(|\nu_k|) = u_k$ . With the help of the one variable function

$$\tilde{\mathcal{C}}^{\text{1eq}}(\lambda) = \frac{1}{\beta M} \sum_k \frac{\lambda}{\nu_k^2 - \lambda^2} \left[ \tilde{\mathcal{G}}_+(\lambda) - \tilde{\mathcal{G}}_+(|\nu_k|) \right] \quad (3.170)$$

the equilibrium correlation function becomes

$$\tilde{\mathcal{C}}^{\text{eq}}(\lambda, \kappa) = \frac{\mathcal{C}^{\text{1eq}}(\lambda) + \mathcal{C}^{\text{1eq}}(\kappa)}{\lambda + \kappa}, \quad (3.171)$$

which clearly displays time translational invariance (TTI). Indeed, the Laplace transform with respect to  $t$  and  $t'$  of a generic function  $f(|t - t'|)$  that depends only on the time difference is equal to  $[\tilde{f}(\lambda) + \tilde{f}(\kappa)]/(\lambda + \kappa)$ , where  $\tilde{f}(\lambda)$  denotes the Laplace transform of  $f(t)$  with respect to  $t$ . Hence, we have  $\mathcal{C}^{\text{eq}}(t, t') = \mathcal{C}^{\text{1eq}}(|t - t'|)$  with the explicit Laplace representation of  $\mathcal{C}^{\text{1eq}}$  in Eq. (3.170). The equilibrium correlation function is thus found without imposing TTI. By imposing TTI Eq. (3.170) can be directly found from Eq. (3.90) by setting  $t' = 0$  which simplifies the expression considerably. Remember that  $\dot{\mathcal{G}}_+(t = 0) = 1$  and  $\mathcal{G}_+(t = 0) = 0$ . By taking the Laplace transform of the result with respect to  $t$  and by using Eq. (3.167) one easily recovers Eq. (3.170).

It is now straightforward to establish the relation between  $\mathcal{C}^{\text{1eq}}(t)$  and  $\mathcal{R}(t)$ . Firstly, we note that since  $\mathcal{C}^{\text{1eq}}(t)$  is an even function of  $t$  its Fourier transform  $\mathcal{C}^{\text{1eq}}(\omega)$  is related to its Laplace transform through

$$\mathcal{C}^{\text{1eq}}(\omega) = \tilde{\mathcal{C}}^{\text{1eq}}(i\omega) + \tilde{\mathcal{C}}^{\text{1eq}}(-i\omega). \quad (3.172)$$

Thus, by using Eqs. (3.160) and (3.170) we have

$$\mathcal{C}^{\text{1eq}}(\omega) = \frac{1}{\beta} \sum_k \frac{i\omega}{\omega^2 + \nu_k^2} \left[ \tilde{\mathcal{R}}(i\omega) - \tilde{\mathcal{R}}(-i\omega) \right]. \quad (3.173)$$

Now, since the Fourier transform of the response function,  $\mathcal{R}(\omega)$ , is related to its Laplace transform via  $\mathcal{R}(\omega) = \tilde{\mathcal{R}}(i\omega)$  due to causality we obtain the quantum FDT in the form

$$\mathcal{C}^{\text{1eq}}(\omega) = \hbar \coth[\omega\beta\hbar/2] \text{Im } \mathcal{R}(\omega), \quad (3.174)$$

where we used the formula  $\sum_k \omega/(\omega^2 + \nu_k^2) = (\beta\hbar/2) \coth[\omega\beta\hbar/2]$ . This result is completely general, in the sense that it applies to any bath, as it should.

### 3.5.4 Asymptotic behavior of $\mathcal{G}_+(t)$ and $\mathcal{C}^{\text{1eq}}(t)$ for Ohmic dissipation

In the case of *Ohmic dissipation* the spectral function has the form

$$S(\omega) = \gamma\omega \quad \text{for } \omega \rightarrow 0. \quad (3.175)$$

For large frequencies one typically introduces a high frequency cutoff function (since the ultra-violet divergence is unphysical) that we choose to be of the Drude-type  $\omega_D^2/(\omega_D^2 + \omega^2)$  where  $\omega_D \gg \omega$  is the high frequency cut-off. The bath kernel

$$\gamma(t) = \gamma\omega_D e^{-\omega_D t} \quad (3.176)$$

then has a finite memory and a simple form in the Laplace domain, namely

$$\tilde{\gamma}(\lambda) = \gamma \frac{\omega_D}{\omega_D + \lambda} . \quad (3.177)$$

We are interested in the equilibration behavior of the correlation function Eq. (3.95) when quantum effects dominate. In order to find the long-time behavior of  $\tilde{\mathcal{C}}^{1\text{eq}}(t)$  and  $\mathcal{G}_+(t)$  we study their small- $\lambda$  behavior. In the very low temperature limit the sum over the Matsubara frequencies in Eq. (3.170) can be replaced by an integral. For  $\lambda \rightarrow 0$  one finds

$$\begin{aligned} \tilde{\mathcal{C}}^{1\text{eq}}(\lambda) &\simeq \int_0^\infty \frac{d\nu}{\pi} \frac{\lambda}{\nu^2 - \lambda^2} \left[ \tilde{\mathcal{G}}_+(\lambda) - \tilde{\mathcal{G}}_+(\nu) \right] \\ &\simeq \frac{1}{\pi} \int_0^{\lambda^{-1}} \frac{d\nu}{\nu^2 - 1} \frac{\lambda^2(\nu^2 - 1) + \lambda(\nu\tilde{\gamma}(\lambda\nu) - \gamma)}{\Omega^4} \\ &\quad + \frac{\lambda}{\pi} \int_1^\infty \frac{d\nu}{\nu^2} \frac{\nu^2 + \nu\tilde{\gamma}(\nu)}{\Omega^2(\nu^2 + \nu\tilde{\gamma}(\nu) + \Omega^2)} + \dots , \end{aligned} \quad (3.178)$$

where the ellipsis stands for higher orders in  $\lambda$ . Now, by observing the ultraviolet behavior of Eq. (3.177) one easily argues that all the terms in the rhs of Eq. (3.178) are of order  $\sim \lambda$ . Therefore, the long time behavior of the Ohmic equilibrium correlation function at zero temperature is

$$C^{1\text{eq}} \sim \frac{1}{t^2} \quad \text{for } t \rightarrow \infty \quad \text{and} \quad \beta\hbar \gg |\Omega^2 - \gamma^2/4|^{-1/2} . \quad (3.179)$$

It is straightforward to show by direct inversion of the Laplace transform that the propagator  $\mathcal{G}^+(t)$  is *exponentially* suppressed for large times (and for Ohmic dissipation) on a typical time scale  $\gamma/2$ , hence we have

$$\mathcal{G}_+(t) \sim e^{-\gamma t/2} \quad \text{for } t \rightarrow \infty . \quad (3.180)$$

Equation (3.180) holds for all temperatures. In the high temperature regime one has  $\nu_k \rightarrow \infty$  so that  $\mathcal{C}^{1\text{eq}}(\lambda) \simeq -\left[\tilde{\mathcal{G}}_+(\lambda) - 1/\Omega^2\right]/(\beta M \lambda)$ . Translated into real time this states that  $\mathcal{G}_+(t)$  is proportional to the derivative of  $\mathcal{C}^{1\text{eq}}(t)$  which is nothing else than the classical FDT. Accordingly, we find

$$C^{1\text{eq}} \sim e^{-\gamma t/2} \quad \text{for } t \rightarrow \infty \quad \text{and} \quad \beta\hbar \ll |\Omega^2 - \gamma^2/4|^{-1/2} . \quad (3.181)$$



---

Dissipative impurity dynamics in a 1D quantum liquid

---

*“Indeed, what could be more rational than the suppression of individuality [...] ?”*  
Herbert Marcuse in “The one-dimensional man”

## 4.1 Introduction to Luttinger liquid theory

One dimensional (1D) quantum liquids are fundamentally different from Fermi liquids. Indeed, Fermi liquid theory predicts individual long-lived excitations, the so-called Landau *quasi-particles*, which are essentially free particles: They have a vanishing scattering cross-section in the perturbative limit of small interactions. Within this theory the interactions only renormalize the effective mass and the effective weight of the spectral function of these quasi-particles. The Matsubara formalism [12] then allows to calculate the effective spectral function from which all interesting equilibrium quantities can be deduced<sup>1</sup>.

Already on the qualitative level one realizes that the notion of individual excitations must be contradictory in 1D. If – say – an electron moves in a 1D liquid of other electrons it has to push a macroscopic number of electrons away in order to be able to advance. Hence, a perturbation in a 1D liquid does not create an individual excitation but rather a collective one and as a consequence, Fermi liquid theory breaks down in 1D. This qualitative picture can be made more precise of course. When constructing a perturbative theory in order to determine the spectral function weight and the effective mass of the electron in the 1D liquid one encounters divergences which are hardly interpretable [10]. The reason is that – as already pointed out – there is no such thing as an effective mass or a spectral function in 1D since the very notion of an individual excitation is fundamentally flawed.

Fortunately, there exists a very beautiful substitute to Fermi liquid theory in 1D, which has been developed from the 1960s onwards [152, 153, 154]. This so-called *Luttinger theory* is

---

<sup>1</sup>Luttinger theory has been first developed for fermions. In the following we will see that the same formalism can be used to describe 1D bosons. See in particular the next subsection on the phenomenological bosonization.

essentially Gaussian for the low energy excitations (which are now collective ones) *regardless of the strength of the interaction*. Thus, even strongly interacting 1D liquids can be elegantly described by Luttinger theory. The heard of this theory is the following observation. Assume for a moment that we deal with fermions. Then the Fermi energy  $E_F$  is typically finite and the term “low energy excitation ” makes sense: Hence, we can concentrate on particle-hole excitations whose energy is small compared to  $E_F$ . In this case, the (*a priori* unknown) exact spectrum of the quadratic part of the generic Hamiltonian describing the 1D liquid can be expanded around  $E_F$  for small energies. The result is a Hamiltonian with a *linear* spectrum, the so called *Tomonaga-Luttinger Hamiltonian*

$$\hat{\mathcal{H}}_0 = \sum_{k,r=\pm} v_F(rk - k_F) \hat{c}_{k,r}^\dagger \hat{c}_{k,r} . \quad (4.1)$$

Here,  $v_F(k_F)$  is the Fermi velocity (momentum) and  $r$  denotes right-moving ( $r = +$ ) and left-moving  $r = -$  particles with creation and annihilation operators  $\hat{c}_{k,r}^\dagger, \hat{c}_{k,r}$ . Note that in 1D particles can only move forward or backwards which forces us to introduce two species of these particles, the right movers and the left movers.

Introducing a linear spectrum amounts to assuming a constant density of states, a common approximation for fermions (the density of states is essentially the derivative of the spectrum times the solid angle element which is equal to one in 1D). The particle-hole excitations now have a well defined energy  $E_{r,q} = v_F(rk + q) - v_Frk = v_Fq$  and a well defined momentum  $q$  independent from  $k$ .

Let us now focus on the interaction term, which is in general present in a realistic theory. In most cases the interaction is quartic in the fermionic operators. Since we expect collective excitations to be the relevant variables we can try a new basis of ladder operators which are quadratic in the  $\hat{c}_{k,r}$ ,

$$\hat{\rho}_{q,r}^\dagger = \sum_k : \hat{c}_{k+q,r}^\dagger \hat{c}_{k,r} : , \quad (4.2)$$

and which consequently mimic density fluctuations. We defined the density in terms of the normal ordered product defined as  $: \hat{A}\hat{B} := \hat{A}\hat{B} - \langle 0|\hat{A}\hat{B}|0\rangle$  for two operators  $\hat{A}$  and  $\hat{B}$ . Indeed, because of the filled Fermi sea the average of  $\hat{c}_{k+q,r}^\dagger \hat{c}_{k,r}$  is formally infinite and has to be removed from the Hamiltonian to yield a finite zero-energy level.

Now, a quartic action is *quadratic* in the  $\hat{\rho}^\dagger, \hat{\rho}$ -basis and is therefore trivial to diagonalize. This is expected from the very construction of the  $\hat{\rho}_{q,r}$  and is not very surprising. The more important observation is that

$$[\hat{\rho}_{q,r}^\dagger, \hat{\rho}_{-q',r'}^\dagger] = -\frac{rqL}{2\pi} \delta_{r,r'} \delta_{q,q'} , \quad (4.3)$$

which is found by correctly using the normal ordered products [10]. Here,  $L$  is the length of the system. Also, the Fermi level trivially verifies  $\hat{\rho}_{q>0,-}^\dagger |0\rangle = 0$  and  $\hat{\rho}_{q<0,+}^\dagger |0\rangle = 0$  such that we can define the two operators for  $q \neq 0$

$$\hat{b}_q^\dagger = \sqrt{\frac{2\pi}{L|q|}} \sum_r \Theta(rq) \rho_{q,r}^\dagger , \quad (4.4)$$

$$\hat{b}_q = \sqrt{\frac{2\pi}{L|q|}} \sum_r \Theta(rq) \rho_{-q,r}^\dagger , \quad (4.5)$$

which satisfy *bosonic* commutation relations  $[\hat{b}_q^\dagger, \hat{b}_{q'}] = \delta_{q,q'}$ . Finally, one finds that  $[\hat{b}_q, \hat{\mathcal{H}}_0] = v_F q \hat{b}_q$ , a remarkable identity, since it tells us that  $\hat{\mathcal{H}}_0$  is *quadratic* in the bosonic density operators although it has been also quadratic in the original fermionic operators. Hence, the free part of the Hamiltonian can also be written as

$$\hat{\mathcal{H}}_0 = \sum_{q \neq 0} v_F |q| \hat{b}_q^\dagger \hat{b}_q, \quad (4.6)$$

where we explicitly used the assumption of a linear spectrum. In conjunction with the observation that a quartic interaction is quadratic in the  $\hat{b}^\dagger, \hat{b}$  we conclude that the linear Tomonaga-Luttinger Hamiltonian with a supplement quartic term is exactly diagonalisable *via* the nonlinear relation (4.2).

Of course, real systems do not have an exactly linear spectrum. However, as long as the spectrum is linear around the Fermi surface up to first order in the excitation energies, the low-energy properties can be exactly calculated with Luttinger liquid theory. Moreover, these low-energy excitations share common universal features which I will present in the next section. Luttinger theory can hence be considered as a universal theory to which many 1D systems “flow” in the renormalization group sense. All interesting quantities, such as correlation functions or spectral densities, can in principle be calculated within Luttinger theory as long as one is interested in the long-range properties of these quantities. The short-range behaviour of the physical systems in question are not accessible within Luttinger theory since they do in general not share any common universal features.

To conclude this introductory part I want to emphasize that there are still notable cases where the spectrum has no such linear part since the first order approximation around the Fermi energy vanishes. In these cases Luttinger theory is simply useless. To cite only one example here I mention spin waves in the ferromagnetic phase, which have a quadratic dispersion at low energies [147].

### 4.1.1 Phenomenological bosonization

The mapping between the fermionic operators and the bosonic density fluctuation operators is commonly referred to as *bosonization*. In this section I present a rather intuitive way of deriving the effective Luttinger Hamiltonian, without directly using the exact relations (4.2) and (4.4) which translate between the two kinds of operators. Moreover, we will see that the bosonization scheme also works for 1D bosons. The notation and concepts which are introduced in this presentation will be used on many occasions in the following. I follow rather closely the pedagogical line which can be found in the well-known reviews on this subject [see, e.g., [10, 155, 156, 157, 158]].

In the previous section we have seen that the collective excitations of a 1D Fermi liquid can be considered as density wave excitations. Hence, it is natural to start from the representation of the density in space,

$$\hat{\rho}(x) = \sum_i \delta(x - \hat{x}_i), \quad (4.7)$$

where the  $\hat{x}_i$  are the position operators of the particles which form the 1D liquid. It is more useful to work with the integrated density represented by a certain monotonic analytical field  $\hat{\phi}_l(x)$  which we require to take the values  $\hat{\phi}_l(x_i) = 2\pi i$  at the position of the  $i$ -th particle and which is a smooth function everywhere else.  $\hat{\phi}_l(x)$  interpolates between the fixed values  $\hat{\phi}_l(x_i) = 2\pi i$  and can hence admit fluctuations. These fluctuations will be governed by a

Hamiltonian which we introduce further below. Note also that here the unidimensionality of the underlying system enters in a crucial way: For the field  $\hat{\phi}_l(x)$  to be well-defined the single particles have to be labeled in a unique way. This can only be achieved in 1D.

With the help of  $\hat{\phi}_l(x)$  the density can be recast as

$$\hat{\rho}(x) = \sum_i \delta(x - \hat{x}_i) = \sum_n |\hat{\phi}'_l(x)| \delta(\hat{\phi}_l(x) - 2\pi n), \quad (4.8)$$

by using the standard formula  $\delta(f(x)) = \sum_n |f'(x_n)|^{-1} \delta(x - x_n)$  (with  $x_n$  the zeros of  $f(x)$ ). The Poisson summation formula then yields

$$\hat{\rho}(x) = \frac{\hat{\phi}'_l(x)}{2\pi} \sum_{p \text{ int}} e^{ip\hat{\phi}_l(x)}, \quad (4.9)$$

where the sum runs over all integer  $p$ . In order to make the notion of density fluctuations more visible in our presentation we introduce the field  $\hat{\phi}(x)$  which is defined relative to a perfect crystalline solution, where the  $i$ -th particles is fixed at  $ai$ : One has  $\hat{\phi}_l(x) = 2\pi\rho_0 x - 2\hat{\phi}(x)$  with  $a$  the lattice spacing and  $\rho_0$  the unperturbed classical (average) density, such that  $\hat{\phi}(x)$  describes the very density waves. The final result reads

$$\hat{\rho}(x) = \left[ \rho_0 - \frac{1}{\pi} \nabla \hat{\phi}(x) \right] \sum_p e^{2p(\pi\rho_0 x - \hat{\phi}(x))}. \quad (4.10)$$

The integer  $p$  can be regarded as a parameter which introduces fluctuations with shorter and shorter wavelengths. Indeed, the  $p = 0$  term corresponds to the coarse-grained density where all high frequency fluctuations are smoothed out. The *smearred density*

$$\rho_{q \simeq 0}(x) \simeq \rho_0 - \frac{1}{\pi} \nabla \hat{\phi}(x) \quad (4.11)$$

valid for small wave vectors  $q \simeq 0$  is sometimes sufficiently accurate for real applications. In virtual all other cases, including the first harmonic term is then sufficient to obtain accurate results. The expression

$$\rho_{q \simeq 0}(x) \simeq \rho_0 - \frac{1}{\pi} \nabla \hat{\phi}(x) + 2\rho_0 \cos[2\pi\rho_0 x - 2\hat{\phi}(x)], \quad (4.12)$$

obtained from Eq. (4.10) by including the  $p = -1, 1$  harmonic terms, is therefore widely used in the literature. Note that during a typical coarse-graining procedure the harmonics cancel each other out when long distances are considered as long as there are no constraints that forbid such a cancellation, such that higher harmonics become relevant even on long-range scales. An important example of a system for which higher harmonics have to be taken into account is the Ising spin chain defined (by definition) on a lattice. As is well known [159] the Ising quantum chain in a transverse field  $h$  can be exactly diagonalized *via* the Jordan-Wigner transformation to yield a theory of free fermions  $\hat{\mathcal{H}} = \sum_k \epsilon_k \hat{c}_k^\dagger \hat{c}_k$  with energies  $\epsilon_k = J \cos ak$  ( $J$  is the ferromagnetic coupling) for  $h = 0$ . The Fermi velocity is readily found to be  $v_F = Ja \sin k_F a$  and the low-energy properties are described by Luttinger theory. In the absence of an external magnetic field the magnetization is zero,  $\langle S_z \rangle = \langle \hat{c}^\dagger(x) \hat{c}(x) \rangle - 1/2 = 0$ , and the ground state is the half-filled fermionic band. What I want to point out here is the fact that in this case  $e^{2p\pi\rho_0 x} = e^{2ip\pi(1/2a)ja} = e^{ip\pi j} = (-1)^{pj}$  (note that  $x = aj$  on the lattice). Hence, for  $p$

even, the higher harmonics give contributions that do not cancel for large  $x$  since they no longer depend on  $x$  anymore. This simple example demonstrates that for models defined on lattices it is in general necessary to keep the relevant harmonics and thus to go beyond the coarse-grained approximation Eq. (4.11).

Starting from the representation of the density (4.10) one can define the field  $\hat{\psi}(x)$  as the “square root” of the density,

$$\hat{\psi}^\dagger(x) = \sqrt{\hat{\rho}(x)} e^{-i\hat{\theta}(x)}, \quad (4.13)$$

where  $\hat{\theta}(x)$  is some operator describing the phase. Since we have by construction  $\hat{\rho}(x) = \hat{\psi}^\dagger(x)\hat{\psi}(x)$ ,  $\hat{\psi}^\dagger$  is therefore a single particle creation operator which can be either bosons or fermions. In the following I will write  $\hat{\psi}_B^\dagger$  for the boson creator and  $\hat{\psi}_F^\dagger$  for the fermion creation operator. We now want to analyze the constraints imposed on the fields  $\hat{\phi}(x)$  and  $\hat{\theta}(x)$  by requiring that the  $\hat{\psi}^\dagger, \hat{\psi}$  be proper bosonic or fermionic ladder operators.

In order for the  $\hat{\psi}_B^\dagger, \hat{\psi}_B$  ( $\hat{\psi}_F^\dagger, \hat{\psi}_F$ ) to verify the bosonic (fermionic) creation and annihilation operator algebra we have to impose the conditions

$$[\hat{\psi}_B(x), \hat{\psi}_B(x')] = \delta(x - x'), \quad (4.14)$$

$$\{\hat{\psi}_F(x), \hat{\psi}_F(x')\} = \delta(x - x'). \quad (4.15)$$

Let us first focus on the bosonic field. For Eq. (4.14) to be satisfied one needs to have

$$[\hat{\rho}(x), e^{-i\hat{\theta}(x')}] = \delta(x - x') e^{-i\hat{\theta}(x)}, \quad (4.16)$$

if one makes the rather natural assumption that  $[\hat{\theta}(x), \hat{\theta}(x')] = 0$ . We can proceed by first inserting the smeared density (4.11) in order to get the right commutation relation at least for large wave lengths. The above relation is then satisfied if

$$\left[ \frac{1}{\pi} \nabla \hat{\phi}(x), \hat{\theta}(x') \right] = -i\delta(x - x'). \quad (4.17)$$

So far we have taken into account only large wave-lengths. What about the shorter wave-lengths fluctuations described by the higher harmonics? The higher harmonic terms in Eq. (4.10) lead in the density-density commutator to expressions of the form

$$[e^{-2pi\hat{\phi}(x)}, e^{-i\hat{\theta}(x')}] = e^{-2pi\hat{\phi}(x)} e^{-i\hat{\theta}(x')} (1 - e^{i\pi p \text{sign}(x-x')}). \quad (4.18)$$

We make the convention  $\text{sign}(0) = 0$ . Then the commutator (4.18) vanishes exactly for  $x = x'$ , while for  $x \neq x'$  terms remain for odd  $p$ . As I have explained in the previous paragraph such odd  $p$  terms usually cancel when coarse-grained, even if the system is defined on a lattice: Remember that it is typically the even  $p$  terms which give rise to non trivial contributions.

If we assume that all assumptions I have enounced up to this point are met, Eq. (4.17) is the right commutation relation for the two fields  $\hat{\phi}$  and  $\hat{\theta}$ . By applying an integration by parts one deduces that

$$\hat{\Pi}(x) \equiv \frac{1}{\pi} \nabla \hat{\theta}(x) \quad (4.19)$$

is the conjugate momentum of  $\hat{\phi}(x)$ .  $\hat{\phi}$  and  $\nabla \hat{\theta}$  are thus canonical fields the action of which can be easily written down [see next section].

The bosonic single particle operator is now easily found by putting all results together and by observing that the square root of a delta function is itself a delta function (up to a normalization). Hence, we have

$$\hat{\psi}_B^\dagger = \left[ \rho_0 - \frac{1}{\pi} \nabla \hat{\phi}(x) \right]^{1/2} \sum_p e^{i2p(\pi\rho_0 x - \hat{\phi}(x))} e^{-i\hat{\theta}(x)}. \quad (4.20)$$

What about the fermion operator  $\hat{\psi}_F^\dagger$ ? The only difference with the bosonic operator is that they have to satisfy anticommutation relations instead of commutation relations. We thus have to introduce some supplement factor that generates the proper minus sign to transform a commutation relation into an anticommutation relation. The answer is easy to guess by using the relation (4.18) with  $p = 1$  which can be viewed as the proper anticommutation relation. The final answer is simply

$$\hat{\psi}_F^\dagger(x) = \hat{\psi}_B^\dagger(x) e^{i\hat{\phi}(x)/2}, \quad (4.21)$$

so that

$$\hat{\psi}_F^\dagger = \left[ \rho_0 - \frac{1}{\pi} \nabla \hat{\phi}(x) \right]^{1/2} \sum_p e^{i(2p+1)(\pi\rho_0 x - \hat{\phi}(x))} e^{-i\hat{\theta}(x)}. \quad (4.22)$$

This transformation from commuting fields into anticommuting fields is also used (although in a different form) in the Jordan-Wigner transformation which transforms spin operators  $\sigma_i^+, \sigma_i^-$ , that commute in different sites, into Fermi operators  $\hat{c}_i^\dagger, \hat{c}_i$  that anticommute, by attaching the proper nonlinear “string” to the spin operators to generate the required minus sign [159].

### 4.1.2 The Tomonaga-Luttinger Hamiltonian

We now write down the Hamiltonian of our 1D system which should only depend on the two conjugate fields  $\hat{\phi}$  and  $\hat{\theta}$ . Let us first focus on the kinetic part of the Hamiltonian. Such a term derives from the kinetic energy (here for the bosonic case)

$$\hat{\mathcal{H}}_{\text{kin}} = \int dx \frac{\hbar}{2m} (\nabla \hat{\psi}^\dagger(x)) (\nabla \hat{\psi}(x)) \simeq \frac{\rho_0}{2m} (\nabla \hat{\theta})^2 + \frac{1}{8m\rho_0} (\nabla \hat{\rho})^2 + \dots, \quad (4.23)$$

where the dots stand for higher derivative terms. Note that all cross terms between  $\hat{\theta}$  and  $\hat{\phi}$  have to vanish. Indeed, for a system with an inversion symmetry one has  $\hat{\rho}(x) = \hat{\rho}(-x)$  which can only be fulfilled if  $\hat{\phi}(-x) = -\hat{\phi}(x)$ . In conjunction with the invariance of the one-particle operator  $\hat{\psi}(-x) = \hat{\psi}(x)$  one also obtains  $\hat{\theta}(-x) = \hat{\theta}(x)$ ; as a consequence (quadratic) mixed terms between  $\hat{\psi}$  and  $\hat{\theta}$  cannot appear.

A typical interaction is bilinear in the density operator,

$$\hat{\mathcal{H}}_{\text{int}} = \frac{\hbar\omega_L}{2} \int dx \hat{\rho}(x) \hat{\rho}(x) \simeq \frac{\hbar\omega_L}{2\pi^2} (\nabla \hat{\phi})^2 + \dots, \quad (4.24)$$

which reconfirms explicitly at this level that the first terms in a gradient expansion of the Hamiltonian contain only quadratic terms in the fields although the underlying theory is interacting. On large scales it is obvious that higher gradient terms are less relevant than the terms explicitly listed above. Hence, the low energy properties (large space scale properties) are governed by the quadratic Tomonaga-Luttinger Hamiltonian

$$\hat{\mathcal{H}}_L = \frac{\hbar}{2\pi} \int dx \left[ \frac{u}{K} (\nabla \hat{\phi})^2 + \frac{uK}{\hbar^2} (\nabla \hat{\theta})^2 \right] + \dots. \quad (4.25)$$

The dimensionless Luttinger parameter  $K$  and the sound velocity  $u$  parametrize this Hamiltonian and they depend on the parameters of the microscopic theory and in particular on the interaction strength  $\hbar w_L$ . Note however that the exact relationship between  $u$ ,  $K$  and  $w_L$  is in general not known and has to be determined with complementary methods such as numerical simulations. The ellipsis stands for all irrelevant operators (in the renormalization group sense), which are subdominant on large scales.

Let us for a moment come back to the expansions (4.23) and (4.24). By converting them to the momentum domain we obtain the spectrum

$$E(k) = \sqrt{\frac{\hbar^3 k^2 w_L \rho_0}{m} + \left(\frac{\hbar^2 k^2}{2m}\right)^2}, \quad (4.26)$$

which is nothing else than the Bogoliubov spectrum of an interacting bosonic liquid [158]. In particular, this spectrum is *linear* for small  $k$  which confirms the underlying assumptions of Luttinger theory that the low energy excitations have a linear spectrum. Interestingly enough, for bosons the non-interacting case  $w_L \rightarrow 0$  is singular and Luttinger liquid theory breaks down. Intuitively this is expected since a non-interacting Bose liquid forms a true BEC (at zero temperature) while each finite interacting destabilizes this condensate (for translationally invariant systems. Trapped Bose liquids may of course condense even if they are weakly interacting). More formally, one can consider – in the bosonic case – the product  $\hbar w_L \rho_0$  as the equivalent of the Fermi energy.

The Luttinger Hamiltonian (4.25) is also found if one starts from a Fermi gas with  $\hat{\psi}_F^\dagger, \hat{\psi}_F$  given in Eq. (4.22). However, for a given interaction strength  $w_L$  and background density  $\rho_0$  the parameters  $u$  and  $K$  are different in the fermionic case from the ones one would find for bosons. Obviously, the non-interacting Fermi gas gives rise to  $K = 1$ . It can be shown that,  $K > 1$  corresponds to fermions with attractive interactions while  $K < 1$  to fermions with repulsive interactions. Since non-interacting fermions are equivalent to impenetrable bosons [160] (bosons with repulsive contact interaction and  $w_L \rightarrow \infty$ ) one has  $K = 1$  for impenetrable bosons, as well. Non-interacting bosons on the other hand are described by  $K \rightarrow \infty$ .  $K < 1$  can only be attained for bosons that are subject to long range repulsive interactions.

Practically all 1D systems which exhibit a linear spectrum at low energies are described by Eq. (4.25). The very form of Eq. (4.25) already specifies most of the outcome of the theory even without knowing the numerical values of  $u$  and  $K$ . In order to completely describe the low-energy properties of the system it is however necessary to know the exact expressions for  $u$  and  $K$ , which cannot be found within the framework of Luttinger theory. Luttinger theory has thus to be combined with other methods to yield a full description of the specific model in question. However, once the two parameters  $u$  and  $K$  are known, the low energy properties of the model are correctly described by Eq. (4.25). In the subsection 4.1.4 I will briefly show how  $u$  and  $K$  can be extracted from simulations in the case of a translationally invariant system.

It is also possible to give an expression of the total momentum operator (or functional) in terms of the two fields  $\hat{\phi}$  and  $\hat{\theta}$  by essentially proceeding in the same way as before when we have derived  $\hat{\mathcal{H}}_L$ . One has

$$\hat{\mathcal{P}}_L = \frac{\hbar}{\pi} \int dx \left[ \rho_0 - \frac{1}{\pi} \nabla \hat{\phi} \right] \nabla \hat{\theta} + \dots, \quad (4.27)$$

where the ellipsis stands – again – for irrelevant terms which only modify the sub-leading behaviour of universal quantities.

### 4.1.3 The interaction between an impurity and a Luttinger liquid

Let me introduce in this subsection the interaction Hamiltonian which models the potential between the impurity and the Luttinger liquid. The formulae of this subsection will be extensively used in the following of this thesis. In its general form the impurity-Luttinger liquid interaction reads

$$\hat{\mathcal{H}}_{IL} = \int dx dy U(x-y) \hat{\rho}(y) \delta(x-\hat{q}), \quad (4.28)$$

where  $U(x-y)$  is an interaction potential,  $\hat{\rho}(y)$  the density of the Luttinger liquid given in Eq. (4.10) and  $\hat{q}$  the position operator of the impurity.

In many applications the atoms behave almost as hard spheres and one can approximate the true interaction by a contact interaction potential

$$U(x-y) = \hbar v \delta(x-y), \quad (4.29)$$

so that Eq. (4.28) can be recast as

$$\hat{\mathcal{H}}_{IL} = \int dx \hbar v \hat{\rho}(x) \delta(x-\hat{q}). \quad (4.30)$$

As shown in formula (4.10) the density has two parts: The coarse-grained density (4.11) and the higher harmonics. If I insert only the  $p = 0$  summand of the rhs of Eq. (4.10) into the above equation I find the so-called *forward scattering* part of the interaction which does not flip the momentum of the Luttinger liquid atoms during a scattering event with the impurity. The higher harmonics lead on the other hand to the so-called *backscattering* part which reverses the momentum of the Luttinger liquid atoms and thus converts left-movers into right-movers and vice versa. In this thesis I will mostly work with the forward scattering interaction Hamiltonian

$$\hat{\mathcal{H}}_{IL} = \int dx \hbar v \left[ \rho_0 - \frac{1}{\pi} \nabla \hat{\phi}(x) \right] \delta(x-\hat{q}), \quad (4.31)$$

which leads, when added to the free Luttinger Hamiltonian (4.25) to a quadratic action in the fields  $\hat{\phi}$  and  $\hat{\theta}$ . The backscattering potential can be analyzed by using Bethe-ansatz methods [161] and renormalization group techniques [13].

The forward scattering Hamiltonian (4.31) can be rewritten (after dropping a constant term) in the Fourier domain as

$$\hat{\mathcal{H}}_{IL} = \sum_k i k U_k \hat{\phi}_k e^{-i k \hat{q}}, \quad (4.32)$$

where I introduced a  $k$ -dependent potential  $U_k$  which has the main purpose of introducing a cutoff scale  $k_c$  for the Luttinger momentum modes. I will use in particular the choice

$$U_k = \hbar v e^{-|k|/k_c}. \quad (4.33)$$

### 4.1.4 The Lieb-Liniger gas as a Luttinger liquid

Let us in this subsection in more detail an important application of Luttinger theory: We are interested in the properties of 1D bosons which interact with a contact potential. This system is described by the so-called *Lieb-Liniger* Hamiltonian

$$\hat{\mathcal{H}} = \sum_{i=1}^N \frac{\hat{p}_i^2}{2m} + \hbar v_L \sum_{i < j=1}^N \delta(\hat{x}_i - \hat{x}_j). \quad (4.34)$$

Note that Eq. (4.34) is integrable [162]. Since we have seen in the previous subsection that the low energy properties of Eq. (4.34) are also described by the Tomonaga-Luttinger Hamiltonian, one can use Eq. (4.34) as a benchmark for Luttinger theory. The integrability of the Lieb-Liniger model allows in particular to find numerical values of  $K$  and  $u$ . Let me demonstrate how to determine  $u$  and  $K$  in practice (I closely follow the analysis presented in [158]):

The model (4.34) is translationally invariant. This symmetry imposes an additional restriction on the two Luttinger parameters. To be more explicit, consider the center of mass position  $\hat{\mathcal{X}} = \frac{1}{N} \int dx x \hat{\rho}(x) = -\frac{1}{N\pi} \int dx x \hat{\phi}'(x) + \dots$ , where we used Eq. (4.11).  $\hat{\mathcal{X}}$  obeys the equation of motion

$$\partial_t \hat{\mathcal{X}} = \frac{i}{\hbar} [\hat{\mathcal{H}}_L, \hat{\mathcal{X}}] = \frac{\hat{\mathcal{P}}}{Nm}. \quad (4.35)$$

Now use the commutator (4.17) in order to compute the second term of Eq. (4.35) and compare it to Eq. (4.27): The final result reads

$$uK = \frac{\hbar\pi\rho_0}{m}. \quad (4.36)$$

For translationally invariant systems there is hence only *one* parameter which has to be determined: The ratio  $u/K$ . Actually, it can be related to the inverse of the macroscopic compressibility at zero temperature  $\kappa_s^{-1}$  [10]:

$$\kappa_s^{-1} = \rho_0 N \frac{\partial^2 E_{GS}(N)}{\partial N^2} = \hbar\pi\rho_0^2 \frac{u}{K}, \quad (4.37)$$

with  $E_{GS}(N)$  the groundstate energy for a system with  $N$  particles. The advantage of Eq. (4.37) is that the stiffness parameter  $\kappa_s$  can be obtained in numerical simulation or by exploiting additional analytic information on the system, such as integrability. By relating  $u$  and  $K$  to “physically observable” quantities, it is thus possible to find numerical values for the Luttinger parameters.

In the case of the Lieb-Liniger gas Eq. (4.36) and Eq. (4.37) can be calculated analytically by using the exact Bethe-Ansatz solution of the ground state energy [162] from which the compressibility  $\kappa_s$  can be derived. It can be shown that the the Luttinger theory then depends only on one dimensionless parameter,  $\gamma = mw_L/\hbar\rho_0$ , the *Lieb-Liniger parameter*. From the exact solution the Luttinger parameter  $K = K(\gamma)$  and the velocity  $u = u(\gamma)$  can be obtained. Although analytical expressions are not available for general  $\gamma$  it is sufficient in most practical situations to know the asymptotic behaviour [163, 158]

$$K(\gamma) \simeq 1 + \frac{4}{\gamma^2} + \mathcal{O}(\gamma^{-3}), \quad \text{for } \gamma \gg 1, \quad (4.38)$$

$$K(\gamma) \simeq \frac{\pi}{\sqrt{\gamma}} \left(1 - \frac{\sqrt{\gamma}}{2\pi}\right)^{-1/2}, \quad \text{for } \gamma \ll 1. \quad (4.39)$$

Note that the asymptotics of  $u$  then follows from Eq. (4.36). We will make use of these relations in Sec. 4.6. Combined with additional information, Luttinger theory predicts the correct low-energy properties of the Lieb-Liniger gas. Since only one parameter  $\gamma$  is needed in order to obtain a full characterization of this Lieb-Liniger gas (note that for lattice systems which violate the translation symmetry the two parameters  $u$  and  $K$  have to be determined independently) Luttinger theory radically simplifies the problem. As soon as  $\gamma(w_L)$  is known the long-range behaviour of all interesting quantities can be easily determined. To cite one example, it can

be shown [10] that the Matsubara density-density correlation function has to behave within the Luttinger framework in general as

$$\langle \hat{\rho}(x, 0) \hat{\rho}(0, 0) \rangle = -\frac{K}{2\pi^2 x^2} + \frac{2}{(2\pi\alpha_+)^2} \left(\frac{\alpha_+}{x}\right)^{2K}, \quad (4.40)$$

where  $\alpha_+$  is a small parameter which is usually related to the initial lattice spacing or, in the continuum limit, which represents a short-range cutoff. The universal properties of the physical system do not depend on  $\alpha_+$ .

While the  $1/x^2$ -decay of the first summand is typical for a Fermi liquid, the second summand shows a characteristic  $1/x^{2K}$ -decay which points to the non-Fermi liquid behaviour of the underlying system. Analogous formulae exist, e.g., for the spin-spin correlation in  $XXZ$ -chains, which again show, that Luttinger liquid theory yields the right – non Fermi-liquid like – long-range behaviour.

## 4.2 Drag force and critical velocities in a 1D quantum liquid

In this section I review some ideas about superfluidity in interaction 1D liquids. If the quantum liquid forms a perfect condensate (i.e. for non-interacting Bose liquids) the drag force on a mobile impurity vanishes. In the opposite Tonks-Girardeau limit of impenetrable bosons (or equivalently non-interacting fermions) the drag force grows linearly with the impurity velocity as long as the impurity moves subsonically. For supersonic impurities the drag force is independent of the velocity. We will also see that an external potential changes this picture. The so-called forward-scattering part of the impurity-liquid interaction becomes important in this case.

In Sec. 4.2.1 I will follow the line of arguments found in [164] to derive a formula for the drag force in a Luttinger liquid. The approach makes use of Fermi's golden rule which allows us to calculate the energy dissipated of the impurity during its motion in the limit of a small interaction between the impurity and the Luttinger liquid. It turns out that one has to distinguish heavy impurities [165] from light impurities which can move through the surrounding quantum liquid without dissipation [166, 167] even though the Luttinger liquid does not form a superfluid. The reason for this lies in the difference between the dispersion relations of a light and an infinite mass impurity. The excitation spectrum of a 1D Lieb-Liniger gas shows a characteristic gap between zero momentum and the Fermi momentum (see Fig. 4.1). Such a gap does not exist in higher dimensions. When the impurity dispersion lies within this gap no dissipation can take place (at first order in the interaction).

In Sec. 4.2.2 I show that the forward scattering part of the interaction term (4.31) becomes important if the impurity is accelerated. The effect has very much in common with standard electromagnetic bremsstrahlung which is emitted when a charge carrier is accelerated.

### 4.2.1 First order dissipation rate: Fermi's golden rule approach

As already announced in the introduction we study the dissipation rate for an impurity in a 1D quantum liquid by using Fermi's golden rule. At zero temperature the quantum liquid is in the ground state  $|0\rangle$ . On the other hand, the impurity initially carries some energy and we assume that it is in some initial state  $|M\rangle$  which is an eigenvector of the impurity Hamiltonian

$$\hat{\mathcal{H}}_I = \frac{\hat{p}^2}{2M_I} + V(\hat{q}), \quad (4.41)$$

where  $M_I$  is the impurity mass,  $\hat{p}$  and  $\hat{q}$  the impurity momentum and position operators and  $V(\hat{q})$  some position dependent external potential. The combined initial impurity-LL state is thus  $|M, 0\rangle$ . We are interested in the transition rate from  $|M, 0\rangle$  to some final state  $|N, n\rangle$ :

$$T_{N,M;n,0} = \frac{2\pi}{\hbar} |\langle N, n | \hat{\mathcal{H}}_{IL} | M, 0 \rangle|^2 \delta(E_n + E_N - E_M), \quad (4.42)$$

where  $E_n$  is the energy of the wave excitation corresponding to the quantum number  $n$  and  $E_N$  ( $E_M$ ) is the energy of the impurity  $N$ -state ( $M$ -state). The energy dissipation per time unit is then given by

$$\dot{E} = - \sum_n \sum_N (E_M - E_N) T_{N,M;n,0}, \quad (4.43)$$

which is related to the drag force  $f(v)$  by  $\dot{E} = -fv$  with  $v$  the impurity velocity. Note that the drag force depends itself on the impurity velocity<sup>2</sup>

In absence of an external potential the impurity energy states are characterized by its momentum states  $|p\rangle$  and Eq. (4.43) simplifies to

$$\dot{E} = - \frac{2\pi}{\hbar} \int dk |U_k|^2 \left( \hbar k - \frac{\hbar^2 k^2}{2m_I} \right) S \left( k, \hbar k - \frac{\hbar^2 k^2}{2m_I} \right), \quad (4.44)$$

where we used the explicit form of the interaction (4.32) and where we introduced the dynamical structure factor

$$S(k, \omega) \equiv \sum_n |\langle n | \delta \hat{\rho}_k | 0 \rangle|^2 \delta(\hbar\omega - E_n). \quad (4.45)$$

$S(q, \omega)$  can be calculated exactly in the Tonks-Girardeau and the Bogoliubov limit and for a Lieb-Liniger gas with intermediate interactions it is known with arbitrary numerical precision. Its form is depicted in Fig. 4.1 for  $\gamma = 20$ . The light shaded region represents the domain in the  $(q, \omega)$ -plane where  $S(q, \omega)$  is zero. The region where  $S(q, \omega)$  is finite is delimited by the upper dispersion  $\omega_+(k)$  (dashed line) and the lower dispersion  $\omega_-(k)$ . Within Luttinger theory the dispersions  $\omega_{\pm}(k)$  are expanded around the forward scattering point ( $k = 0$ ) and the backscattering point  $k = 2k_F$  up to linear order: Luttinger theory assumes  $\omega_{\pm}(k) = u|k|$  around  $k = 0$  and  $\omega_- = u|k - 2k_F|$  around  $k = 2k_F$ . Consequently, Luttinger theory correctly describes the interaction between a heavy impurity and a 1D liquids only when the impurity velocity is small. However, when  $m_I$  is finite Luttinger theory can be employed in many cases even for supersonic impurities: The impurity dispersion crosses  $\omega_-$  if

$$m_I(v + u)^2 \geq 4\hbar k_F u. \quad (4.46)$$

As long as the typical momentum  $\hbar k_0 = m_I(v + u)$  lies in the linear part of the Bogoliubov spectrum of the 1D liquid,  $S(k_0, \hbar k_0 - \hbar^2 k_0^2 / 2m_I)$  is well described by Luttinger theory: More specifically, this is the case whenever  $m_I(u + v)^2 \ll \hbar \omega_L \rho_0$ .

As pointed out before, the impurity emits excitons whenever its dispersion crosses the region where the DST is nonzero. It is thus clear that an impurity with infinite mass dissipates energy at all velocities due to the backscattering part of  $S(k, \omega)$ . It can be shown that the drag force scales in this case as

$$f \sim v^{2K-1} \quad (4.47)$$

<sup>2</sup>It is important to understand that the above formula does *not* imply that the dynamics are Markovian. Here, the constant velocity of the impurity is imposed by hand and therefore not a dynamical quantity. A classical particle moving with constant velocity  $v$  and linearly coupled to a harmonic oscillator bath dissipates energy with  $f(v) \sim v$  regardless of the bath characteristics.

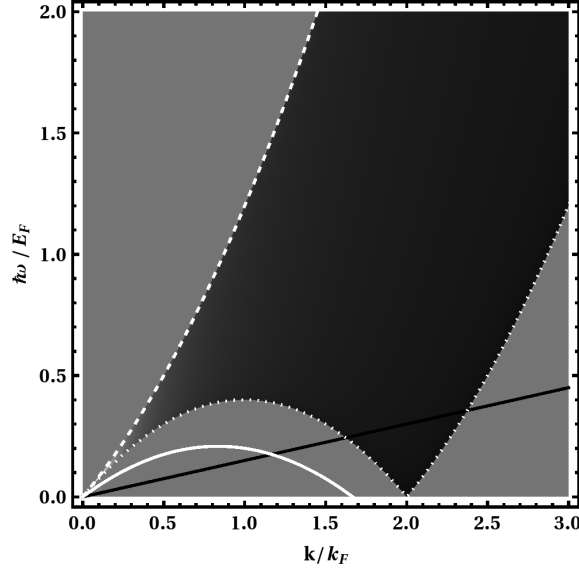


Figure 4.1: Dynamical structure factor (DSF) for a Lieb-Liniger gas with  $\gamma = 20$ . The solid lines represent the dispersion relations for a heavy impurity (black) and a light impurity (white) whereas the dashed line represents the upper dispersion  $\omega_+(k)$  of the Lieb-Liniger gas and the dotted line its lower dispersion  $\omega_-$ .

for small impurity velocities  $v$ . On the other hand, a light impurity emits excitons only if Eq. (4.46) is fulfilled, which thus defines the region in the  $(m_I, v)$ -plane where an impurity can move at a constant velocity *without friction*. We insist that this result is only valid if the impurity is not subject to any potential energy. As we will show in the next section an impurity trapped in a harmonic potential always dissipates energy.

If  $v > u$  the dispersion of a light impurity crosses twice the *forward scattering* part of  $S(k, \omega)$ . But since within Luttinger theory  $S(q, \omega)$  shrinks to a line around  $k = 0$  the forward scattering part does not contribute to the drag force  $f$  and for a general Lieb-Liniger gas this contribution is negligible whenever Luttinger theory can be applied. In many applications where a static impurity is considered, the forward scattering part of the interaction can be in practice absorbed into a redefinition of the field  $\phi$  [10].

#### 4.2.2 Forward scattering Bremsstrahlung of accelerated impurities

We begin with the full Hamiltonian with a forward scattering term [see Eqs. (4.25), (4.31) and (4.41)] of an untrapped impurity-Luttinger liquid system. After transforming the resulting Hamiltonian into momentum space it is straightforward to show that

$$\hat{\mathcal{H}} = \frac{u}{2} \sum_k \left[ \hat{\Pi}_k \hat{\Pi}_{-k} + k^2 \hat{\phi}_k \hat{\phi}_{-k} \right] + \sqrt{\frac{K}{\pi \hbar}} \sum_k ik U_k \hat{\phi}_k e^{-ik\hat{q}} + \frac{\hat{p}^2}{M_I}. \quad (4.48)$$

Note that I rescaled the fields according to  $\hat{\phi}_k \mapsto \sqrt{(\pi K/\hbar)} \hat{\phi}_k$  and  $\hat{\Pi}_k \mapsto \sqrt{(\hbar/\pi K)} \hat{\Pi}_k$ .

I now analyze the equations of motion obtained from the Hamiltonian (4.48). The idea is that one can solve these equations if the trajectory of  $\hat{q}(t)$  is imposed by hand. One thus *demand*s that the impurity moves according to a certain evolution prescription in order to find the force which the surrounding fluid exerts on the impurity.

The equations of motion read in the momentum domain:

$$\ddot{\hat{\phi}}_k(t) + u^2 k^2 \hat{\phi}_k(t) = iuk \sqrt{\frac{K}{\pi\hbar}} U_k^* e^{ik\hat{q}(t)}, \quad (4.49)$$

$$M_I \ddot{\hat{q}}(t) + \kappa \hat{q}(t) = -\sqrt{\frac{K}{\pi\hbar}} \sum_k k^2 U_k e^{-ik\hat{q}(t)} \hat{\phi}_k(t). \quad (4.50)$$

If the impurity is not accelerated, then

$$\hat{q}(t) = \hat{q}(0) + \hat{v}t, \quad (4.51)$$

with  $\hat{v} = \hat{p}(0)/M_I$ . Hence, for an impurity with constant velocity the solution to Eq. (4.49) reads

$$\hat{\phi}_k(t) = \hat{A}_k(t; \hat{v}) e^{ik\hat{v}t} + \hat{g}_k e^{iukt} + \hat{h}_k e^{-iukt}, \quad (4.52)$$

with the coefficients

$$\begin{aligned} \hat{A}_k(t; \hat{v}) &= iuk U_k^* \sqrt{\frac{K}{\pi\hbar}} \frac{e^{ik\hat{q}(0) + i\hbar k^2 t / 2M_I}}{u^2 k^2 - \hat{v}^2 k^2}, \\ \hat{g}_k &= \frac{1}{2} \left[ \hat{\phi}_k(0) + \frac{1}{iuk} \dot{\hat{\phi}}_k(0) - \hat{A}_k(0; \hat{v}) - \hat{A}_k(0; \hat{v}) \frac{\hat{v}}{u} \right], \\ \hat{h}_k &= \frac{1}{2} \left[ \hat{\phi}_k(0) - \frac{1}{iuk} \dot{\hat{\phi}}_k(0) - \hat{A}_k(0; \hat{v}) + \hat{A}_k(0; \hat{v}) \frac{\hat{v}}{u} \right]. \end{aligned} \quad (4.53)$$

The first term on the right-hand-side of Eq. (4.52) describes a density cloud that moves together with the impurity creating a local density hole around the impurity, while the two last terms describe the very wave excitation with sound velocity  $u$ . For instance, in the limit  $\omega_c \rightarrow \infty$  we have for a mobile impurity with *constant* velocity

$$\hat{\rho}(x, t) \sim \sum_k ik \hat{A}_k(t; \hat{v}) e^{ik\hat{v}t - ikx} \sim \delta(x - \hat{q}(t)), \quad (4.54)$$

meaning that the LL density profile follows the impurity, thus creating a *dressed* local impurity. Such a constantly moving density cloud does not have any back-effect on the impurity as can be seen by inserting the first term of the rhs of Eq. (4.52) into Eq. (4.50). We thus confirm directly that no dissipation takes place at zero temperature if only the forward scattering is retained. As pointed out before this approximation becomes exact for light impurities [see Eq. (4.46)].

However, if the impurity is accelerated with a constant acceleration  $a$  the picture drastically changes. The density cloud part of the solution to the EOM (4.49) reads by using  $\hat{q} - \hat{q}(0) = at^2$ :

$$\begin{aligned} \hat{\phi}(x, t) &= \frac{1}{2u} \int_0^t dt' \int_{x-u(t-t')}^{x+u(t-t')} dx' \sqrt{\frac{K}{\pi\hbar}} U \delta'(x' - at'^2) \\ &= \sqrt{\frac{K}{\pi\hbar}} \frac{U}{2u} \int_0^t dt' \left\{ \delta(x + u(t-t') - \frac{1}{2}at'^2) - \delta(x - u(t-t') - at'^2) \right\}. \end{aligned} \quad (4.55)$$

For  $t < u/a$  we find the solution [see Fig. 4.2]

$$\hat{\phi}(x, t) = \sqrt{\frac{K}{\pi\hbar}} \frac{U}{2u} \begin{cases} (u^2 + 2ax + 2aut)^{-1/2} & , -ut < x < at^2 \\ -(u^2 + 2ax - 2aut)^{-1/2} & , at^2 < x < ut \\ 0 & \text{else .} \end{cases} \quad (4.56)$$

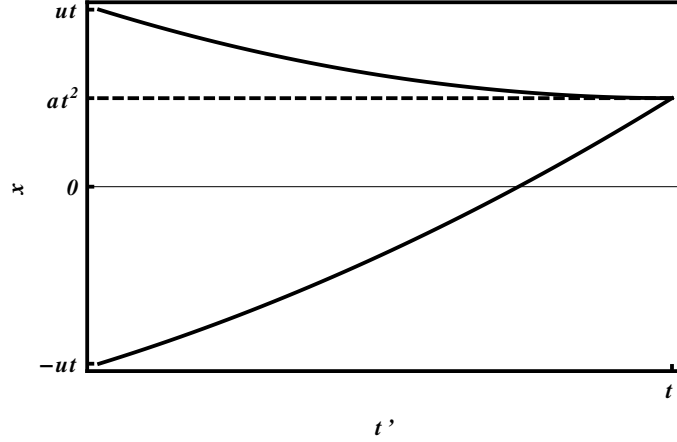


Figure 4.2: The function  $f_{\pm}(t') = at'^2/2 \pm u(t - t')$  (see main text for details).

The classical energy associated to Eq. (4.56) is then found to be

$$\Delta E = \frac{KU^2 au}{8\pi\hbar} \left\{ \frac{1}{(u^2 + 2a^2t^2 - 2aut)^2} - \frac{1}{(u^2 + 2a^2t^2 + 2aut)^2} \right\}. \quad (4.57)$$

For  $t = u/a$  the rhs of Eq. (4.57) diverges, which is when the impurity velocity  $v = at$  has attained the Luttinger speed of sound  $u$ . In this case the Bremsstrahlung becomes infinite and the assumptions of a constant acceleration breaks down. However, for small times Eq. (4.57) makes sense and it shows that an accelerated impurity emits phonons much as an accelerated charge emits electromagnetic radiation. It is therefore clear that Eq. (4.57) describes the analogue of the Bremsstrahlung phenomenon. Note that Eq. (4.57) was derived by only considering the forward scattering potential which is the dominant part for a light impurity. Eq. (4.57) is thus only valid in the case  $m_I(v + u)^2 \ll 4\hbar k_F u$ .

### 4.2.3 Backscattering: Renormalization group approach

In the last subsections we focused on light impurities for which backscattering effects can be neglected to a large extent. The full problem of describing a moving impurity in a Luttinger liquid subject to forward and backscattering effects is not analytically solvable. Nonetheless, by combing analytical expressions based on the Bethe ansatz with heavy numerical methods Mathy et al. [161] were able to access the regime of high energy impurities strongly interacting with the surrounding liquid. More specifically, they considered an impurity which is injected into the Luttinger liquid. When the impurity has an initial velocity which exceeds the Luttinger liquid sound velocity, the impurity velocity sharply drops beneath the sound speed and subsequently shows damped oscillations around some average velocity (smaller than the sound speed). This intriguing behaviour has been explained by an entangled state between the impurity and particle-hole excitations in the Luttinger liquid. Indeed, they showed within a simple approach that the superposition of an “exciton state” (the Fermi sea plus the impurity and a hole) and a “polaron state” (Fermi sea plus the impurity and a particle-hole pair excitation) was sufficient to describe the oscillating behaviour of the wave function. Note also that since the final impurity velocity does not drop to zero the entangled state between the impurity and

the surrounding liquid does not lead to an energy flow directed from the impurity to the quantum liquid. This intriguing behaviour – which is in sharp contrast to the Fermi's golden rule approach – has to my knowledge not been explained, yet.

The simpler case of a static impurity can be tackled by considering the renormalization group equation of the backscattering amplitude. It was Kane and Fisher [13] who first solved this problem. The main ingredient is the observation that the free action of a Luttinger liquid can be written in two different ways,

$$\mathcal{S}_L = \frac{1}{2\pi K} \int dx dt \left[ \frac{1}{u} \dot{\phi}^2 + u(\nabla\phi)^2 \right] = \frac{K}{2\pi} \int dx dt \left[ \frac{1}{u} \dot{\theta}^2 + u(\nabla\theta)^2 \right]. \quad (4.58)$$

This duality relation between the two conjugate fields  $\phi$  and  $\theta$  will be very useful in the following.

Consider first a weak barrier in a Luttinger liquid modeled by the interaction Hamiltonian

$$\hat{\mathcal{H}}_{\text{int}} = \int dx U(x) \hat{\rho}(x), \quad (4.59)$$

where  $U(x) = \hbar w \delta(x)$ . By using the decomposition of the density the forward scattering part reads  $-(1/\pi) \nabla\phi(x=0)$ . It can be absorbed in a redefinition of the field (since the impurity is immobile) according to  $\tilde{\phi}(x) = \phi(x) - \frac{K}{u} \int_0^x dx' U(x')$  in the action. The interesting physics comes rather from the backscattering part of the density  $U_{\text{back}} \sim \cos[2\phi(x=0)]$ . By decomposing the field  $\phi(x)$  into  $\phi_{<}(x)$ , which consists solely of slow momentum modes, and into  $\phi_{>}(x)$  which regroups the high momentum modes, the Wilson renormalization group scheme amounts to averaging over the high momentum modes: We are thus interested in  $\langle \cos(2\phi(0)) \rangle_{>} = \cos(2\phi_{<}(0)) \exp[-\langle \phi_{>}(0)^2 \rangle_{>}/2]$ , where the subscript  $>$  indicates that the average with respect to  $e^{-\mathcal{S}_L}$  is only taken over the high momentum modes. By using Eq. (4.58) we find  $\langle \cos(2\phi(0)) \rangle_{>} = e^{-K d\ell} \cos(2\phi_{<}(0))$  with  $d\ell$  a small parameter. The resulting renormalization equation for the backscattering part  $U_{\text{back}}$  of the coupling  $w_L$ <sup>3</sup> is then found to be

$$\partial_\ell U_{\text{back}} = (1 - K) U_{\text{back}}. \quad (4.60)$$

Here,  $\ell$  is the renormalization scale parameter. When the potential reaches the strong coupling regime one can use an intuitive picture to devise a strong-coupling perturbation theory. If  $w$  was infinite it would cut the Luttinger liquid into two independent halves. However, for large but finite  $w$  tunneling processes may occur which make some bosons (or fermions) hop from one side to the other. A reasonable candidate for a strong-coupling Hamiltonian is thus [13]

$$\hat{\mathcal{H}} = \hat{\mathcal{H}}_1 + \hat{\mathcal{H}}_2 + U_{\text{tun}} [\hat{\psi}_1^\dagger(0) \hat{\psi}_2(0) + \text{h.c.}], \quad (4.61)$$

where  $U_{\text{tun}}$  is a small tunneling element and where the two subscripts 1 and 2 denote the two half-chains. By going back to Eq. (4.20) it is clear that  $U_{\text{tun}} [\hat{\psi}_1^\dagger(0) \hat{\psi}_2(0) + \text{h.c.}] \sim U_{\text{tun}} \cos 2\hat{\theta}(0)$ . The above renormalization group argument can now be repeated by simply using the dual representation of the action (4.58). The final result reads:

$$\partial_\ell U_{\text{tun}} = (1 - K^{-1}) U_{\text{tun}}. \quad (4.62)$$

<sup>3</sup>Note that the unrenormalized forward scattering and backscattering have the same coupling constant  $w$ . However, they do not renormalize in the same way such that it becomes necessary to introduce a new coupling  $U_{\text{back}}$  which stands for the backscattering, only.

This second renormalization equation beautifully connects to Eq. (4.60): Indeed, if  $K < 1$  the barrier potential  $U_{\text{back}}$  grows until perturbation theory breaks down and the strong-coupling regime takes over. The tunneling element subsequently decreases which indicates that  $U_{\text{back}}$  further increases beyond the weak-coupling regime. The inverse is of course true as well. For  $K > 1$  the tunneling element  $U_{\text{tun}}$  increases until the renormalization flow of  $U_{\text{back}}$  resumes. Hence, it is natural to assume that the renormalization equation (4.60) [or alternatively Eq. (4.62)] describe the right physics over the whole parameter space.

#### 4.2.4 Drag force and quantum stirring in a Luttinger liquid

Another approach to measuring the drag force in quantum liquids is quantum stirring [see [168] for the details]. For one-dimensional gases such a quantum stirring can be set up by “pulling” a laser through the quantum liquid. The fraction of stirred particles can then be taken as a measure for the superfluid behaviour. Note that a moving laser corresponds to a moving barrier, i.e. to a moving impurity with infinite mass. Let us consider  $N$  bosons confined to a ring of circumference  $L$ . Due to Galilean invariance we have  $uK = \pi\hbar\rho_0/m$  [see Eq. (4.36)]. The barrier moves with constant velocity  $V$  which can be modeled by the time-dependent potential  $U(x, t) = U_0\delta(x - Vt)$ . The interaction Hamiltonian reads

$$\hat{\mathcal{H}}_{\text{int}} = \int dx U(x, t)\hat{\rho}(x) \simeq \hbar w \left[ \rho_0 - \frac{1}{\pi}\nabla\hat{\phi}(Vt) + 2\rho_0 \cos(2\pi\rho_0 Vt - 2\hat{\phi}(Vt)) \right], \quad (4.63)$$

where we used only the most relevant harmonics to model the Luttinger density  $\rho_0$ . The forward scattering term proportional to  $\nabla\hat{\phi}$  represents a slowly varying chemical potential and can be absorbed in  $\hat{\mathcal{H}}$  by a redefinition of the field  $\hat{\phi} \mapsto \hat{\phi} - (K/u)\int^x dx' U(x')$ . The last term in Eq. (4.63) represents the backward scattering whose renormalization I have presented in the previous subsection.

We are interested in the fraction of stirred particles  $N_{\text{st}}/N$  which is related to the total particle current through  $\hat{N}_{\text{st}} = \frac{1}{2\pi}\int_0^t dt' \hat{I}(t')$ . In the weak barrier limit one can perform the following perturbation analysis: By using the standard formulae for the particle densities of right (left) movers [10],  $\hat{\rho}_{R(L)} = \rho_0/2 \pm \nabla\hat{\theta} - \nabla\hat{\phi}$ , we find the stirred current operator up to first order

$$\hat{I} = \frac{i}{\hbar}[\hat{N}_L, \hat{\mathcal{H}}_{\text{int}}], \quad (4.64)$$

with  $\hat{N}_L = \int dx \hat{\rho}_L(x)$ . By using the bosonized expressions for the density and the stirring Hamiltonian the authors of [168] find

$$\hat{I} = i\hbar w_L \rho_0 e^{i2\hat{\phi}(Vt)} e^{2\pi i \rho_0 Vt}. \quad (4.65)$$

Linear response theory now yields the average backscattering current

$$I \simeq i \int_{-\infty}^t dt' \langle [\hat{I}(t), \hat{\mathcal{H}}_f(t')] \rangle_{\mathcal{S}_0} = \frac{(2\pi)^{2K-1} (\hbar w_L)^2}{\Gamma_E(2K) (\hbar u)^2} \left( \frac{V}{u} \right)^{2K-2} 2\pi \rho_0 V, \quad (4.66)$$

where we took the thermodynamic limit,  $N, K \rightarrow \infty$  with  $N/L = \rho_0$ , in the last step. The fraction of stirred particles is then given by  $\hat{N}_{\text{st}}/N = I/(2\pi\hat{\rho}V)$ . Note that Luttinger liquid theory is only valid for small stirring energies, i.e. for  $V \ll u$ . Let us take some limits of Eq. (4.66). First, the non-interacting boson limit is attained for  $K \rightarrow \infty$ . In this case  $I = 0$  (note that  $V < u$ ) as it should: Indeed, the non-interacting bosons form a condensate which

behaves as a superfluid for  $V < u$  (superfluidity abruptly breaks down at  $V = u$ ). The Tonks-Girardeau limit of impenetrable bosons is equivalent to  $K = 1$ . In this case  $N_{st}/N = (w_L/u)^2$  independently of  $V$ . The drag force is then proportional to  $V$  and thus behaves adiabatically (or Ohmic).

Interestingly enough, one can find a similar formula in the large barrier limit. The fundamental reason lies in the duality  $\hat{\phi} \leftrightarrow \hat{\theta}$  of the action (4.58) which allows a weak-coupling and a strong-coupling perturbation theory. Indeed, the large barrier cuts the ring into two pieces and the bosons can hop from one side to the other *via* a small tunneling element  $U_{\text{tun}}$  which can be treated as a small perturbation. It can be shown that the resulting interaction Hamiltonian reads  $\hat{\mathcal{H}}_{\text{int}} = U_{\text{tun}} \cos(2\pi\hat{\theta}(Vt))$  [168]. By repeating the above analysis we find

$$I = \frac{(2\pi)^{2/K-1} U_{\text{tun}}^2}{(\rho_0 \hbar u)^2 \Gamma_E(2/K)} \left(\frac{V}{u}\right)^{2/K-2} 2\pi \rho_0 V. \quad (4.67)$$

How does the strong coupling equation (4.67) relate to the weak coupling formula (4.66)? We have seen in Sec. 4.2.3 that the backscattering barrier  $U_{\text{back}}$  scales under renormalization as  $\partial_\ell U_{\text{back}} = (1 - K)U_{\text{back}}$ .  $U_{\text{back}}$  becomes thus irrelevant as soon as  $K > 1$ : By noting that  $V$  represents the true velocity scale the factor  $(V/u)^{K-1}$  in Eq. (4.66) is nothing else than the renormalization factor of the bare coupling  $w$ . If  $K < 1$  the interaction  $w$  is relevant. Upon decreasing  $V$  the renormalized  $w^{\text{ren}} = w(V/u)^{K-1}$  grows until perturbation breaks down, i.e. when  $V \sim u(w/u)^{1/(1-K)}$ . The behaviour beyond this point is then described by the strong coupling perturbation theory described above. Accordingly, the formulae (4.66) and (4.67) are consistent with the renormalization group approach by Kane and Fisher [see Sec. 4.2.3].

### 4.3 Trapped Luttinger liquids

In this pedagogical chapter I will focus on trapped bosonic Luttinger liquids. This part of the thesis is meant as a pedagogical bridge to Sec. 4.6 where I present new theoretical results that have been obtained for a particular experimental configuration of an impurity immersed in a trapped ultracold 1D gas. Thus, let me briefly discuss the experimental techniques which allow for the creation of such ultracold vapors of bosonic atoms. Trapped atoms are typically confined in 3D geometries in real experiments. However, by tuning the external potential to render it very anisotropic it is possible to obtain quasi-1D condensates [169, 170, 171, 172]. Another possibility is to use 2D arrays of effective 1D optical tubes [173, 146] or atom chips [174], a technique which I will not discuss at all here.

The most important trapping technique of atoms is the so-called ‘‘optical trapping’’. Ultracold atoms are trapped in a configuration of standing light waves which can be generated by using interference of external laser sources. More precisely, if we assume that the atom is equivalent to a two-level system (the Alkali atoms such as  $^{87}\text{Rb}$  come closest to this simplified view) a *red-detuned* laser (i.e. one whose frequency is slightly below the characteristic transition frequency of the atom in question) creates an attractive force whereas *blue-detuned* laser (the opposite of red-detuned laser) acts as a repulsive force. Indeed, within the simplest model, the Heisenberg energy uncertainty relation allows the atom to absorb photons with a frequency slightly detuned. Since the subsequent emission process is isotropic, the momentum and the kinetic energy of the atom are changed on average. If the laser is red-detuned, the atoms thus accumulate in regions of high light intensity while they are attracted to regions of low light intensity if the laser is blue-detuned. One simple application of this trapping method are 2D arrays

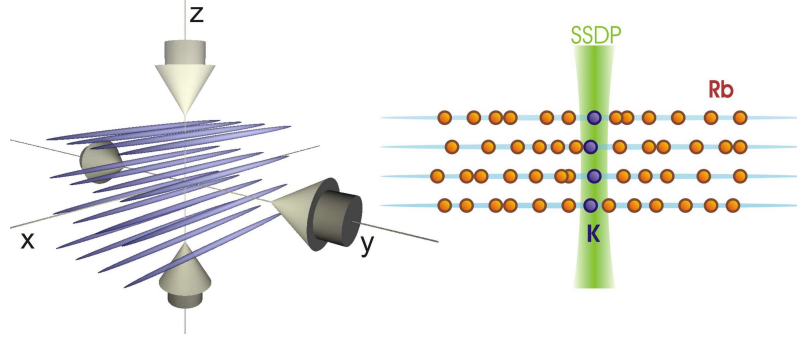


Figure 4.3: Sketch of a 2D array of 1D optical tubes. Taken from [146], which reports on the experiment that I will analyze in more detail in the following.

of standing waves. They are such that the atoms are confined to the “trenches” thus creating a system of many effective 1D systems which are separated by a “transverse” potential wall. The various 1D tubes itself are subject to a residual “longitudinal” potential which is much weaker. The system remains effectively one-dimensional as long as the thermal energy of the atoms is small compared to the transverse potential strength. We show a sketch of a typical experimental situation in Fig. 4.3. Let us now turn to the theoretical description of such trapped 1D liquids. Hereafter, Sec. 4.6 will deal with impurity dynamics in such a trapped Luttinger liquid.

### 4.3.1 Ground state of a trapped Lieb-Liniger gas: Thomas-Fermi approximation and Tonks-Girardeau regime

A longitudinal trapping potential breaks the translation invariance of the quantum gas. As we have seen already in Sec. 4.1.4, all parameters of a translationally invariant Lieb-Liniger liquids depend only on the Lieb-Liniger parameter  $\gamma$ , the presence of the external potential thus fundamentally changes the properties of the quantum gas. Moreover, it is obvious on intuitive grounds that the trap leads to an inhomogeneous density profile of the 1D gas, thus leading in principle to a breakdown of Luttinger theory itself. Fortunately, it is possible to develop a static and even a dynamic theory which makes use of the same hydrodynamic-like collective excitations as observed in a standard Luttinger liquid. As one can easily imagine, in view of developing a theory of such collective excitations it is necessary to first gain an insight into the groundstate properties of a trapped Lieb-Liniger gas, or more precisely its zero-temperature density profile. As we have seen in Sec. 4.1.4 the physics of the untrapped Lieb-Liniger gas are determined by  $\gamma = mw_L/\hbar\rho_0$ . In the presence of a harmonic external potential (I only consider harmonic potentials throughout this chapter) another dimensionless quantity can be formed,

$$\alpha_{\text{ho}} = \frac{mw_L\ell_{\text{ho}}}{\hbar}, \quad (4.68)$$

where  $\ell_{\text{ho}} = \sqrt{\hbar/m\Omega}$  is the typical quantum oscillator length scale. The parameter  $\alpha_{\text{ho}}$  can be regarded as the ratio between  $\ell_{\text{ho}}$  and the typical interaction length  $\ell_{\text{int}} = \hbar^2/mg$  and it fully characterizes the strength of the external potential. Indeed,  $\alpha_{\text{ho}} \gg 1$  corresponds to a weak external potential whereas  $\alpha_{\text{ho}} \ll 1$  corresponds to the regime where the potential determines the particle motion rather than the interaction.

In the regime of weak interactions, i.e.  $\gamma \ll 1$ , we can regard the 1D liquid as a quasi-BEC for which the Gross-Pitaevskii equation holds. For a weakly interacting Bose system

Gross [175] and Pitaevskii [176] found an evolution equation for the dynamical condensate wave function by using a mean-field like approach. It takes in general the form of a non-linear Schrödinger equation. By applying this equation [see also Eq. (4.76)] to our problem one derives the static density profile [158]

$$\rho_0(x) = \frac{\mu}{g} \left[ 1 - \frac{x^2}{r_{\text{TF}}^2} \right]. \quad (4.69)$$

I have introduced the Thomas-Fermi radius  $R_{\text{TF}} = \sqrt{2\mu/(m\Omega^2)}$ . The chemical potential  $\mu$  can be found by requiring that  $\int_{-r_{\text{TF}}}^{r_{\text{TF}}} dx \rho_0(x) = N$ , with  $N$  the number of particles, from which we find

$$\mu = \mu_{\text{TF}} = \hbar\Omega \left( \frac{3N\alpha_{\text{ho}}}{\sqrt{32}} \right)^{2/3}. \quad (4.70)$$

This is the so-called Thomas-Fermi approximation which is valid as long as  $\gamma \ll 1$ . In the inhomogeneous case  $\rho_0$  is the mean density defined by  $\rho_0 \simeq N/r_{\text{TF}}$ . By using this identity one has  $\gamma = \alpha_{\text{ho}} r_{\text{TF}}/N\ell_{\text{ho}}$  which gives in conjunction with Eq. (4.70) and the definition of  $r_{\text{TF}}$ :

$$\gamma \sim (\alpha_{\text{ho}}^2/N)^{2/3}. \quad (4.71)$$

Hence, the Thomas-Fermi regime is attained if  $(\alpha_{\text{ho}}^2/N)^{2/3} \ll 1$ , i.e. either if  $\alpha_{\text{ho}} \ll 1$  for any  $N$  or if  $N \gg \alpha_{\text{ho}}^2$ . It is intuitive clear that the weak coupling regime requires large number of particles as reflected by the last equation.

Let us now focus on the opposite limit  $\alpha_{\text{ho}} \gg 1$  and  $N \ll \alpha_{\text{ho}}^2$ . This case corresponds to the Tonks-Girardeau regime of impenetrable bosons. By virtue of the exact mapping between these bosons and free fermions [160] the Hamiltonian of the full system reads

$$\mathcal{H}_{TG} = \sum_n E_n c_n^\dagger c_n, \quad (4.72)$$

where  $E_n = \hbar\Omega n + 1/2$  are the energy levels of the harmonic oscillator. At zero temperature all energy levels are occupied up to the Fermi energy  $E_F = \hbar\Omega N + 1/2$  and the ground state is a factorizing state of eigenstate of the harmonic oscillator. It is not difficult to find the final density distribution:

$$\rho_0 = \frac{m\Omega r_{\text{TF}}}{\pi\hbar} \left[ 1 - \frac{x^2}{r_{\text{TF}}^2} \right]^{1/2}, \quad (4.73)$$

and the chemical potential  $\mu_{\text{TG}} = N\hbar\Omega$ .

Finally, the non-interacting regime is attained when  $\mu \ll \hbar\Omega$ . In this case interactions are so weak that the trapped gas forms a true BEC condensate. At zero temperature the density profile is thus equal to the one of the harmonic oscillator, i.e. a Gaussian  $\rho_0 \sim e^{-x^2/\ell_{\text{ho}}^2}$ .

Both Eqs. (4.69) and (4.73) can be found within a more general approach by using an energy functional. Let us assume that the ground state energy of a given density profile  $\rho_0$  can be written as an integral  $E[\rho_0] = \int dx e[\rho_0(x)]$  where  $e[\rho_0]$  is the energy density of a uniform interacting Bose gas with density  $\rho_0$ . The above approach thus makes sense if the density does not vary too much and it is therefore sometimes called the *local density approximation*. We now add the external potential  $V_e(x)$  and a Lagrange multiplier  $\lambda$  so that the total energy reads

$$E_{\text{tot}}[\rho_0] = \int dx e[\rho_0(x)] + (V_e(x) - \lambda)\rho_0(x). \quad (4.74)$$

By fixing the particle number one has to determine  $\lambda$  self-consistently. The difficulty lies in the fact that the energy density  $e[\rho_0]$  is in general unknown. However, in the weakly interacting limit we have  $e[\rho_0] = g\rho_0^2/2$  which follows directly from mean-field arguments. In the opposite Tonks-Girardeau limit the relevant energy scale is the Fermi energy. In order to find the energy density we consider a small interval around  $x$  where the density is quasi constant. Consider only the fermions left from our interval: They already occupy some states. The supplementary Fermi energy due to the additional small interval scales as the squared of the number particles, i.e.  $\rho_0(x)^2$ , and the total energy of the gas up to  $x$  thus scales as  $\rho(x)_0^3$ . Accordingly, we have  $E[\rho_0] \sim \int dx \rho_0^3(x)$  for the Tonks-Girardeau gas.

By varying  $E_{\text{tot}}$  with respect to  $\rho_0(x)$  and by using  $V_e(x) = \kappa x^2$  one can now find an equation for the local density  $\rho_0(x)$ . In the weak-interacting limit and in the Tonks-Girardeau regime Eq. (4.69) and Eq. (4.73) are then recovered once the Lagrange multiplier is eliminated. The space dependent chemical potential is found by assuming that the density  $\rho_0(x)$  varies so slowly that the gas in a small finite interval around  $x$  can be assumed to be in equilibrium. The whole liquid can then be divided into segments, each of which is in quasi-equilibrium. Standard thermodynamics yields in this case the very useful relation

$$\mu(\rho_0) = \left( \frac{\partial e[\rho_0]}{\partial \rho_0} \right)_{\rho_0 = \rho_0(x)}, \quad (4.75)$$

valid within the local density approximation. If an analytic expression of  $\mu$  as a function of  $\rho_0$  is given, equation (4.75) allows one to find  $\rho(x)$  by combining it with the solution of Eq. (4.74).

### 4.3.2 Hydrodynamic excitations in a trapped Luttinger liquid

Let us now discuss the properties of trapped 1D gases at finite temperatures. As in a standard Luttinger liquid, the excitations are collective and a systematic ‘‘hydrodynamic’’ theory can be developed in the Thomas-Fermi regime for these excitations. I closely follow the pedagogical line of [169, 177, 158] in this section. Let me first focus on the non-interacting case. As demonstrated in the experiment by Ketterle [178] a sharp crossover from a classical gas to a BEC takes place when the temperature is lowered.

It is generally believed that this sharp crossover stems from the discrete nature of the energy spectrum. A direct consequence of this observation is the fact that interactions will destroy such a sharp crossover by smearing out the energy spectrum. Indeed, in the presence of low momentum collective fluctuations the spectrum becomes quasi continuous. Therefore, we can formulate a heuristic criterion for the presence of the sharp crossover which is characteristic for the classical-BEC transition. The interaction energy per particle has to be much smaller than the level spacing  $\hbar\Omega$  (we assume as before that the gas is trapped in a harmonic potential). At low temperatures the gas is in its ground state such that the average interaction per particle reads  $\hbar w_L N(m\Omega/\hbar)^{1/2}$ . By using Eq. (4.68) the criterion for a sharp crossover translates into  $\alpha_{\text{ho}} \ll 1/N$ . If this condition is not met the Thomas-Fermi regime dominates. The crossover is not sharp anymore and collective excitations dominate the low energy spectrum. How would one proceed in 2D or 3D to find the excitations of a weakly interacting quantum gas?

Let us begin with the Gross-Pitaevskii equation [175, 176] for a weakly interacting Bose gas with interaction potential  $V(x - x') = \hbar w_L \delta(x - x')$ , chemical potential  $\mu$ , atomic mass  $m$  and wave function  $\Psi(\vec{x}, t)$ :

$$i\hbar\partial_t\Psi(\vec{x}, t) = \left[ -\frac{\hbar^2}{2m} - \mu + \int dx' V(x - x') |\Psi(\vec{x}, t)|^2 \right] \Psi(\vec{x}, t). \quad (4.76)$$

Let us now set  $\Psi(\vec{x}, t) = \sqrt{\rho(\vec{x}, t)}e^{i\theta(\vec{x}, t)}$ , then we find from Eq. (4.76) the two equations [179]

$$\partial_t \rho + \frac{\hbar}{m} \nabla \cdot (\rho \nabla \theta) = 0, \quad (4.77)$$

$$\partial_t \theta + \left[ \frac{\hbar}{2m} (\nabla \theta)^2 + w_L \rho - \frac{\hbar}{2m} \frac{\nabla^2 \sqrt{\rho}}{\sqrt{\rho}} \right] = 0. \quad (4.78)$$

The first equation is nothing else than the continuity equation, while the second equation describes the evolution of the phase field  $\theta$ . Furthermore, these equations are valid for *superfluids* of arbitrary dimensions and internal interactions (their range of validity extends beyond the realm of the Gross-Pitaevskii regime). If one assumes a slowly varying density profile the above equations simplify to the standard (classical) Euler equations for the flow of a *non-viscous fluid*. In other words, the hydrodynamics approach described by the Eqs. (4.77) and (4.78) governs (beyond other systems) the dynamics of a 1D gas in the Thomas-Fermi regime [158]. However, if one leaves this weakly interacting regime it is not *a priori* clear how to adapt the hydrodynamic approach.

One can circumvent this difficulty by directly using the phenomenological bosonization approach in Sec. 4.1.1, with the only difference that the background density  $\rho_0(x)$  is not constant. The Hamiltonian then reads

$$\int dx \left[ \frac{\hbar^2 \rho_0(x)}{2m} (\nabla \hat{\theta})^2 + \frac{\hbar^2 (\nabla \delta \hat{\rho})^2}{8m \rho_0(x)} + \frac{\hbar w_L}{2} (\delta \hat{\rho})^2 \right] + \dots, \quad (4.79)$$

with  $\delta \rho = \hat{\rho} - \rho_0$  the density fluctuation. The ellipsis stands for higher order fluctuation terms. I also used the same symmetry arguments as before to show that no term linear in  $\delta \hat{\rho}$  can arise. I now give a short review of the arguments developed in [169] which allow to analyze the different regimes Eq. (4.79) gives rise to. First of all, at high temperatures we can treat the fluctuations of  $\delta \hat{\rho}$  and  $\hat{\theta}$  as classical variables. Since Eq. (4.79) is quadratic, we can compute the correlation functions  $\langle (\rho(x) - \rho(x'))^2 \rangle$  and  $\langle (\theta(x) - \theta(x'))^2 \rangle$  if we make the simplification  $\rho_0(x) = \rho_0 = \text{const}$  in Eq. (4.79). The result for the density correlations at temperature  $\beta^{-1}$  reads:

$$\langle (\rho(x) - \rho(x'))^2 \rangle = \beta^{-1} \sqrt{\frac{8m\rho_0}{\hbar^3 w_L}} \left[ 1 - e^{-\sqrt{8m g \rho_0} |x-x'|/\hbar} \right]. \quad (4.80)$$

By using the relation (4.70) for the chemical potential, Eq. (4.68) and the typical length scale  $R_{\text{TF}} = \sqrt{2\mu/(m\Omega^2)}$ , valid for the trapped Bose gas in the Thomas-Fermi regime, we find

$$\langle (\rho(x) - \rho(x'))^2 \rangle / \rho_0^2 \sim \beta^{-1} \frac{1}{\hbar \Omega N}. \quad (4.81)$$

Hence, the relative density fluctuation is negligible provided

$$\beta^{-1} < \beta_d^{-1} = \hbar \Omega N. \quad (4.82)$$

Below the crossover temperature  $\beta_d^{-1}$  the Bose gas behaves as a weakly interacting gas with the density profile (4.69). Above  $\beta_d^{-1}$  the gas is essentially classical. By a similar calculation for the phase [169] one arrives at a second crossover temperature  $\beta_{ph}^{-1} = \hbar \Omega \beta_d^{-1} / \mu$  below which both phase and density fluctuations are negligible; the gas then forms a true BEC, and above which only phase fluctuations are present. The gas is then called a *quasi-condensate*. The phase diagram is given in Fig 4.4. Having identified the different regimes of the trapped Bose gas let us

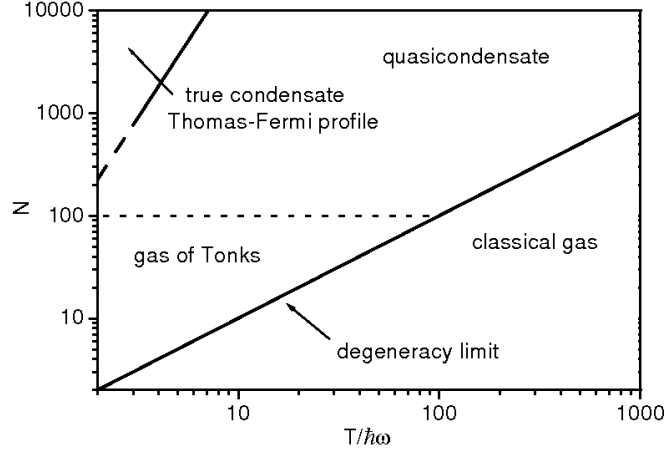


Figure 4.4: Different regimes of a 1D Bose gas [169, 158]. Above the degeneracy temperature  $\beta_d^{-1}$  the gas essentially behaves classical whereas it forms a true BEC below  $\beta_{ph}^{-1}$ . In between the number of particles discriminates between the weak-interacting (Thomas-Fermi) regime and the strong interacting (Tonks-Girardeau) regime.

now discuss the collective interactions. One way to describe these fluctuations is to generalize the standard Tomonaga-Luttinger Hamiltonian to a non-uniform background density. Evidence that such a generalization can be performed has been found by, e.g., Citro et al. [180, 181, 182]. The inhomogeneous Tomonaga-Luttinger Hamiltonian is given by

$$\hat{\mathcal{H}}_{L,inh} = \frac{\hbar}{2\pi} \int_{-R}^R dx \left[ \frac{u(x)K(x)}{\hbar^2} (\nabla \hat{\theta})^2 + \frac{u(x)}{K(x)} (\nabla \hat{\phi})^2 \right], \quad (4.83)$$

and it describes well the excitation spectrum of an inhomogeneous Luttinger liquid as long as the local density approximation holds. Note that Eq. (4.83) is the direct generalization of Eq. (4.25) for inhomogeneous background densities. The unperturbed density profile  $\rho_0(x)$  is an external information which is complementary to the Hamiltonian (4.25) which describes the thermal excitations. It can be derived from the methods presented in the previous subsection. The Luttinger parameters can be expressed in terms of the background density  $\rho_0(x)$  and the chemical potential  $\mu(x)$  which are assumed to be known. One has

$$u(x)K(x) = \frac{\hbar\pi\rho_0(x)}{m} \quad (4.84)$$

and

$$\frac{u(x)}{K(x)} = \frac{\partial_{\rho_0}\mu[\rho_0(x)]}{\pi}, \quad (4.85)$$

which resembles a lot the relation (4.36) for a translationally invariant system although this symmetry is broken here [180].

Let us pursue our analysis by focusing on the equations of motion which derive from the path integral built upon Eq. (4.83). We find that

$$\hbar^2 \dot{\phi}(x, t) = u(x)K(x)\theta(x, t), \quad (4.86)$$

$$\dot{\theta}(x, t) = \hbar^2 \nabla \left[ \frac{u(x)}{K(x)} \nabla \phi(x, t) \right]. \quad (4.87)$$

If we introduce the density fluctuation operator  $\delta\hat{\rho} = -\nabla\hat{\phi}/\pi$  and the “velocity” operator  $v = \hbar\nabla\hat{\theta}/m$  we see that Eqs. (4.86) and (4.87) are equivalent to the linearized version of the hydrodynamic equations (4.77) and (4.78) [see [158, 179]]. Combining these two equations and using the boundary condition

$$\phi(R, t) = \phi_1 \quad \text{and} \quad \phi(-R, t) = \phi_0, \quad (4.88)$$

we arrive at a single equation for  $\phi$ :

$$\ddot{\phi}(x, t) = u(x)K(x)\nabla\left[\frac{u(x)}{K(x)}\nabla\phi(x, t)\right]. \quad (4.89)$$

The Fourier decomposition of Eq. (4.89) leads to

$$-\omega_n^2\phi_n = u(x)K(x)\nabla\left[\frac{u(x)}{K(x)}\nabla\phi(x, t)\right], \quad (4.90)$$

where the boundary conditions translate into  $\phi_n(\pm R) = 0$ , and where the orthogonality relation

$$\int dx \frac{\phi_n(x)\phi_{n'}(x)}{u(x)K(x)} = \delta_{n,n'} \quad (4.91)$$

holds. Citro et al. [182] found the expansion of the field operators in terms of bosonic creation and annihilation operators  $b_n^\dagger, b_n$ :

$$\hat{\phi}(x) = \phi_0 - \pi \frac{\int_{-R}^x dx' K(x')/u(x')}{\int_{-R}^R dx' K(x')/u(x')} \hat{N} + \sum_n \frac{\pi}{2\omega_n} [\hat{b}_n^\dagger + \hat{b}_n] \hat{\phi}_n(x), \quad (4.92)$$

$$\hat{\Pi}(x) \equiv \nabla\hat{\theta}(x)/\pi\hbar^2 = \sum_n \sqrt{\omega_n} 2\pi \frac{\phi_n(x)}{iu(x)K(x)} [\hat{b}_n^\dagger - \hat{b}_n]. \quad (4.93)$$

$\hat{N}$  is the operators of the number of particles. The fields  $\hat{\Pi}(x)$  and  $\hat{\phi}(x)$  satisfy the canonical commutation relation. The Hamiltonian (4.83) can be rewritten in terms of the  $\hat{b}_n^\dagger, \hat{b}_n$  as

$$\hat{\mathcal{H}}_{L,\text{inh}} = \frac{\pi N^2}{2 \int_{-R}^R dx' K(x')/u(x')} + \sum_n \omega_n \hat{b}_n^\dagger \hat{b}_n. \quad (4.94)$$

The solution of the eigenvalue problem (4.90) gives access to the eigenmodes of the trapped Luttinger liquid. Let us assume the gas is trapped in a harmonic potential with frequency  $\Omega$  – as is the standard situation in this manuscript. By using Eq. (4.85) in conjunction with Eq. (4.90) we find

$$\rho_0(x)\nabla\left[\partial_{\rho_0}\mu(x)\nabla\hat{\phi}_n(x)\right] = -\omega_n^2\hat{\phi}_n(x) \quad (4.95)$$

One solution is given by  $\hat{\phi}(x) = A\rho_0(x)$  with some proportionality constant  $A$ . Indeed, in this case  $\partial_{\rho_0}\mu(x)\nabla\hat{\phi}(x) = A d\mu(x)/dx = -Am\Omega^2 x$  by definition. Thus, the differential equation is satisfied for  $\omega = \Omega$ . This solution describes the center-of-mass oscillations of the gas cloud in the harmonic trap (the so-called “Kohn mode”) [182].

An exact solution for the eigenvalue equation (4.95) is found by making the assumption that  $u(x) = u_0\sqrt{1-x^2/R^2}$  and  $K(x) = K_0\sqrt{1-x^2/R^2}$  for  $\alpha > -1/2$ . Such profiles are obtained for instance in the case  $\mu(\rho_0) \sim \rho_0^\gamma$  with  $\alpha = 1/\gamma - 1/2$ . From Eq. (4.84) it immediately follows that the Thomas-Fermi gas is described by  $\alpha = 1/2$  and the Tonks gas by

$\alpha = 0$ . For general  $\alpha$  the eigenmodes are obtained in terms of ultraspherical polynomials while the eigenfrequencies have the form

$$\omega_n^2 = \frac{u_0^2}{R^2} (n+1)(n+2\alpha+1). \quad (4.96)$$

In the Tonks limit the eigenfunctions can be expressed in terms of the simpler Chebychev polynomials while in the opposite Thomas-Fermi limit they can be written in terms of Legendre polynomials. Their explicit form – which I will not give here – can be found in [182].

## 4.4 A Luttinger liquid as a quantum bath

The evolution of impurities in a Luttinger liquid (LL) has attracted much attention in recent years [147, 183, 151, 184] since this problem can be explicitly realized with cold atom systems. In particular, modern techniques allow one to tune the interspecies interaction strength [185, 186, 187] so that it has become possible to study the diffusion of a minority species within an ensemble of majority atoms, as a function of the interaction and the trapping potential [146].

In this part of our work we apply the non equilibrium formalism developed in the chapter 3 to such an impurity–LL system. In particular, we seek to mimic the experimental process described in [146] with our theoretical description. In this experiment the impurity atom is trapped in a 1D harmonic potential together with an ensemble of a different kind of atoms that form the LL. The impurity is initially localized at the center of the confining potential by a laser blade. When the whole impurity–LL system reaches equilibrium the impurity is released. The equal-times position correlation function of the impurity,  $\mathcal{C}(t, t)$ , then shows damped oscillations which strongly suggest that the impurity is *de facto* a quantum Brownian particle moving in a quantum liquid bath.

In the following we will present a precise description of the impurity motion in the LL from the quantum Brownian motion point of view. The LL itself will play the role of an exotic quantum bath that we here characterize. While this quantum Brownian motion approach has limited success it serves as an excellent starting point for the more sophisticated analysis presented in Sec. 4.6.

### 4.4.1 The impurity model

The impurity and the atoms constituting the bath are all confined in a harmonic potential. We therefore take the Hamiltonian of the impurity,  $\hat{\mathcal{H}}_S$ , to be of the standard form Eq. (3.32) without external force ( $H = 0$ ) and with the harmonic potential  $V(\hat{q}) = \frac{M\Omega^2}{2}\hat{q}^2$ . We assume that the interaction Hamiltonian between the position operator  $\hat{q}$  of the impurity and the density of the boson liquid is of the form

$$\hat{\mathcal{H}}_{SB} = \int dx dy U(x-y) \hat{\rho}(y) \delta(x-\hat{q}), \quad (4.97)$$

with the density operator  $\hat{\rho}(x)$  of the LL approximately described by

$$\hat{\rho}(x) \simeq \rho_0(x) - \frac{1}{\pi} \nabla \hat{\phi}(x), \quad (4.98)$$

where  $\rho_0(x)$  is the unperturbed density of the fluid in the 1D trap and  $\hat{\phi}(x)$  is the density variation. The Hamiltonian of the free LL reads

$$\hat{\mathcal{H}}_B = \frac{\hbar}{2\pi} \int dx \left[ \frac{uK}{\hbar^2} (\pi\hat{\Pi}(x))^2 + \frac{u}{K} (\nabla\hat{\phi}(x))^2 \right], \quad (4.99)$$

where  $\hat{\Pi}(x)$  and  $\hat{\phi}(x)$  are conjugate operator fields. Equation (4.99) describes the low-energy properties of a Lieb-Liniger gas [188] with a contact interaction potential  $\hbar w_L \delta(x)$ . The parameters  $u$  (with the dimension of a velocity) and  $K$  (dimensionless) have to be determined numerically for general  $w_L$ . In order to reduce the complexity of the problem we will assume the background density  $\rho_0$  to be constant in the following. Accordingly, we define

$$\rho_0 \equiv \frac{1}{L} \int dx \rho_0(x), \quad (4.100)$$

where  $L$  is a length scale of the order of the length of the trap. Note that in this modeling we have not added the quadratic confining potential to the LL.

Since the Bose gas is confined in a space of length  $L$ , the wave vectors are quantized with values  $k_n = \pi n/L$  with  $n$  an integer. The Fourier representation of Eq. (4.97) is

$$\hat{\mathcal{H}}_{SB} = \frac{1}{\sqrt{L}} \sum_n \tilde{U}_{k_n} e^{ik_n \hat{q}} \left[ -\frac{ik_n}{\pi} \tilde{\phi}(k_n) \right], \quad (4.101)$$

where we used  $\delta(x-x') = (1/L) \sum_n e^{ik_n(x-x')}$  and we neglected a constant contribution. We assume that the potential  $U$  has the form

$$\tilde{U}_k = \hbar v e^{-|k|/k_c}, \quad (4.102)$$

with some finite cutoff  $k_c$  that depends on the microscopic properties of the interaction. The parameter  $v$  has the dimension of a velocity and it determines the strength of the impurity–bath interaction potential.

After redefining the fields according to

$$\hat{\phi}(x) \mapsto \sqrt{(\pi K/\hbar)} \hat{\phi}(x) \quad (4.103)$$

and

$$\hat{\Pi}(x) \mapsto \sqrt{(\hbar/\pi K)} \hat{\Pi}(x), \quad (4.104)$$

one introduces the bosonic ladder operators

$$\hat{b}_k = \sqrt{\frac{|k|}{2\hbar}} \left( \tilde{\phi}(k) + \frac{i}{|k|} \tilde{\Pi}(k) \right) \quad (4.105)$$

and

$$\hat{b}_{-k}^\dagger = \sqrt{\frac{|k|}{2\hbar}} \left( \tilde{\phi}(k) - \frac{i}{|k|} \tilde{\Pi}(k) \right), \quad (4.106)$$

which describe bosonic density wave excitations with sound velocity  $u$  [10]. The full Hamiltonian now takes the form of the Fröhlich polaron Hamiltonian, which in the second quantization language reads

$$\begin{aligned} \hat{\mathcal{H}} = & \sum_{k \in \{k_n\}} \hbar u |k| \hat{b}_k^\dagger \hat{b}_k + \frac{\hat{p}^2}{2M} + \frac{M\Omega^2}{2} \hat{q}^2 \\ & - \frac{1}{\sqrt{L}} \sum_k \left( \frac{K}{2\pi|k|} \right)^{1/2} \tilde{U}_k \left[ (ik e^{ik\hat{q}}) \hat{b}_k^\dagger + (ik e^{ik\hat{q}})^* \hat{b}_k \right]. \end{aligned} \quad (4.107)$$

For each  $k$  mode the coupling between the operator  $e^{ik\hat{q}}$  and the bath operators  $\hat{b}_k^\dagger$  and  $\hat{b}_k$  is bilinear, so we can use the general results derived in Sec. 3.3.2 by considering that  $e^{ik\hat{q}}$  represents a different operator for each  $k$  that is coupled to one harmonic oscillator. The resulting influence functional is hence a sum of one-particle–one-oscillator influence functionals. By using Eq. (3.130) we thus find

$$\begin{aligned} \Phi[q^+, q^-, q^0] = & - \sum_k \left\{ \int_0^{\beta\hbar} d\tau \int_0^\tau d\sigma K_k(-i\tau + i\sigma) e^{ikq^0(\tau)} e^{-ikq(\sigma)} \right. \\ & + i \int_0^{\beta\hbar} d\tau \int_0^t ds K_{-k}^*(s - i\tau) e^{ikq^0(\tau)} \left[ e^{-ikq^+(s)} - e^{-ikq^-(s)} \right] \\ & \left. - \int_0^t ds \int_0^s du \left[ e^{ikq^+(s)} - e^{ikq^-(s)} \right] \left[ K_{-k}(s - u) e^{-ikq^+(u)} - K_{-k}^*(s - u) e^{-ikq^-(u)} \right] \right\}. \end{aligned} \quad (4.108)$$

Note that, since in the initial Hamiltonian there is no counter-term the counter-terms in Eq. (3.130) are absent in Eq. (4.108). The  $k$ -dependent kernel reads

$$K_k(\theta) = \frac{1}{L} \frac{K|k|}{2\pi\hbar} |\tilde{U}_k|^2 \frac{\cosh[u|k|\beta\hbar/2 - i\theta u|k|]}{\sinh[u|k|\beta\hbar/2]}. \quad (4.109)$$

A well known feature of the Fröhlich polaron Hamiltonian (4.107) is its polaronic mass shift which leads to an effective impurity mass  $M^* > M$  greater than the “bare mass” [50]. Another process described by this Hamiltonian is that during a collision between the impurity and an LL atom the former loses momentum  $\hbar k$  by creating a density wave excitation  $b_k^\dagger$  in the LL. However, the LL is itself confined in a harmonic potential and one may expect to have some momentum transfer absorbed (or provided) from the LL to the optical trap. We will in this section simply assume that the spring constant of the optical potential is renormalized by such a process in such a way that it balances the polaronic mass shift and we will henceforth work with the bare Hamiltonian (4.107) before turning to the more sophisticated analysis presented in Sec. 4.6.

If the oscillations are small (if the impurity potential is sufficiently steep) we can expand the  $e^{ik\hat{q}}$  in Eq. (4.108) to second order in  $k$ . Note that the linear order vanishes in Eq. (4.108)

due to the symmetry  $k \mapsto -k$ . Ignoring the zero-th order in  $k$  we can make the replacements

$$\begin{aligned}
 e^{ikq^0(\tau)}e^{-ikq^0(\sigma)} &\mapsto -\frac{k^2}{2} [q^0(\tau) - q^0(\sigma)]^2, \\
 e^{ikq^0(\tau)} [e^{-ikq^+(s)} - e^{-ikq^-(s)}] &\mapsto k^2 q^0(\tau) [q^+(s) - q^-(s)] - \frac{k^2}{2} [q^+(s)^2 - q^-(s)^2], \\
 [e^{ikq^+(s)} - e^{ikq^-(s)}] \times [K_{-k}(s-u)e^{-ikq^+(u)} - K_{-k}^*(s-u)e^{-ikq^-(u)}] \\
 &\mapsto k^2 [q^+(s) - q^-(s)] [K_k(s-u)q^+(u) - K_k^*(s-u)q^-(u)] \\
 -\frac{k^2}{2} [q^+(s)^2 - q^-(s)^2] (K_k(s-u) - K_k^*(s-u)). & \tag{4.110}
 \end{aligned}$$

#### 4.4.2 Steep potential: The Luttinger bath and the initial condition

If the external potential is steep we expect the Gaussian approximation of the Fröhlich Hamiltonian (4.110) to be valid. Up to this order in  $k$  each  $k$ -mode plays the role of one bath harmonic oscillator. Accordingly, for  $L \rightarrow \infty$  we define the spectral density as

$$\begin{aligned}
 S(\omega) &= \frac{\pi}{L} \sum_{k \in \{k_n\}} \frac{K|k|^3}{2\pi\hbar} |\tilde{U}_k|^2 \delta(\omega - u|k|) \\
 &\simeq \frac{K\omega^3 \hbar v^2}{\pi u^4} e^{-\omega/\omega_c} = \frac{\pi\mu}{4} \left(\frac{\omega}{\omega_c}\right)^3 e^{-\omega/\omega_c}, \tag{4.111}
 \end{aligned}$$

with  $\omega_c = u|k_c|/2$  and

$$\mu = \frac{4\hbar K \omega^2 \omega_c^3}{\pi^2 u^4}. \tag{4.112}$$

Hence, the bath induces *super-Ohmic* dissipation with a power law behavior  $S(\omega) \sim \omega^3$  for small  $\omega$ . This is the main difference from the analysis presented in Sec. 3.3.

In terms of the fundamental kernel [c.f. Eq. (3.131)]

$$K(\theta) = \int_0^\infty \frac{d\omega}{\pi} S(\omega) \frac{\cosh[\omega(\beta\hbar/2 - i\theta)]}{\sinh[\omega\beta\hbar/2]} \tag{4.113}$$

and with  $\int_0^{\beta\hbar} d\tau K^*(s - i\tau) = M\gamma(s)$  and  $\int_0^s du [K(s-u) - K^*(s-u)] = -iM\gamma(0) + iM\gamma(s)$ , where  $\gamma(s)$  is defined in Eq. (3.145), we obtain

$$\begin{aligned}
 \Phi[q^+, q^-, q^0] &= \frac{1}{4} \int_0^{\beta\hbar} d\tau d\sigma K(-i\tau + i\sigma) [q^0(\tau) - q^0(\sigma)]^2 \\
 &\quad - i \int_0^{\beta\hbar} d\tau \int_0^t ds K^*(s - i\tau) q^0(\tau) [q^+(s) - q^-(s)] \\
 &\quad + \int_0^t ds \int_0^s du [q^+(s) - q^-(s)] [K(s-u)q^+(u) - K^*(s-u)q^-(u)] \\
 &\quad + \frac{iM\gamma(0)}{2} \int_0^t ds [q^+(s)^2 - q^-(s)^2]. \tag{4.114}
 \end{aligned}$$

The first line in Eq. (4.114) shows that only the non-local part of  $K(-i\tau + i\sigma)$  contributes. Hence we can replace the first line by  $\frac{1}{2} \int_0^{\beta\hbar} d\tau d\sigma k(-i\tau + i\sigma) q^0(\tau) q^0(\sigma)$ . Furthermore, we

see that the last line in Eq. (4.114) exactly represents the counter-term proportional to  $\mu$ . By rewriting Eq. (4.114) in terms of the kernels  $K_R$  and  $\gamma$  [see Eqs. (3.136) and (3.145)] and using the transformed variables  $x = (q^+ + q^-)/2$  and  $\bar{x} = q^+ - q^-$  the action becomes

$$\begin{aligned}
 \Sigma[x, \bar{x}, q^0, x_i, x_f, \bar{x}_i] &= i \int_0^{\beta\hbar} d\tau \left[ \frac{M}{2} \dot{q}^0(\tau)^2 + \frac{M\Omega^2}{2} q^0(\tau)^2 + \frac{1}{2} \int_0^{\beta\hbar} d\sigma k(\tau - \sigma) q^0(\tau) q^0(\sigma) \right] \\
 &+ \int_0^{\beta\hbar} d\tau \int_0^t ds K^*(s - i\tau) q^0(\tau) \bar{x}(s) \\
 &+ \int_0^t ds \left[ M \dot{\bar{x}}(s) \dot{x}(s) - M\Omega^2 \bar{x}(s) x(s) - M \bar{x}(s) \frac{d}{ds} \int_0^s du \gamma(s - u) x(u) \right] \\
 &+ \frac{i}{2} \int_0^t ds \int_0^t du K_R(s - u) \bar{x}(s) x(u) + \frac{i\hbar}{2\Delta^2} \left[ x_i^2 + \frac{\bar{x}_i^2}{4} \right]. \tag{4.115}
 \end{aligned}$$

We remind the reader of the main approximations used so far. First, we used the Gaussian approximation (4.110) of the Fröhlich Hamiltonian. Second, in order for the action (4.115) to make sense we assumed  $\Omega$  to be large enough, so that non Gaussian effects are not too important. Note, that the mass and the potential renormalization can modify the oscillation amplitude and the final width of the impurity position. Finally, we interpreted the laser blade that initially localizes the impurity at the center of the quantum liquid as an initial position measurement with outcome  $q_m = 0$  and uncertainty  $\Delta$ . The effect of the initial position measurement is incorporated into the action via the last term of the rhs of Eq. (4.115). If the localization is performed itself by a very steep trapping potential with frequency  $\Omega_0$  the particle is in its harmonic oscillator (with respect to  $\Omega_0$ ) ground state at initial time. We then have

$$\epsilon^{-2} = 2\Omega_0. \tag{4.116}$$

This approximation is disputable since one could also consider the initial localization of the impurity as stemming from an initial trapping potential. The subsequent release of the impurity would then rather be described by a quench in the harmonic potential [see Sec. 3.4.2]. However, in real experiments the “high temperature” regime  $\hbar\beta\Omega \ll 1$  prevails. From the discussion in Secs. 3.4.1 and 3.4.2 we know that in this case the difference between the particle motion after an initial position measurement and the one after an initial localization due to an initial trapping potential (followed by a quench in the potential) is blurred. Since it is technically easier to deal with a position measurement we prefer this method to a quench in the trapping potential. Note that the “high temperature” regime is not equivalent to the classical regime, as we pointed out in Sec. 3.4.1 as it does not fulfill the “macroscopic measurement” condition  $\Delta \gg \lambda_T$  with  $\lambda_T$  the thermal de Broglie–wavelength of the impurity. For more details go back to the discussion in Sec. 3.4.1.

### 4.4.3 Signature of a Luttinger liquid bath

A typical experimental scenario consists in holding the impurity in the center of the trap at  $t < 0$  and switching off the localizing potential at  $t = 0$  to let the impurity move in the residual harmonic potential. Let us for a moment forget about the potential renormalization and the mass shift. By using the results found in Sec. 3.4.1 we find in the limit  $\epsilon \rightarrow 0$  (which corresponds to

an almost perfect localization of the impurity at  $t = 0$ )

$$\begin{aligned} \tilde{\mathcal{C}}(\lambda, \kappa) &\simeq \frac{\hbar}{4M\epsilon^2} \tilde{\mathcal{G}}_+(\lambda) \tilde{\mathcal{G}}_+(\kappa) - \frac{M}{\hbar\Lambda} \tilde{\mathcal{C}}^{\text{1eq}}(\lambda) \tilde{\mathcal{C}}^{\text{1eq}}(\kappa) \\ &\quad + \frac{1}{\lambda + \kappa} \left[ \tilde{\mathcal{C}}^{\text{1eq}}(\lambda) + \tilde{\mathcal{C}}^{\text{1eq}}(\kappa) \right]. \end{aligned} \quad (4.117)$$

In the time domain the correlation function reads

$$\begin{aligned} \mathcal{C}(t, t') &\simeq \frac{\hbar}{4M\epsilon^2} \mathcal{G}_+(t) \mathcal{G}_+(t') - \frac{M}{\hbar\Lambda} \mathcal{C}^{\text{1eq}}(t) \mathcal{C}^{\text{1eq}}(t') \\ &\quad + \mathcal{C}^{\text{1eq}}(|t - t'|). \end{aligned} \quad (4.118)$$

For the moment, experimental measurements focus on the equal-time correlation (which corresponds to the time-dependent variance of the position)

$$\mathcal{C}(t, t) \simeq \frac{\hbar}{4M\epsilon^2} \mathcal{G}_+^2(t) - \frac{M}{\hbar\Lambda} \mathcal{C}^{\text{1eq}}(t)^2 + \mathcal{C}^{\text{1eq}}(0). \quad (4.119)$$

The formula Eq. (4.119) is valid for all kinds of baths and for very small polaronic effects and potential renormalization.

In order to gain further insight into the dynamics of the impurity we need to understand the contribution of each of the three terms in Eq. (4.119).

We start from the analysis of the propagator  $\mathcal{G}_+(t)$ . To determine its time-dependence we need the specific form of the spectral density of the LL bath (4.111). In terms of the function

$$\begin{aligned} g(z) &= \frac{1}{2} \int_0^\infty d\zeta \zeta^2 e^{-\zeta} \frac{z^2}{\zeta^2 + z^2} \\ &= \frac{z^2}{2} - \frac{z^4}{2} \int_0^\infty d\zeta \frac{e^{-\zeta}}{\zeta^2 + z^2} \end{aligned} \quad (4.120)$$

the Laplace transform of the damping kernel  $\tilde{\gamma}(\lambda)$  [see Eqs. (3.145)] can be recast as

$$\lambda \tilde{\gamma}(\lambda) = \frac{\mu}{M} g(\lambda/\omega_c) \quad (4.121)$$

and the propagator (which is proportional to the linear response function) reads

$$\tilde{\mathcal{G}}_+(\lambda) = \frac{1}{\lambda^2 + \frac{\mu}{M} g(\lambda/\omega_c) + \Omega^2}. \quad (4.122)$$

Our objective is to find the oscillation frequency and the damping of the impurity motion in the small coupling limit. Thus, we need the inverse Laplace transform of Eq. (4.122) which can be expressed in terms of the Bromwich integral,

$$\mathcal{G}_+(t) = \frac{1}{2\pi i} \int_{c-i\infty}^{c+i\infty} d\lambda e^{\lambda t} \tilde{\mathcal{G}}_+(\lambda), \quad (4.123)$$

where the real number  $c$  is greater than the real part of all poles of  $\tilde{\mathcal{G}}_+(\lambda)$ . The integral in Eq. (4.123) can be solved by displacing the complex contour towards the left and by evaluating the encountered residues. Hence, we seek for the complex points at which the denominator of Eq. (4.122) vanishes, that is  $z^2 + \mu' g(z) + \Omega^2/\omega_c^2 = 0$  with

$$z = i\sigma - \Gamma, \quad \text{where } \frac{\Gamma}{\sigma} \ll 1 \quad \text{and} \quad \mu' = \frac{\mu}{M\omega_c^2}. \quad (4.124)$$

Note that  $z$ ,  $\sigma$ ,  $\Gamma$  and  $\mu'$  are dimensionless and  $\sigma$  and  $\Gamma$  real. From Eq. (4.123) it is clear that  $\Gamma$  corresponds to the exponential damping (measured in units of  $\omega_c$ ) of the propagator and hence  $\Gamma$  has to be positive (whereas  $\sigma$  is the oscillating frequency measured in units of  $\omega_c$  and can be positive or negative). Thus, the first singularities encountered when displacing the contour towards the left are the imaginary axis for which  $g(z)$  is obviously singular when  $\text{Re } z = 0$ . In other words, we have to account for the difference  $g(i\sigma + 0^+) - g(i\sigma - 0^+)$  when displacing the integration contour past the imaginary axis. We will come back to this point in just a few lines. The integral in the second term of the rhs of Eq. (4.120) can be recast as

$$\begin{aligned} I(-\Gamma, \sigma) &\equiv \int_0^\infty d\zeta \frac{e^{-\zeta}}{\zeta^2 + z^2} \\ &\simeq \frac{1}{|\sigma|} \int_0^\infty d\zeta \frac{e^{-|\sigma|\zeta}}{\zeta^2 - 1 - 2i\Gamma/\sigma} \\ &\simeq \frac{1}{|\sigma|} \left[ A(|\sigma|) + \text{sign} \left[ \frac{\Gamma}{\sigma} \right] \frac{i\pi}{2} e^{-|\sigma|} \right] \\ &\quad + \frac{|\Gamma|}{\sigma^2} \left[ \frac{\pi}{2} (1 + |\sigma|) e^{-|\sigma|} + i \text{sign} \left[ \frac{\Gamma}{\sigma} \right] B(|\sigma|) \right], \end{aligned}$$

where we expanded the denominator of the integrand to first order in  $\Gamma/\sigma$  and we defined

$$\begin{aligned} A(\sigma) &= \sinh \sigma \text{Chi } \sigma - \cosh \sigma \text{Shi } \sigma, \\ B(\sigma) &= \sigma [\cosh \sigma \text{Chi } \sigma - \sinh \sigma \text{Shi } \sigma] \\ &\quad + \cosh \sigma \text{Shi } \sigma - \sinh \sigma \text{Chi } \sigma, \end{aligned}$$

where Shi and Chi are the hyperbolic sine and cosine integrals, respectively. The contribution from the crossing of the imaginary axis is now easily obtained:  $\Delta I \equiv I(0^+, \sigma) - I(-0^+, \sigma) = -i\pi e^{-|\sigma|}/\sigma$ . After adding  $-z^4 \Delta I/2$  to  $g(z)$  we thus obtain for  $\text{Re } z < 0$

$$\begin{aligned} g(z) &\simeq -\frac{\sigma^2}{2} + \frac{i\pi\sigma^3}{4} e^{-|\sigma|} - \frac{\sigma^3}{2} A(\sigma) \\ &\quad - \frac{\pi\Gamma\sigma^2}{4} (1 + |\sigma|) e^{-|\sigma|} - \pi\Gamma\sigma^2 e^{-|\sigma|}, \end{aligned} \quad (4.125)$$

where we neglected all real terms of  $\mathcal{O}((\Gamma/\sigma)^2)$  and all imaginary terms of  $\mathcal{O}(\Gamma/\sigma)$ .

At the poles, the real and the imaginary part of the denominator  $z^2 + \mu'g(z) + (\Omega/\omega_c)^2$  vanish simultaneously. By using the form of  $g(z)$  just derived we see that this can be achieved with the choices

$$\Gamma = \frac{\pi\mu'}{8} \sigma^2 e^{-|\sigma|}, \quad (4.126)$$

$$\frac{\Omega^2}{\omega_c^2} = \sigma^2 + \frac{\mu'}{2} [\sigma^3 A(\sigma) + \sigma^2] + 2\Gamma^2(5 + |\sigma|). \quad (4.127)$$

Note the symmetry  $\sigma \mapsto -\sigma$  in Eq. (4.127). Equations (4.126) and (4.127) determine the oscillating behavior of  $\mathcal{G}_+(t)$ :  $\Gamma$  corresponds to the damping and  $\sigma$  to the frequency of the oscillation (both quantities measured in units of  $\omega_c$ ). We assumed the damping  $\Gamma$  to be small compared to  $\sigma$  which by virtue of Eq. (4.126) translates into

$$\mu' \ll \frac{4}{\pi\sigma} e^\sigma \geq \frac{4e}{\pi} \approx 3.461. \quad (4.128)$$

The behavior of the oscillating frequency  $\sigma$  (measured in units of  $\omega_c$ ) strongly depends on the trapping frequency  $\Omega/\omega_c$ . Figure 4.5 shows the dependence of  $|\sigma|$  on  $\mu' = \mu/(M\omega_c^2)$  and on  $\Gamma$  for the case  $\Omega/\omega_c = 3.0$ . When  $\hbar\beta\Omega \ll 1$  (as in [146]) the properties of the oscillations of  $\mathcal{G}_+(t)$  coincide with the ones for  $\mathcal{C}^{1\text{eq}}(t)$  [see App. 3.5.2]. Then, by observing Eq. (4.119) one deduces that the actual oscillation frequency of  $\mathcal{C}(t, t)$  and its damping are rather  $2\sigma$  and  $2\Gamma$ , respectively. As can be seen for moderate to high trapping frequencies there is an *increase* of the oscillator frequency followed by a decrease induced by the bath [see Fig. 4.5]. Such a behavior is not observed for small frequencies (compared to  $\omega_c$ ). The experimental results in [146] confirm such a “peak” although very few data-points are shown in this paper and the error bars are quite large so it is hard to draw firm conclusions on the actual experimental behavior at this stage. The “peak” in the curve of the oscillation frequency can be used in further experiments to determine whether the bath is actually described by a LL or not since it is a direct consequence of the non-Ohmic spectral density (4.111). In Fig. 4.6 we show the

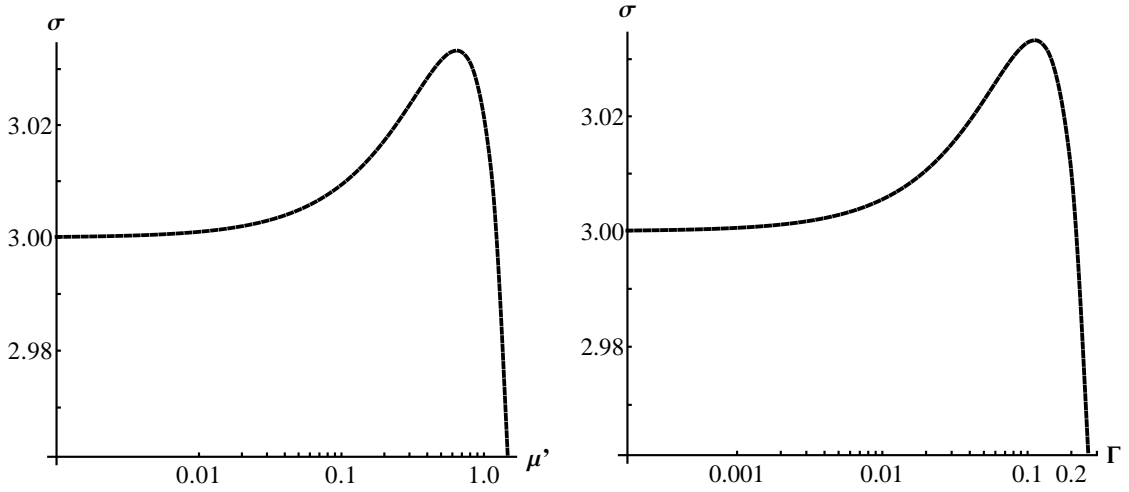


Figure 4.5: Dependence of the oscillator frequency  $\sigma$  on the impurity-bath coupling  $\mu' = \mu/(M\omega_c^2)$  (left image) and on the damping  $\Gamma$  [see Eq. (4.126)] (right image) for  $\Omega/\omega_c = 3.0$  obtained from Eq. (4.127). A logarithmic scale has been used.

correlator Eq. (4.119) for values of the impurity–bath coupling ( $\mu' = 0.5$  and  $\mu' = 0.2$ ) in the “high temperature” regime  $\beta\hbar\Omega \ll 1$  typical for experiments. The parameters were chosen to be  $1/(4\epsilon^2\omega_c) = 10$  in both images for the thick lines,  $\Omega/\omega_c = 1.0$  in the upper and  $\Omega/\omega_c = 3.0$  in the lower image. The thin line in the upper image has been obtained with  $1/(4\epsilon^2\omega_c) = 50$ . The curves qualitatively agree with the experimental data [146]. One clearly recognizes the *increase of the oscillation frequency* induced by an increase in the coupling  $\mu'$  for  $\Omega/\omega_c = 3.0$ . See however Sec. 4.6 for more details and a critical comparison of this effect with the ones induced by the frequency renormalization due to the non-homogeneity of the Luttinger liquid and the polaronic mass shift. The typical oscillation width in experiments is about  $15\mu\text{m}$  with a frequency of  $\sigma \simeq 550\text{s}^{-1}$ . The final position width of a (high temperature) quantum Brownian particle is given by  $1/(\beta M\Omega^2)$  [8]. With the mass  $M$  of the  $^{41}\text{K}$  atoms used as an impurity and the bath temperature  $T \approx 350\text{nK}$  in [146] this yields  $\sqrt{C(t, t)} \approx 15\mu\text{m}$  which is even quantitatively the right value. Hence, quantum Brownian motion captures many main features of the impurity dynamics observed in [146]. The limits of the present approach will be discussed in the conclusion and Sec. 4.6.

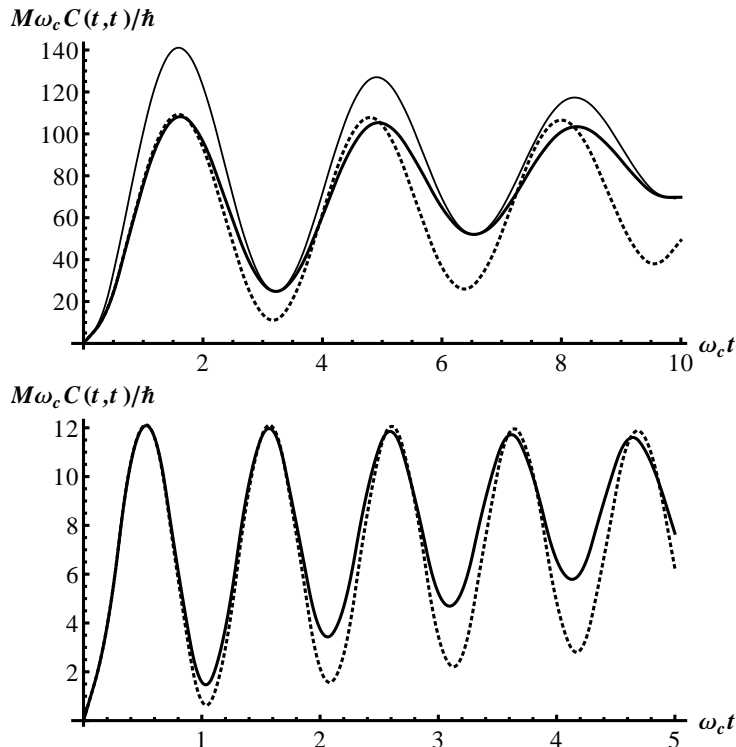


Figure 4.6: Theoretical results for the variance of the impurity position  $C(t, t)$  after its quantum Brownian motion induced by a LL bath in the “high temperature”-regime which is experimentally available. We chose  $1/(4\epsilon^2\omega_c) = 10$  for the thick lines in both images, and  $\Omega/\omega_c = 1.0$  in the upper and  $\Omega/\omega_c = 3.0$  in the lower image. The impurity-quantum liquid couplings are  $\mu' = 0.5$  (thick straight lines) and  $\mu' = 0.2$  (thick dotted lines), respectively. In the upper image the thin line has been obtained with  $1/(4\epsilon^2\omega_c) = 50$  and  $\mu' = 0.5$ .

## 4.5 Some notions about polaron theory

At this point it becomes important to provide the reader with some background information on *polarons*. The polaron concept will be used in Sec. 4.6 which presents the main novel results of the present chapter.

In lattices where the characteristic phonon frequencies are sufficiently low, an electron which passes by the atomic ions deforms the background lattice in such a way that an effective potential for the electron is created. Holstein, Fröhlich and Lieb [189, 190, 191] studied these phenomenon, by approximating the background lattice by a continuous polarizable medium. In this case one calls the moving charge carrier a large polaron. If the motion is sufficiently slow, the reaction of the polaron on the medium can follow the polaron as an ionization cloud, thus creating a free quasiparticle with an enhanced mass.

When the polaron binding energy exceeds the half-bandwidth of the electron band in the system, all states are “dressed” by phonons. This is the so-called strong-coupling regime where the finite bandwidth becomes important so that the continuum limit can not be applied. In this case the polarons are called *small polarons* and they have been studied in, e.g. [192, 193], to cite just a few.

In the next subsection we will discuss the case where the medium is not polarizable by

an electric charge carrier, but rather deformable by a mobile localized moving density, i.e., an impurity. This physical difference, however, does not need any specific approach and the impurity-Luttinger liquid system can be considered as a polaron-lattice system with a modified interaction potential. Since we are interested in continuum systems the large polaron, or weak-coupling, regime is relevant for us.

The so-called Fröhlich polaron model is defined by the Hamiltonian

$$\hat{\mathcal{H}} = \frac{\hat{p}^2}{2M} + \sum_{\vec{q}} U_{\vec{q}} e^{i\vec{q}\cdot\vec{r}} \left[ \hat{b}_{\vec{q}}^\dagger + \hat{b}_{-\vec{q}} \right] + \sum_{\vec{q}} \hbar\omega_p \hat{b}_{\vec{q}}^\dagger \hat{b}_{\vec{q}}, \quad (4.129)$$

where  $\hat{p}$  and  $M$  are the momentum operator and the mass of the polaron, and  $\hat{b}_{\vec{q}}^\dagger, \hat{b}_{\vec{q}}$  phonon creation and annihilation operators. The Fourier transformed potential  $U_{\vec{q}}$  is given by

$$U_{\vec{q}} = i\sqrt{\frac{4\pi\alpha}{V}} \left( \frac{\hbar}{2M\omega_p} \right)^{1/4} \frac{\hbar\omega_p}{|\vec{q}|}, \quad (4.130)$$

where  $\omega_p$  is the longitudinal optical phonon frequency,  $V$  the volume of the crystal and  $\alpha$  the so-called Fröhlich coupling constant:

$$\alpha = \frac{e^2}{\hbar c} \left( \frac{mc^2}{2\hbar\omega_p} \right)^{1/2} \left[ \frac{1}{E_\infty} - \frac{1}{E_0} \right]. \quad (4.131)$$

Here,  $e$  is the charge of the electron and  $E_0$  and  $E_\infty$  are the static and high-frequency dielectric constants. Since these coupling constants are model dependent I will not use them anymore. It is only important to note that  $V_{\vec{q}} \sim 1/|\vec{q}|$ .

We are interested in the groundstate of Eq. (4.129). If the interaction between the polaron and the phonons can be neglected the system is in the unperturbed groundstate

$$|\vec{k}, 0\rangle = e^{i\vec{k}\cdot\vec{r}} |0\rangle, \quad (4.132)$$

where  $e^{i\vec{k}\cdot\vec{r}}$  is the polaron plane wave and  $|0\rangle$  the phonon vacuum. We can now apply perturbation theory by assuming that the coupling is weak. By using standard Schrödinger perturbation theory the first order energy correction is given by the diagonal elements of the interaction term,

$$\sum_{\vec{q}} U_{\vec{q}} e^{i\vec{q}\cdot\vec{r}} \left[ \hat{b}_{\vec{q}}^\dagger + \hat{b}_{-\vec{q}} \right], \quad (4.133)$$

which vanish identically, obviously. The interaction (4.133) conserves the total momentum at each scattering event. Hence, the second order perturbation leads to

$$\delta E_{\vec{k}} = - \sum_{\vec{q}} \frac{|V_{\vec{q}}|^2}{(\vec{k} - \vec{q})^2/2M + \omega_p - \vec{k}^2/2M}. \quad (4.134)$$

By transforming the momentum sum into an integral one finds the result:

$$E_{\vec{k}} \equiv \frac{\vec{k}^2}{2M} + \delta E_{\vec{k}} = \frac{\vec{k}^2}{2M} - \frac{\alpha(2M\omega_p^3)^{1/2}}{|\vec{k}|} \arcsin \left[ |\vec{k}|/\sqrt{2M\omega_p} \right], \quad (4.135)$$

which in the limit of a slow polaron motion simplifies to

$$E_{\vec{k}} = \frac{\vec{k}^2}{2M^*} - \alpha\omega_p. \quad (4.136)$$

The second term of the rhs of the above equation is a constant  $\vec{k}$ -independent energy shift which does not contribute to the dispersion relation of the polaron. However, in the first term I defined

$$M^* = \frac{M}{1 - \alpha/6} > M, \quad (4.137)$$

which we call henceforth the *effective mass* of the polaron. Thus, we found that the mass of the polaron is enhanced by the photon cloud which leads to a dressed polaron.

This lowest order perturbation method can be largely improved. Feynman had 1955 the idea to transform the polaron Hamiltonian (4.129) into an action in which the photon degrees of freedom are integrated out [190]. One then finds an influence functional very similar to the ones already encountered in this thesis. The effective polaron action is given by

$$\mathcal{S} = \int_0^{\hbar\beta} d\tau \frac{\dot{x}^2(\tau)}{2} - \frac{\alpha}{2^{3/2}} \int_0^{\hbar\beta} d\tau \int_0^{\hbar\beta} d\sigma \frac{e^{-|\tau-\sigma|}}{|x(\tau) - x(\sigma)|}, \quad (4.138)$$

where I restrict this analysis to a one-dimensional problem so that the polaron coordinate  $x$  is a scalar. The action (4.138) has a very appealing form. Indeed, the interaction term describes a particle which interacts with itself *via a retarded* Coulomb interaction. The retardation is mediated by the  $e^{-|\tau-\sigma|}$ -term in the numerator. Eq. (4.138) is non Gaussian and therefore not integrable. However, in [190] Feynman replaced the Coulomb-potential by a squared potential and performed a variational calculus by minimizing the non specified coupling constant. More precisely, let us do the replacement

$$\frac{\alpha}{2^{3/2}} \frac{e^{-|\tau-\sigma|}}{|x(\tau) - x(\sigma)|} \mapsto C e^{-w|\tau-\sigma|} (x(\tau) - x(\sigma))^2. \quad (4.139)$$

$C$  and  $w$  are constants which have to be determined by minimizing the ground state energy  $E$  by the well-known upper bound variational calculus which leads to

$$E = E_0 - \lim_{\beta \rightarrow \infty} \frac{1}{\beta} \langle \mathcal{S} - \mathcal{S}_0 \rangle_0, \quad (4.140)$$

with  $E_0$  the free energy and  $\mathcal{S}_0$  the trial action (i.e. the one with  $C$  and  $w$ ). The average is taken with respect to  $\mathcal{S}_0$ . It can be shown that the weak coupling expansion of Eq. (4.140) leads after a short calculation to

$$M^*/M \simeq 1 + \frac{\alpha}{6} + 0.025\alpha^2 + \dots. \quad (4.141)$$

Eq. (4.141) generalizes Eq. (4.137) beyond the first order in  $\alpha$ . In [146] the authors presented results for the effective mass of an impurity in a 1D liquid by using a similar Feynman variational ansatz as described above, albeit with a density-density coupling rather than a Coulomb potential. Note that such an impurity is coupled *via* a similar polaronic-like interaction to the surrounding liquid, although the potential is different in the impurity case [see Sec. 4.6].

Apart from the effective mass the mobility and the effective polaron radius have also attracted interest [149]. I will not go into detail, here, nor will I discuss more sophisticated methods to tackle the polaron problem such as the diagrammatic Monte Carlo algorithm [194].

Devreese et al. [195] introduced another approach to find Eq. (4.137) [beyond other results]. They used the Hamiltonian (4.129) directly to write the Heisenberg equations of motion. By imposing a constant velocity of the polaron the equations become solvable and one finds again the first-order result Eq. (4.129). This approach neglects the back-reaction of the phonons on themselves *via* the particle interaction. It is hence equivalent to a linear response theory where such back-reactions are commonly neglected. Since the approach I present in Sec. 4.6 is also based on equations of motion I will not present the approach by Devreese et al. which is very similar to the one in Sec. 4.6.

## 4.6 An impurity in a trapped 1D gas: Dynamical linear response theory

*“Make things as simple as possible, but not simpler.”*

Albert Einstein

In this section I present results which were obtained [23] during my PhD on the motion of impurities in trapped 1D Bose liquids. Diffusion in such low dimensional quantum liquids has been a major field of research in the last decade [165, 196, 197, 198, 166, 167, 199, 164, 200, 10, 146]. In one-dimensional (1D) liquids of interacting bosons a moving impurity is subject to a drag force [199] and dissipates energy for all velocities even at zero temperature [200] as we have also seen in Sec. 4.2.1. The experimental design of artificial 1D impurity–quantum liquid systems has now become possible by confining cold atoms in optical nanotubes. Using these techniques, the diffusion of impurity atoms in contact with a Luttinger liquid (LL) with tunable impurity-LL interaction has been recently studied [146] by making use of a Feshbach resonance which allows for controlling the interaction strength [185]. The experimental scenario is thus the following:

Both the Luttinger liquid and the impurity are confined in an effective 1D optical tube with the *same* residual longitudinal potential. This longitudinal potential will be assumed to be harmonic. For times  $t < 0$  the impurity is localized in the center of the nanotube. At  $t = 0$  it is released and it starts its mostly stochastic diffusion motion in the Luttinger liquid. By measuring several quantities such as the mean position width of the impurity one can characterize these dynamics. Note that due to the external trapping potential the minority atoms undergo damped oscillations which directly confirm that dissipation takes place in this system.

In Ref. [183] the authors attempted to describe the impurity dynamics within the Gross-Pitaevskii approach at zero temperature. Such a Gross-Pitaevskii approach has also been employed in [201] where the authors found a strange “atome blockade” which leads to a self-trapping of the *a priori* untrapped impurities in the non-homogeneous Luttinger liquid. Peotta et al. [151, 184] recently studied the trapped impurity-Luttinger liquid system with a dynamical numerical renormalization group method (albeit their trapping potential is not harmonic). In the original paper [22] [see Sec. 4.4] we followed an alternative way by applying quantum Brownian motion theory to the impurity problem. In this section I will pursue an alternative approach by considering the impurity atom as a quantum Brownian particle. The quantum liquid then plays the role of an exotic quantum bath and it can be dealt with using Luttinger theory [see Sec. 4.4]. Also, as already pointed out in [146, 22, 183] the impurity atom acquires an effective mass due to its interaction with the LL which can be related to the well-known polaron

paradigm where a charge carrier acquires an effective mass (which exceeds his bare mass) when passing past a charged lattice [see [191, 192, 193, 202] and Sec. 4.5]. I will not go into details since this polaronic mass shift is not the main focus of this study. I will only make use of the linear response approach using the equations of motions of the impurity which had also been successfully applied by [195].

In the conclusion chapter 5 I will compare the different results obtained in these papers with the results I shall present in the following.

Quite obviously, the external trapping potential leads to an inhomogeneous density profile of the LL with non-trivial effects on the impurity motion. In this section I combine several independent ideas that will allow us to: (a) estimate the mass shift of the impurity, (b) evaluate the effect of the non-homogeneous density profile of the LL as well as, to a first approximation, the renormalization of the confining potential, (c) use the non-equilibrium formalism of quantum Brownian motion developed in [22] to reproduce the data in [146] *quantitatively*.

I repeat here the free Hamiltonian of an impurity with mass  $M_I$ , in an optical trap modeled by a harmonic potential with spring constant  $\kappa$ , which reads

$$\hat{\mathcal{H}}_I = \frac{\hat{p}^2}{2M_I} + \frac{\kappa}{2}\hat{q}^2, \quad (4.142)$$

with  $\hat{p}$  and  $\hat{q}$  the momentum and position operators.

The impurity interacts with an LL which is confined by the same potential [146]. For the sake of simplicity we will incorporate the effects of the trap on the LL later. The low energy excitations of an unconfined 1D quantum liquid are described by the Tomonaga-Luttinger Hamiltonian

$$\begin{aligned} \hat{\mathcal{H}}_L &= \frac{\hbar}{2\pi} \int dx \left[ \frac{uK}{\hbar^2} (\pi\hat{\Pi}(x))^2 + \frac{u}{K} (\nabla\hat{\phi}(x))^2 \right] \\ &= \sum_{k \neq 0} \hbar u |k| \hat{b}_k^\dagger \hat{b}_k, \end{aligned} \quad (4.143)$$

with the two canonically conjugate bosonic fields  $\hat{\Pi}(x)$  and  $\hat{\phi}(x)$  [10, 158].  $\hat{\phi}$  is related to the LL particle density through  $\hat{\rho}(x) = \rho_0 - (1/\pi)\hat{\phi}'(x)$ . In the second quantization language the Hamiltonian can be equally expressed in terms of bosonic operators  $\hat{b}_k^\dagger$  and  $\hat{b}_k$  which we define below. The dimensionless coefficient  $K$  and the sound velocity  $u$  totally characterize the low energy properties of such a 1D system. For translationally invariant cases they only depend on the Lieb-Liniger parameter  $\gamma = M_L w_L / \hbar \rho_0$ , with  $M_L$  the mass of the bosons,  $\hbar w_L$  the strength of the interaction and  $\rho_0$  the density of the LL [158].

We model the impurity-LL interaction through

$$\hat{\mathcal{H}}_{IL} = \int dx dy U(x-y) \hat{\rho}(y) \delta(x-\hat{q}), \quad (4.144)$$

with  $U(x)$  the interaction potential,  $\hat{\rho}(x)$  the LL density and  $\hat{q}$  the impurity position operator. In Fourier space we define  $\hat{\phi}(x) = L^{-1/2} \sum_k e^{-ikx} \hat{\phi}_k$  with  $k = 2\pi n/L$  and  $n \in \mathbb{Z}$ . The full Hamiltonian is then  $\hat{\mathcal{H}} = \hat{\mathcal{H}}_L + \hat{\mathcal{H}}_{IL} + \hat{\mathcal{H}}_I$ , with  $\hat{\mathcal{H}}_I$  defined in Eq. (4.142) and

$$\hat{\mathcal{H}}_L = \frac{u}{2} \sum_k \left[ \hat{\Pi}_k \hat{\Pi}_{-k} + k^2 \hat{\phi}_k \hat{\phi}_{-k} \right], \quad (4.145)$$

$$\hat{\mathcal{H}}_{IL} = \sqrt{\frac{K}{\pi\hbar}} \sum_k ik U_k \hat{\phi}_k e^{-ik\hat{q}}. \quad (4.146)$$

Note that we rescaled the fields according to  $\hat{\phi}_k \mapsto \sqrt{(\pi K/\hbar)}\hat{\phi}_k$  and  $\hat{\Pi}_k \mapsto \sqrt{(\hbar/\pi K)}\hat{\Pi}_k$ . In terms of  $\hat{b}_k^\dagger, \hat{b}_k$  the (rescaled) field reads  $\hat{\phi}_k = \sqrt{\hbar/2|k|}(b_{-k}^\dagger + b_k)$ . We choose  $U_k = \hbar w/\sqrt{L} e^{-u|k|/2\omega_c}$  with some cutoff wave vector  $\omega_c/u$  depending on the microscopic properties of the coupling. Equation (4.146) considers only the so-called forward impurity-LL scattering. The backward scattering potential  $U_{\text{back}}$  is not relevant in our case since we consider light impurities [see Sec. 4.2.1 and [200, 166, 167]].

### 4.6.1 The experimental evidence

In [146] the impurities are initially localized at the center of the potential tubes with a laser blade that creates another harmonic potential well with spring constant  $\kappa_0 > \kappa$ . After their subsequent release they undergo stochastic dynamics that resemble the ones of a damped harmonic oscillator. Catani *et al.* measured the equal-time correlation function  $\mathcal{C}(t, t)$  and they drew the following conclusions:

(I) The oscillation frequency  $\Omega_I$  is virtually not affected by the value of the impurity-LL interaction  $\hbar w$ .

(II) Equations (4.142)-(4.146) resemble the well-known Fröhlich polaron Hamiltonian that should result in the impurity mass renormalization,  $M_I \mapsto M_I^*$ , as a function of the interaction  $\hbar w$ . Point (I) then indicates that in parallel to the mass renormalization the potential spring constant should be renormalized as well,  $\kappa \rightarrow \kappa^*$ , in such a way that  $\Omega_I^* \equiv \sqrt{\kappa^*/M_I^*}$  remained equal to  $\Omega_I$ .

(III) The initial kinetic energy of the impurity can be estimated from the high temperature equipartition theorem to be  $\sim 1/\beta$  (note that  $\hbar\beta\sqrt{\kappa_0/M_I} \approx 0.1$  in [146]) by assuming that the impurity has equilibrated with the LL before its release. The amplitude after one oscillation  $q_a$  should therefore scale as  $\sim 1/\sqrt{\kappa^*}$  when neglecting dissipation such that  $\kappa^* q_a^2 \sim 1/\beta$  due to energy conservation. Furthermore,  $\sqrt{\kappa/\kappa^*} \sim \sqrt{M_I/M_I^*}$  due to point (I). The increase of  $\kappa^* \sim M_I^*$  is clearly observed when  $\hbar w$  is ramped up (see Fig. 4.7). Note that for  $w/w_L \gtrsim 5$  the 1D regime is not ensured any longer which explains the ‘‘saturation’’ of  $\kappa^*$  for large values of  $w$  (not described by the effective 1D theory).

(IV) The final (equilibrium) width of the impurity cloud is independent of  $\hbar w$ .

We notice that (IV) is at odds with (II). From the theory of quantum Brownian motion we know that  $\lim_{t \rightarrow \infty} \mathcal{C}(t, t) \simeq 1/(\beta\kappa^*)$  for a harmonic potential with spring constant  $\kappa^*$  [8]; therefore, the dependence of  $\kappa^*$  on  $\hbar w$  should entail a dependence of the cloud width with the same parameter. Accordingly, a more thorough analysis of the coupled systems is needed to correctly interpret the experimental evidence. In the following I examine the points (I)-(IV) in detail and I propose a way out this *conundrum*.

### 4.6.2 The dynamical mass shift

It is well-known that a charged particle acquires an effective mass when it interacts with lattice vibrations through a Coulomb potential [191, 192, 193, 202]. Equations (4.145)-(4.146) describe such a polaron with the only difference that the interaction is not Coulomb-like. In the following we estimate the polaronic mass shift in our problem by using the equations of motion

(EOM) for  $\hat{\phi}_k(t)$  and  $\hat{q}(t)$  (see [195] for the use of EOM in this context):

$$\ddot{\hat{\phi}}_k(t) + u^2 k^2 \hat{\phi}_k(t) = iuk \sqrt{\frac{K}{\pi\hbar}} U_k^* e^{ik\hat{q}(t)}, \quad (4.147)$$

$$M_I \ddot{\hat{q}}(t) + \kappa \hat{q}(t) = -\sqrt{\frac{K}{\pi\hbar}} \sum_k k^2 U_k e^{-ik\hat{q}(t)} \hat{\phi}_k(t). \quad (4.148)$$

Suppose that the impurity is not accelerated during a small time interval, then we can make the Ansatz

$$\hat{q}(t) = \hat{q}(0) + \hat{v}t \quad (4.149)$$

with  $\hat{v} = \hat{p}(0)/M_I$  and  $[\hat{q}(t), \hat{\phi}_k(t)] \approx 0$ . The solution to Eq. (4.147) for small  $t$  reads

$$\hat{\phi}_k(t) = \hat{A}_k(t; \hat{v}) e^{ik\hat{v}t} + \hat{g}_k e^{iukt} + \hat{h}_k e^{-iukt}, \quad (4.150)$$

with the coefficients

$$\begin{aligned} \hat{A}_k(t; \hat{v}) &= iuk U_k^* \sqrt{\frac{K}{\pi\hbar}} \frac{e^{ik\hat{q}(0) + i\hbar k^2 t / 2M_I}}{u^2 k^2 - \hat{v}^2 k^2}, \quad (4.151) \\ \hat{g}_k &= \frac{1}{2} \left[ \hat{\phi}_k(0) + \frac{1}{iuk} \dot{\hat{\phi}}_k(0) - \hat{A}_k(0; \hat{v}) - \hat{A}_k(0; \hat{v}) \frac{\hat{v}}{u} \right], \\ \hat{h}_k &= \frac{1}{2} \left[ \hat{\phi}_k(0) - \frac{1}{iuk} \dot{\hat{\phi}}_k(0) - \hat{A}_k(0; \hat{v}) + \hat{A}_k(0; \hat{v}) \frac{\hat{v}}{u} \right]. \end{aligned}$$

The first term on the right-hand-side of Eq. (4.150) represents a density cloud that moves together with the impurity, while the two last terms describe the very wave excitation. For instance, in the limit  $\omega_c \rightarrow \infty$  we have for a mobile impurity with *constant* velocity

$$\hat{\rho}(x, t) \sim \sum_k ik \hat{A}_k(t; \hat{v}) e^{ik\hat{v}t - ikx} \sim \delta(x - \hat{q}(t)), \quad (4.152)$$

meaning that the LL density profile follows the impurity, thus creating a *dressed* local impurity. It is important to note that this simple picture has to be altered when the impurity is accelerated. We will come back to this point later.

The combined system of the impurity and the density cloud has an effective mass which exceeds the bare impurity mass. As an illustration, we consider the initial conditions  $\hat{\phi}_k(0) = \hat{A}_k(0; 0)$  and  $\dot{\hat{\phi}}_k(0) = 0$ . If the impurity is immobile [i.e.  $\hat{q}(t) = \hat{q}(0)$ ] these initial conditions lead to the static solution  $\hat{\phi}_k(t) = \hat{A}_k(0; 0)$  which describes a static density cloud without wave excitations. Suppose now that the impurity is instantaneously accelerated to some constant velocity  $\hat{v}$ , then we obtain from Eq. (4.150)  $\hat{\phi}_k = \hat{A}_k(t, \hat{v}) e^{ik\hat{v}t} - i\hat{A}_k(0; 0) \frac{\hat{v}}{u} \sin ukt$ . Hence, upon acceleration energy is carried away by a wave excitation, such that the kinetic energy of the impurity is less than the external energy provided. To be more specific, by using Eq. (4.145) the average energy of such a wave excitation is found to be  $E_k = \frac{uk^2}{2} (v/u)^2 A_k(0; 0) A_{-k}(0; 0)$  with  $v^2 = \langle \hat{v}^2 \rangle$ . We define the dynamical effective impurity mass through

$$M_I^* = (1 + \mu) M_I, \quad (4.153)$$

with the interaction-dependent correction  $\mu = 2\hbar\omega_c^2 K / (\pi^2 M_I u^4)$ . Then, by instantaneously providing an amount of energy  $E$ , the impurity acquires after acceleration a (mean) velocity

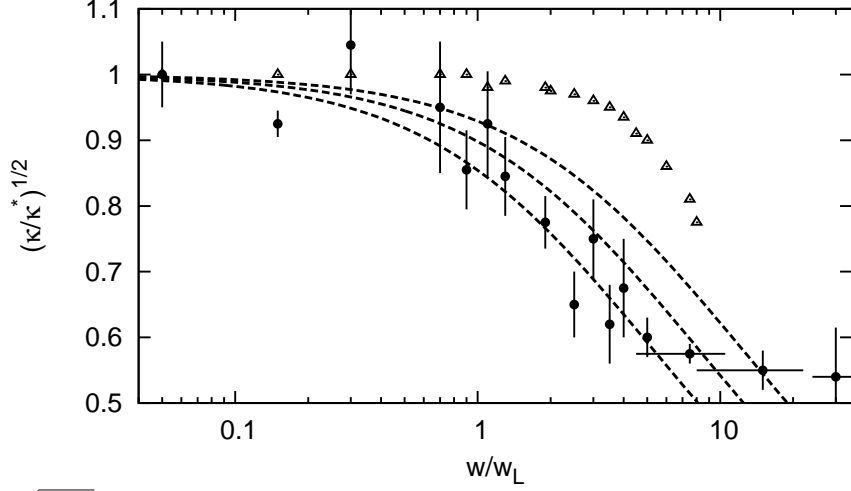


Figure 4.7:  $\sqrt{\kappa/\kappa^*}$  versus the impurity-LL coupling  $w/w_L$ . Lines obtained from Eq. (4.153) with (from left to right)  $\gamma = 0.25$ ,  $\gamma = 0.35$  and  $\gamma = 0.5$ . Experimental data points are taken from [146]. Triangular points: Result from Feynman's variational theory [146].

given by  $E = M_I^* v^2/2$ . It is straightforward to generalize this calculation to the case where the impurity has already a velocity  $\hat{v}_0$  before the acceleration: One simply replaces  $\mu$  by

$$\mu(v_0) = \frac{\mu}{(1 - v_0^2/u^2)^2}, \quad (4.154)$$

where we used the classical mean value  $v_0^2$  instead of  $\hat{v}_0^2$ . In the following we consider  $M_I^*$  as the true impurity mass. Note, that our definition of the dynamical effective mass differs from the effective mass usually defined via the impurity self-energy diagram.

### 4.6.3 The potential renormalization

Ref. [146] indicates that the spring constant of the optical trap is renormalized as well. We will show here that the effect of the external potential on the LL indeed leads to a renormalization of the potential felt by the impurity. In the same spirit as in the previous paragraph we study the effects of the external potential, which we previously neglected, *via* its action on the density cloud. The force exerted by the external harmonic potential on the density cloud is given by

$$\hat{F} = - \int_{-L/2}^{L/2} dx \kappa x \hat{\rho}(x) = \kappa \hat{q} \frac{uK}{\pi \hbar (u^2 - \hat{v}^2)} \sqrt{LU_0^*}, \quad (4.155)$$

where we used Eq. (4.150) to express  $\hat{\rho}(t)$ . By considering the combined impurity and the density cloud system as one entity,  $\hat{F}$  acts in the end on the impurity itself. Interestingly enough,  $\hat{F}$  changes sign when  $\hat{v}$  exceeds the sound speed  $u$  such that the subsonic and supersonic regimes are quantitatively different. In [146] the impurity moves with supersonic speed ( $\sqrt{\langle \hat{v}^2 \rangle} \approx 8.5 \text{ mm/s}$  while  $u \approx 3 \text{ mm/s}$  typically) so that  $\hat{F}$  leads to an *increase* of the effective external potential. In the following we approximate  $\hat{v}^2$  by its mean value  $v^2 \equiv \langle \hat{v}^2 \rangle$ .

The idea behind this approximation is the following: If we take the mean of Eq. (4.155) with respect to the impurity wavefunction (written in the momentum domain) divergences appear as soon as  $v$  approaches  $u$ . But in this case the formula (4.155) is certainly wrong. Indeed, one has to bear the meaning of the approximation so far made in the mind. By imposing a constant

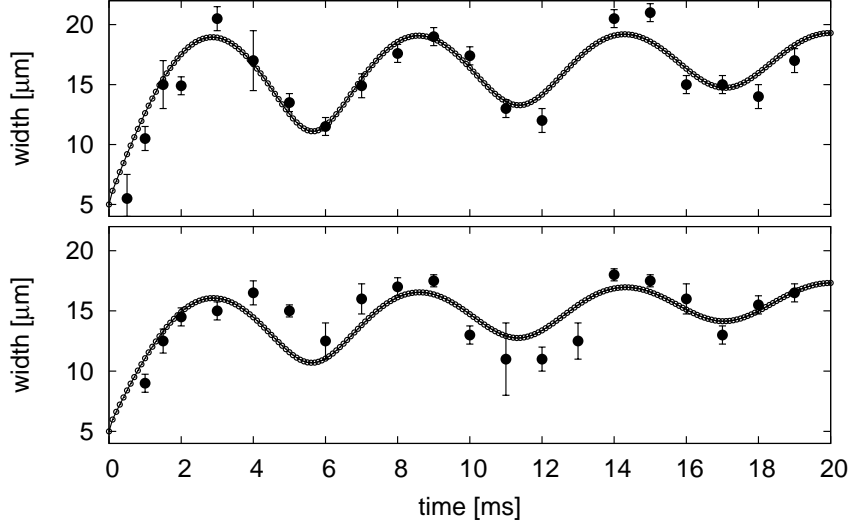


Figure 4.8:  $\sqrt{C(t,t)}$  for  $\Omega_I/\omega_c = 2.5$ ,  $\gamma = 0.45$  and  $w/w_L = 1(4)$  in the upper (lower) image. Points: Experimental data from [146]. Lines: Solution to Eq. (4.164) with  $\Omega_I^* = \Omega_I$ .

impurity velocity one actually assumes that the acceleration of the impurity is small within the time interval one considers. However, in Sec. 4.2.2 we have learned that the dissipation of an accelerated impurity diverges when the impurity velocity approaches the sound velocity. Therefore, even the tiniest deviation from the linear relation (4.149) produces a huge dissipation in the vicinity of the sound speed and the time interval within which the ansatz (4.149) remains valid shrinks to zero.

Accordingly, it is difficult to take the average of  $\hat{F}$  with respect to a wavefunction if this wavefunction allows for arbitrary momenta. In order to stay in the range of validity of Eq. (4.155) it is therefore necessary to directly average  $\hat{v}^2$  and to require that  $\hat{v}^2$  not too close to  $u$ .

Intuitively, the potential renormalization can be easily understood. When the impurity creates a density exciton it has to push the LL atoms up the optical potential to be able to create the density cloud. Therefore it loses more energy than what the density wave would cost. The inverse is true as well. By absorbing an exciton the impurity gains more energy than the exciton provides since potential energy is freed during the absorption process. Equation (4.155) leads to the effective spring constant

$$\kappa^* = (1 + \tilde{\mu}(v))\kappa, \quad (4.156)$$

where  $\tilde{\mu}(v) = \frac{Kw}{\pi}u/(v^2 - u^2)$ . In conjunction with Eq. (4.154) we thus obtain for the effective potential frequency

$$(\Omega_I^*)^2 = \frac{1 + \tilde{\mu}(v)}{1 + \mu(v)}\Omega_I^2. \quad (4.157)$$

In Fig. 4.7 we compare the prediction in Eq. (4.156) to the experimental data [146]. The best curves are obtained for  $\gamma \approx 0.25 - 0.35$ . Note that all the constants are determined by the experimental setup. However, since it is difficult to define  $\gamma$  for a non-homogeneous density we plotted results for  $\gamma = 0.5$  and  $\gamma = 0.35$  and  $\gamma = 0.25$  for illustration. If the non-homogeneous density profile is approximated by an homogeneous one the parameters used in the experimental setup in [146] lead to  $\gamma \approx 0.45$ .

#### 4.6.4 Long time dynamics

In the previous two paragraphs we studied the potential renormalization and the impurity mass shift by assuming that the impurity velocity was constant. Only then is the impurity cloud perfectly localized around the impurity position. It is clear that such an approximation can only hold for short times in the system we consider. For instance, while Eq. (4.156) can still be considered as a realistic approximation up to the first oscillation maximum of the impurity, it certainly fails to describe the correct physics for  $t \rightarrow \infty$ . The general solution to Eq. (4.150) is

$$\hat{\phi}_k(t) = \int_0^t ds \frac{\sin uk(t-s)}{uk} e^{ik\hat{q}(s)} + \text{wave excitations} , \quad (4.158)$$

which leads to a density cloud of the form  $\hat{\rho}(x, t) \sim \int_0^t ds \delta[x - \hat{q}(s) - u(t-s)] - \delta[x - \hat{q}(s) + u(t-s)]$ . In the case of an exponentially damped oscillating impurity this density cloud depends only on past values of  $\hat{q}$  when  $t$  is large and hence, for  $t \rightarrow \infty$ , the influence of  $\hat{q}(t)$  on  $\hat{\rho}(x, t)$  becomes negligible.

To put it in other words, for  $t \rightarrow \infty$  the density cloud is independent of the impurity such that its dynamics decouple from those of  $\hat{q}(t)$ : The LL has no dynamical effects on the impurity and one concludes that the LL neither renormalizes the impurity mass nor the external potential. Accordingly, the final width of the impurity reads

$$\mathcal{C}(t, t) \simeq \frac{1}{\beta\kappa} \quad \text{for } t \rightarrow \infty \quad (4.159)$$

and not  $1/\beta\kappa^*$ . We have thus found that dynamical quantities depend on the renormalized values  $\kappa^*$  and  $M_I^*$  while final equilibrium quantities have to be computed with the bare values  $\kappa$  and  $M_I$ . We insist on the fact that this behaviour has been observed by [146] where the final impurity position width is not renormalized in contrast to the potential renormalization that is observed at short times (see Fig. 4.7).

#### 4.6.5 The impurity influence functional

We now use the Keldysh formalism to derive an effective out of equilibrium action for the dynamical impurity position. The action of the free oscillator (described by  $\mathcal{H}_I$  with the parameters  $M_I^*$  and  $\kappa^*$ ) is complemented by

$$\begin{aligned} \mathcal{S}_{inf}[q^+, q^-, q^0] = & \sum_k \left\{ -i \int_0^{\beta\hbar} d\tau \int_0^\tau d\sigma \Gamma_k(-i\tau + i\sigma) e^{ikq_0(\tau) - ikq_0(\sigma)} \right. \\ & + \int_0^{\beta\hbar} d\tau \int_0^t ds \Gamma_k^*(s - i\tau) e^{ikq_0(\tau)} \left[ e^{-ikq^+(s)} - e^{-ikq^-(s)} \right] \\ & + i \int_0^t ds \int_0^s du \left[ e^{ikq^+(s)} - e^{ikq^-(s)} \right] \left[ \Gamma_{-k}(s - u) e^{-ikq^+(u)} - \Gamma_{-k}^*(s - u) e^{-ikq^-(u)} \right] \left. \right\} \\ & + \frac{\hbar\beta\kappa_0}{4} \left[ q_i^2 + q_i'^2 \right], \end{aligned} \quad (4.160)$$

where  $q^+(s)$ ,  $q^-(s)$  are the dynamical Keldysh branches with  $q^+(0) = q_i$  and  $q^-(0) = q_i'$ , and  $q_0(\tau)$  is the path over the initial condition (with imaginary time  $\tau$ ) [22]. The last line in the right-hand-side of Eq. (4.160) describes the initial localization due to the laser blade which

we interpreted as an initial position measurement with width  $1/\kappa_0\beta$ . Damping stems from the impurity-bath coupling which induces the kernel [8]:

$$\Gamma_k(\theta) = \frac{K|k||U_k|^2 \cosh[u|k|(\beta\hbar/2 - i\theta)]}{2\pi\hbar \sinh[u|k|\beta\hbar/2]}, \quad (4.161)$$

with  $\theta = s - i\tau$ . In order to understand the effects induced by the non linear impurity-LL coupling in Eq. (4.146) we expand Eq. (4.160) to second order in  $q$ . The result can be found in chapter 3 and [22] and the correlation function can be calculated:

$$\mathcal{C}(t, t) \simeq \frac{\hbar^2\beta\kappa_0}{4} \mathcal{R}^2(t) - \kappa^*\beta \mathcal{C}^{\text{eq}}(t)^2 + \frac{1}{\kappa^*\beta}, \quad (4.162)$$

Here,  $\mathcal{R}(t)$  and  $\mathcal{C}^{\text{eq}}(t)$  are the response and equilibrium correlation functions in the high temperature limit  $\hbar\beta\Omega_I \ll 1$  which prevails in the experiment. In the Laplace domain they read  $\tilde{\mathcal{R}}(z) = (1/M_I^*)[z^2 + z\omega_c\tilde{\alpha}(z) + (\Omega_I^*)^2]^{-1}$  and  $\tilde{\mathcal{C}}^{\text{eq}}(z) = (1/\beta z)[1/\kappa^* - \tilde{\mathcal{R}}(z)]$ . Linear response and correlator depend only on the ‘‘damping kernel’’

$$\alpha(t) = \int_0^\infty d\omega \frac{\mu M_I}{M_I^*} \left(\frac{\omega}{\omega_c}\right)^2 e^{-\omega/\omega_c} \cos \omega t. \quad (4.163)$$

As we pointed out, the final equilibrium value should be rather  $1/\kappa\beta$  [22] than  $1/\kappa^*\beta$  that would follow from Eq. (4.162). We conclude that, while the Gaussian approximation of Eq. (4.160) [see [22] for details] yields a realistic description of the impurity dynamics for short times, it cannot deliver the right correlation function for large times, where a crossover from the effective constants  $\kappa^*$  and  $M_I^*$  to bare quantities takes place. Since our approach does not provide us with an explicit expression of  $\kappa(t)$  and  $\Omega_I(t)$  we directly construct an approximate correlator

$$\begin{aligned} \mathcal{C}(t, t) \approx & \frac{\hbar^2\beta\kappa_0}{4} \mathcal{R}^2(t) - \kappa^*\beta \mathcal{C}^{\text{eq}}(t)^2 + \frac{1}{\kappa^*\beta} \\ & + (1 - e^{-\Gamma\Omega_I t}) \left( \frac{1}{\kappa\beta} - \frac{1}{\kappa^*\beta} \right), \end{aligned} \quad (4.164)$$

which interpolates between the two asymptotic expressions (4.162) and (4.159). Here,  $\Gamma$  is the effective damping induced by the Luttinger bath. For small to moderate damping it is given by  $\Gamma \simeq \frac{\pi}{8}\mu(\Omega_I/\omega_c)e^{-\Omega_I/\omega_c}$  [see (4.126)]. We expect Eq. (4.164) to be a realistic approximation of the impurity position width.

#### 4.6.6 Discussion of the results

In [146]  $^{41}\text{K}$  atoms play the role of the impurities moving in optical 1D tubes through a Luttinger liquid made of  $^{87}\text{Rb}$  atoms. Both the  $^{41}\text{K}$  and the  $^{87}\text{Rb}$  are confined in the same longitudinal optical potential with the (bare) potential frequency  $\Omega_I = 550\text{s}^{-1}$  ( $390\text{s}^{-1}$ ) for  $^{41}\text{K}$  ( $^{87}\text{Rb}$ ). We interpret the initial localization (with  $\kappa_0 \approx 150\kappa$ ) of the impurities as a position measurement. The experimental temperature is such that  $\hbar\Omega_I\beta \simeq 10^{-2}$  which ensures the high temperature regime. The mean squared velocity is obtained to be  $\sqrt{v^2} \approx 8.5 \text{ mm/s}$  which exceeds the typical sound velocity  $u \approx 3 \text{ mm/s}$  so that the impurity moves in the supersonic regime.

As pointed out before, the mass has to be renormalized in such a way that  $\Omega_I^*$  remains approximately constant over a wide range of  $w/w_L$ . This can be achieved by a suitable choice of  $\omega_c$ , the only free parameter in our theory. For  $\gamma = 0.35$  the choice  $\omega_c/\Omega_I = 40 - 50$  leads to a variation of 10 % for  $\Omega_I^*$  in the range  $0 < w/w_L < 5$ . However, since the mass and potential shifts decrease during equilibration the oscillation frequency can slightly change in time. Thus, for large times  $\Omega_I^*$  approaches  $\Omega_I$  in any case. Hence, in order to experimentally observe the  $\Omega_I^*$  predicted by Eq. (4.157) one cannot average over many periods as was done in [146]. It is therefore not straightforward to make a direct precise quantitative comparison between Eq. (4.157) and the experimental findings, although we think that the evidence in [146] clearly indicates that the mass renormalization counteracts the potential shift to a large extent.

Finally, we compare Eq. (4.164) to experimental data in Fig. 4.8. In [146]  $\sqrt{\mathcal{C}(t, t)}$  has an offset of about  $5\mu\text{m}$  which we add to our theoretical results. Moreover, for small interactions ( $w/w_L \lesssim 1$ ) there is a residual damping in the experiment due to inter-impurity collisions in tubes with several impurity atoms [146] which is of course not covered by our theory. We therefore use the data from [146] for the damping constant ( $\Gamma \approx 0.03$  for  $w/w_L = 1$ ) in  $\alpha(t)$ . As pointed out before  $\Omega_I^*$  can slightly vary during the equilibration process. However, this effect is not expected to be observable within the experimental error bars and therefore we approximate  $\Omega_I^*$  by  $\Omega_I$  for all times. The match between the experimental data and our theoretic curves is quite impressive.

In Sec. 4.4 I argued that non-trivial effects on  $\Omega_I$ , produced by the super-Ohmic spectral density in the damping kernel (4.163), could be observed for  $\omega_c \approx 0.3\Omega_I$ . Here, a second effect, which is potentially more important, has been described. I think that in the experiment described here  $\omega_c$  is much larger such that the effects of the polaronic mass shift and the potential renormalization (which were previously neglected in Sec. 4.4 largely dominate the influence of the non-Ohmic spectral density.

In summary we gained a thorough theoretical understanding of the experimental data in [146]. We calculated the effective potential spring constant with an EOM approach, which is expected to be correct for short times, and we obtained a result without any undetermined parameter [see Fig. 4.7]. We argued that due to memory effects neither a potential nor a mass renormalization can take place in the long time limit. One question not resolved yet concerns the precise mechanism that links the mass and potential shifts which I hope will be revealed by future experiments. Finally, using the analytic results developed in Sec. 4.4 for the Brownian motion of a particle coupled to an exotic environment, after an initial position measurement, and with a phenomenological correction to the asymptotic limit, we described the experimental data for  $\mathcal{C}(t, t)$  very accurately.



---

Conclusion and Outlook

---

*“Even if I knew that tomorrow the world would go to pieces, I would still plant my apple tree.”*  
 Martin Luther

In this thesis I presented the main aspects of the research I conducted during my PhD at the LPTHE at Pierre-et-Marie Curie university in Paris. The thesis consists of three main research chapters. Let me here summarize the main achievements and compare our results to other approaches in the literature.

### 5.1 Critical dynamics driven by colored noise

In chapter 2 I thoroughly studied the purely dissipative critical dynamics of a model with an  $N$ -component order parameter in  $D$  spatial dimensions, coupled to an *equilibrium* thermal bath which provides a colored thermal noise. We argued that the upper critical dimensionality of the model is  $D_c = 4$  and we used the framework of the field-theoretical  $\epsilon$ -expansion to account for the effects of non-Gaussian fluctuations in  $4 - \epsilon$  spatial dimensions.

Within the Gaussian approximation – valid for  $D > D_c$  – the equilibrium dynamic exponent  $z$  which controls the different scaling of space and time takes the values

$$z_0 = \begin{cases} z_0^{(\text{col})} = 2/\alpha & \text{for } \alpha < 1, \\ z_0^{(\text{w})} = 2 & \text{for } \alpha \geq 1, \end{cases} \quad (5.1)$$

where  $\alpha$  characterizes the *algebraic* long-time decay of the two-time correlation function of the noise, see Eq. (2.4). For  $\alpha = 1$  one recovers the white-noise result  $z_0^{(\text{w})} = 2$ . The non-equilibrium ‘initial slip exponent’  $\theta$ , instead, vanishes. Depending upon the value of  $\alpha$  the asymptotic long-time dynamics is effectively equivalent to one driven by white noise (Ohmic bath) for  $\alpha > \alpha_c$ , whereas the effect of the colored noise is relevant for  $\alpha < \alpha_c$ . Within the Gaussian approximation  $\alpha_c = 1$ , as demonstrated by the change in behavior of  $z_0$  given in Eq. (5.1).

In dimensions  $D < 4$  the critical behavior is modified due to the relevance of the interaction term and of the non-Gaussian fluctuations. The value  $\alpha_c$  which controls the cross-over between the white-noise and the colored-noise dominated behaviors is modified by  $N$ -dependent corrections of order  $\epsilon^2$  and it therefore separates the two corresponding regions in the parameter space  $(\alpha, D, N)$ , named W and C in Fig. 2.5, respectively. The dynamical critical exponent  $z$  is given by

$$z = \begin{cases} z^{(\text{col})} \equiv \frac{2}{\alpha} + \eta_\gamma = \frac{2}{\alpha} \left[ 1 - \frac{N+2}{4(N+8)^2} \epsilon^2 \right] + \mathcal{O}(\epsilon^3) & \text{within region C ,} \\ z^{(\text{w})} \equiv 2 + \eta_w = 2 + \frac{N+2}{(N+8)^2} \left[ 3 \ln \frac{4}{3} - \frac{1}{2} \right] \epsilon^2 + \mathcal{O}(\epsilon^3) & \text{within region W .} \end{cases} \quad (5.2)$$

The  $N$ -dependent curve Eq. (2.90) which separates regions W and C in the  $(\alpha, D)$ -plane is illustrated in Fig. 2.5 for  $N = 1, 4, \infty$ . Some comments are in order:

- (i) Upon decreasing  $D$ , the region W within which the Ohmic result is recovered extends beyond the Gaussian value  $\alpha_c = 1$ .
- (ii) The correction to the Gaussian value  $z_0$  is positive within region W ( $z_0 = 2$ ) and negative within region C ( $z_0 = 2/\alpha$ ).
- (iii) The exponent  $z$  is a continuous function of  $\epsilon$  and  $\alpha$ : At the transition line between regions W and C one has  $z^{(\text{w})} = z^{(\text{col})}$ , as can be easily verified by using Eq. (2.90).
- (iv) In the large- $N$  limit the  $\epsilon^2$  correction vanishes and the dynamic exponent  $z$  and  $\alpha_c$  take their Gaussian values  $z_0$  and  $\alpha_c = 1$ , respectively. This is also consistent with the large- $N$  result reported in Sec. 2.2.2

For random initial conditions, i.e., with vanishing correlations and average order parameter, we determined the general scaling forms of the dynamic correlation functions. Within region C, such scaling forms differ from the ones valid in the presence of white noise only, studied in Ref. [82] and recovered within region W. We determined the corresponding initial-slip exponent  $\theta$  up to order  $\mathcal{O}(\epsilon)$  in the presence of colored noise. It is given by

$$\theta = \frac{(N+2)}{4(N+8)} d(\alpha) \Gamma_E(\alpha) \epsilon + \mathcal{O}(\epsilon^2), \quad (5.3)$$

and the plot of the ratio between this value  $\theta$  and the reference  $\theta_{\alpha=1}$  for the white noise is reported in Fig. 2.8. Note that in the white-noise limit  $\alpha = 1$  we recover the large- $N$  result  $\theta_{\alpha=1} = \epsilon/4$  [see Sec. 2.2.2].

In non-equilibrium conditions we also calculated the long-time limit  $X^\infty$  of the FDR for general  $\alpha$  and  $N$ . The value of  $X^\infty$  in the presence of white noise is known analytically up to  $\mathcal{O}(\epsilon^2)$  [91] and numerically via Monte Carlo simulations in various dimensions for models belonging to the universality class of the  $O(N)$  model with dissipative dynamics (see, e.g., [86] for a review). We proved that this result is recovered within region W. Instead, if the colored noise is dominant [ $\alpha < \alpha_c(D, N)$ ], i.e., within region C, we showed that  $X^\infty = 0$ . Therefore, the associated effective temperature is infinite, analogously to what is found in sub-critical coarsening [93, 94]. Our result for  $X^\infty$  within the Gaussian approximation is only in partial agreement with the corresponding one derived in [48] for an anomalously diffusing particle — i.e., of a fractional Brownian motion — which our model reduces to within such an approximation. Indeed, in the presence of a super-Ohmic noise  $\alpha > \alpha_c = 1$ , one finds

$X^\infty = 1$  [48] and super-diffusion  $z < 2$  for the fractional Brownian motion, while we argue that  $X^\infty = X_0^\infty = 1/2$  and normal diffusion  $z = z_0^{(w)} = 2$  in our field theoretical model. This is due to the fact that even in the absence of a white-noise effective vertex in the original model, non-Gaussian fluctuations (induced by the interactions) generate it and turn it into the dominant one for  $\alpha > \alpha_c \leq 1$  such that the white-noise result is recovered.

In conclusion, noises correlated in time may affect significantly the equilibrium and non-equilibrium dynamical properties of systems close to critical points. In this respect it is important to note that the distinction between super-Ohmic ( $\alpha > 1$ ) and sub-Ohmic ( $\alpha < 1$ ) thermal baths does not fully correspond to having irrelevant (white) and relevant (colored) long-time correlations of the noise, respectively. Indeed, as shown in Fig. 2.5, even a weakly sub-Ohmic noise with  $\alpha_c(D, N) < \alpha < 1$  is actually equivalent (in the RG sense) to an Ohmic (white) noise in the physical dimensions  $D = 3$  and  $D = 2$  as far as the dynamical properties in the long-time limit are concerned. In addition, in the presence of interactions, a super-Ohmic bath does not result in a super-diffusive behavior ( $z < 2$ ) but rather in the anomalous diffusion induced by the equivalent white noise, in contrast to what happens for the free fractional Brownian motion.

The field-theoretical predictions for the relaxational Markov critical dynamics of systems belonging to the universality class considered here have been put to the numerical test both via Monte Carlo simulations and by solving the Langevin equations with a variety of different methods (see, e.g., [87] and references therein). An instance of non-Markovian dynamics of the  $\phi^4$ -theory with a noise exponentially correlated in time was investigated in [203]. However, in this case one does not expect the long-time dynamics of the system to be affected by the finite memory of the noise. Dealing numerically with power-law correlated Gaussian noise is a significantly harder problem which remains basically open due to the difficulties in generating such kind of random process, see, e.g., [47, 204] and references therein.

## 5.2 Out-of-equilibrium quantum Brownian motion

After the study of classical critical out-of-equilibrium systems I focused on dissipative quantum systems, in particular on quantum Brownian motion. The chapter 3 is devoted to the study of such non equilibrium dynamics of a quantum Brownian particle coupled to a quantum thermal bath of harmonic oscillators for generic Gaussian initial conditions. We found a closed expression for the non equilibrium correlation function, which we showed to be easy to derive from variations of a generating functional Eq. (3.87). We used the analysis in [8] as a starting point to obtain this generating functional by employing path integral methods. We then showed that factorizing initial conditions (where the bath and the particle are initially uncoupled) are a special case of the non-factorizing initial conditions on which a position measurement has been performed. We demonstrated the correctness of our approach by deriving the equilibrium correlation function without imposing time-translational invariance (presented in App. 3.5.3).

We applied this general formalism to the study of three physical situations. First, we studied the equilibration process of a trapped particle after an initial position measurement. In this case we considered Ohmic dissipation. While the classical (high temperature) correlator relaxes exponentially on a time scale  $\gamma^{-1}$ , the low temperature correlator  $C(t, t')$  in the strongly quantum regime shows an algebraic relaxation of the form  $1/(tt')^2$  which is independent of the dissipation strength  $\gamma$ . Therefore, the information that an initial measurement on the system has been performed persists for a very long time. We then showed that the equilibration process is

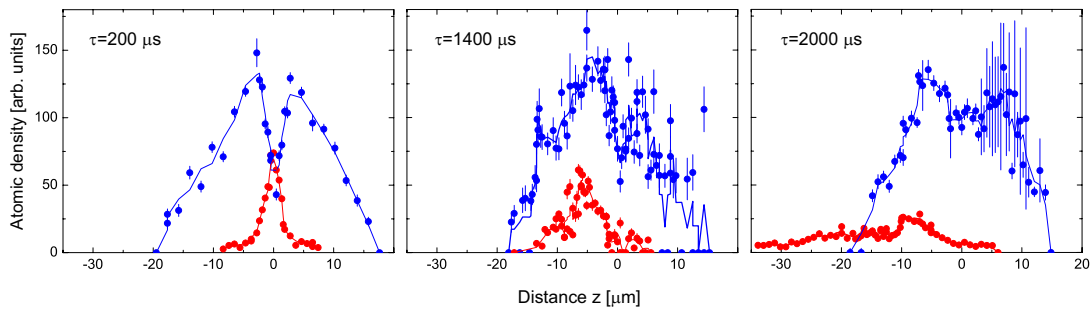


Figure 5.1: Figure from Palzer et. al [148]. The majority atoms (blue atoms are trapped *via* an optical potential. At initial time the trapping is switched off for the impurities (red atoms) which subsequently are pulled downwards (here: to the left) by gravity.

different if, instead of a position measurement, a sudden quench in the trapping potential is performed at the initial time. We showed that in this case the relaxation is exponential in time even in the quantum regime with the slight difference that at very low temperatures the relaxation time is of order  $2\gamma^{-1}$  rather than  $\gamma^{-1}$  for high temperatures. Accordingly, the relaxation due to quantum fluctuations is almost as effective as thermal relaxation in this case.

### 5.3 Impurity dynamics in 1D Bose liquids

Sec. 3.3 (which is a part of chapter 3) provided us with useful formulae for the study of impurity dynamics in trapped Luttinger liquids. We showed that the quantum Brownian influence functional is a good starting point for these impurity dynamics in 1D quantum liquids. In particular, quantum Brownian motion leads to damped oscillations for the impurity and to the correct final position width. On the other hand, we pointed out that this approach has many limitations. Indeed, the polaronic effects and the potential renormalization cannot be described by standard quantum Brownian motion since the impurity-Luttinger liquid coupling is a density-density coupling and therefore nonlinear in the impurity position coordinate: Note that standard quantum Brownian motion is modeled *via* a *linear* impurity-bath coupling. In Sec. 4.6 we showed how it is possible to understand the mass shift and the potential renormalization by using a simple approach based on the equations of motion of the impurity and the coupled quantum liquid. As we have pointed out, the external potential is enhanced *via* the surrounding *trapped* quantum liquid bath for sufficiently fast impurities. This has dramatic consequences. Recently Palzer et al. [148] experimentally studied an impurity-Luttinger liquid system with a vertical geometry. The external optical potential has to be such that it retains the impurity against gravity in the center of the surrounding cloud of majority atoms (the Luttinger liquid). This process is shown in Fig. 5.1. When the external potential is switched off for the impurities (but not for the Luttinger liquid) the impurities are pulled out of the majority atom cloud by gravity as one would expect intuitively.

However, this system has recently also been simulated by using the Gross-Pitaevskii equations. In 1D one can construct an approach which is valid for weak *and* strong internal interactions within the quantum liquid, since strongly interacting bosons are equivalent to weakly interacting fermions in 1D. In [201] the authors showed that – after switching off the external potential for the impurities only – the impurity atoms are trapped in the Luttinger liquid for a

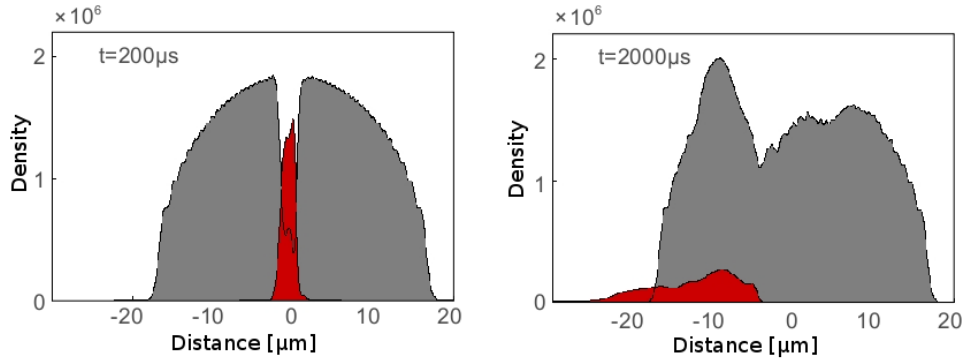


Figure 5.2: Figure from Rutherford et. al [201]. The minority atoms (red) are pulled out of the cloud of majority atoms (gray) by gravity. The system has been simulated within a Gross-Pitaevskii approach.

sufficiently great coupling strength, although they do not feel the external potential anymore. To be more precise, while the majority atoms were still subject to the external optical trap, the external potential was switched off for the minority atoms (the impurities) very much as in the experiment. As in the experiment by Palzer et. al one would expect that gravity pulls them immediately out of the majority cloud. This is indeed the case for small to moderate coupling strengths [see Fig. 5.2]. But, as shown in [201] there is a quite sharp threshold value of the atom interaction strength (the interspecies interaction is equal the impurity-Luttinger liquid interaction in this particular article) beyond which the impurities are “blocked” within the majority cloud. See Fig. 5.3 for a visual representation of the phenomenon. Such an intriguing

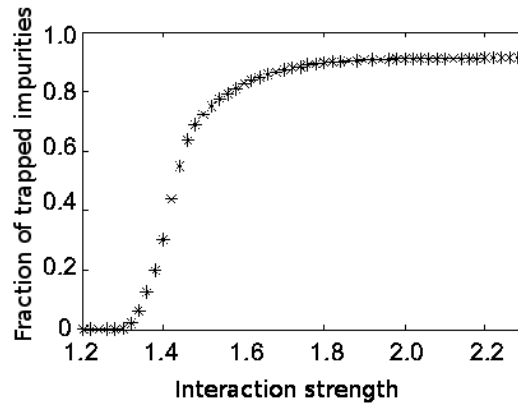


Figure 5.3: Figure from Rutherford et. al [201] showing the fraction of impurity atoms which remain within the atom cloud of majority atoms (despite gravity) versus the interaction strength (here  $w = w_L$ ) measured in units of  $10^{-36}$  Jm. A quite sharp crossover can be observed for  $w \approx 1.4 \cdot 10^{-36}$  Jm.

behaviour can be well explained by the results found in Sec. 4.6. Indeed, the *trapped* Luttinger liquid has a non homogeneous density which leads to an *effective potential* for the impurities (characterized by the potential constant  $\kappa_{\text{imp}}$ ) even if they are indifferent towards the external optical potential. This happens according to the formula

$$\kappa_{\text{imp}} = \tilde{\mu}(v)\kappa, \quad (5.4)$$

with

$$\tilde{\mu}(v) = \frac{Kw}{\pi} u / (v^2 - u^2), \quad (5.5)$$

where I used the results in Sec. 4.6. Above some threshold value of  $w$  this effective potential exceeds gravity and the impurities cannot “drop on the floor” anymore, according to our formula. Hence, Eq. (5.4) predicts a sharp transition value  $w_c$  beyond which the impurities cannot leave the surrounding cloud anymore (at least for short time intervals for which Eq. (5.4) is valid).

At last, let me discuss the formula (5.5) when  $v^2 < u^2$ . First of all, I insist again on the fact that Eq. (5.5) is not valid when  $v^2 \approx u^2$ . However, one can imagine cases where  $v^2$  is much smaller than  $u^2$ . For instance, when the interaction between the impurity and the Luttinger liquid becomes very weak, we can argue that – for zero temperature – the typical impurity velocity is determined by its ground state momentum with respect to the harmonic oscillator potential. If we take the numerical values found in [146] we can deduce that  $v^2/u^2 \approx 0.1$  in this case. The effective potential is thus lowered for  $w/w_L \rightarrow 0$  and  $\beta \rightarrow \infty$ . At first glance such an effect is very surprising. Note however that, in the limiting case where  $v^2$  vanishes, it might be quite intuitive to expect an impurity to be expelled from the region in the quantum liquid of higher density towards the ones with a lower density, i.e. from the center of the liquid outwards. In our analysis we replaced the inhomogeneous density profile of the quantum liquid by a homogeneous one while including the potential energy of the wave excitations. This is supposed to preserve the effects of the inhomogeneous background density. For an impurity immersed in a Bose-Einstein condensate such an expulsion has indeed been investigated in [205]. It is however beyond the scope of this thesis to compare our results to the ones in [205] or to decide if any comparison can be done. In summary, I hope very much that a future research project will shed more light on this fascinating effect and in particular on the formula (5.5).

An impurity-Bose liquid system has also been recently simulated by a time-dependent density matrix renormalization group (TDMRG) method by Peotta et. al [151, 184]. The TDMRG has to be performed on discrete lattices (with sites labeled by  $i$ ) and the author chose the Hamiltonian

$$\hat{\mathcal{H}}_L = -J_1 \sum_i [\hat{b}_i^\dagger \hat{b}_{i+1} + \text{h.c.}] + U_1 \sum_i (\hat{b}_i^\dagger \hat{b}_i)^2 + \sum_i W_i \hat{b}_i^\dagger \hat{b}_i, \quad (5.6)$$

$$\hat{\mathcal{H}}_I = -J_2 \sum_i [\hat{a}_i^\dagger \hat{a}_{i+1} + \text{h.c.}] + V_2(t) \sum_i (i - i_0)^2 \hat{a}_i^\dagger \hat{a}_i, \quad (5.7)$$

$$\hat{\mathcal{H}}_{IL} = U_{12} \sum_i \hat{b}_i^\dagger \hat{b}_i \hat{a}_i^\dagger \hat{a}_i. \quad (5.8)$$

The  $\hat{b}_i^\dagger, \hat{b}_i$  model the background Bose liquid while  $\hat{a}_i^\dagger, \hat{a}_i$  are the impurity operators. The terms proportional to  $J_1$  and  $J_2$  represent the kinetic hopping term of the Bose liquid and of the impurity, respectively. Note that the majority ( $\hat{b}_i^\dagger, \hat{b}_i$ )-bosons are simply described by the Bose-Hubbard model and their number is fixed in this problem. The  $V_2(t)(i - i_0)^2$ -term describes a harmonic potential for the impurity with a time-varying amplitude. This allows to mimic the initial trapping of the impurity (with a strong  $V_2$ ) and its subsequent release after which the impurity feels only a weak longitudinal potential (a weak  $V_2$ ). Up to this point the system described by Eq. (5.6) is exactly the discretized version of the system studied in this thesis.

However, the author of [151] chose for the Bose liquid an external trapping  $W_i$  which is essentially zero in a wide range of the bulk and raises smoothly at the edges. This notable

difference with the harmonic trapping potential of the Luttinger liquid studied in Sec. 4.6 leads to remarkable differences for the impurity dynamics which I will discuss further below. Let me first discuss the most remarkable result by Peotta et al. who found that Luttinger theory is only applicable in a small range of parameters. This raises questions about the validity of our own analysis which heavily relies on Luttinger theory.

Peotta et al. pointed out that the system in question could lie outside the realm of Luttinger liquid theory. They found, to be more precise, a non symmetric damping constant when the impurity-Luttinger liquid coupling is reversed,  $w \mapsto -w$ , which is in conflict with our formula [see the definition of  $\mu$  right after Eq. (4.153)]. However, it should be pointed out that the Lieb-Liniger parameter in the system we studied is rather small ( $\gamma \approx 0.25 - 0.5$ ) while  $\gamma \gtrsim 10$  in the simulation by Peotta et al. The weakest intra-bath interaction strength which they considered is  $U_1/J_2 = 0.1$  corresponding to  $\gamma \approx 1$ . In this case Luttinger theory seems to be reliable for  $U_{12}/J_2 \leq 0.1$  which corresponds to  $w/w_L \leq 1$  in our notations. Unfortunately, the authors did not consider smaller Lieb-Liniger parameters in [151, 184] so that it is not possible to *directly* verify if a system with  $\gamma \approx 0.25 - 0.5$  can be described by Luttinger theory when  $w$  is large so that it lies in a range which relevantly stretches beyond  $w/w_L = 1$ . Fortunately, we can confirm the validity of our approach *indirectly*, because the results in [151, 184] indicate that the range of validity of Luttinger theory strongly increases when  $U_1/J_2$  is further decreased. Therefore, we can deduce from the results in [151, 184] that Luttinger theory is applicable markedly beyond  $w/w_L = 1$  in our case and it is highly probable that this is also true in the whole range  $0 < w/w_L \lesssim 5$  which we consider in this work. It is thus possible to apply Luttinger theory in our problem.

Let us now discuss the major difference between the simulation in [151] and the experiment [146]. Indeed, as wished by the author of [151] the Bose liquid has an almost homogeneous density profile in their simulations within a wide range around the center of the cloud. If we go back to Sec. 4.6 we should therefore expect that the effective potential renormalization  $\kappa \mapsto \kappa^* > \kappa$  disappears or is at least diminished (since the Bose gas is still confined in [151] and not translationally invariant which leads intuitively to a decreased, albeit non-zero, potential renormalization). If we go back to the discussion in Sec. 4.6 these circumstances have two consequences. First of all, the amplitude of the first oscillation maximum should not dramatically increase upon ramping up the impurity-Luttinger liquid coupling  $\hbar w$ . Second, the final width of the impurity cloud should be equal to the mean width during the first amplitudes. Indeed, as I have pointed out, the potential renormalization only works for small times; at large times the potential renormalization disappears. Therefore, if the potential is enhanced by the surrounding Luttinger liquid, a difference between the mean impurity cloud width at small times and at large times, respectively, has to appear. As can be seen in Fig. 5.4 the simulation results confirm this picture. First, compare Fig. 5.4 to Fig. 4.8. The simulation by Peotta et al clearly indicates that the average impurity width does not change during equilibration. As discussed above such a behaviour hints to a vanishing potential renormalization. Compare now Fig. 5.4 to Fig. 4.7. For great values of  $\gamma$  (here,  $\gamma \approx 10$ ) the curve in Fig. 4.7 is greatly shifted to the left. Therefore, upon changing  $w/w_L$  from 0.2 to 0.6 we expect an amplitude decrease of about 50% which is clearly not observed in Fig. 5.4. Note however, that the simulation performed in [151, 184] focuses on a regime which lies beyond the Luttinger paradigm. A comparison between our results and the findings of Peotta et al. is therefore always built on somewhat shaky grounds.

To summarize, the numerical results by Peotta et al. confirm our approach (or at least they do not refute it) in the sense that Peotta et al. do not find a strong potential renormalization although such a potential shift is measured in the experiment [146]. Our theory is thus vali-

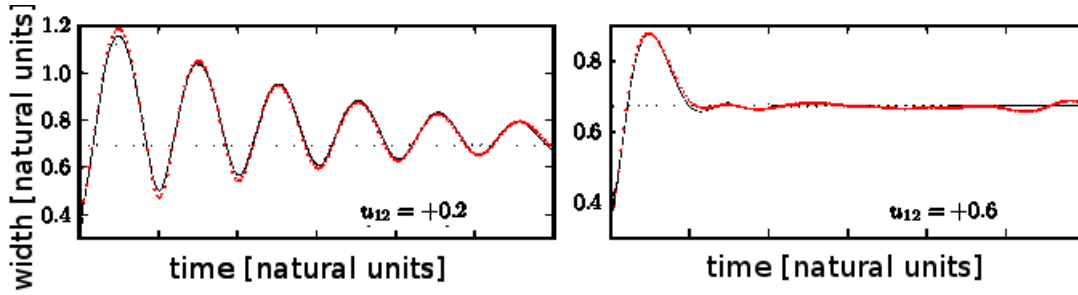


Figure 5.4: Figure from Peotta et. al [151, 184] depicting the impurity position width versus time for two different couplings between the impurity and the Bose liquid,  $u_{12} = w/w_L$  in our notations. The Lieb-Liniger parameter can be found by using  $\gamma = U_1/(2J_1\langle b_i^\dagger b_i \rangle)$  [151] from which we find  $\gamma = 1/\langle b_i^\dagger b_i \rangle \approx 10$  with  $U_1/J_2 = 1$ ,  $J_2 = 2J_1$  and  $\langle b_i^\dagger b_i \rangle \approx 0.1$  in [184].

dated self-consistently since if it can be applied to the regime considered by Peotta et al., the only difference between the two physical systems studied in the simulation [184] and the experiment [146], respectively, lies in the different trapping of the bosons. It is then clear that the non-homogeneity of the boson density profile – strongly present in the experiment but only weakly in the simulation – induces the potential shift. Finally, this interpretation beautifully overlaps with the results in Sec. 4.6.

In summary, our results have been independently confirmed by several other studies, although these studies did not directly investigate the potential renormalization. We are confident that a future numerical or experimental study of this issue will confirm our intuition of the interplay between a non-homogeneous density profile and the impurity potential shift by directly addressing this fascinating phenomenon.

## 5.4 Outlook

The RG methods introduced in chapter 2 can probably be applied to critical membrane dynamics with colored noise. Although the relevant Ginzburg-Landau functional has a form different from the standard  $\phi^4$ -functional, the idea to construct an RG flow and to analyze separately the white-noise and the colored-noise vertices is certainly a good starting point for the analysis of the effects of colored noise on this critical systems found in biochemistry.

More theoretically, we worked on the critical large- $N$  approximation of the  $\phi^4$ -theory driven by colored noise in order to generalize the analysis by Janssen [see [82] and Sec. 2.2.2]. I hope to find soon results which confirm our RG analysis. Among other possible extensions of the present work, I also mention the problem of understanding the effects of colored noise on sub-critical coarsening. The dynamic scaling hypothesis states that the late-stage phase ordering kinetics is governed by a length scale  $L(t)$  that, in models with no quenched disorder, typically grows in time as a power-law  $L(t) \simeq \lambda(T)t^{1/z_d}$ . The dynamic exponent  $z_d$  (generically different for the dynamic exponent  $z$  at criticality) depends upon the kind of order parameter and the conservation laws [17] while the prefactor  $\lambda(T)$  typically depends only weakly upon temperature  $T$ , is non-universal, and it vanishes upon approaching a critical point. (The matching with the critical growth is explained in [206].) In presence of colored noise this growth law might be modified, since heavily correlated thermal noise might have an aggregate effect strong enough to alter the domain growth, which is usually exclusively driven by the surface curvature: Note

that for white noise one typically expects thermal fluctuations not to affect the domain growth law [17].

Quantum Brownian motion has still many unexplored research fields to offer. From decoherence to exotic baths, such as spin baths [126], many questions and problems have not been investigated, yet. I will not go into details here and I refer the reader to the extremely vast literature on the subject. Let me however point out two things. I have introduced the formulae (3.23) and (3.24) which allow for an exact diagonalized form of the reduced density matrix of a Gaussian quantum Brownian particle. From its diagonal nature quantities such as the purity and the von Neumann entropy are easily calculated. The discussion around (3.24) can thus be extended to study decoherence effects. Note that these formulae can be applied as long as the initial condition can be expanded on Gaussian functions. This is in particular true for Schrödinger cat states consisting, e.g., of two displaced superposed Gaussian wave packets. In this context another type of Brownian motion can be explored. Indeed, there are two ways of coupling a quantum harmonic oscillator to a quantum bath. The possibility, which has not been analyzed in the present study, consists in introducing a  $a^\dagger b_i + a b_i^\dagger$ -coupling with  $b_i^\dagger, b_i$  the bath operators and  $a^\dagger, a$  the creation and annihilation operators of the quantum harmonic oscillator which – due to the coupling described above – is damped. Such a coupling conserves the total number of excitations and the dynamics are therefore not ergodic in the sense that the total Hilbert space factorizes into invariant subspaces each characterized by the total number of excitations. Since this Hilbert space is “smaller” than the one of standard quantum Brownian motion one expects that decoherence is weaker. I hope to address this question in a future study.

Let me comment now the results of chapter 4. I think it is very important that future experiments give us a deeper empirical understanding of how impurities behave in 1D quantum liquids. The effective potential imposed on the impurity, which stems from the interaction of a *trapped* Luttinger liquid with the impurity, is an intriguing phenomenon. Numerical simulations have shown that such an effective potential can even lead to a complete “blocking” of the impurities within the cloud of trapped majority atoms, which is strong enough to counteract gravity [201]. Unfortunately, to date no experiments have examined this question. The dependence of the oscillation frequency on the interaction strength is rather easy to measure. Also, in a vertical geometry where gravity can fully exert its influence, or in a tilted optical potential, it is well within reach to experimentally reproduce the self-trapping of impurities and to measure the threshold interaction strength which in turn gives information about the effective potential. From a theoretical point of view, the results of the linear response theory presented in Sec. 4.6 should be reproducible by methods such as the local density approximation. It would be most satisfactory to build a bridge between the formulae found in Sec. 4.6 and more conventional methods, possibly with some support from numerical simulations. Also, the influence of the back-scattering potential on the results derived in Sec. 4.6 is still quite mysterious. Unfortunately, studying dynamical phenomena of impurities in 1D quantum liquids beyond the weak-coupling regime (weak interactions as well as slow impurities) by taking into account the full Hamiltonian with the backscattering terms is very difficult and involves generally Bethe-ansatz methods combined with massively paralleled computation. Recently, Mathy et al. [161] found an intriguing behaviour of an impurity in such numerical simulations of a strongly coupled impurity after it is shot into a 1D liquid with supersonic speed. Accordingly, impurity

dynamics in 1D liquids show utterly unexpected phenomena as soon as the background liquid and/or the impurity are in regimes notoriously difficult for a theoretical analysis, such as strong coupling or external trapping.

This has been probably a difficult manuscript for the reader. I presented many different aspects of today's non-equilibrium physics which are not always related one to another. While it was passionate during my PhD to gain an insight into so many different fields of physics, I considered as a challenge to write this finale manuscript in a comprehensible way. As the reader has certainly realized, the present thesis is structured around the three main research chapters. I have decided to keep this threefold structure also in the last chapter 5 of my thesis. I very much hope that, despite this way of presenting the results, the reader was able to enjoy the parts of the thesis he found interesting.

## CHAPTER 6

---

### Bibliography and index of most important symbols

---

“ $10^2 + 11^2 + 12^2 = 13^2 + 14^2$ ”  
famous proverb

rhs	right hand side of an equation
lhs	left hand side of an equation
$\beta$	inverse temperature $\beta = 1/k_B T$
$D$	dimensionality; sometimes the diffusion constant
$R(t, s)$	two-time classical non equilibrium position response function
$C(t, s)$	two-time classical non equilibrium position correlation function
$Q(t)$	Mean displacement in classical Brownian motion
$Q_F(t)$	Mean displacement in free quantum Brownian motion
$g$	coupling constant in chapter 2
$\mathcal{H}$	General symbol for the Hamiltonian
$\mathcal{S}$	General symbol for the action
$\gamma$	Chapter 2: Colored-noise vertex. Chapter 3: Coupling strength of the bath. Chapter 4: Lieb-Liniger parameter which totally characterizes a 1D gas with contact interactions
$\Gamma(t - s)$	Noise memory kernel in chapter 2
$\Gamma_E(x)$	Euler's Gamma function
$\alpha$	Characteristic exponent of the colored noise: $\Gamma(t) \sim t^{-\alpha}$
$\epsilon$	equal to $4 - D$ in chapter 2; measures the width of the initial Gaussian wave function in chapter 3
$z$	Dynamic exponent governing the scaling relation between space and time $t \sim x^z$
$\eta$	static anomalous dimension of the field $\phi$ in chapter 2
$\theta$	non-equilibrium initial slip exponent in chapter 2
$\hat{\theta}(x)$	Field describing the phase in Luttinger theory

$\gamma_w$	White-noise vertex
$\bar{\phi}(x)$	Response field
$\gamma^{n,\bar{n}}$	One-particle irreducible vertex functions with $n$ external $\phi$ -lines and $\bar{n}$ external $\bar{\phi}$ -lines
$\alpha_c(D, N)$	crossover $\alpha$ beyond which the colored noise becomes relevant
$E_{\alpha,\beta}(x)$	Mittag-Leffler function
$X(\vec{p}; t, t')$	Fluctuation-dissipation ratio
$X^\infty$	large time zero-momentum fluctuation-dissipation ratio
$\beta^\infty$	Effective temperature for coarsening
$\hat{p}, \hat{p}_n$	Momentum operators
$\hat{q}, \hat{q}_n$	Position operators
$\Omega$	Frequency of the external potential for the quantum Brownian particle or impurity
$M$	Mass of the quantum Brownian particle or impurity
$\gamma(t)$	Damping kernel in quantum Brownian motion
$\hat{\rho}_0(t)$	Initial density matrix
$\hat{\rho}_R(t)$	Reduced density matrix
$\mathcal{R}(t, t')$	Response function in quantum Brownian motion
$\mathcal{C}(t, t')$	Position correlation function in quantum Brownian motion
$\mathcal{G}_+(t)$	“Propagator” in quantum Brownian motion, related to the response function
$\nu_k$	Matsubara frequencies
$\hat{\Pi}(q)$	Projection operator on some state centered around $q$
$F(t), G(t)$	External sources in quantum Brownian motion ch. 3
$\mathcal{J}[F, G]$	Generating functional of all non equilibrium correlation functions of the damped quantum harmonic oscillator
$\hat{a}^\dagger, \hat{a}$	Harmonic oscillator creation and annihilation operators
$\hat{b}^\dagger, \hat{b}$	Bosonic particle creation and annihilation operators
$\hat{c}^\dagger, \hat{c}$	Fermionic particle creation and annihilation operators
$E_F, v_F, k_F$	Fermi energy, Fermi velocity and Fermi momentum
$\hat{\Pi}(x)$	Conjugate momentum field in Luttinger theory
$\hat{\mathcal{H}}_{IL}$	Interaction Hamiltonian between the impurity and the Luttinger liquid
$u$	Sound velocity in a Luttinger liquid
$K$	Luttinger parameter: $K = 1$ corresponds to non-interacting fermions or impenetrable bosons
$w$	Coupling strength between the atoms in the 1D quantum liquid
$U(x), U_k$	Potential (in Fourier space) between the impurity and the 1D quantum liquid
$w_L$	Coupling strength between the impurity and the Luttinger liquid
$\hat{\rho}(x)$	density operator of the Luttinger liquid
$\rho_0$	Background density of the Luttinger liquid
$S(\omega)$	Spectral density of the bath
$r_{TF}$	Thomas-Fermi radius
$\alpha_{ho}$	Dimensionless quantity which measures the strength of the external potential
$\mu$	Chemical potential; redefined coupling constant in Sec. 4.6.
$M^*$	Effective mass

$\kappa^*, \kappa$  (Effective) external potential spring constant

---

## Bibliography

---

- [1] A. EINSTEIN, *Annalen der Physik* **17**, 549 (1905).
- [2] N. G. VAN KAMPEN, *Stochastic processes in physics and chemistry*, Elsevier, 2007.
- [3] C. GARDINER, *Stochastic Methods. A Handbook for Natural and Social Sciences*, Springer, 2009.
- [4] J. P. BOUCHAUD and A. GEORGES, *Physics Reports* **195**, 127 (1990).
- [5] P. SCHRAMM and H. GRABERT, *Phys. Rev. A* **34**, 4515 (1986).
- [6] H. GRABERT, P. SCHRAMM, and G.-L. INGOLD, *Phys. Rev. Lett.* **58**, 1285 (1987).
- [7] P. SCHRAMM and H. GRABERT, *J. Stat. Phys.* **49**, 767 (1987).
- [8] H. GRABERT, P. SCHRAMM, and G.-L. INGOLD, *Phys. Rep.* **168**, 115 (1988).
- [9] A. CALDEIRA and A. LEGGETT, *Annals of Physics* **374**, 149 (1983).
- [10] T. GIAMARCHI, *Quantum Physics in One Dimension*, Clarendon Press, Oxford, 2003.
- [11] E. M. LIFSHITZ, L. P. PITAEVSKII, and L. D. LANDAU, *Course of Theoretical Physics: Physical Kinetics*, Pergamon press, 1980.
- [12] J. W. NEGELE and H. ORLAND, *Quantum Many-Particle Systems*, Westview Press, 1998.
- [13] C. L. KANE and M. P. A. FISHER, *Phys. Rev. B* **46**, 15233 (1992).
- [14] T. GIAMARCHI and H. J. SCHULZ, *Phys. Rev. B* **37**, 325 (1988).
- [15] L. F. CUGLIANDOLO, Course 7: Dynamics of Glassy Systems, in *Slow Relaxations and nonequilibrium dynamics in condensed matter*, edited by J.-L. BARRAT, M. FEIGELMAN, J. KURCHAN, and J. DALIBARD, volume 77 of *Les Houches*, pp. 161–171, Springer Berlin/Heidelberg, 2003.
- [16] L. F. CUGLIANDOLO, *Out of equilibrium dynamics in classical and quantum systems*, Beg Rohu Summer School, 2009.
- [17] A. J. BRAY, *Adv. in Phys.* **43**, 357 (1994).
- [18] S. K. MA, *Modern Theory of critical phenomena*, Benjamin Reading, 1976.
- [19] J. ZINN-JUSTIN, *Quantum Field Theory and Critical Phenomena*, Clarendon Press, Oxford, 1996.
- [20] G. PARISI, *Statistical Field Theory*, Addison Wesley, New York, 1988.
- [21] J. BONART, L. F. CUGLIANDOLO, and A. GAMBASSI, *J. Stat. Mech.* , P01014 (2012).

## BIBLIOGRAPHY

---

- [22] J. BONART and L. F. CUGLIANDOLO, *Phys. Rev. A* **86**, 023636 (2012).
- [23] J. BONART and L. F. CUGLIANDOLO, *Europhys. Lett.* **101**, 16003 (2013).
- [24] J. BONART, *arXiv*, arXiv:1307.3378 (2013).
- [25] A. RANÇON and J. BONART, *arXiv*, arXiv:1307.5768 (2013).
- [26] R. J. GLAUBER, *J. Math. Phys.* **4**, 294 (1963).
- [27] P. C. HOHENBERG and B. I. HALPERIN, *Rev. Mod. Phys.* **49**, 435 (1977).
- [28] B. I. HALPERIN and P. C. HOHENBERG, *Phys. Rev.* **177**, 952 (1969).
- [29] S. M. ALLEN and J. W. CAHN, *Acta Metallurgica* **27**, 1085 (1979).
- [30] D. A. HUSE, *Phys. Rev. B* **7845**, 34 (1986).
- [31] H. E. HURST, *Trans. Am. Soc. Civ. Eng.* **116**, 770 (1951).
- [32] H. E. HURST, *Nature* **180**, 44 (1957).
- [33] B. B. MANDELBROT and J. W. V. NESS, *SIAM Rev.* **10**, 422 (1968).
- [34] B. B. MANDELBROT, *The fractal geometry of nature*, W. H. Freeman, New York, 1983.
- [35] H. C. BERG, *Random walks in biology*, Princeton University Press, 1983.
- [36] M.-A. MIVILLE-DESCHÊNES, F. LEVRIER, and E. FALGARONE, *The Astrophysical Journal* **593**, 831 (2003).
- [37] L. C. G. ROGERS, *Mathematical Finance* **7**, 95 (1997).
- [38] T. LUNDAHL, W. J. OHLEY, S. M. KAY, and R. SIFFERT, *IEEE Transactions on medical imaging* **5**, 152 (1986).
- [39] Z. ZHANG, O. G. MOURITSEN, K. OTNES, T. RISTE, and M. J. ZUCKERMANN, *Phys. Rev. Lett.* **70**, 1834 (1993).
- [40] E. S. KIKKINIDES and V. N. BURGANOS, *Phys. Rev. E* **59**, 7185 (1999).
- [41] J. L. A. DUBBELDAM, V. G. ROSTIASHAVILI, A. MILCHEV, and T. A. VILGIS, *Phys. Rev. E* **83**, 011802 (2011).
- [42] A. TALONI, A. CHECHKIN, and J. KLAFTER, *Phys. Rev. Lett.* **104**, 160602 (2010).
- [43] A. M. CHURILLA, W. A. GOTTSCHALKE, L. S. LIEBOVITCH, L. Y. SELECTOR, A. T. TODOROV, and S. YEANDLE, *Annals of biomedical engineering* **24**, 99 (1996).
- [44] P. ALLEGRINI, M. BUIATTI, P. GRIGOLINI, and B. J. WEST, *Phys. Rev. E* **57**, 4558 (1998).
- [45] L. C.-L. LIN, N. GOV, and F. L. H. BROWN, *The Journal of Chem. Phys.* **124**, 074903 (2006).
- [46] I. A. MARTINEZ, S. RAJ, and D. PETROV, *European Biophysics Journal* **41**, 99 (2012).
- [47] A. ZOIA, A. ROSSO, and S. N. MAJUMDAR, *Phys. Rev. Lett.* **102**, 120602 (2009).
- [48] N. POTTIER, *Physica A* **317**, 371 (2003).
- [49] P. HÄNGGI and P. JUNG, in *Advances in Chemical Physics*, edited by I. PRIGOGINE and S. A. RICE, volume 89, p. 239, John Wiley and Sons, 1995.
- [50] U. WEISS, *Quantum dissipative systems*, World Scientific Publishing Co., Singapore, New Jersey, London, Hong Kong, 2008.
- [51] M. J. BOWICK and A. TRAVESSET, *Physics Reports* **344**, 255 (2001).
- [52] T. FRANOSCH, M. GRIMM, M. BELUSHKIN, F. M. MOR, G. FOFFI, L. FORRÓ, and S. JENEY, *Nature* **478**, 85 (2011).

## BIBLIOGRAPHY

---

- [53] P. HÄNGGI, P. TALKNER, and M. BORKOVEC, *Rev. Mod. Phys.* **62**, 251 (1990).
- [54] P. HÄNGGI, *Chem. Phys.* **180**, 157 (1994).
- [55] J. MASOLIVER, B. J. WEST, and K. LINDENBERG, *Phys. Rev. A* **34**, 1481 (1986).
- [56] U. SEIFERT and S. DIETRICH, *Europhys. Lett.* **3**, 593 (1987).
- [57] E. MEDINA, T. HWA, M. KARDAR, and Y.-C. ZHANG, *Phys. Rev. A* **39**, 6 (1989).
- [58] H. K. JANSSEN, E. FREY, and U. C. TÄUBER, *Eur. Phys. J. B* **9**, 491 (1999).
- [59] E. KATZAV, *Phys. Rev. E* **68**, 046113 (2003).
- [60] P. DUTTA and P. M. HORN, *Rev. of Mod. Phys.* **53**, 497 (1981).
- [61] M. J. KIRTON and M. J. UREN, *Adv. in Phys.* **38**, 367 (1989).
- [62] F. N. HOOGE, T. G. M. KLEINPENNING, and L. K. L. VANDAMME, *Rep. Prog. Phys.* **44**, 479 (1981).
- [63] M. B. WEISSMAN, *Rev. of Mod. Phys.* **60**, 537 (1988).
- [64] A. HAJIMIRI and T. H. LEE, *IEEE Journal of solid-state circuits* **33**, 179 (1998).
- [65] H. M. JAEGER and S. R. NAGEL, *Science* **2555**, 1523 (1992).
- [66] M. PACZUSKI, S. MASLOV, and P. BAK, *Phys. Rev. E* **53**, 414 (1996).
- [67] T. HWA and M. KADAR, *Phys. Rev. A* **45**, 7002 (1992).
- [68] M. TAKAYASU, *Fractals* **1**, 860 (1993).
- [69] P. C. IVANOV, L. A. N. AMARAL, A. L. GOLDBERGER, S. HAVLIN, M. G. ROSENBLUM, and H. E. STANLEY, *CHAOS* **11**, 641 (2001).
- [70] T. G. DEWEY and J. G. BANN, *Biophysical Journal* **63**, 594 (1992).
- [71] R. F. VOSS, *Phys. Rev. Lett.* **68**, 3805 (1992).
- [72] E. LUIJTEN and H. W. J. BLÖTE, *Phys. Rev. B* **56**, 8945 (1997).
- [73] P. C. MARTIN, E. D. SIGGIA, and H. H. ROSE, *Rev. Rev. A* **8**, 423 (1973).
- [74] C. DE DOMNINICIS, *J. Phys. Colloques* **37**, C1 (1976).
- [75] R. BAUSCH, H. K. JANSSEN, and H. WAGNER, *Z. Phys. B* **24**, 113 (1976).
- [76] B. I. HALPERIN, P. C. HOHENBERG, and S. MA, *Phys. Rev. B* **10**, 139 (1974).
- [77] B. I. HALPERIN, P. C. HOHENBERG, and S. MA, *Phys. Rev. B* **13**, 4119 (1976).
- [78] B. I. HALPERIN, S. MA, and P. C. HOHENBERG, *Phys. Rev. Lett.* **29**, 1548 (1972).
- [79] P. C. HOHENBERG and B. I. HALPERIN, *Rev. Mod. Phys.* **49**, 435 (1977).
- [80] C. DE DOMNINICIS and L. PELITI, *Phys. Rev. B* **18**, 353 (1978).
- [81] A. ONUKI, *Phase transition dynamics*, Cambridge University Press, Cambridge, 2002.
- [82] H. K. JANSSEN, B. SCHAUB, and B. SCHMITTMANN, *Z. Phys. B* **73**, 539 (1989).
- [83] P. CALABRESE, A. GAMBASSI, and F. KRZAKALA, *J. Stat. Mech.* , P06016 (2006).
- [84] P. CALABRESE and A. GAMBASSI, *J. Stat. Mech.* , P01001 (2007).
- [85] H. K. JANSSEN, in *From Phase Transitions to Chaos—Topics in Modern Statistical Physics*, edited by G. GYÖRGYI, I. KONDOR, L. SASVÀRI, and T. TÉL, p. 68, World Scientific, Singapore, 1992.

## BIBLIOGRAPHY

---

- [86] P. CALABRESE and A. GAMBASSI, *J. Phys. A* **38**, R133 (2005).
- [87] Y. OZEKI and N. ITO, *J. Phys. A* **40**, R149 (2007).
- [88] J.-P. BOUCHAUD and M. POTTERS, *Theory of Financial Risk and Derivative Pricing: From Statistical Physics to Risk Management*, Cambridge University Press, 2003.
- [89] R. ZWANZIG, *J. Stat. Phys.* **9**, 215 (1973).
- [90] K. KAWASAKI, *J. Phys. A* **6**, 1289 (1973).
- [91] P. CALABRESE and A. GAMBASSI, *Phys. Rev. E* **66**, 066101 (2002).
- [92] C. ARON, G. BIROLI, and L. F. CUGLIANDOLO, *J. Stat. Mech.* , P11018 (2010).
- [93] F. CORBERI, E. LIPPIELLO, and M. ZANNETTI, *J. Stat. Mech.* , P07002 (2007).
- [94] L. F. CUGLIANDOLO, *J. Phys. A: Math. Theor.* **44**, 483001 (2011).
- [95] B. B. MANDELBROT and J. W. VAN NESS, *SIAM Review* **10**, 4 (1968).
- [96] M. LE BELLAC, *Quantum and Statistical Field Theory*, Oxford University Press, Oxford, 1991.
- [97] H. W. DIEHL, S. DIETRICH, and E. EISENRIEGLER, *Phys. Rev. B* **27**, 2937 (1983).
- [98] H. HAUBOLD, A. MATHAI, and R. SAXENA, *J. App. Math.* **2011**, 298628 (2011).
- [99] L. F. CUGLIANDOLO, J. KURCHAN, and L. PELITI, *Phys. Rev. E* **55**, 3898 (1997).
- [100] L. F. CUGLIANDOLO and J. KURCHAN, *J. Phys. Soc. Japan (Supplement A)* **69**, 247 (2000).
- [101] C. GODRÈCHE and J. M. LUCK, *J. Phys. A* **33**, 9141 (2000).
- [102] P. CALABRESE and A. GAMBASSI, *J. Stat. Mech.* , P07013 (2004).
- [103] A. CRISANTI and F. RITORT, *J. Phys. A* **36**, R181 (2003).
- [104] L. F. CUGLIANDOLO, J. KURCHAN, and G. PARISI, *J. Phys. I* **4**, 1641 (1994).
- [105] P. CALABRESE and A. GAMBASSI, *Acta Phys. Slov.* **52**, 335 (2002).
- [106] P. CALABRESE and A. GAMBASSI, *Phys. Rev. E* **65**, 066120 (2002).
- [107] G. SCHÖN and A. ZAIKIN, *Phys. Rep.* **5**, 237 (1990).
- [108] A. J. LEGGETT, S. CHAKRAVARTY, A. T. DORSEY, M. P. A. FISHER, A. GARG, and W. ZW-  
ERGER, *Rev. Mod. Phys.* **59**, 1 (1987).
- [109] P. HÄNGGI, P. TALKNER, and M. BORKOVEC, *Rev. Mod. Phys.* **62**, 251 (1990).
- [110] R. FEYNMAN and F. VERNON, *Ann. Phys.* **24**, 118 (1963).
- [111] J. SCHWINGER, *J. Math. Phys.* **2**, 407 (1961).
- [112] G. AGARWAL, *Phys. Rev. A* **4**, 739 (1971).
- [113] N. POTTIER and A. MAUGER, *Physica A* **282**, 77 (2000).
- [114] G. INGOLD, in *Coherent Evolution in Noisy Systems*, volume 611, p. 1, Springer-Verlag Berlin, 2002.
- [115] B. HU, J. PAZ, and Y. ZHANG, *Phys. Rev. D* **45**, 2843 (1992).
- [116] R. KARRLEIN and H. GRABERT, *Phys. Rev. E* **55**, 153 (1997).
- [117] G. W. FORD, M. KAC, and P. MAZUR, *J. Math. Phys.* **6**, 504 (1965).
- [118] C. W. GARDINER and P. ZOLLER, *Quantum Noise*, Springer Berlin Heidelberg New York, 2004.
- [119] S. A. BALBUS, J. BONART, H. N. LATTER, and N. O. WEISS, *MNRAS* **400**, 176 (2009).

## BIBLIOGRAPHY

---

- [120] H. N. LATTER, J. BONART, and S. A. BALBUS, *MNRAS* **405**, 1831 (2010).
- [121] S. CHAKRAVARTY, *Phys. Rev. Lett.* **49**, 681 (1982).
- [122] A. O. CALDEIRA and A. J. LEGGETT, *Phys. Rev. Lett.* **46**, 211 (1981).
- [123] A. J. BRAY and M. A. MOORE, *Phys. Rev. Lett.* **49**, 1545 (1982).
- [124] H. GRABERT, U. WEISS, and P. HÄNGGI, *Phys. Rev. Lett.* **52**, 2193 (1984).
- [125] J. M. KOSTERLITZ, *Phys. Rev. Lett.* **37**, 1577 (1976).
- [126] N. V. PROKOFEV and P. C. E. STAMP, *Rep. Prog. Phys.* **63**, 669 (2000).
- [127] M. SCHLOSSHAUER, A. P. HINES, and G. J. MILBURN, *Phys. Rev. A* **77**, 022111 (2008).
- [128] K. M. FORSYTHE and N. MAKRI, *Phys. Rev. Lett.* **81**, 5710 (1998).
- [129] J. SHAO and P. HÄNGGI, *Phys. Rev. Lett.* **81**, 5710 (1998).
- [130] P. SCHRAMM and H. GRABERT, *Journal Stat. Phys.* **49**, 767 (1987).
- [131] R. BULLA, N.-H. TONG, and M. VOJTA, *Phys. Rev. Lett.* **91**, 170601 (2003).
- [132] M. VOJTA, N.-H. TONG, and R. BULLA, *Phys. Rev. Lett.* **94**, 070604 (2005).
- [133] A. WINTER, H. RIEGER, M. VOJTA, and R. BULLA, *Phys. Rev. Lett.* **102**, 030601 (2009).
- [134] A. CHIN, J. PRIOR, S. F. HUELGA, and M. B. PLENIO, *Phys. Rev. Lett.* **107**, 160601 (2011).
- [135] P. HÄNGGI and G. INGOLD, *CHAOS* **15**, 026105 (2005).
- [136] L. F. CUGLIANDOLO, T. GIAMARCHI, and P. L. DOUSSAL, *Phys. Rev. Lett.* **96**, 217203 (2006).
- [137] L. F. CUGLIANDOLO and G. S. LOZANO, *Phys. Rev. Lett.* **80**, 4979 (1998).
- [138] L. F. CUGLIANDOLO and G. S. LOZANO, *Phys. Rev. B* **59**, 915 (1999).
- [139] L. F. CUGLIANDOLO, D. R. GREMPER, G. S. LOZANO, H. LOZZA, and C. A. DA SILVA SANTOS, *Phys. Rev. B* **66**, 014444 (2002).
- [140] M. P. KENNETT and C. CHAMON, *Phys. Rev. Lett.* **86**, 1622 (2001).
- [141] M. P. KENNETT, C. CHAMON, and Y. YE, *Phys. Rev. B* **64**, 224408 (2001).
- [142] G. BIROLI and O. PARCOLLET, *Phys. Rev. B* **65**, 094414 (2002).
- [143] C. ARON, G. BIROLI, and L. F. CUGLIANDOLO, *Phys. Rev. B* **82**, 174203 (2010).
- [144] L. V. KELDysh, *J. Exptl. Theoret. Phys.* **47**, 1515 (1964).
- [145] E. CALZETTA, A. ROURA, and E. VERDAGUER, *Physica A* **319**, 188 (2003).
- [146] J. CATANI, G. LAMPORESI, D. NAIK, M. GRING, M. INGUSCIO, F. MINARDI, A. KANTIAN, and T. GIAMARCHI, *Phys. Rev. A* **85**, 023623 (2012).
- [147] M. ZVONAREV, V. CHEIANOV, and T. GIAMARCHI, *Phys. Rev. Lett.* **99**, 240404 (2007).
- [148] S. PALZER, C. ZIPKES, C. SIAS, and M. KÖHL, *Phys. Rev. Lett* **103**, 150601 (2009).
- [149] J. T. DEVREESE and A. S. ALEXANDROV, *Rep. Prog. Phys.* **72**, 066501 (2009).
- [150] J. TEMPERE, W. CASTEELS, M. K. OBERTHALER, S. KNOOP, E. TIMMERMANS, and J. T. DEVREESE, *Phys. Rev. B* **80**, 184504 (2009).
- [151] S. PEOTTA, *Nonequilibrium dynamics of strongly correlated one-dimensional ultracold quantum gases*, PhD thesis, Scuola Normale Superiore di Pisa, 2012.
- [152] S. TOMONAGA, *Prog. in Theor. Phys.* **5**, 544 (1950).

## BIBLIOGRAPHY

---

- [153] J. M. LUTTINGER, *J. Math. Phys.* **4**, 1154 (1963).
- [154] D. MATTIS and E. LIEB, *J. Math. Phys.* **6**, 304 (1965).
- [155] C. L. KANE, Lectures on Bosonization, Boulder summer school July 2005, 2005.
- [156] D. SENECHAL, An introduction to bosonization, 1999.
- [157] J. VAN DELFT and H. SCHOELLER, *Annalen Phys.* **7**, 225 (1998).
- [158] M. A. CAZALILLA, R. CITRO, T. GIAMARCHI, E. ORIGNAC, and M. RIGOL, *Rev. Mod. Phys.* **83**, 1405 (2011).
- [159] S. SACHDEV, *Quantum Phase Transitions*, John Wiley and Sons, Ltd., 2007.
- [160] M. GIRARDEAU, *Journal of Math. Phys.* **1**, 516 (1960).
- [161] C. J. M. MATHY, M. B. ZVONAREV, and E. DEMLER, *Nature Physics* **8**, 881 (2012).
- [162] E. H. LIEB and W. LINIGER, *Physical Review* **130**, 1605 (1963).
- [163] M. A. CAZALILLA, *J. Phys. B* **37**, S1 (2004).
- [164] A. Y. CHERNY, J.-S. CAUX, and J. BRAND, *Phys. Rev. A* **80**, 043604 (2009).
- [165] A. H. CASTRO NETO and M. P. A. FISHER, *Phys. Rev. A* **53**, 9713 (1995).
- [166] M. SCHECKTER, A. KAMENEV, D. M. GANGARDT, and A. LAMACRAFT, *Phys. Rev. Lett.* **108**, 207001 (2012).
- [167] M. SCHECKTER, D. M. GANGARDT, and A. KAMENEV, *Annals of Physics* **327**, 639 (2012).
- [168] R. CITRO, A. MINGUZZI, and F. W. J. HEKKING, *Rhys. Rev. B* **79**, 172505 (2009).
- [169] D. S. PETROV, G. V. SHLYAPNIKOV, and J. T. M. WALRAVEN, *Phys. Rev. Lett.* **85**, 3745 (2000).
- [170] F. SCHRECK, L. KHAYKOVICH, K. L. CORWIN, G. FERRARI, T. BOURDEL, J. CUBIZOLLES, and C. SALOMON, *Phys. Rev. Lett.* **87**, 080403 (2001).
- [171] S. DETTMAR, D. HELLWEG, P. RYTTY, J. J. ARLT, W. ERTMER, K. SENGSTOCK, D. S. PETROV, G. V. SHLYAPNIKOV, H. KREUTZMANN, L. SANTOS, and M. LEWENSTEIN, *Phys. Rev. Lett.* **87**, 160406 (2001).
- [172] A. GÖRLITZ, J. M. VOGELS, A. E. LEANHARDT, C. RAMAN, T. L. GUSTAVSON, J. R. ABO-SHAEER, A. P. CHIKKATUR, S. GUPTA, S. INOUE, T. ROSEN BAND, and W. KETTERLE, *Phys. Rev. Lett.* **87**, 130402 (2001).
- [173] M. GREINER, I. BLOCH, O. MANDEL, T. HÄNSCH, and T. ESSLINGER, *Phys. Rev. Lett.* **87**, 160405 (2001).
- [174] R. FOLMAN, P. KRÜGER, D. CASSETTARI, B. HESSMO, T. MAIER, and J. SCHIEDMAYER, *Phys. Rev. Lett.* **84**, 4749 (2000).
- [175] E. P. GROSS, *J. Math. Phys.* **4**, 195 (1963).
- [176] L. P. PITAEVSKII, *Sov. Phys. JETP* **40**, 646 (1961).
- [177] D. S. PETROV, D. GANGARDT, and G. V. SHLYAPNIKOV, *Journal de Physique* **116**, 3 (2004).
- [178] W. KETTERLE and N. VAN DRUTEN, *Phys. Rev. A* **54**, 656 (1996).
- [179] C. MENOTTI and S. STRINGARI, *Phys. Rev. A* **66**, 043610 (2002).
- [180] R. CITRO, S. D. PALO, E. ORIGNAC, P. PETRI, and M.-L. CHIOFALO, *Phys. Rev. A* **75**, 051602 (2007).
- [181] P. PETRI, S. D. PALO, E. ORIGNAC, R. CITRO, and M.-L. CHIOFALO, *Phys. Rev. A* **77**, 015601 (2008).

## BIBLIOGRAPHY

---

- [182] R. CITRO, S. D. PALO, E. ORIGNAC, P. PETRI, and M.-L. CHIOFALO, *New Journal of Physics* **10**, 045011 (2008).
- [183] T. H. JOHNSON, M. BRUDERER, Y. CAI, S. R. CLARK, W. BAO, and D. JAKSCH, *Europhys. Lett.* **98**, 26001 (2012).
- [184] S. PEOTTA, D. ROSSINI, P. SILVI, G. VIGNALE, R. FAZIO, and M. POLINI, *Phys. Rev. Lett.* **110**, 015302 (2013).
- [185] G. THALHAMMER, G. BARONTINI, L. D. SARLO, J. CATANI, F. MINARDI, and M. INGUSCIO, *Phys. Rev. Lett.* **100**, 210402 (2008).
- [186] V. PEANO, M. THORWART, C. MORA, and R. EGGER, *New J. Phys.* **7**, 192 (2005).
- [187] M. OLSHANII, *Phys. Rev. Lett.* **81**, 938 (1998).
- [188] E. H. LIEB and W. LINIGER, *Phys. Rev.* **130**, 16051616 (1963).
- [189] H. FRÖHLICH, *Adv. Phys.* **3**, 325 (1954).
- [190] R. P. FEYNMAN, *Phys. Rev.* **97**, 660 (1955).
- [191] E. H. LIEB and K. YAMAZAKI, *Phys. Rev.* **111**, 728 (1958).
- [192] T. HOLSTEIN, *Annals of Physics* **8**, 325 (1959).
- [193] T. HOLSTEIN, *Annals of Physics* **8**, 343 (1959).
- [194] A. S. MISHCHENKO and N. V. PROKOF'EV, *Adv. Phys.* **3**, 325 (1954).
- [195] J. T. DEVREESE, R. EVRARD, and E. KARTHEUSER, *Phys. Rev. B* **12**, 3353 (1975).
- [196] B. DAMSKI, *Phys. Rev. A* **73**, 043601 (2006).
- [197] V. HAKIM, *Phys. Rev. E* **55**, 2835 (1997).
- [198] T. FUKUHARA, A. KANTIAN, M. ENDRES, M. CHENEAU, P. SCHAUSS, S. HILD, D. BELLEM, U. SCHOLLWÖCK, T. GIAMARCHI, C. GROSS, I. BLOCH, and S. KUHR, *arXiv*, 1209.6468 (2012).
- [199] G. E. ASTRAKHARCHIK and L. P. PITAEVSKII, *Phys. Rev. A* **70**, 013608 (2004).
- [200] A. Y. CHERNY, J.-S. CAUX, and J. BRAND, *Frontiers of Physics* **7**, 54 (2011).
- [201] L. RUTHERFORD, J. GOOLD, T. BUSCH, and J. F. MCCANN, *Phys. Rev. A* **83**, 055601 (2011).
- [202] H. SPOHN, *Annals of Physics* **175**, 278 (1987).
- [203] J. M. SANCHO, J. GARCÍA-OJALVO, and H. GUO, *Physica D* **113**, 331 (1998).
- [204] J.-L. BARRAT and D. RODNEY, *J. Stat. Phys.* **144**, 679 (2011).
- [205] S. A. CHIN and H. A. FORBERT, *Physics Lett. A* **272**, 402 (2000).
- [206] A. SICILIA, J. ARENZON, A. J. BRAY, and L. F. CUGLIANDOLO, *Phys. Rev. E* **76**, 061116 (2007).